The role of pulvinar during perceptual decision-making and thalamic interactions with cardiac and respiratory activity in macaques

Dissertation

for the award of the degree

"Doctor rerum naturalium"

of the Georg-August-Universität Göttingen

within the doctoral program Systems Neuroscience
appendant to the Göttingen Graduate Center for Neurosciences, Biophysics, and Molecular Biosciences (GGNB)

of the Georg-August University School of Science (GAUSS)

submitted by

Kristin Kaduk

from Rostock

Göttingen 2022

Thesis Committee

Dr. Igor Kagan (supervisor)
Cognitive Neuroscience Laboratory, German Primate Center

Prof. Dr. Melanie Wilke
Department of Cognitive Neurology, University Medical Center Göttingen

Dr. Caspar Schwiedrzik
Department of Neural Circuits and Cognition, European Neuroscience Institute

Members of the Examination Board

Referee: Dr. Igor Kagan (supervisor)
Cognitive Neuroscience Laboratory, German Primate Center

2nd Referee: Prof. Dr. Melanie Wilke
Department of Cognitive Neurology, University Medical Center Göttingen

Further members of the Examination Board

Dr. Caspar Schwiedrzik
Department of Neural Circuits and Cognition, European Neuroscience Institute

Prof. Dr. Alexander Gail
Sensorimotor Laboratory, German Primate Center

Prof. Dr. Thomas Bayer
Department of Molecular Psychiatry, University Medical Center Göttingen

Prof. Dr. Ralf Heinrich
Department of Cellular Neurobiology, University of Göttingen

Date of oral examination: 23.08.2022

doi:10.53846/goediss-10065

Table of Contents

Summary

The dorsal pulvinar (dPul), a higher-order thalamic hub, is instrumental in spatial orienting and selecting stimuli in our environment by gating cortico-thalamic-cortical communication. However, its precise role in perceptual decision-making, particularly under conditions of spatial competition and varying perceptual difficulty, is less understood. Moreover, dPul's reciprocal connections with the central autonomic network (CAN) hint at its potentially profound influence on how the brain and physiological systems, such as the heart, interact. This thesis explores how the dPul modulates visuospatial cognition, influences perceptual decision processes, and potentially interacts with cardiac and respiratory activity to better understand heart-brain interactions.

Chapter 2 examines the dorsal pulvinar's role in visuospatial cognition by injecting GABA-A agonist THIP into dPul during a color discrimination task with varying difficulty. Utilizing Signal Detection Theory, we predict either a decrease in dprime if dPul inactivation affects perceptual discrimination or a shift in response criterion if dPul inactivation affects spatial orienting. We observed criterion shifts away from contralesional stimuli after inactivation for both difficulty levels, especially when competing peripheral stimuli in opposite hemifields were present. Additionally, saccade latency for the contralesional selection increased, while dprime and overall accuracy remained largely unaffected after inactivation. Using a more epoch-specific perturbation, Chapter 3 builds on this and Dominguez-Vargas et al.'s 2017 findings about increased contraversive target selection in free-choice trials after dPul microstimulation starting after the target onset ("late"). Late dPul microstimulation had little impact on contraversive criterion and dprime. We primarily observed criterion shifts away from ipsiversive stimuli, manifesting as reluctance to select ipsiversive stimuli. After early microstimulation, similar effects were observed as in the inactivation study. Together, our results underline the critical contribution of the dorsal pulvinar to spatial orienting while being less important for perceptual discrimination.

In Chapter 4, we tested whether the dPul generally interacts with the CAN and cardiovascular system beyond a specific emotional content remains unknown. We found that suppressing the neural activity of the dPul pharmacologically decreased the heart and respiration rates of two out of three monkeys. Moreover, the RMSSD, as a measure of the heart rate variability, decreased after dPul inactivation in one monkey (M1). We conclude that suppressing the dorsal pulvinar's neural activity impacts the heart and respiration rate, emphasizing the crucial role of the dPul in arousal-related processing. In the electrophysiology study, a significant proportion of thalamic neurons displayed robust coupling between their spiking activity and the cardiac cycle during the task (ventral posterior lateral nucleus (VPL): 88%, dPul and mediodorsal thalamus (MD): 68%). After analyzing the signal-to-noise ratio and firing rate changes, we found no sign of instability from potential cardiac mechanical influences. The identified link between dPul and the heart's rhythm indicates dPul's role in integrating multisensory and arousal-related signals. This insight enhances our understanding of heart-brain dynamics. Considering the medial pulvinar's high density of alpha receptors, it raises questions regarding an intertwined neural mechanism for spatial attention and arousal in the dPul. Together, these results prompt a re-evaluation of the thalamus's function in neuro-cardiological processes.

Acknowledgments

First and foremost, I would like to express my gratitude to Dr. Igor Kagan, my Ph.D. supervisor, for his constant directional guidance and support in technical aspects. He empowered me to find the solution to diverse scientific problems. I am also deeply grateful to Prof. Dr. Melanie Wilke for being a great mentor and collaborator that was always ready to exchange scientific thoughts. I have greatly appreciated the opportunity both of you gave me to work with non-human primates and apply different technologies to gain insights into the neural mechanisms of visuospatial cognition.

A heartfelt thanks go to Dr. Caspar Schwiedrizik for his helpful scientific discussions and accompaniment of the projects over the years. I also thank the remaining members of my examination board, Prof. Dr. Alexander Gail, Prof. Dr. Thomas Bayer, and Prof. Dr. Ralf Heinrich.

I thank Prof. Dr. Stefan Treue and Prof. Dr. Alexander Gail for valuable learning experiences, scientific support, and social gatherings of the Department of Cognitive Neuroscience. Special thanks go to Dr. Daniela Trinca Bertazzi Lazzarini for the fantastic technical support on-site, for working hand in hand to perform MRI scans or inactivation experiments, and for the encouraging conversations in the setup during a long experimental day.

Many thanks also to members of the Cognitive Neuroscience Laboratory (CNL) for their essential and fruitful discussions and mutual support during the everyday life of a Ph.D. Special thanks go to Dr. Lukas Schneider for guiding me through monkeypsych and the different analysis pipelines until the last day of my Ph.D. Thanks to Sina Plümer for taking care of my monkeys and for support with handling and cleaning the electrodes. Thanks to Leonore Burchhardt for teaching me handling and training the animals. My gratitude extends to all other colleagues who supported me, practically, scientifically, or personally. All the people mentioned above have contributed significantly to a friendly and enriching working atmosphere.

Special thanks go to Dr. Fadila Hadj-Bouziane, who accompanied me during my doctorate with encouraging words and professional input. It was my pleasure working together with you all these years on our scientific project that had a significant and inspiring impact on me during my Ph.D.

Thank you for the close and intense scientific collaboration over all the year goes to the five rhesus monkeys: Norman, Cornelius, Curius, Bacchus, and Magnus for contributing more than anyone else to these Ph.D. projects.

I would like to thank all the staff at System Neuroscience and the GGNB office for their efforts. I greatly appreciate this fantastic graduate school's diverse course offerings and opportunities. Special thanks go to Dr. Christina Stier for the continuous exchange as a colleague and friend.

I am grateful to the mentors, coordinators, and mentees of the Dorothea Schlözer Program at the University of Göttingen for their time and the valuable impulses they have given me in the last part.

I am grateful for the friendships that support me immensely in different ways. Special thanks to Annika Köhne, Dr. Ilyas Kuhlemann, Elfriede Steigerwald, Simone Santalucia, Vivien Hülsen, and finally but most importantly, Jorge Cabrera Moreno for all the exciting scientific and non-scientific discussions.

I am particularly grateful to my parents, brother, cousins, and grandparents, who supported me in every conceivable way and helped me flourish in my scientific work and the many other colorful facets of life. It is a great privilege of learning and benefiting from a stimulating and warm family environment. An especially heartfelt thanks goes to Dr. Felix Bracharz, who went on this journey with me and continues to do so, bringing his endless support and love along at every step.

1. Introduction

The brain is arguably the most complex organ in the human body. This jelly-like tissue mass contains billions of neurons interlinked through trillions of connections. The visualization of individual neuronal bodies, axons, and dendrites was pivotal to today's neuroscience, which mainly started with the work of histologists and pathologists, specifically in 1873 when Camillo Golgi introduced the Golgi staining procedure (Golgi, 1873). After refining Golgi's technique, Santiago Ramón y Cajal proposed in 1906 that the nervous system, including the brain and spinal cord, can be separated into individual neurons distinct from one another (Cajal, 1906). Together with the notion that individual neurons have a specific receptive field, i.e., visual field or areas of the skin that they respond to exclusively, these discoveries position the individual neuron as the structural and functional unit of the nervous system (so-called neuron doctrine). Neurons use biophysical processes and chemical messengers to transmit signals and are clustered in anatomical and functional regions. The first evidence that certain differentiable functions are localized in different parts of the nervous system came from a long series of clinical and experimental discoveries throughout the 19th century. Together, the neuron doctrine and functional localization are the core of the conceptual foundations of neuroscience; and replaced the view of the brain and central nervous system as a "black box"[1].

Investigating the nervous system and its underlying computations is necessary to understand behavior – as most behaviors are related to and result from the central nervous system functions. The brain activity underlies every simple behavior, such as walking or eating, as well as complex cognitive actions, such as speaking and problem-solving. Neuroscience evolved as a research discipline to broadly understand the nervous system and its impact on behavior and cognitive functions. Neuroscientists investigate the most complex organ in the human body. Therefore, neuroscientists had to break down the nervous system into smaller parts to understand the brain's temporally and spatially multiscale structure to explain behavior.

Visual perception (vision) is the ability to receive and interpret visual stimuli of the surroundings through the light that enters our eyes, which is the dominant sensory modality in humans and non-human primates. Up to 54% of the macaque neocortex is involved in visual processing (Van Essen et al., 1990), and vision is, to date, the most studied sensory system. Selecting a

[1] The term "black box" refers to any complex system where we can measure the inputs and outputs of the system but not the underlying inner units and computations.

behaviorally salient stimulus in complex environmental settings requires efficiently perceiving and evaluating behaviorally relevant information at different spatial locations. Most studies investigating the neural processes of visuospatial target selection emphasize interactions in frontoparietal cortical networks. In this framework, the sensory input information is relayed via the thalamus to the cortex, where the main distributed computations are going on, leading finally to a percept of the action as an output. Thus, the classical perspective on how the nervous system is related to perception and action is *corticocentric*. Indeed, this perspective is common and shared in a good article by Passingham and colleagues demonstrates that the function of any cortical area can be determined by its intrinsic and extrinsic cortical connections (Passingham et al., 2002). The author limited their review to the extrinsic connections to the cerebral cortex without considering the afferents and efferents from the subcortical brain areas. Today, neuroscientists know that transthalamic connections parallel any direct cortical link.

The view of the thalamus as a passive relay of sensory signals to the cortex changed radically, especially with the publication of Sherman and Guillery's articles, reviews, and books about the lateral geniculate nucleus (LGN), demonstrating that even LGN, a first-order thalamic nucleus, modulates the transmitted neural signal to the cortex (Sherman & Guillery, 1996, 2002, 2013). Furthermore, some so-called higher-order thalamic nuclei receive inputs mainly from the cortex, introducing the idea that, on the one hand, signal transmission is converging in the thalamus. On the other hand, the cortex may strongly influence which signals are relayed to other cortical regions via ascending thalamocortical projections. The anatomical arrangement between the thalamus and cortical areas and the insights from functional studies about perception and cognition implies that the thalamus may be more actively involved in coordinating corticocortical communication than previously realized. Specifically, different thalamic nuclei have distinct anatomical connections with the cortex that hint toward specific functional roles of the thalamic nuclei. I noticed that the thalamus functions are described vaguely and broadly by stating that specific thalamic nuclei are crucial for relaying, convergence, integration or/ and regulation/modulation of cortical communication. These descriptions of the functions are indicated in many reviews about the thalamus.

Still, we cannot yet explain the underlying neural mechanisms that describe how or which information is integrated to regulate cortical communication. How are the different thalamic nuclei relay, modulate or regulate other cognitive processes with the cortex? What is the specific function of different thalamic nuclei in cognition and perception? These questions belong to the twenty-three currently unresolved problems in system neuroscience identified and listed by Van Hemmen

and Sejnowski in their book (van Hemmen & Sejnowski, 2006). Many questions about the thalamus remain unanswered until today.

The investigation of one specific thalamic nucleus has excellent potential to give crucial insights into some of these questions. The dorsal pulvinar is a higher-order thalamic nucleus with a complex organization that is causally linked to visuospatial cognition. Humans and animals with damage to the pulvinar show spatial orienting and visuomotor behavior problems. The dorsal pulvinar has extensive and reciprocal connections with higher-order cortical areas, such as the prefrontal and parietal cortex, and subcortical regions, such as the superior colliculus and amygdala. This diverse connectivity profile identifies the dorsal pulvinar as a unique brain hub well situated to integrate cortical information and modulate the circuitry involved in spatial attentional orienting, sensory-guided action, and interaction with the central autonomous network. Thus, the dorsal pulvinar combines processed complex sensory inputs from the cortex with limbic influences. Yet it remains to be determined how the dorsal pulvinar contributes to sensory-guided actions with perceptual decision-making and cardiovascular regulation via its distinct interconnection. The presented work of this dissertation focuses on causally perturbating the neural activity of the dorsal pulvinar (pharmacological inactivation and electrical microstimulation) to investigate its involvement in visuospatial and perceptual decision-making as well as the link between the dorsal pulvinar and the autonomous network.

Overview of chapters

The central part of this dissertation consists of two general chapters and three research manuscript-style chapters (chapters 2-4). Here, I will shortly summarize their content.

Chapter 1 (General Introduction) summarizes the literature about the thalamic nuclei, the pulvinar focusing on the functional role of the pulvinar in attentional processing and sensory-guided actions. The function of the pulvinar is highly interconnected with its cytoarchitecture and anatomical connections; therefore, the chapter starts there. This chapter outlines the different functions of the pulvinar in perception and cognition, focusing mainly on non-human primate studies. Still, the general discussion will take it further to compare with studies done on humans. It also gives a short overview of perceptual decision-making, which psychophysics task have been used to investigate perceptual decision-making and describe the color discrimination saccade task used in every study of this dissertation in relation to other tasks used to investigate the functional contribution of the pulvinar.

Chapter 2 is a manuscript presenting the change in visually-guided selection behavior after a pharmacological inactivation of the dorsal pulvinar. The data emphasize the critical contribution of dorsal pulvinar to spatial orienting while being less critical for perceptual discrimination.

Chapter 3 is a manuscript complementing the previous chapter by resolving at which processing stages pulvinar might affect perceptual decision-making by applying time-resolved electrical microstimulation.

Chapter 4 is a manuscript containing two experimental studies (inactivation, electrophysiology) exploring heart-brain interactions: whether and how dorsal pulvinar is related to the cardiovascular system.

Chapter 5, a General Discussion, summarizes the main results of the individual studies about dorsal pulvinar involvement in perceptual-decision making and autonomic control, discussing experimental results, limitations, and future directions to provide the reader with a conceptual overview and general conclusions of the presented work.

1.1 The pulvinar complex

The pulvinar is the largest thalamic nuclei in the posterior end of the primate thalamus and has dramatically expanded during primate evolution compared to other thalamic nuclei. Its change in size is comparable to the changes in the prefrontal cortex, and its largest dimensions were reached in the human pulvinar. The pulvinar or part of it is often called the lateral posterior thalamic nucleus in all non-primate mammals (see review in Lyon, 2007). The primate pulvinar is better described as a pulvinar complex consisting of several nuclei with distinct functional properties and connectivity profiles. Although some nuclei of the pulvinar complex have a putatively homologous region in other animals (e.g. rats and cats), specifically the medial/dorsal pulvinar that is the main focus of the work presented in this dissertation seems to be unique to the primate pulvinar.

1.1.1 Structure of the pulvinar complex

Based on the classical cytoarchitecture and fiber myelination, early anatomical studies segmented the pulvinar into at first three and then four major divisions: anterior, medial, lateral, and inferior pulvinar (Olszewski, 1952; Walker, 1938).

These subnuclei consist of a mix of morphologically and neurochemically distinct cell types (Jones, 1985). Like other thalamic nuclei, the pulvinar contains two main populations of neurons; glutamatergic thalamocortical projection neurons (also called thalamocortical relay cells) and local gamma-aminobutyric acid (GABA)ergic interneurons (also called Golgi type II neuron). The projection-interneuron ratio is about 7:3 in the lateral and inferior pulvinar and 9:2 in the medial pulvinar (Gattass et al., 2018). The soma of the relay neurons is usually small and round and exhibits a radial dendritic pattern and thin dendritic appendages. The pulvino-cortical projections from glutamatergic relay neurons have been further characterized and compared to neurons in the extrastriate cortex (Rockland, 1996, 1998, 2019). For the lateral part of the inferior pulvinar and lateral pulvinar, the non-giant pulvinocortical relay neurons cluster together. The giant relay cells tend to be solitary and are enmeshed with large terminals after the first branch point (Imura & Rockland, 2007). The somata of the projection neurons in the medial pulvinar are generally smaller and rounder than those found in the lateral and inferior pulvinar (Ma et al., 1998). Within the medial pulvinar, some interneurons with widespread collateral differ from the typical thalamic interneurons with their very localized axonal distributions. These long-range interneurons had been only identified within the medial pulvinar (Imura & Rockland, 2006). It has been suggested that these neurons interconnect the micro-units of the medial pulvinar and might support the

integration of information. GABA is the most important inhibitory neurotransmitter in the brain, and it is present in all thalamic interneurons. To understand better the cytoarchitecture of the pulvinar and especially how the neurons branch into several areas, where they converge on targets of cortico-cortical projections is crucial for the questions of how thalamic nuclei regulate communication among cortical regions to know.

The originally cytoarchitectonically defined divisions of the pulvinar in 4 major subnuclei do not correspond well with the connectivity-based and functional properties of the pulvinar. This discrepancy led to further studies using new histochemical techniques in combination with connectivity which argue for a partly different parcellation dividing the lateral pulvinar into a dorsal and ventral part and differentiating subnuclei in the medial and inferior pulvinar (Homman-Ludiye et al., 2020; Kaas & Lyon, 2007). The cytoarchitectonic and myeloarchitectonic segregation of the pulvinar complex was an essential piece of information to improve the targeting of specific nuclei in neurophysiological studies. It was necessary to combine the results of cytoarchitecture, fiber myelination, structural and functional connectivity, as well as neurophysiological and behavioral studies to investigate the role of the different nuclei of the pulvinar in cognition. We know today that the pulvinar complex consists of several nuclei with distinct connectivity profiles and functional properties.

However, the pulvinar organizational structure is partly still under active re-evaluation. Nowadays, approximately eight to ten different subnuclei of the pulvinar have been identified using more elaborated modern techniques such as immunostaining and histochemistry (Homman-Ludiye & Bourne, 2019). Assuming the overriding rule of brain anatomy that segregation of structure implies separation of function also applies to the pulvinar complex, neurophysiological studies investigating the role of the pulvinar complex in cognition might need to target more specific subnuclei of the pulvinar to resolve its secrets.

1.1.2 Subdivisions via cortical-thalamo-cortical connections

Identifying the inputs to a thalamic nucleus can also give insight into the source and type of information this nucleus processes or relays. Because of this reason, many studies investigated the anatomical connections to and away from the pulvinar. The inferior pulvinar receives inputs and projects to the striate and extra-striate cortex (Adams et al., 2000; Stepniewska et al., 1994). As the early visual cortex is organized according to retinotopic maps, the anatomical connections to the inferior pulvinar are also topographically managed so that neighboring neurons in the visual

cortex project to neighboring neurons in the inferior pulvinar. In this regard, V1 projections to the pulvinar are near V2's projections but further from V4's.

The ventral part of the lateral pulvinar also has organized retinotopic maps, which connect with the visual cortex (Gutierrez et al., 1995). By considering the retinotopic organization of the ventral part of the lateral pulvinar, the cortical connections, and distinctive chemoarchitectonic features of the lateral pulvinar, the ventral part of the lateral pulvinar is more appropriate to be considered part of the retinotopically organized inferior pulvinar (Baldwin & Bourne, 2017; Gutierrez et al., 2000; Kaas & Lyon, 2007). Therefore, together they form the ventral pulvinar (vPul). The ventral pulvinar also receives direct inputs from the retina (O'Brien et al., 2001).

Current evidence suggests that the ventral pulvinar of primates consists of at least five nuclei (Kaas & Baldwin, 2020). The anatomical connections of these nuclei can be grouped according to Mishkin and colleagues' two visual streams proposed in 1983. Visual information is processed in two paths of interconnected visual areas in primates. The ventral stream processes visual information for object identification (ventral stream, 'what' pathway), and the other is processing locations in space (dorsal stream, 'where' pathway) (Mishkin et al., 1983). The lateral pulvinar ventrolateral (PLvl) and central lateral nucleus of the inferior pulvinar (PIcl) project to the ventral stream of cortical processing for perception, and the other three nuclei, the posterior nucleus of the inferior pulvinar (PIp), medial nucleus of the inferior pulvinar (PIm), and central medial nucleus of the inferior pulvinar (PIcm), contribute to the dorsal stream for visually directed actions (Kaas & Baldwin, 2020; Kaas & Lyon, 2007).

By contrast, the dorsal part of the lateral pulvinar does not interconnect with retinotopically organized cortical areas (Gutierrez et al., 1995). Instead, it is connected to the temporal areas TEO and TE, the posterior parietal, temporal-parietal, and superior parietal regions, and dorsolateral prefrontal cortex, as well as to the dorsal and ventral premotor cortices (Adams et al., 2000; Asanuma et al., 1985; Gutierrez et al., 2000; Hardy & Lynch, 1992; Shipp, 2003; Webster et al., 1993). This pattern of connections of the dorsal part of the lateral pulvinar is more similar to the medial pulvinar. The medial pulvinar is reciprocally interconnected to the parietal (LIP, MIP, VIP area 7) and prefrontal cortex (FEF, dlPFC), orbitofrontal cortex, insula, cingulate, superior and inferior temporal sulcus regions, such as MST (Hardy & Lynch, 1992; Kaas & Baldwin, 2020; Kaas & Lyon, 2007; Preuss, 2007). More details about the localization of afferent and efferent projections of the medial pulvinar were described in marmosets (Homman-Ludiye et al., 2020). The identified anatomical connectivity profiles result in classification related to the cortical-thalamic-cortical connections, grouping broadly the dorsal part of the lateral pulvinar and

the medial pulvinar together, forming the dorsal pulvinar. The brachium, a fiber bundle, originating in the superior colliculus, marks a rough separation between the dorsal and ventral pulvinar. These global anatomical connectivity profiles underlie the described dorso-ventral functional gradient and guided electrophysiology and perturbation studies in non-human primates investigating the contribution of the pulvinar in complex behaviors.

1.1.3 Neural mechanisms of pulvinar's cortico-thalamic-cortical connections

Given that there are several input sources to the dorsal pulvinar, this raises the possibility that a variety of information is transmitted from the cortex to the pulvinar. Studies highlight the pulvinar's extensive and reciprocal anatomical connections to subserve the integration and modulation of cortical information depending on the behavioral context (e.g., Benarroch, 2015; Saalmann & Kastner, 2011). In my view, we need to consider more essential details about these interconnections, such as the density of nerve fibers, overlapping projections, and their synaptic characteristic, to better understand how pulvinar acts as a hub of transthalamic corticocortical communication.

The dorsal pulvinar has a patchy distribution of cortical terminals, leading to the proposition of a mosaic organization of afferents to the dorsal pulvinar. In the previously outlined classification of anatomical connections, it was emphasized that these cortical connections of the dorsal pulvinar are reciprocal. However, the relative density of nerve fibers that runs from the dorsal pulvinar towards the cortex (corticopetal) compared to nerve fibers that originate in the cortex (corticofugal) varies. For example, the anterior part of the temporal cortex has a reciprocal connection with the medial pulvinar. Still, medial pulvinar projections to the anterior part of the temporal cortex (corticopetal) were denser than the corresponding corticofugal projections (Romanski et al., 1997).

Similarly, the granular insular cortex was more densely labeled with terminals from neurons originating in the medial pulvinar. In contrast, the dysgranular proportion of the insula had more neurons connecting to the medial pulvinar (Romanski et al., 1997). Finally, the caudal superior temporal sulcus, the superior temporal gyrus, the posterior cingulate cortex, and the inferior parietal areas show balanced reciprocal afferent and efferent projections to the medial pulvinar.

In addition to the density of nerve fibers, the specific location in the nuclei varies; for example, two distinct areas of the posterior parietal cortex, the lateral intraparietal area (LIP) and area 7a, receive the majority of their thalamic input from distinct zones within the dorsal pulvinar (Shipp, 2003). Although both nuclei are adjacent areas in the posterior parietal cortex, they participate in

recognizably different cortical circuits. Notably, while the dorsal part of the medial pulvinar has dense interconnections with area 7a, the connections to areas LIP span the junction of the lateral pulvinar and medial pulvinar (Asanuma et al., 1985; Hardy & Lynch, 1992). The interaction between the FEF, LIP, and dorsal pulvinar is critical for attentional and visuospatial decision-making. Yet, the possible underlying computations about the convergence of the signal and its modulation are unknown.

In addition to the cortical inputs, the medial pulvinar also receives subcortical inputs from the non-retinorecipient deep layers of the superior colliculus. It also receives minor input from the superficial layers of the superior colliculus and brain stem nuclei that include the nucleus of the optic tract and the lateral terminal nucleus (Baldwin et al., 2011; Benevento & Fallon, 1975; Benevento & Standage, 1983; Elorette et al., 2018). Unlike the other pulvinar nuclei, the medial part of the medial pulvinar projects to the anterior region of the lateral nucleus of the amygdala (Aggleton et al., 1980; Elorette et al., 2018; Jones & Burton, 1976; Romanski et al., 1997). Several studies suggested dorsal pulvinar involvement in arousal-related emotional processing (Maior et al., 2010; Rafal et al., 2015; Van Le et al., 2013) and a subcortical route rapidly transferring information from the retina to the amygdala without interferences. The possibility of dorsal pulvinar participating in this subcortical pathway has been debated (Bertini et al., 2018; Pessoa & Adolphs, 2010), and the open question remains whether the projection from the superior colliculus and the projection to the amygdala in the dorsal pulvinar overlap.

What is the essential synaptic organization of the cortico-thalamic projections to be the anatomical foundation for the pulvinar role in integrating, mediating, and modulating signals between cortical areas? A characteristic synaptic organization of these cortico-thalamic projections has been identified. Like other thalamic relays, the medial pulvinar receives cortical inputs predominantly from neurons located in cortical layer 6, with other weaker projections arising from neurons in layer 5 (Homman-Ludiye & Bourne, 2019). From the somata of medial pulvinar neurons, moderate numbers of primary dendrites extend a short distance before branching into many secondary branches. Two distinct cell types for cortical-thalamic projections were identified based on the diameters of their dendritic tree in macaque and squirrel monkeys (Ma et al., 1998). The first type of afferents originates from giant cortical-layer-5 pyramidal cells, which are directly excitatory (or driving). The second afferent cell type has small to medium synaptic terminals mainly originating in cortical-layer six cells that might be modulatory. Although it has been suggested that these distinct projections have different functional influences on the thalamus, it has not been directly tested until recently.

This principle is also confirmed for the ventral pulvinar, where afferent connections of early visual brain areas to the ventral pulvinar originate in layer 5 of V1 with excitatory influence (Bourassa et al. 1995). Neurons originating in layer 6 of V2 are thought to modulate information processing between visual areas (Saalmann & Kastner, 2011, Saalmann et al., 2012). Notably, the afferents from the prefrontal cortex originate from layer 6 to the medial pulvinar, which is different for the insula, the parietal, and temporal cortices, where the afferents originate from layer five and layer 6 (Romanski et al., 1997). In particular, the pulvinar relay cells transmit the already processed message of the cortex to other cortical regions depending on the influence of their modulators.

All in all, the cortical and subcortical projections, in combination with their synaptic structure in the pulvinar, suggest that the pulvinar has the potential to converge corticothalamic projections and regulate information flow between cortical and also subcortical regions. Thus, the dorsal pulvinar can transfer crucial behaviorally relevant information from the sensory cortex to higher-order cortices that differentiate the dorsal pulvinar from other thalamic nuclei.

1.1.4 The pulvinar – is it a higher-order thalamic relay or a connector hub?

The pulvinar had been classified as a higher-order thalamic relay according to the criteria outlined by Sherman and Guillery in several research articles and books. Still, it is better described as a connector hub for the communication between networks (Bridge et al., 2015).

The core of the classification for low- and higher-order thalamic relays was solely based on the source of their inputs. Higher-order relays receive their driving input from layer 5 of the cortex, and low-order relays receive their driving input from subcortical sources, such as the retina. It was hypothesized that the source inputs of a thalamic nucleus determine which information is relayed and modulated, hinting toward its functionality. This classification scheme for the thalamus had been mainly inferred from the lateral geniculate nucleus as the best-studied thalamic structure that receives visual information from the retina and projects to the primary visual cortex (Sherman, 2017; Sherman & Guillery, 2002). The LGN's structural and functional features were used to interpret data from other thalamic structures. Pulvinar cortical afferents, their overlapping projection zones, and their specific properties, as outlined in detail, classify all pulvinar subnuclei accordingly as higher-order thalamic nuclei (Kanai et al., 2015).

This classification as a higher-order thalamic relay has several limitations. For example, the anatomical connections of the dorsal pulvinar include subcortical and limbic structures, which question the classification scheme focusing solely on cortical connections. And the excitatory inputs of different thalamic nuclei vary (Rovo et al., 2012), as described in more detail in the

previous section on the pulvinar. Halassa & Sherman (2019) state that the conclusion raised from studying the lateral geniculate nucleus (LGN) as an example for understanding the involvement of the thalamus in cognition is limited. They suggest convergence [2] as another crucial feature(Byrne, 2013) to distinguish between distinct thalamic nuclei and their involvement in circuits (Halassa & Sherman, 2019). For example, the retinogeniculate synapses share basic receptive field properties and show little convergence of driver inputs meaning that the transformation of information passed on to the cortex is limited.

While the structural connectivity is relatively fixed, a significant modification of information due to convergence from different cortical areas onto single thalamic neurons is possible, as shown on the rodent somatosensory thalamus (Groh et al., 2014), and might depend on behavioral demands. In this regard, the dynamic synaptic connectivity might vary as a function of different strengths and weights of the inputs and behavioral demands. Some evidence about the degree of cortical input convergence onto single thalamic neurons and its link with cognitive processing can also be inferred from specifically designed functional studies (Berman & Wurtz, 2011; Rikhye et al., 2018; Zhou et al., 2016). The recent literature about integrating sensory and cognitive signals in the pulvinar has been summarized by Bridge and colleagues (2015). Still, many open questions remain. How do pulvinar neurons converge cortical and subcortical inputs to be involved in the different circuits related to arousal-related emotional, visual oculomotor, and attentional processing? How are these multisensory signals integrated on the neuronal level with either overlapping projections from different brain regions on a single neuron or a group of neurons with interconnections inside the pulvinar? And what is the underlying neural mechanism of the pulvinar in the thalamocortical system that the signal of some inputs strengthen to mediate and regulate the cortical information transfer?

[2] Convergence allows a neuron to receive inputs from many neurons in a network (Byrne, 2013).

1.1.5 Debate about the functional specialization of the pulvinar complex

So far, I have described that the pulvinar complex is heavily interconnected with multiple cortical and subcortical areas and can be differentiated accordingly into a dorsal and ventral part. The heterogenetic connectivity profile positions the different subnuclei of the pulvinar complex in unique positions to integrate diverse information and regulate the cortico-cortical transmission according to behavioral context (Shipp, 2003). Despite the topographic properties of the thalamocortical network and the functional role of the cortical-thalamic-cortical regulation and transmission of signals being largely unknown, it is clear that pulvinar as higher-order thalamic nuclei participates in information transfer with multiple cortical functional networks (Hwang et al., 2017). Some broad agreement about the functions of the pulvinar complex exists that are summarized and discussed in reviews focusing strongly on the pulvinar's contribution to visual, visuomotor, or attentional processing, as well as its contribution to integrating converging and diverging cortical and subcortical information (Bourgeois et al., 2020; Bridge et al., 2015; Grieve et al., 2000; Kaas & Lyon, 2007; Robinson & Petersen, 1992; Saalmann & Kastner, 2011). Nevertheless, it has been proven difficult to define a specific and distinguishable role of the different sub-nuclei of the pulvinar complex in perception and cognition. Even it has been stated that the pulvinar's functional role has remained elusive (Bridge et al., 2015; Fiebelkorn & Kastner, 2019).

In contrast to these statements stands the summary of the research on the primate pulvinar related to the function of the pulvinar in perception and cognition presented in the next section of this dissertation. Its primary focus lies in non-human primate pulvinar and important lesion studies in patients encompassing the pulvinar. The summary hints that the pulvinar might have more than one functional role related to the different behavioral demands of the environment and the functional connections to different neural circuits, such as the spatial attention network or the central autonomous network. However, an overarching theory is still missing that explains how these various functions of the pulvinar are united into a model with specific assumptions that can be further tested.

Like other thalamic nuclei, the pulvinar contains two main populations of neurons; glutamatergic thalamocortical projection neurons (also called thalamocortical relay cells) and local gamma-aminobutyric acid (GABA)ergic interneurons (also called Golgi type II neuron). The properties of these neurons in the pulvinar were measured as voltage changes (action potentials) using single-unit recordings in non-human primates. At the same time, they were either anesthetized, awake, or performing a task. The findings of the studies are described in the following. The first electrophysiology study systematically investigated the neuronal activity of the primate pulvinar recorded in anesthetized squirrel monkeys in lateral, inferior, and medial pulvinar, showing the three subdivisions of the pulvinar have contralateral visual receptive fields (Mathers & Rapisardi, 1973). Most pulvinar neurons respond phasically to the onset of contralateral presented visual stimuli, show broad tuning to object orientation, and weak directional preference for moving stimuli (Petersen et al., 1985). Neural activity in the pulvinar is related to eye and reach movements towards an object with behavioral significance or visual fixation of such objects (Acuna et al., 1983, 1990; Cudeiro et al., 1989; Magariños-Ascone et al., 1988; Perryman et al., 1980; Robinson et al., 1990; Yirmiya & Hocherman, 1987). Evidence from early electrophysiology studies supports that visual and oculomotor signals converge within the neural activity of the pulvinar neurons and that the pulvinar is primarily devoted to visual processing (Grieve et al., 2000).

In particular, the neuronal properties, such as the receptive fields of the ventral pulvinar, seem to reflect its cortical input. The receptive fields of ventral pulvinar neurons (encompassing inferior pulvinar and ventral part of lateral pulvinar) are arranged in precise retinotopic maps of the visual field that agree with their anatomical connections to cortical neurons in the early visual cortices (diffusion tractography in humans: Arcaro et al., 2015; in monkeys: Bender, 1988). The inferior pulvinar receives projections from the retina, the superior colliculus's superficial layer, and projects to the cortical area MT that carries saccadic suppression signals (Berman & Wurtz, 2011). Ventral pulvinar neurons show mainly responses during or after the saccade (Berman & Wurtz, 2011; Petersen et al., 1985; Robinson et al., 1986), and its neurons exhibit response modulation by eye position (Robinson et al., 1990), that has been recently also confirmed for the dorsal pulvinar (Schneider et al., 2019). In contrast, the neurons in the dorsal pulvinar do not show a clear retinotopic organization (Benevento & Miller, 1981; Benevento & Port, 1995; Petersen et al., 1987). Some neurons in the dorsal pulvinar respond to eye movement, encode the static eye position, and combine spatial encoding in eye-centered and non-retinocentric coordinates (Schneider et al., 2019). Still, they are crudely tuned for saccade direction and amplitude.

While the dorsal pulvinar is not retinotopically organized, its neurons have large receptive fields and exhibit space-specific visual, visuomotor, and motor enhancement responses (Schneider et al., 2021). The same neurons respond to visual cues during saccade execution phases in visual saccade task, exhibiting an overall preference for a contralateral visual cue, peri- and post-saccadic responses. Similar response properties of the neurons related to eye movements were also reported in the frontal eye field and the parietal cortex, anatomically connected with the pulvinar (Acuna et al., 1990). The neural properties of dorsal pulvinar neurons in non-human primates partially resemble its reciprocal connection with the cortex, such as the parietal cortex. For example, enhancement for visual stimuli indicates an upcoming saccade target (Robinson, 1993).

Furthermore, the neurons in the dorsal pulvinar respond to visual, auditory, and/or somatosensory stimulation (Gattass et al., 1978; Yirmiya & Hocherman, 1987). In addition, the neural activity in the pulvinar is modulated by the arousal level, and a consistent physiological response of neurons in the pulvinar occurs only when the visual stimulus serves as an immediate saccade target (Bender, 1982; Bender & Youakim, 2001; Gattass et al., 1978, 1979; Yirmiya & Hocherman, 1987).

Some dorsal pulvinar neurons exhibit modulation to two important cues for social behavior, face orientation and gaze direction (Nguyen et al., 2013). Some visually responsive dorsal pulvinar neurons responded to facial expressions of humans, either with a short latency (<100ms) or long (>300ms). In addition, evidence from single-unit activation in medial and lateral pulvinar (Maior et al., 2010) supported findings from patients (Ward et al., 2005, 2007) that neural activity in the pulvinar is related to recognizing fearful faces. Although the existence of an anatomical path to rapidly transferring information from the retina to the amygdala without interference has been heavily criticized (Pessoa & Adolphs, 2010, 2011), evidence is converging from tracer studies in non-human primates (Baldwin et al., 2011; Benevento & Fallon, 1975; Elorette et al., 2018) and diffusion-weighted imaging in human (Kragel et al., 2021; McFadyen et al., 2019; Rafal et al., 2015) about overlapping anatomical connections between the superior colliculus, pulvinar, and amygdala. Additional evidence was provided by a study of hemianopic patients with pulvinar lesions, where implicit processing of fearful stimuli was perturbed compared with hemianopic patients without a pulvinar lesion (Bertini et al., 2018). The dorsal pulvinar is linked to arousal-related emotional processing and multisensory integration (Froesel et al., 2021; Gattass et al., 1978; Vittek et al., 2022). By describing the variety of responses of neurons in the dorsal pulvinar,

the reader can anticipate the variety and possibilities for the discussed functions relating to the role of the pulvinar in perception and cognition.

A recurrent theme regarding the function of the pulvinar is its role in selective attention. Selective attention is a cognitive function that guides behavior by selecting and prioritizing relevant or salient sensory information. Acuna and colleagues stated already 1983 that pulvinar neurons reliably respond to intentional or attentional behaviors, which, therefore, can be utilized as states to control the activity of pulvinar neurons (Acuna et al., 1983). Attentional spatially selective modulation occurred in the dorsal pulvinar and (rarely) in the ventral pulvinar (Bender & Youakim, 2001; Fiebelkorn et al., 2019; Petersen et al., 1985; Robinson et al., 1986; Robinson & Petersen, 1992). The role of pulvinar in selective attention is further supported by studies in human patients with unilateral thalamic lesions, including the pulvinar, demonstrated deficits in orienting or responding to visually or behaviorally salient stimuli in the contralesional hemifield (Arend, Machado, et al., 2008; Arend, Rafal, et al., 2008; Danziger et al., 2001, 2004; Karnath et al., 2002; Lucas et al., 2019; Snow et al., 2009). These findings are in partial agreement with monkey lesion studies that can specifically target the pulvinar and its distinct subnuclei, showing a contralesional visuospatial deficit after unilateral pharmacological inactivation or electrical microstimulation of the dorsal pulvinar (Desimone et al., 1990; Dominguez-Vargas et al., 2017; Komura et al., 2013; Petersen et al., 1987; Wilke et al., 2010, 2013).

Such visuospatial deficits can manifest behaviorally in several ways. One possible manifestation is that the inactivation causes impairment of spatial attentional orienting to cued targets in contralesional hemifield, decreasing performance in a detection task or a color discrimination manual response tasks (Desimone et al., 1990; Petersen et al., 1987). The ventral pulvinar has no direct anatomical connections to the parietal and prefrontal cortex Feld (Baizer et al., 1993), but the visuospatial deficits are similar to the dorsal pulvinar. Notably, by recording simultaneously in the ventral pulvinar, extrastriate cortex (V4), and inferior temporal cortex (IT), Zhou and colleagues confirm that neurons in the ventral pulvinar have sensory properties similar to those of neurons in V4 and the effects of attention were weaker and later in the ventral pulvinar than V4 (Zhou et al., 2016). After suppressing the neural activity in the ventral pulvinar pharmacologically, visual responses in V4 changed even below the level typically found without attention. Together these findings suggest that the ventral pulvinar relays mainly sensory information and is not modulating cortical responses according to attentional demands because the attentional latencies of the pulvinar occur not earlier than in V4. Unlike in the ventral pulvinar, the firing rate of FEF

neurons in a visual search task is strongly modulated by attention, and this modulation occurs significantly earlier than in V4 (Zhou & Desimone, 2011).

In contrast to the ventral pulvinar, it was proposed that the dorsal pulvinar has a more similar role in attention to the posterior parietal cortex according to the attentional impairments after inactivation. Dorsal pulvinar's bidirectional connectivity with higher-order cortical regions, including the frontal eye fields (FEF) and the lateral intraparietal area (LIP) (Gutierrez et al., 2000; Hardy & Lynch, 1992; Romanski et al., 1997; Selemon & Goldman-Rakic, 1988), suggest a unique position for integrating and regulating cortical interaction in the attention network. An electrophysiology study shows the increased coupling between mediodorsal pulvinar with FEF and LIP during spatial attention (Fiebelkorn et al., 2019). In particular, mediodorsal pulvinar regulates cortical activity during an engagement at the attentional location related to enhanced perceptual sensitivity. LIP regulates thalamic activity during the non-engaged periods related to diminished perceptual sensitivity. The contradictory evidence for the involvement of the pulvinar in attentional processing is sparse and restricted to one study where after lesioning the ventro-lateral pulvinar, no effect on attentional performance in a visual search task was observed (Bender & Butter, 1987). The pulvinar complex is part of multiple functional circuits, transmitting and regulating bottom-up and top-down sensory information to the many sensory, associative, and subcortical areas.

Another behavioral manifestation of the visuospatial deficits after unilateral perturbation of the pulvinar is that the inactivation causes a target selection bias away from contralesional hemifield, which was observed in the free-choice saccade task (Wilke et al., 2010, 2013). Such inactivation-induced bias could be alleviated by presenting only a single target or increasing the reward for contralesional targets but less so by perceptual saliency manipulations (Wilke et al., 2013). Based on these findings that inactivation of the dorsal pulvinar impairs target selection, it could be inferred that the dorsal pulvinar is involved in transforming the sensory inputs to making a choice by integrating and prioritizing information to enable goal-directed action (Phillips et al., 2021). However, no spatial choice selectivity for the upcoming saccade was found for the dorsal pulvinar, neither in the delay nor in pre-saccadic activity or on the population level in a memory-guided saccade task (Schneider et al., 2021). In this study, the delay period activity was mainly characterized by a gradual suppression of firing relative to the initial fixation period. Only a small subset showed classical sustained or ramping up activity enhancement in the delay period and before performing the action to indicate the selection, frequently observed in frontoparietal areas, such as LIP and FEF. These different functions of the dorsal pulvinar are not mutually exclusive

and could depend on other behavioral, psychological, and physiological demands and their related neural circuit. Dorsal pulvinar neurons represent perceptual confidence during visual categorization (Komura et al., 2013). The pulvinar contributes to sensory detection and selection by processing sensory inputs related to emotional values, intrinsic salience, and extrinsic behavioral relevance. In this case, the dorsal pulvinar might weigh and prioritize information based on the reliability of sensory evidence (Phillips et al., 2021). This computation would be useful for attentional prioritization, multisensory integration, selective attention, and perceptual decision-making.

1.2 Perceptual decision-making

The long-standing interest of neuroscientists in the neural mechanism of decision-making gained even more attraction 30 years ago with flourishing research on perceptual decision-making, e.g., Hanks & Summerfield, 2017). Perceptual decision-making is defined as a cognitive process that uses sensory information to guide behavior in relationship to the external world by gathering information through the senses, evaluating and integrating it according to the subject's current goals and internal state, and finally, using the accumulated knowledge to produce motor responses (Hauser & Salinas, 2014; Kelly & O'Connell, 2015). The main difference between value-based and perceptual decision-making is that the latter relies on decisions about sensory properties, while the former use sensory properties to infer associated values. Notably, most perceptual decisions in animals (who work under a positive reinforcement schedule) also have value-based components because typically, only a "correct" response is rewarded (Schultz, 2015).

Perceptual decisions are decisions typically made in the presence of perceptual uncertainty. If we want to measure and understand how we decide under conditions of uncertainty, a common framework is the Signal detection theory (Stanislaw & Todorov, 1999). The goal of the Signal detection theory is to estimate two main parameters. The first parameter, dprime, indicated how well signal and noise could be discriminated. The second parameter, called criterion, reflects the response strategy of the participant. To apply Signal detection theory, the data are categorized to where stimuli were either present or absent in relation to the categorization of the participant as having the stimulus present or absent, resulting in four categories: hits as correct detected present stimulus, miss, as not detected presented stimulus, correct rejection as correct notice of the

absent of a stimulus and false alarms as wrongly detected absent stimulus. The Signal detection theory is broadly applied to study decision-making under various uncertainties.

One widely used category of a psychophysical task to investigate perceptual decision-making is the two-alternative forced-choice task (2AFC). In a perceptual variant, the participant is presented with noisy stimuli. The participants must integrate and evaluate the available sensory information to report their perceived response according to the rules of the task by making a pre-defined motor response. The two-alternative forced-choice task can be adapted to specific research questions. There are four classical psychophysical approaches to investigating decision-making under sensory uncertainty. Each approach can be characterized by an elementary question that can be asked about the magnitude of a sensation (Hauser & Salinas, 2014).

The work presented in this dissertation uses a novel variant of the perceptual discrimination task. In the following, I will outline the two standard perceptual decision tasks, the classical random dot motion discrimination task and the visual search task. In particular, I will emphasize studies where these tasks had been used to investigate the function of the pulvinar. Afterward, I will describe our color discrimination task to explain why this task was chosen to study perceptual decision-making in the dorsal pulvinar.

1.2.1 The core ideas of the two standard perceptual decision tasks

One of the most studied two-alternative forced-choice (2AFC) tasks is the random dot motion discrimination task (Newsome & Pare, 1988). Its visual stimulus is the random-dot pattern (RDP) consisting of a cloud of dots in which a certain percentage of these dots move coherently in a given, fixed direction. In contrast, the remaining dots, presented simultaneously, are moving in random directions. The signal decreases with a lower rate of dots moving coherently, and sensory uncertainty increases. The participants indicated which of two possible motion directions they perceived by responding to one of the two choice targets associated with the two possible movement directions. The difficulty of the perceptual judgment can be tightly controlled by varying the coherence, i.e., the percentage of dots that move together.

The random-dot motion discrimination task has rarely been used in research on the pulvinar. In one study, Komura and colleagues used a random dot motion discrimination task where the monkey indicated whether the dots moved downwards or upwards from the previously cued colored dots; in the absence of competing distractors in the opposite hemifield (Komura et al.,

2013). Additionally, two studies investigating the functional pathway starting from the superficial layers of the superior colliculus through the inferior pulvinar to cortical area MT used a random dot pattern to map the receptive field and determine directional tuning for each pulvinar neuron (Berman & Wurtz, 2008, 2010).

Another widely used psychophysical task is the visual search task (see reviews, Chan & Hayward, 2013; Eckstein, 2011). To select objects we are interested in, we first need to search where they are. Visual search requires judging whether a currently viewed object matches an internal representation of the target, which necessitates discriminating specific object features and the orienting in space. The visual search task involves actively scanning the visual environment to locate a predefined target (object or feature) among other behaviorally irrelevant non-targets (distractors). The most straightforward version consists of a target standing out from a group of constant stimuli, often described as the “pop-up” phenomenon. However, more objects or/and more features make the visual stimulus noisier and the visual search more complex, resulting in an N-alternative choice task, except for the “pop-up” version. Usually, participants search until they are confident of a decision. The visual search task has been used as an experimental paradigm with diverse minor adjustments to study the pulvinar contributions to visual attention, mainly in humans (Bender & Butter, 1987; Lucas et al., 2019; Strumpf et al., 2013; Van der Stigchel et al., 2010).

The match-to-sample task can be considered a specific variant of the visual search paradigm with trial-by-trial target instruction. The match-to-sample task assesses the ability to judge whether a sensory stimulus matches an internally represented pattern, e.g., Moreira et al., 2018. The typical trial of the task begins by presenting a participant with a visual stimulus (target) known as the sample that needs to be remembered. After a delay, the participants must identify and indicate which test stimulus matches the previously shown sample stimulus from a subsequent set of stimuli. The match-to-sample task is also frequently used to investigate memory processes by varying the delay time between the sample and the test stimulus.

A related variant of the above psychophysics task is the color-based perceptual decision task, where colored objects must be compared to and discriminated from a previously indicated target color. When the target and “distractor” (i.e. non-matching color) are very similar or presented very briefly, this becomes a difficult perceptual discrimination task that requires attentional allocation. When and how the information about the target is presented to the participant leads to different versions of the task. One variant was used to investigate the functions of the pulvinar by combining perceptual and attentional components by Desimone et al. (1990). The attentional task

features are related to the original spatial cueing task or Posner task (Posner, 1980). In the initial Posner task, a valid cue is presented in the exact location or same hemifield as the subsequent target, and in the case of an invalid cue, it is shown in the opposite hemifield. The target properties are usually known to the participants before. Participants must respond to the target immediately after discrimination/detection by either making a saccade to the target or pressing a corresponding button. The success rate and the response reaction times can be analyzed.

The cue itself does not provide information about the correct response. To dissociate the effects of eye movements and attentional processing, participants must usually fixate on a fixation spot in the middle of the screen during the presentation of the cue. The original study used 80% valid to 20% invalid cues. The primary and often replicated effect is that valid cues lead to faster response times, and invalid cues lead to slower responses than when there is no or a neutral cue. Numerous studies conducted in recent decades have used the Posner spatial cueing paradigm for eliciting, measuring, and characterizing attentional orienting in space (Caldani et al., 2020; Doricchi et al., 2010). The initial spatial cueing task is a detection task. Suppose another stimulus is presented at a different location but still simultaneously with the target. This stimulus is either behaviorally relevant where the target and the additional stimulus need to be discriminated, or the stimulus is irrelevant (distractor) and must be ignored.

The Posner task had been used with and without a distractor to investigate attentional processing by either recording from or to inactivate the dorsal pulvinar in monkeys (Petersen et al., 1987) or examining the behavior of patients with thalamic lesions encompassing the pulvinar (Rafal & Posner, 1987). The combination of the Posner task with the color discrimination task was used by Desimone et al. (1990), who called their task ‘color discrimination task with a spatial attentional cue’. A shortly presented spatial signal not only cues the target's spatial location but also indicates which stimulus is the target. The target was the stimulus presented at the exact location at the cue, and the animals had to indicate the target's color using a lever (Desimone et al., 1990). The task was utilized with and without a distractor color. In the distractor condition, the cue was followed by two differently colored stimuli, one of which (cued) was the target and one a distractor. This study is essential for the presented work in Chapter 2 and Chapter 3 of this dissertation because it also supports the idea that the dorsal pulvinar is involved in resolving the spatial competition when multiple response options compete against each other. At the same time, information is collected to bias this competition between representations at different levels of neuronal processing until one option is selected.

1.2.2 Color discrimination saccade selection task

The core idea of the color discrimination saccade selection task I used in my thesis is to respond according to the following predefined and learned rules. The visual stimulus, such as a red dot, indicates that a saccade must be made to the dot to gain a reward. Yellow and orange dots (easy – yellow, difficult - orange) represented visual stimuli to continue fixating when only distractors (s) were presented. Thereby, all stimuli were behaviorally relevant. Despite their behavioral relevance, the yellow and orange stimuli, indicating that there is no target for a saccade, are called distractors in the following for easy reference. The level of sensory uncertainty (perceptual difficulty) was determined by the color similarity of the target (T, red) and the distractor (D, easy – yellow, difficult - orange).

Both stimuli were presented alone or with a second stimulus (saccade-target or distractor) in the opposite hemifield, determining the level of spatial competition —these resulted in three main stimulus conditions, single stimuli, double stimuli same, and double different stimuli. In conditions with a single peripheral stimulus, either one stimulus (target) requiring a saccade or distractor requiring to continue central fixation was presented in the left or the right hemifield. The participants were shown two dots in opposite hemifields in the condition with two peripheral stimuli. Two equally rewarded saccade targets were presented in double-target trials, and the monkey could choose either for the response. The two distractors with identical colors were shown in double distractor trials, requiring maintaining central fixation. In trials where a saccade target and distractor were presented simultaneously in opposite hemifields, the subject must make a saccade to the red dot (target) and ignore the other stimulus. The current task is based on the classical visually-guided (direct) saccade task, where the appearance of a target and simultaneous disappearance of the fixation point instructs the monkey to make an immediate (within allotted reaction time, typically 500 ms) saccade.

Further studies added two equally rewarded targets presented in opposite hemifields to study value-based decision making and visuomotor functioning in the pulvinar. This two-target free-choice version was either a visually-guided saccade task, or a memory-guided saccade small or large reward was utilized (Dominguez-Vargas et al., 2017; Schneider et al., 2021; Wilke et al., 2010, 2013). In these studies, a peripheral saccade response was always required, and no difficult perceptual discrimination was involved.

To add a perceptual discrimination component, the color similarity of the distractor to the target was introduced, creating sensory uncertainty between the target and distractors. Furthermore, an

additional response option, central fixation, needed to be added as the correct response for the distractor(s) trials. This new color discrimination task involves specific contextual demands to investigate the possible functions of the dorsal pulvinar, perceptual decision making, and spatial orienting. The task demands are fast perceptual color discrimination between target and distractor, varying perceptual difficulty related to the color of the distractor, spatial competition between stimuli (either between two peripheral stimuli or between central fixation and peripheral stimulus), and stimulus-congruent saccade responses. The target colors were either red or yellow or green or blue. The distractor was colored randomly or consistently a different color from the target. The reported level of performance at baseline is around 90% or higher, indicating that this color discrimination task was easy to perform correctly for the animals.

The ability to correctly discriminate competing stimuli and initiate contextually appropriate behaviors is a crucial feature of our variant of color discrimination to investigate the role of dorsal pulvinar in perceptual decision-making. Multiple response options compete against each other, while information is collected to bias this dependency between multiple representations until one option is selected with an action (Cisek, 2006). Our findings confirm that dorsal pulvinar is involved in the spatial competition related to the inactivation-induced effect in the results of the single stimulus condition compared to the null effects for the single target condition in Wilke et al. (2010). Hence, dorsal pulvinar inactivation impairs the representation and/or selection of contralesional targets under spatial competition, that is, when a response to a contralesional stimulus must be activated in preference to a conflicting ipsilesional or central presented response option. Support also comes from a one monkey case in Desimone et al. (1990), where both target and the conflicting stimulus (distractor) were placed in the same visual field leading to no spatial competition between hemifields and no significant effect of pulvinar inactivation on performance was observed. These findings suggest that the pulvinar plays a critical role in target selection under competition between hemifields. Desimone & Duncan (1995) proposed interpreting their findings after unilateral pulvinar inactivation as formulated in the biased competition theory. In this theory, unilateral dorsal pulvinar inactivation puts the contralesional hemifield at a disadvantage for selection by biasing the ongoing competition for the neuronal representation of multiple stimuli leading to the observed bias “away from contra”. They claim that pulvinar resolves the competition for the neural representation of multiple stimuli by two proposed neural mechanisms enhancing target representations and filtering out distracting stimuli. So, neural representations of multiple stimuli also compete for attention. When various stimuli compete for attention, attending to one option biases the competition by enhancing the neuronal activity representing this response

option within their receptive field. Selective attention can bias the competition via bottom-up and top-down mechanisms (Beck & Kastner, 2009; Markowitz et al., 2011)

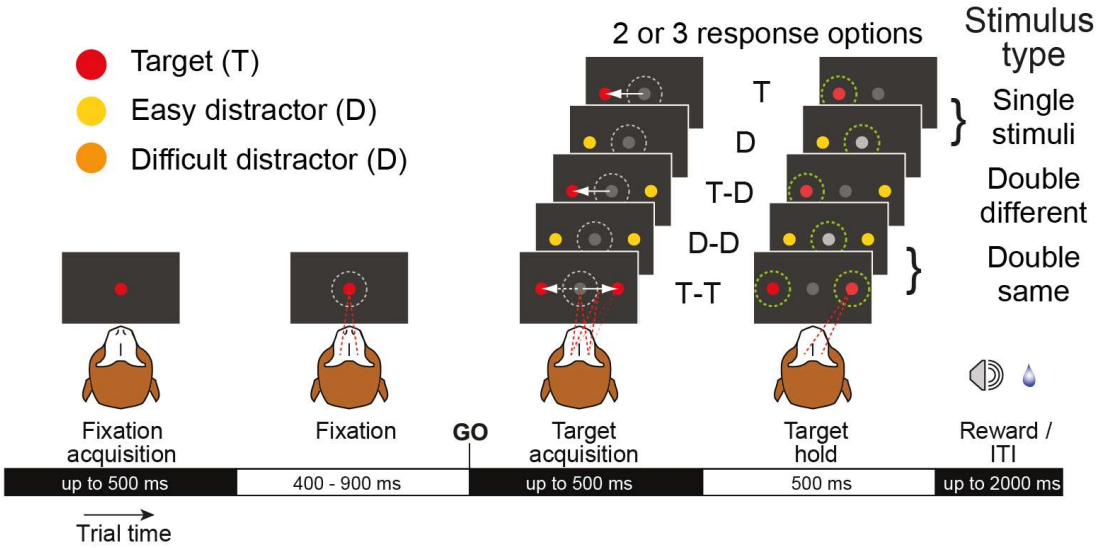

Figure 1.1. Task design. Two monkeys performed a color discrimination task where the perceptual difficulty was determined by the color similarity of the target (T, red) vs. distractor (D, easy - yellow, difficult - orange). Target or distractor was presented alone or with a second stimulus (distractor or target) in the opposite hemifield. Monkeys had to saccade to the target and continue fixating when only distractor(s) were presented.

Table 1.1. Relationship between stimulus conditions and the features of the color discrimination task.

Trial type	**Stimuli**	**Reward for …**	**Discrimination to from …**	**Spatial competition between …**
Single stimuli	one target	Selection of target	Memorized representations of the target or/and distractor	one hemifield & fixation
	one distractor	Fixation		one hemifield & fixation
Double same stimuli	two targets	Selection of one of the targets		two hemifields
	two distractors	Fixation		two hemifields
Double different stimuli	one target and one distractor	Selection of target	Memorized representations or the stimulus presented in the opposite hemifield	two hemifields two hemifields

1.3 Research rationale of the dissertation

The main research questions of this dissertation are:

- What are the visuospatial and perceptual effects after causally perturbing the dorsal pulvinar in the context of perceptual uncertainty and spatial competition?
- Is there a relationship between cardiac, respiratory and neural activity in the dorsal pulvinar?

For each research question, a suitable organism must be carefully chosen to investigate the underlying neural processes of interest and generalize the findings. The first stated research question involves complex cognitive abilities, where humans might be the most appropriate organism to study decision-making under perceptual uncertainty. Still, this research also aims to investigate the underlying neuronal mechanisms of perceptual decision-making where using healthy human subjects is considered ethically unjustifiable, with some exceptions. Given the invasive experimental procedure necessary to investigate a thalamic nucleus lying deep inside the brain combined with demanding cognitive behaviors, such as decision-making, pointed clearly to the rhesus monkey as an optimal model organism to investigate these research questions.

Although the view of the thalamus as a passive relay of sensory information to and across the cortex is obsolete, more evidence for the central role of the thalamus in integrating and actively regulating signal transmission related to cognition is still needed to test the generality of this hypothesis. In addition, the involvement of the thalamus in the cardiovascular system was suggested as early as 1891 (Ott, 1891). Still, the contribution of higher-order thalamic nuclei to autonomic control of sensory and cognitive processing remains unclear. The dorsal pulvinar is a well-suited candidate region to investigate further the thalamus's integrative function in cognition and perception. The pulvinar complex participates in information transfer with multiple cortical functional networks, such as the central autonomous network (CAN) or multisensory networks (Bridge et al., 2015; Froesel et al., 2021; Shipp, 2003). The dorsal pulvinar is interconnected with the parietal and prefrontal cortex, orbitofrontal cortex, insula, cingulate, and superior and inferior temporal cortex. Current evidence points that afferents from the deep layer of the superior colliculus co-localize with projections to the amygdala (Benevento & Standage, 1983; Elorette et al., 2018; Romanski et al., 1997). This specific connectivity profile of the dorsal pulvinar, including cortical and subcortical regions, identifies the dorsal pulvinar as a unique thalamic nucleus

interacting with the circuitry related to selecting behaviorally relevant stimuli and with the central autonomous network. Thus, the dorsal pulvinar can integrate processed complex sensory inputs from the cortex with limbic influences and transmits this information to the cortex or the amygdala.

The role of dorsal pulvinar in perceptual decision-making. In particular, the connectivity with the frontoparietal cortex, specifically FEF and LIP (Hardy & Lynch, 1992), identifies the dorsal pulvinar as a suitable thalamic hub to interact with and modulate the circuitry involved in spatial attentional orienting and selection of behaviorally salient stimuli (Bourgeois et al., 2020; Grieve et al., 2000; Kaas & Baldwin, 2020; Sherman & Guillery, 2002). Accordingly, studies in human patients with unilateral thalamic lesions, including the pulvinar, demonstrated deficits in orienting or responding to visually or behaviorally salient stimuli in the contralesional hemifield (Arend, Machado, et al., 2008; Arend, Rafal, et al., 2008; Danziger et al., 2001; Karnath et al., 2002; Lucas et al., 2019). These findings are in partial agreement with monkey lesion studies that can specifically target the pulvinar and its distinct subnuclei, showing a contralesional visuospatial deficit after unilateral pharmacological inactivation or electrical microstimulation of the dorsal pulvinar (Desimone et al., 1990; Dominguez-Vargas et al., 2017; Komura et al., 2013; Petersen et al., 1987; Wilke et al., 2010, 2013). Previous work on pulvinar focused mainly on attentional processing or oculomotor behavior and neglected the effect of perceptual factors such as the perceptual difficulty of a decision in conditions of spatial competition on goal-directed behaviors. Therefore, it remains unclear whether the perturbation of the dorsal pulvinar during perceptual decision will lead to perceptual impairment or a more general orienting deficit. To address this research gap, the two studies in this dissertation used a color discrimination saccade selection task that included specific contextual demands – fast perceptual color discrimination between target and distractor (saccade-stimulus and fixation-stimulus), varying perceptual difficulty related to the color of the distractor, spatially competing between stimuli and stimulus-congruent saccade responses. The first study investigated whether unilateral dorsal pulvinar inactivation leads to a perceptual deficit or a spatial selection bias. In the second study, the results of the pharmacological inactivation study were complemented by resolving which processing stage pulvinar exerts its effect on perceptual decision-making by applying electrical microstimulation with the necessary temporal and spatial precision. The Signal Detection Theory dissociates the impact of perceptual discrimination (dprime) and spatial selection (response criterion). A decrease in dprime was expected if dorsal pulvinar affects perceptual discrimination and a shift in response criterion if dorsal pulvinar is mainly involved in spatial orienting.

The neural interaction of the dorsal pulvinar with the cardiovascular system. The dorsal pulvinar has reciprocal connections with all major nodes of the central autonomous network (amygdala, insula, cingulate and prefrontal cortex). This identifies the dorsal pulvinar as a well-suited candidate region to integrate neuronal signals from and to the autonomic nervous system. A consensus is yet to be reached, but the research converges on the conclusion that the dorsal pulvinar seems to be critical for the fast, subcortical processing of threatening information (Almeida et al., 2015; Bertini et al., 2018; Kragel et al., 2021; Maior et al., 2010; Soares et al., 2017; Van Le et al., 2013; Ward et al., 2005, 2007). The medial pulvinar is an area of overlapping projections that seems to connect the non-retinotopic layers of the superior colliculus with the amygdala (Benevento & Fallon, 1975; Elorette et al., 2018; McFadyen et al., 2019; Rafal et al., 2015; Romanski et al., 1997). However, whether the dorsal pulvinar generally affects the cardiovascular system beyond this specific emotional content remains unknown. Historically, Poirier and Schulmann (1954) stimulated the pulvinar's posterior part electrically, leading to respiratory arrest and blood pressure changes. This was supplemented by studies done in human patients that reported relationships between pulvinar damage and impaired oxygen regulation, or a reduction of gray matter volume of the pulvinar in patients with a high risk for sudden cardiac death (Rosenberg et al., 2006; Wandschneider et al., 2015; Woo et al., 2003).

Since disentangling the contribution of a specific brain region to cardiac activity is experimentally challenging in human patients, we first examined the impact of local reversible pharmacological inactivation of dorsal pulvinar on cardiac and respiratory activity in awake monkeys. The aim was to probe the causal relationship between the central autonomic system and the dorsal pulvinar. In a second experiment, we examined the neural activity of the dorsal pulvinar with extracellular recordings while recording cardiac and respiration activity simultaneously. The relationship between the firing rate of dorsal pulvinar neurons and the cardiac cycle was investigated and compared to the previously published cardiovascular-related neural activity in the ventral posterior lateral nucleus (VPL).

The studies presented in this dissertation on the dorsal pulvinar support the idea of co-localizing different functions in the dorsal pulvinar. The dorsal pulvinar has been suggested as a region of convergence through its overlapping interconnection with visual, auditory, and somatosensory cortices and premotor areas (Cappe et al., 2009). A recent review has presented the primary evidence supporting this hypothesis about the pulvinar's role in integrating sensory information from other modalities (Froesel et al., 2021). Furthermore, a recent study shows that dorsal pulvinar is implicated in multisensory integration, mainly sub-additive and suppressive (Vittek et

al., 2023). In this regard, the diverse connectivity profile with cortical and subcortical interconnections implies additionally a unique position of the dorsal pulvinar in integrating signals related to cortical processing with cardiovascular/autonomic influences.

2. Chapter

Dorsal pulvinar inactivation leads to spatial selection bias without perceptual deficit

Kristin Kaduk, Melanie Wilke, Igor Kagan

Manuscript in preparation

Authors contributions

Conceptualization: KK, MW, IK. Data curation: KK. Formal analysis: KK, IK. Funding acquisition: MW, IK. Project Administration: IK. Supervision: MW, IK. Visualization: KK, IK. Writing—Original draft preparation: KK, IK. Writing—Review & editing: KK, MW, IK.

Acknowledgments

We thank Lydia Gibson and Uwe Zimmermann for developing the color discrimination task, Lukas Schneider for help with the monkeypsych experimental task software, and Daniela Lazzarini, Sina Plümer, Klaus Heisig, and Dirk Prüße for technical support. We also thank Stefan Treue, Alexander Gail, the Decision and Awareness Group, the Sensorimotor Group, and the Cognitive Neuroscience Laboratory for helpful discussions. Supported by the Hermann and Lilly Schilling Foundation, German Research Foundation (DFG) grants WI 4046/1-1 and Research Unit GA1475-B4, KA 3726/2-1, CNMPB Primate Platform, and funding from the Cognitive Neuroscience Laboratory.

Keywords: perceptual decision, eye movements, distractors, spatial choice, macaque

Summary of the chapter

The dorsal pulvinar has been implicated in visuospatial attentional and perceptual confidence processing. Pulvinar lesions in humans and monkeys lead to spatial neglect symptoms including an overt spatial saccade bias during free choices. But it remains unclear whether the dorsal pulvinar perturbations and lesions during target selection that relies on a perceptual decision will lead to a perceptual impairment or a more general orienting deficit. To address this question, we reversibly inactivated the unilateral dorsal pulvinar by injecting GABA-A agonist THIP while two macaque monkeys performed a color discrimination saccade response task with varying perceptual difficulty. We used Signal Detection Theory to dissociate perceptual discrimination (d-prime) and spatial selection bias (response criterion) effects. We expected a decrease in d-prime if dorsal pulvinar affects perceptual discrimination and a shift in response criterion if dorsal pulvinar is mainly involved in spatial orienting. After inactivation, we observed response criterion shifts away from contralesional stimuli, especially when two competing peripheral stimuli in opposite hemifields were present, for both difficulty levels. Notably, the d-prime and overall accuracy remained largely unaffected. Our results underline the critical contribution of the dorsal pulvinar to spatial orienting while being less important for perceptual discrimination, resolving a debate on perception vs action bias.

Introduction

Visual scenes contain multiple spatial locations that serve as potential saccades targets. Selecting a target in complex scenes requires efficiently perceiving and evaluating behaviorally relevant information at different spatial locations. Many studies investigating the neural processes of visuospatial target selection emphasize interactions in frontoparietal cortical networks (Corbetta and Shulman, 2011; Fiebelkorn et al., 2018; Adam et al., 2020). These direct cortical connections are paralleled by indirect routes through higher-order thalamic nuclei such as the pulvinar, raising the question of how the pulvinar contributes to the selection of behaviorally relevant stimuli to guide visuospatial decision-making (Halassa and Kastner, 2017; Sherman, 2017).

The primate pulvinar consists of several nuclei – anterior, medial, lateral and inferior - with distinct functional properties and connectivity profiles. The dorsal part of the pulvinar (dPul) encompasses the anterior and medial pulvinar and the dorsal part of the lateral pulvinar (Gutierrez et al., 2000; Stepniewska, 2003; Arcaro et al., 2015; Baldwin and Bourne, 2017). These nuclei developed together with the association cortices in the course of primate evolution and are reciprocally connected to the parietal and prefrontal cortex, orbitofrontal cortex, insula, cingulate, superior and inferior temporal cortex (Kaas and Lyon, 2007; Preuss, 2007; Kaas and Baldwin, 2020). This extensive connectivity profile identifies the dorsal pulvinar as a unique brain hub well situated to interact with and modulate the circuitry involved in spatial attentional orienting and target selection (Grieve et al., 2000; Sherman and Guillery, 2002; Shipp, 2003; Saalmann and Kastner, 2015; Bourgeois et al., 2020; Kagan et al., 2021). Studies in human patients with unilateral thalamic lesions encompassing the pulvinar demonstrated deficits related to orienting or responding to perceptually or behaviorally salient stimuli in the contralesional hemifield (Danziger et al., 2001; Karnath et al., 2002; Arend et al., 2008b, 2008a; Lucas et al., 2019). Similar to neglect/extinction in patients, monkey studies using targeted reversible unilateral pharmacological inactivation of the dorsal pulvinar induced contralesional visuospatial deficits (Petersen et al., 1987; Desimone et al., 1990; Wilke et al., 2010, 2013; Komura et al., 2013). Such deficits manifest behaviorally in several ways. First, the inactivation causes impairment of spatial attentional orienting to cued targets in contralesional hemifield, decreasing performance in detection or color-contingent manual response tasks (Petersen et al., 1987; Desimone et al., 1990). Second, the confidence about contralesional perceptual categorization but not the categorization itself has been reported to decrease after the inactivation, in the absence of competing distractors in the opposite hemifield (Komura et al., 2013). Third, a target selection bias away from contralesional hemifield was observed in a free-choice saccade task (Wilke et al., 2010, 2013). Such inactivation-induced bias could be

alleviated by presenting only a single target or increasing the reward for contralesional targets but less so by perceptual saliency manipulations (Wilke et al., 2013).

The above causal perturbation findings, and the results of electrophysiological recordings (Robinson and Petersen, 1992; Benevento and Port, 1995; Bender and Youakim, 2001; Dominguez-Vargas et al., 2017; Fiebelkorn et al., 2019; Schneider et al., 2019, 2021), on the one hand, implicate dPul in attentional allocation and perceptual processing, but on the other, are also compatible with a role in more general spatial orienting bias. Different task demands might be one reason for such interpretational ambiguity. In particular, studies that used attentional cueing and perceptual discrimination employed paradigms where manual responses (e.g. button presses) were dissociated from the spatial position of the visual stimuli. At the same time, our previous choice tasks always required a saccade towards a peripheral target and did not involve difficult perceptual discrimination (Wilke et al., 2010, 2013; Dominguez-Vargas et al., 2017). Therefore, it remains unclear if perceptual factors contribute to contralesional visuospatial deficits in conditions of spatial competition and target-congruent saccade actions.

In the current study we used a color discrimination saccade selection task to address this question with two essential new features. Firstly, we included easy and difficult (i.e. perceptually similar to a target) distractors that should not be selected with a saccade. Secondly, we introduced an option to maintain central fixation as a correct response when only distractor(s) were presented. The task involved three different stimulus types – single stimuli, double “same” stimuli (target-target or distractor-distractor) and double different stimuli. Single stimuli included a peripheral target or a distractor and a central fixation option, resulting in low spatial competition. The double stimuli included left and right peripheral stimuli and a fixation option, adding competition between hemifields. Using Signal Detection Theory (Stanislaw and Todorov, 1999; Macmillan and Creelman, 2004), we investigated whether unilateral dPul inactivation leads to a perceptual deficit or a spatial selection bias. Suppose the dorsal pulvinar is mainly involved in spatial orienting. In that case, we expected a shift in the criterion manifesting as a selection bias away from the contralesional hemifield, regardless of whether a target or a distractor is presented. But if the dorsal pulvinar is involved in discriminating targets from distractors, we expected a contralesional perceptual sensitivity deficit, manifesting as a decrease in d-prime. Furthermore, if dPul is mainly relevant for regulating the competition between hemifields, we expected a more substantial effect of inactivation in double stimuli conditions.

Methods

Experimental procedures

All experimental procedures complied with the ARRIVE guidelines (https://arriveguidelines.org) and were conducted in accordance with the European Directive 2010/63/EU, the corresponding German law governing animal welfare, and German Primate Center institutional guidelines. The procedures were approved by the responsible government agency (Niedersaechsisches Landesamt fuer Verbraucherschutz und Lebensmittelsicherheit (LAVES), Oldenburg, Germany).

Two adult male rhesus monkeys (*Macaca mulatta*), weighing 9 kg and 10.5 kg, served as subjects (monkey 1, Cornelius, M1; monkey 2, Curius, M2). For both monkeys, the surgical procedures for implanting an MRI-compatible headpost and chambers, and small within-chamber craniotomies, were the same as described in Dominguez-Vargas et al. (2017). The inactivation locations in the dorsal pulvinar were estimated based on anatomical MRI as described in more detail in the previous work (Dominguez-Vargas et al., 2017; Kagan et al., 2021). Based on the MRI images, we planned where to target the dorsal pulvinar (the grid hole and depth) using the software Planner (Ohayon and Tsao, 2012) and BrainVoyager (Version 2.4.2, 64-bit; Brain Innovation). To confirm the inactivation locations, we performed MRI contrast agent gadolinium injections (**Figure 1A**).

The neural activity was reversibly suppressed using the GABA-A agonist 4,5,6,7-tetrahydro isoxazole [5,4-c]-pyridine-3-ol (THIP hydrochloride; Tocris). The THIP was dissolved in phosphate-buffered saline (PBS). The solution (pH 7.0-7.5) was sterile filtered with a hydrophobic PTFE membrane filter (pore size: 0.2 µm, Sartorius) before injection via a sterile 50 or 60 mm length 31 gauge sharp-tip steel cannula (Plastics One). The solution was delivered at a rate of 0.25 µl/min using a 0.1 ml glass-tight Hamilton syringe driven by a digital infusion pump (Harvard Apparatus). The injection volume per session was 4.5-5 µl of 10 mg/ml of THIP for monkey 1 (dPul in the left hemisphere) and 1.5 µl for monkey 2 (dPul in the right hemisphere). The injected volume was determined for each monkey separately in pilot sessions in which the monkey could perform the task without nystagmus and showed an ipsilesional spatial bias for target-target (free choice) stimuli as in prior reports (Wilke et al., 2010, 2013). The “free-choice” selection bias during target-target trials demonstrated a successful inactivation procedure.

Every experimental session started with a pre-injection testing period, followed by the injection, a 30-40 min waiting period, and the post-injection testing period. We conducted 7 inactivation sessions interleaved with 7 control (no actual injection) sessions for each monkey. In total, M1

performed 15222 trials and M2 performed 10945 trials. The control sessions were performed with the same timing of events as the inactivation sessions.

Behavioral paradigm

The monkeys were sitting in a dark room in a custom-made primate chair with the head restrained 30 cm away from a 27" LED display (60 Hz refresh rate, model HN274H, Acer Inc. USA). The gaze position of the right eye was monitored at 220 Hz using an MCU02 ViewPoint infrared eye tracker (Arrington Research Inc. USA). A MATLAB-based task controller (https://github.com/dagdpz/monkeypsych, MATLAB version R2012b, The MathWorks, Inc., USA) and the Psychophysics Toolbox (Brainard, 1997) were used to control stimulus presentation.

Color discrimination task. Two monkeys performed a color discrimination task (**Figure 2.1B**) where the perceptual difficulty was determined by the color similarity of the target (T, red) vs. distractor (D, easy – yellow, difficult – orange). Target or distractor was either presented alone or with a second stimulus (distractor or target) in the opposite hemifield, determining the level of spatial competition. Monkeys had to saccade to the target or continue fixating when only distractor(s) were presented. Each trial started with the presentation of a red fixation spot. The monkey initiated each trial by acquiring eye fixation by entering the 5° radial window around the fixation spot within 500 ms after the onset of the fixation spot. After maintaining fixation for 500-900 ms, the fixation spot turned gray, and one or two peripheral dots simultaneously appeared (go-signal). Red dots represented targets, whereas yellow and orange dots represented distractors. In conditions with a single peripheral stimulus, either one target or one distractor was presented in the left or the right hemifield. In conditions with two peripheral stimuli, the monkey was shown two dots in opposite hemifields. In double-target trials, two equally-rewarded targets were presented, and the monkey could choose either as a saccade target. In double-distractor trials, two distractors were shown, which had to be ignored by maintaining central fixation. In target-distractor trials, a target was presented with a distractor in the opposite hemifield. The monkey was required to make a saccade towards the target while ignoring the distractor. The monkey had to choose within 500 ms (target acquisition epoch). As soon as the eye position entered the 5° radial window around one of the stimuli, the stimulus was selected, and the monkey was not allowed to reverse his decision. The chosen stimulus, either the selected peripheral dot for saccade responses or the fixation spot for maintaining eye fixation, turned bright to confirm the monkey's selection. After fixating the selected stimulus for another 500 ms (target hold epoch), correct responses were followed by the reward tone, a fluid reward, and an inter-trial interval (ITI) of 2000 ms. Incorrect answers were followed by the error tone, no liquid reward, and an ITI of 2000 ms.

All stimuli were matched in luminance (dim stimuli: 11 cd/m^2, bright stimuli: 35 cd/m^2) and size (1° diameter). Targets and distractors were displayed at one of three locations per hemifield (six locations in total) with an eccentricity of 20° of visual angle. Stimulus locations were arranged concentrically around the fixation spot at 0° (mid-left), 20° (up left), 160° (upright), 180° (mid-right), 200° (down right), and 340° (down left). They were presented on a horizontal or a diagonal axis in conditions with two peripheral stimuli. All experimental conditions (stimulus type, difficulty level, spatial location) were pseudorandomized. Trials aborted before the monkey selected a stimulus returned to the pool of trials from which the next trial was chosen randomly.

Distractor color determination. After initial training of the task with an easy yellow distractor, we determined the difficult distractor color (orange) for the experiment based on the results of a psychophysical assessment (six sessions in each monkey). The goal of the assessment was to determine a distractor color that could be correctly discriminated from the target with 70 - 80% accuracy. To this end, the monkeys performed a color discrimination test with five distractor colors of different perceptual difficulty ranging from yellow (easy, RGB [60 60 0]) to red-orange (difficult, M1: [128 11 0]; M2: [128 23 0]). All trial conditions were presented in a pseudorandomized order. The perceptual difficulty was defined as the RGB value ratio between green (G) and red (R). A stimulus with a G/R ratio of 1 is a yellow distractor (60 60 0) which is perceptually very different from the target color ([128 0 0]) with a G/R ratio of 0. We chose an orange color as the difficult distractor color (M1: G/R ratio = 0.09, M2: G/R ratio = 0.18, see Supplementary Information, **Suppl. Figure S2.1**). The corresponding accuracy values were fitted by the cumulative normal function using Palamedes toolbox (Prins and Kingdom, 2009) in MATLAB 2019b (The MathWorks, Inc. USA).

Equalizing spatial choice behavior. In the beginning of each task training session, the left-right choice behavior in target-target trials was approximately equalized by shifting the entire stimulus array (both central and peripheral stimuli) with respect to the body midline, if a substantial hemifield bias was present (Dominguez-Vargas et al., 2017). In all subsequent experimental sessions, the stimulus array was adjusted by the same amount (0° from the midline for M1 and by 5° for M2).

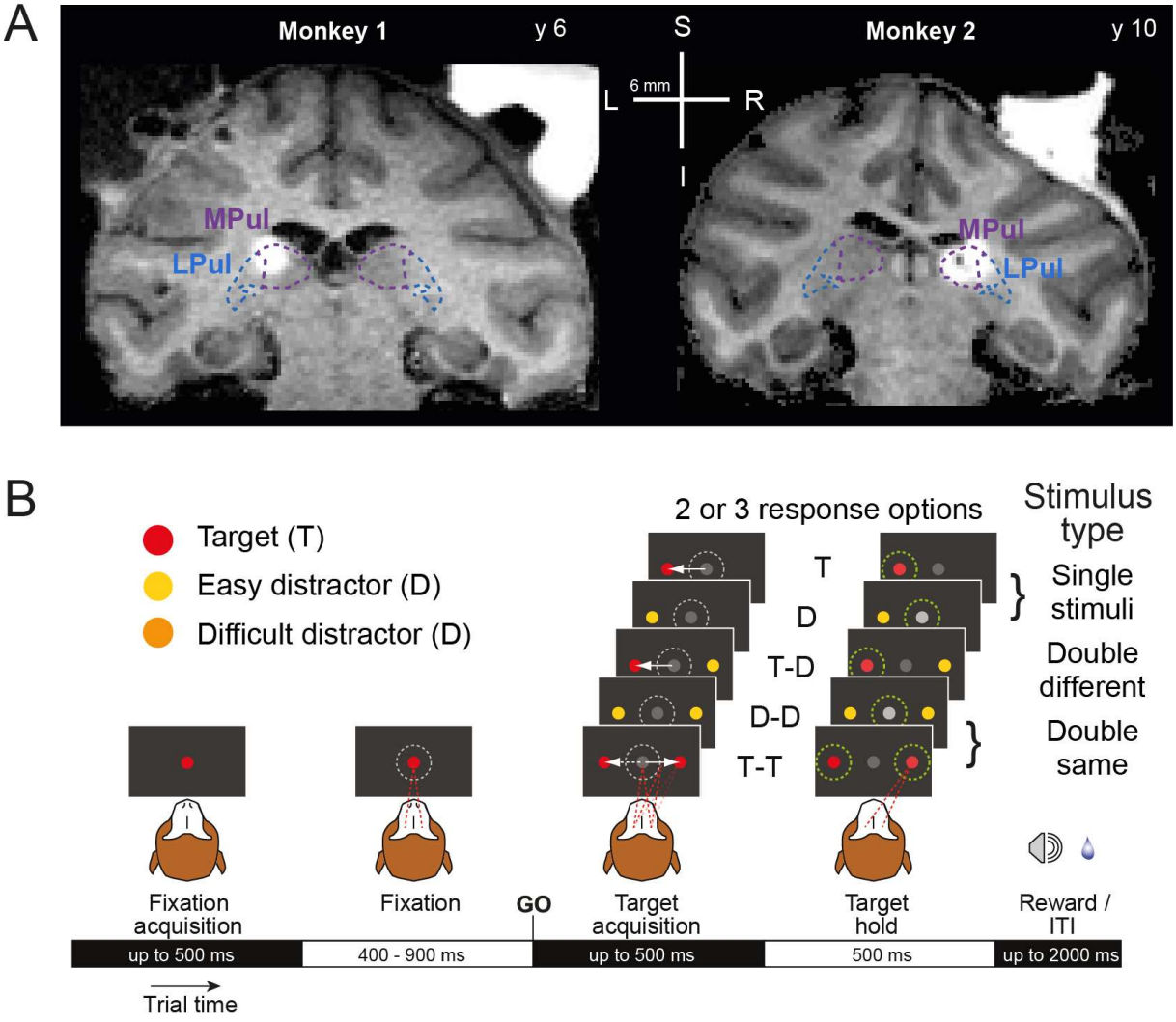

Figure 2.1. Inactivation sites and task design. (A) MR images show the inactivation sites visualized with co-injection of gadolinium MR contrast agent (ratio: 1:200 saline) ~20 min following the injection (for M1: 2 μl and M2: 3 μl, respectively) and the overlaid borders of medial pulvinar (MPul) and lateral pulvinar (LPul). (B) Two monkeys performed a color discrimination task where the perceptual difficulty was determined by the color similarity of the target (T, red) vs. distractor (D, easy - yellow, difficult - orange). Target or distractor was presented alone or with a second stimulus (distractor or target) in the opposite hemifield. Monkeys had to saccade to the target and continue fixating when only distractor(s) were presented.

Data analysis

We analyzed the behavioral data from two monkeys for the “post-injection” testing period, with seven injections and seven control sessions for each monkey. Data analysis were performed using MATLAB R2015a. The analysis focuses on the saccade latencies, accuracy, and Signal Detection Theory variables to evaluate if there is a significant statistical difference between control and inactivation sessions. Accuracy was defined as the proportion of correct and rewarded trials among all trials in a specific condition (e.g. correct hits and rejections for all

single stimuli trials, regardless of the hemifield). For calculating the saccade latencies, we used all completed saccades to the target.

Saccade definition

All eye movements with a minimum velocity of 200 °/s and a minimum duration of 30 ms were considered saccades. To detect a saccade, the instantaneous saccade velocity was calculated sample by sample as the square root of the sum of squared interpolated (220 Hz to 1 kHz) and smoothed (12 ms moving average rectangular window) horizontal and vertical eye position traces, and smoothed again (12 ms moving average rectangular window). Saccade onset was defined as the first eye position change after the go-cue that exceeded a velocity threshold of 200°/s. Saccade end was defined as the first point in time when eye velocity dropped below 50°/s after saccade onset.

Signal Detection Theory

To address our two alternative hypotheses, whether the contralesional visuospatial deficit is a consequence of a contralesional perceptual discrimination deficit or spatial selection bias, we used the Signal Detection Theory to assess changes in perceptual sensitivity index (d-prime) and response criterion after unilateral reversible dorsal pulvinar inactivation. D-prime measures how well the monkeys discriminate targets from distractors (Eq. 1); z represents z-score calculated using normal inverse cumulative distribution function (*norminv* function in MATLAB). The response criterion indicates the tendency to select a stimulus in a specific hemifield regardless if it is a target or distractor (Eq. 2).

$$\mathrm{d}' = \mathrm{z}(\text{False alarm rate}) - \mathrm{z}(\text{Hit rate}) \quad (1)$$

$$\mathrm{c} = -0.5(\mathrm{z}(\text{Hit rate}) + \mathrm{z}(\text{False alarm rate})) \quad (2)$$

The data were analyzed separately for each monkey (M1 and M2), for each difficulty level (yellow and orange distractor), and stimulus type (single, double same, and double different stimuli). To compare the effect of inactivation per hemifield, we calculated the signal detection theory variables separately for the contralesional and ipsilesional hemifield relative to the side of inactivation (see the details in the Supplementary Information, **Suppl. Figures S2.2-S2.4**). An increase of the criterion signifies decreased selection of the contralateral stimulus ("less contra") and vice versa.

Statistical analysis

The statistical analysis was performed using R (version 4.1.2, R Core Team, 2022) and MATLAB 2014b. First, to assess whether the accuracy differs between the three stimulus types (single stimuli, double same, and double different stimuli) for each difficulty level in the control sessions due intended consequence of our task design, we conducted a mixed ANOVA followed by post-hoc tests to determine whether the three stimulus types differed significantly (corrected for multiple comparisons using Bonferroni correction).

The main aim of the study was to investigate the effects of dorsal pulvinar inactivation compared to control (no perturbation) sessions on different dependent variables. Accuracy was analyzed with three-way mixed ANOVAs: Difficulty level (easy, difficult) × Stimulus type (single, double same, double different) × Perturbation (inactivation, control). The d-prime and criterion were analyzed with four-way mixed ANOVAs: Difficulty level (easy, difficult) × Stimulus type (single, double same, double different) × Perturbation (inactivation, control) × Hemifield (contra, ipsi). Although the four-factor mixed ANOVA includes all possible interactions, it cannot directly answer our research question: whether dPul inactivation affects the criterion or d-prime, differently for the three stimulus types and the two perceptual difficulty levels. To assess whether there was a statistical difference between the inactivation sessions and control sessions in the d-prime and criterion, we conducted independent sample t-tests separately for the stimulus position (contralesional and ipsilesional hemifield), the stimulus type (single, double same, and double different), and the difficulty level (difficult and easy). Due to a small sample size, we also calculated non-parametric tests (Wilcoxon rank sum test), leading to comparable results (**Suppl. Table S8**).

Simulations

We numerically simulated different scenarios of stimulus selection corresponding to the two alternative hypotheses (response bias and perceptual sensitivity deficit). These simulations aimed to visualize the effects of unilateral inactivation on selection behavior and resulting STD variables for each scenario, and to compare the changes derived from the predictions of each hypothesis with the data. One group of scenarios represents the response criterion hypothesis, where we expect a decrease both in contralesional hit rate and false alarm rate after the inactivation, resulting in a shift of criterion away from the contralesional hemifield – i.e. towards “less contra”. The other group of scenarios represents the perceptual discrimination hypothesis, where we expect a decrease in the contralesional hit rate and an increase in false alarm rate, resulting in decreased contralesional d-prime. In brief, the proportions of hits,

misses, correct rejections, and false alarms were defined for the control condition (no inactivation), approximately based on the actual monkey performance. A specific bias or perceptual deficit on these proportions was introduced to estimate resulting hits, misses, correct rejections, and false alarms in the "inactivated" condition. The resulting criterion and d-prime values were calculated for the control and the inactivated conditions.

For each scenario, the simulated data consisted of 200 trials (100 target trials and 100 distractor trials) separated into four different outcomes: hits, misses, false alarms and correction rejections. The proportion of selection for one specific stimulus type and one difficulty level is set in each scenario. An example of a specific selection pattern is illustrated for the scenario "single stimulus – difficult distractor – response criterion hypothesis" (**Table 1**). Before inactivation, the (contralateral) selection pattern is: hits: 0.7 fraction of target selection (correct, 70 trials), misses: 0.3 fraction staying on the central fixation spot when a target is presented (incorrect, 30 trials); correct rejections 0.6 fraction staying when a difficult distractor is presented (correct, 60 trials) and false alarms: 0.4 fraction selecting the distractor (incorrect, 40 trials). The hit rate is 0.7, and the false alarm rate is 0.4 resulting in a criterion of -0.14 and a d-prime of 0.77. According to the prediction of response bias hypothesis, after the inactivation the monkey should select less often stimuli presented in the contralesional hemifield regardless whether a target or a distractor is shown. We therefore expect a decrease of hits and false alarms, and an increase of misses and correct rejections, resulting in a decrease of the contralesional hit rate and false alarm rate. In this example, we chose an inactivation-induced decrease in contralesional selection by 0.2 (20 trials) for the hit and false alarm rates, resulting in shift of the criterion towards "less contra" (increase of the criterion). Notably, the d-prime is also changing slightly. To visualize how the hit rate, the false alarm rate, the criterion and the d-prime are related, we visualized for each combination of the false alarm rate and the hit rate the resulting values of criterion and d-prime. All simulations were done in MATLAB. The code is publically available at https://github.com/dagdpz/perceptual-dis.

Table 1. An example selection pattern for the simulated hypothetical scenario "single stimulus – difficult distractor – response bias hypothesis". This example is illustrated in **Figure 2.4A**.

	Before inactivation	**Inactivation effect**	**After inactivation**
Hits	0.70	- 0.2	0.50
Misses	0.30	+ 0.2	0.50
Correct rejections	0.60	+ 0.2	0.80
False alarms	0.40	- 0.2	0.20
Hit rate	0.70	- 0.2	0.50
False alarm rate	0.40	- 0.2	0.20
criterion	**-0.14**		**0.42**
d-prime	**0.77**		**0.84**

Results

We investigated whether local unilateral injection of THIP suppressing the dorsal pulvinar neuronal activity (**Figure 2.1A**) causes a contralesional perceptual discrimination deficit or a spatial selection bias. Two monkeys performed a color discrimination task between red targets and distractors (orange stimuli as difficult distractors and yellow stimuli as easy distractors) in three stimulus type conditions (single stimuli, double same stimuli, double different stimuli, **Figure 2.1B**). We analyzed the following dependent variables: saccade latency, accuracy, d-prime, and response criterion. The main statistical analysis focused on the comparison between control vs. inactivation sessions.

The effect of dorsal pulvinar inactivation on saccade latency

The saccade latency is a sensitive measure of the effect of dorsal pulvinar inactivation. According to previous work, we expected either faster ipsilesional saccades (Wilke et al. 2010) or/and slower contralesional saccades (Wilke et al. 2013). A three-way mixed ANOVA (see details in **Suppl. Table S1**) was performed to compare the effect of the within-factors “Stimulus Type” (Single / Double Same / Double Different) and “Hemifield” (Contra- / Ipsilateral hemifield) and the between-factor “Perturbation” (Control / Inactivation sessions) on saccade latency. We found a statistically significant Stimulus type × Hemifield × Perturbation interaction for both monkeys (3-way interaction: M1: $F(2,22) = 4.64$, $p = .021$; M2: $F(2,24) = 3.74$, $p = .039$), as well as the Hemifield × Perturbation interaction for M1 (2-way interaction: M1: $F(1,11) = 21.81$, $p = .001$; M2: $F(1,12) = 3.74$, $p = .08$).

In agreement with our expectations about the inactivation effects, both monkeys significantly slowed down after dorsal pulvinar inactivation during contralesional target selection for both difficulty levels in all three stimulus types (independent t-test, **Table 2.2**, **Figure 2.2**). The consistent inactivation effect across stimulus types and difficulty levels on the contralesional saccade latency indicated a successful pharmacological manipulation. The saccade latency effects for ipsilesional target selection were less pronounced and only reached significance for the double same stimuli (independent t-test, **Table 2.2**, **Figure 2.2**).

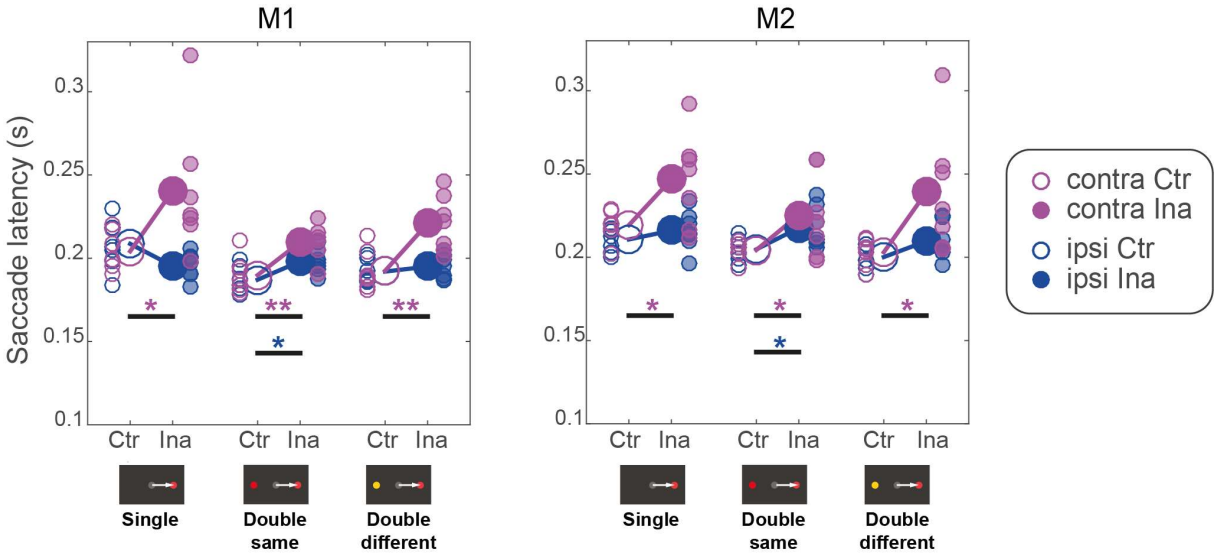

Figure 2.2. Inactivation effects on saccade latency to the target. The saccade latency is displayed separately for control (empty circles, "Ctr") and inactivation (filled circles, "Ina") sessions for each stimulus type and hemifield (icons below horizontal axis show example stimulus display for one hemifield). Small circles display single sessions; large circles display the mean across sessions. We tested the difference between control and inactivation saccade latency of selecting either contralesional (magenta) or ipsilesional (blue) stimuli (independent t-test, one star *, $p < .05$; two stars **, $p<0.01$).

Table 2.2. Results of the independent t-test for the comparison of saccade latency in control vs inactivation sessions. The significant effects are in bold font.

Stimulus type	Hemifield	Monkey 1 (M1)		Monkey 2 (M2)	
		t-value	p-value	t-value	p-value
Single stimuli	**contra**	**2.31**	**.039**	**2.47**	**.029**
	ipsi	2.07	.061	0.99	.342
Double same stimuli	**contra**	**3.21**	**.008**	**2.19**	**.049**
	ipsi	**2.81**	**.016**	**2.43**	**.032**
Double different stimuli	**contra**	**3.62**	**.004**	**2.54**	**.026**
	ipsi	0.80	.44	1.91	.081

The effects of stimulus type and inactivation on accuracy

The apparent difference between accuracy for easy vs difficult discrimination in the control sessions (**Figure 2.3**) was the intended consequence of our task design (since the accuracy level was manipulated experimentally by adjusting the distractor difficulty, we do not present the corresponding statistical comparison). However, when we analyzed each difficulty level separately, we also observed accuracy differences between the three stimulus types during difficult discrimination (repeated measures one-way ANOVA, within-factor "Stimulus Type"; for the difficult discrimination: monkey M1: $F(2,20) = 132.26$, $p < .001$; monkey M2: $F(2,20) = 115.96$, $p < .001$; for the easy discrimination: M1: $F(2,20) = 2.23$, $p = .15$; M2: $F(2,20) = 2.54$, $p = .12$). In both monkeys, the accuracy was highest for the double different stimuli and lowest

in the double same stimuli for the difficult distractor (post-hoc tests; **Suppl. Table S2.2**). This difference in accuracy suggests that the three stimulus types elicited different behavioral strategies (for instance, direct comparison between hemifields for double different stimuli vs. only memorized representations of targets and distractors in double same and single stimuli; see later).

We next analyzed the effects of inactivation on accuracy using a three-way mixed ANOVA with within-factors “Stimulus Type” (Single / Double Same / Double Different) and “Difficulty” (Difficult / Easy discrimination) and between-factor “Perturbation” (Control / Inactivation sessions). This analysis (see details in **Suppl. Table S2.3**) revealed no main effect of the factor “Perturbation” and no statistically significant interactions with this factor for M1. However, the main effect of the “Perturbation” and the two-way interaction between Stimulus Type × Perturbation was significant for M2 ($F(1,12) = 9.4$, $p = .01$, $F(2,24) = 6.4$, $p = .006$).

The results for M2 were followed up to investigate the effect of inactivation by applying post-hoc tests. M2 showed a significant decrease in accuracy for single stimuli for the easy distractor ($t(1,12) = -2.26$, $p = .04$) and for double different stimuli for both difficulty levels (difficult: $t(1,12) = -2.67$, $p = .02$; easy: $t(1,12) = -3.73$, $p = .003$) but not for double same stimuli (difficult: $t(1,12) = 0.18$, $p = .86$; easy: $t(1,12) = 1.48$, $p = .16$) or difficult single stimuli ($t(1,12) = 0.86$, $p = .4$) (**Figure 2.3**). These effects will be addressed with the Signal Detection Theory analysis below.

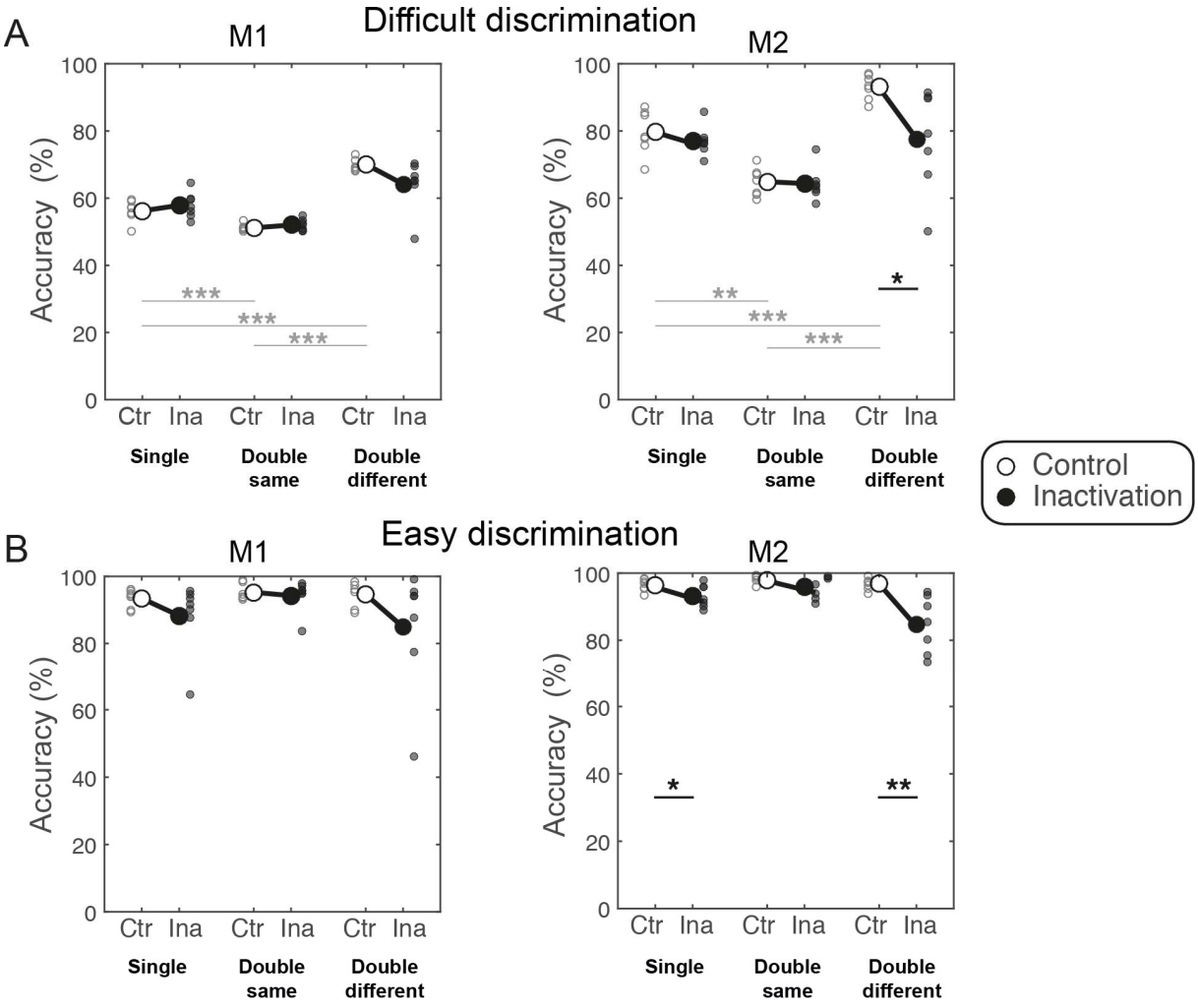

Figure 2.3. Inactivation effects on accuracy. The accuracy is displayed separately for control (Ctr) and inactivation (Ina) sessions for each stimulus type and difficulty level. Small circles depict single sessions, and large circles indicate the mean across sessions. Two statistical analyses are presented: the difference between control and inactivation sessions (black connecting lines and stars) and the difference in accuracy between stimulus types (single, double same, double different) for the control sessions (gray connecting lines and stars). (A) Difficult discrimination. The inactivation did not affect the accuracy, besides a decrease in the double different condition in M2. Considering only the control sessions, the accuracy significantly varied between stimulus types. (B) Easy discrimination. The inactivation affected accuracy for M2 for single and double different conditions. The accuracy in the control condition was very high and did not vary between stimulus types. Independent t-test, one star *, $p < .05$; two stars **, $p<0.01$; three stars ***, $p<0.001$.

The effect of inactivation on criterion and d-prime

We adopted the Signal Detection Theory approach to differentiate between the spatial selection bias by calculating the response criterion and the deficit in perceptual discrimination between stimuli by calculating d-prime. To assess at first all possible interaction effects on criterion and d-prime, a four-factor mixed ANOVA was used per monkey, including within-factors “Stimulus Type” (Single / Double Same / Double different), “Difficulty” (Difficult / Easy discrimination) and “Hemifield” (Contra- / Ipsilesional) and between-factor “Perturbation”

(Control / Inactivation sessions). This ANOVA revealed that there was a significant interaction of all four factors (Stimulus Type × Difficulty × Hemifield × Perturbation) only in M1 for the d-prime ($F(2,24) = 3.87$, $p = .035$) but not for the criterion and not in M2 (criterion: $F(2,24) = 0.33$, $p = .72$, d-prime: $F(2,24) = 0.33$, $p = .72$). Related to the perturbation, for the criterion M1 showed a three-way Stimulus Type × Difficulty × Perturbation interaction ($F(2,24) = 8.69$, $p = .001$), and two two-way interactions (Perturbation × Difficulty, $F(1,12) = 17.86$, $p = .001$ and Perturbation × Stimulus Type, $F(2,24) = 17.30$, $p < .001$); and for the d-prime, a three-way Perturbation × Hemifield × Stimulus Type interaction ($F(2,24) = 3.99$, $p = .032$). Likewise, M2 showed two two-way interactions (Perturbation × Stimulus Type, $F(2,24) = 7.82$, $p = .002$; Perturbation × Hemifield, $F(2,24) = 6.71$, $p = .024$) for the criterion; and for the d-prime, a main effect of Perturbation ($F(1,12) = 10.00$, $p = .008$) and a two-way Stimulus Type × Perturbation interaction ($F(2,24) = 8.76$, $p = .001$) (see the details in the in **Suppl. Table S2.4**).

Although the four-factor mixed ANOVA includes all possible interactions, it is difficult to interpret and it cannot directly answer our research question, such as whether dPul inactivation affects the criterion or d-prime, differently for the three stimulus types and the two perceptual difficulty levels. In both monkeys, we observed interactions of the factors “Perturbation” and “Hemifield”, and we had *a priori* hemifield-specific predictions. To test these predictions, in the sections below we continue the analysis of d-prime and criterion focusing on a two-factor mixed ANOVA (see the details in the **Suppl. Table S2.5 and S2.6**) with the within-factor “Hemifield” (Contra- / Ipsilesional) and the between-factor “Perturbation” (Control / Inactivation sessions), plus the corresponding post-hoc t-tests, separately for each stimulus type and difficulty.

The effect of inactivation for single stimuli

The single stimuli condition involves a perceptual judgment between making a saccade to a peripheral target or continuing fixating as the correct response to a peripheral distractor (low spatial competition between a central “stay” and peripheral “go” options). To evaluate a deficit in discrimination versus a spatial selection bias, we divided trials into hits, misses, correct rejections, and false alarms separately for stimuli presented in the contralesional hemifield (opposite to the side of inactivation) or ipsilesional hemifield to calculate the hit rate, false alarm rate, d-prime and criterion for each hemifield (**Suppl. Figure S2.2**). Since we used two distractors: one easy distractor (yellow) that was perceptually clearly different from the red target and the other (orange) distractor required a difficult perceptual discrimination, we analyzed these two distractor conditions separately, contrasting them to target trials. Here and in the next sections, we first describe quantitative predictions using simulated data and then the actual data separately for difficult and easy discrimination.

During difficult discrimination, if dorsal pulvinar inactivation causes a spatial selection bias, we expect a similar decrease in contralesional hit rate and false alarm rate, resulting in a criterion shift towards “less contra” (**Figure 2.4A**). If the inactivation causes a contralesional perceptual discrimination deficit, we expect a decrease in the contralesional hit rate and an increase in the false alarm rate, resulting in decreased contralesional d-prime (**Figure 2.4A**). We did not expect changes to the ipsilesional criterion and d-prime.

In the target trials, the contralesional hit rate decreased after the inactivation significantly for M2 (independent t-test; M1: $t(1,12) = 1.1$, $p = .29$; M2: $t(1,12) = -2.89$, $p = .01$). For difficult discrimination (**Figure 2.4B**), the contralesional false alarm rate also decreased, but this effect did not reach significance (M1: $t(1,12) = 1.15$, $p = .27$; M2: $t(1,12) = 1.6$, $p = .14$). The two-way mixed-effect ANOVA with factors “Perturbation” and “Hemifield” performed on d-prime and criterion showed no significant interaction of “Perturbation” × “Hemifield” in either monkey, and only a significant main effect of “Perturbation” in M2 on criterion ($F(1,12) = 6.40$, $p = .026$; see **Suppl. Table S2.5**). Accordingly, M2 showed a significant shift of the contralesional criterion towards “less contra” (M2: $t(1,12) = 3.07$, $p = .01$; the effect was similar but did not reach significance in M1, $t(1,12) = 1.21$, $p = .25$). Neither monkey showed a decrease in contralesional d-prime after inactivation (M1: $t(1,12) = -0.36$, $p = .73$; M2: $t(1,12) = -1.26$, $p = .23$). In line with our predictions, in both monkeys neither ipsilesional d-prime nor the ipsilesional criterion exhibited any changes (d-prime M1: $t(1,12) = -0.41$, $p = .69$; M2: $t(1,12) = -1.98$, $p = .07$; criterion M1: $t(1,12) = -0.99$, $p = .34$; M2: $t(1,12) = 0.15$, $p = .89$).

During easy discrimination, if dorsal pulvinar inactivation causes a spatial selection bias, we expect a decrease in the contralesional hit rate but now no change in false alarm rate due to a “ceiling effect” (already very low false alarm rate in the control sessions). This will result in a shift of criterion towards “less contra” combined with a decrease in contralesional d-prime (**Figure 2.4C**). For completeness, if the inactivation causes a contralesional perceptual discrimination deficit, one expects a decrease in contralesional hit rate and an increase in false alarm rate (although given the easy discriminability of the yellow distractor, we did not expect such an increase in the actual behavior). This would result in decreased contralesional d-prime but no change in criterion (**Figure 2.4C**).

Indeed, in both monkeys during easy discrimination (**Figure 2.4D**), the false alarm rate was already near zero, so there was no room to exhibit any inactivation-induced decrease (independent t-test; contra M1: $t(1,12) = 0.02$, $p = .98$; M2: $t(1,12) = -0.3$, $p = .7$; ipsi M1: $t(1,12) = 0.95$, $p = .36$; M2: $t(1,12) = -0.6$, $p = .6$). In a two-way mixed-effect ANOVA on d-prime and criterion, there was no significant main effect for “Perturbation” or any interaction between “Perturbation” and “Hemifield” in both monkeys (in M2, the interaction for the criterion showed a trend, $F(1,12) = 4.59$, $p = .053$, see **Suppl. Table S2.6**). Accordingly, M2 showed a significant

shift for the contralesional criterion towards “less contra” (M1: $t(1,12) = 0.85$, $p = .41$; M2: $t(1,12) = 2.63$, $p = .02$), but also a decrease in contralesional d-prime (M1: $t(1,12) = -1.49$, $p = .16$; M2: $t(1,12) = 2.27$, $p = .04$). This decrease in d-prime was due to the “ceiling effect” of already very low false alarm rate, as predicted in the simulation.

To sum up, under conditions of low spatial competition, after inactivation both monkeys showed a shift in response criterion manifesting as reluctance to select stimuli in the contralesional hemifield for both difficulty levels, significant in monkey M2.

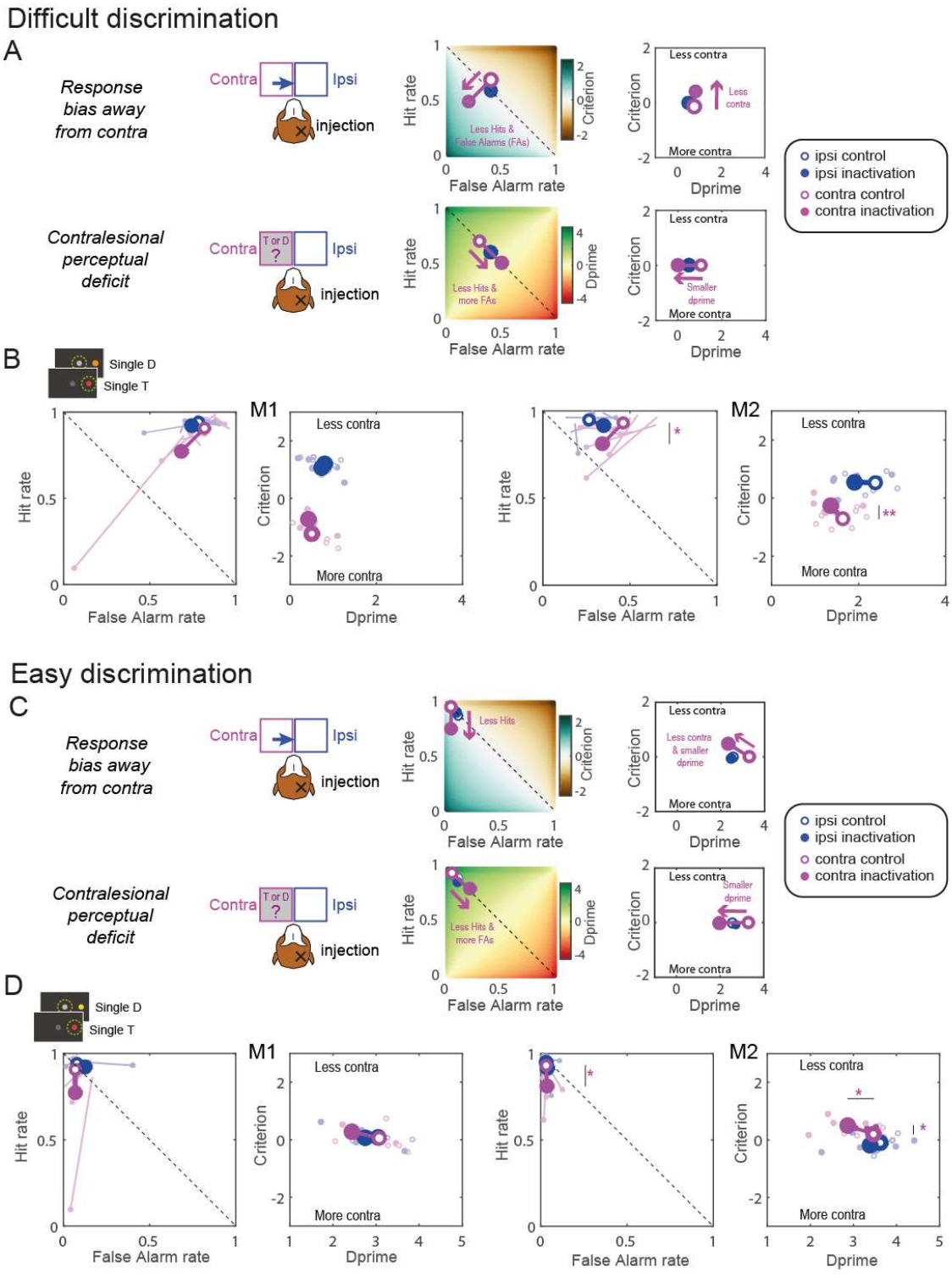

Figure 2.4. Predictions and results for single stimuli. (A) Illustration of the two alternative hypotheses for the difficult discrimination using simulated data showing the expected changes in hit rate, false alarm rate, d-prime and criterion after unilateral dPul inactivation. The color-coded background in the hit rate vs false alarm rate plots reflects the corresponding criterion or d-prime. Positive shifts of the criterion are defined as towards “Less contra” (and vice versa). (B) Inactivation effects on signal detection variables for the difficult discrimination (orange distractor); the data are displayed separately for each monkey, in each monkey the left panel shows the ipsilesional (blue) and contralesional (magenta) false alarm rate and hit rate, the right panel shows the ipsilesional and contralesional criterion and d-prime. Small circles display single sessions; large circles display the mean across sessions. (C) Illustration of the two alternative hypotheses for the easy discrimination. (D) Inactivation effects on signal detection

variables for the easy discrimination (yellow distractor). Abbreviations: T – target, D – distractor, contra – contralesional, ipsi – ipsilesional.

The effect of inactivation for double same stimuli

Previous studies suggested that dorsal pulvinar becomes most relevant in the case of spatial competition between hemifields (Desimone et al., 1990; Wilke et al., 2013; Dominguez-Vargas et al., 2017). Here, two equally rewarded targets or two distractors were presented in the periphery during the double same stimuli condition, eliciting a high competition between hemifields for visual representation and response selection. The monkeys chose between continuing fixating or making a saccade to one of the two peripheral stimuli (**Suppl. Figure S2.3**).

As for the single stimuli, if dorsal pulvinar inactivation causes a spatial selection bias during inter-hemifield competition, we expect a similar decrease in contralesional hit and false alarm rates. Necessarily, such a decrease has to result in either (i) a corresponding increase in ipsilesional hit rate and false alarm rate, or (ii) an increase of central fixation selection. Both monkeys tended to select peripheral stimuli over the central fixation, even after inactivation, as shown with a non-hemifield-selective criterion analysis ("stay" vs. "go", **Suppl. Table S2.7**). Therefore, we expected a shift for both contralesional and ipsilesional criteria towards "less contra" (**Figure 2.5A**). If dorsal pulvinar inactivation causes a contralesional perceptual discrimination deficit, similarly to the single stimuli condition we expect a decrease in contralesional hit rate and an increase in contralesional false alarm rate, resulting in a reduction of contralesional d-prime (**Figure 2.5A**). We did not have strong predictions for the ipsilesional discrimination: it might remain unaffected, as for single stimuli (and instead, only fixation selection might change to counterbalance the contralesional changes, the possibility we illustrate here), or it might improve as a consequence of ipsilesional hit rate increase and ipsilesional false alarm rate decrease.

The contralesional hit rate decreased significantly for both monkeys (independent t-test; M1: $t(1,12) = -4.24$, $p < .001$; M2: $t(1,12) = -4.78$, $p < .001$), and ipsilesional hit rate increased significantly (M1: $t(1,12) = 4.36$, $p < .001$; M2: $t(1,12) = 3.28$, $p = .01$). For difficult discrimination displayed in **Figure 2.5B**, the ipsilesional false alarm rate significantly increased for both monkeys (M1: $t(1,12) = 3.25$, $p = .01$; M2: $t(1,12) = 3.23$, $p = .01$), and contralesional false alarm rate significantly decreased for M1 (M1: $t(1,12) = -2.79$, $p = .02$; M2: $t(1,12) = -2.04$, $p = .065$). The two-way mixed-effect ANOVA performed on d-prime and criterion showed no significant "Perturbation" × "Hemifield" interaction (see **Suppl. Table S2.5**). For the criterion, a significant main effect for "Perturbation" was observed for both monkeys (M1: $F(1,12) = 9.65$, $p = .009$; M2: $F(1,12) = 10.43$, $p = .007$). Both monkeys showed a significant shift of the

contralesional and ipsilesional criterion towards “less contra” (M1 contra: $t(1,12) = 2.68$, $p = .02$, ipsi: $t(1,12) = 3.74$, $p = .003$; M2 contra: $t(1,12) = 2.87$, $p = .014$, ipsi: $t(1,12) = 3.8$, $p = .003$). Neither monkey showed a significant change in contralesional d-prime ($p > .05$).

During easy discrimination, as for the single stimuli, for the spatial selection bias hypothesis we expect a decrease in contralesional hit rate and no observable decrease in false alarm rate (again due to the ceiling effect on already very low false alarm rate), and a corresponding increase in ipsilesional hit rate, but no increase in false alarm rate, due to easy discriminability of the distractor. These changes should result in a shift for both contralesional and ipsilesional criteria towards “less contra” combined with a change in d-prime values (**Figure 2.5C**). For the contralesional perceptual discrimination deficit hypothesis, we expect a decrease in the contralesional hit rate and an increase in the false alarm rate resulting in a decrease in contralesional d-prime (**Figure 2.5C**).

For the criterion, we found a significant main effect for “Perturbation” in both monkeys (M1: $t(1,12) = 8.30$, $p = .014$; M2: $t(1,12) = 31.20$, $p < .001$). For the d-prime, we found significant interaction of “Perturbation” × “Hemifield” in M1 ($F(1,12) = 11.99$, $p = .005$; **Suppl. Table S2.6**). To further evaluate the selection behavior for easy discrimination, we examined the results of the follow-up tests and compared them with the hypothesis-driven simulations. For easy discrimination (**Figure 2.5D**), the false alarm rate was already near zero, so there was no room to exhibit any inactivation-induced decrease: the contralesional false alarm rate did not show an effect (independent t-test; M1: $t(1,12) = -0.94$, $p = .2$; M2: $t(1,12) = 1.82$, $p = .09$). The ipsilesional false alarm rate slightly increased, significant for one monkey (M1: $t(1,12) = 1.37$, $p = 0.37$; M2: $t(1,12) = 2.32$, $p = .04$). Consequently, both monkeys showed a significant shift for the contralesional and ipsilesional criterion towards “less contra” (M1 contra: $t(1,12) = 2.83$, $p = .015$, ipsi: $t(1,12) = 2.66$, $p = .021$; M2 contra: $t(1,12) = 3.6$, $p = .004$, ipsi: $t(1,12) = 7.66$, $p < .001$). Both monkeys also showed a significant decrease in contralesional d-prime (M1: $t(1,12) = -2.32$, $p = .039$; M2: $t(1,12) = -2.30$, $p = .04$), due to the already very low false alarm rate, and M1 showed an increase in ipsilesional d-prime (M1: $(1,12) = 3.31$, $p = .006$, M2: $(1,12) = -0.38$, $p = .71$), due to increase in ipsilesional hit rate but without corresponding increase in ipsilesional false alarm rate. Overall, the data for both difficulty levels are consistent with the spatial selection bias hypothesis.

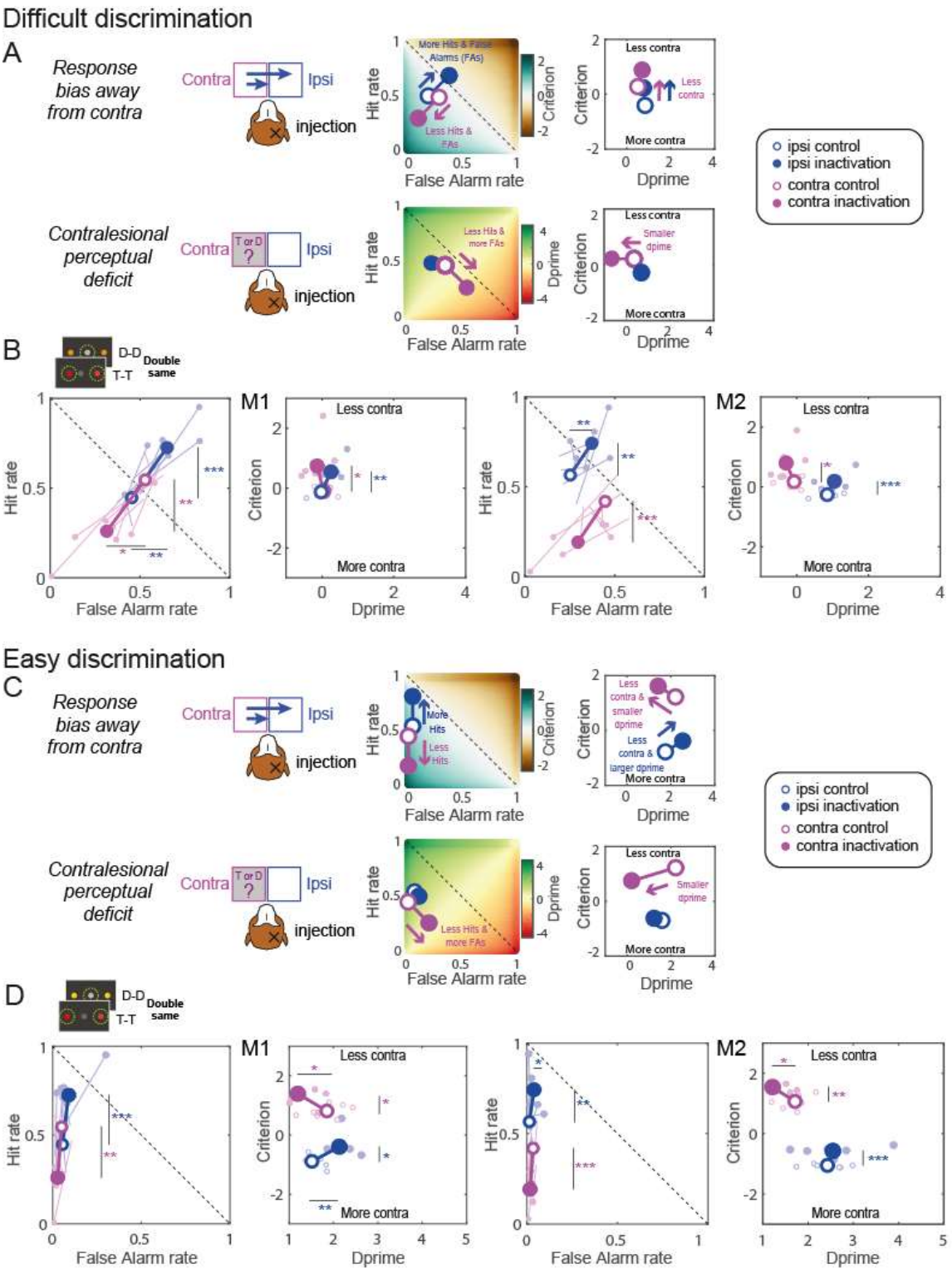

Figure 2.5. Predictions and results for double same stimuli. Same format and notations as in Figure 4. (A) Illustration of the two alternative hypotheses for the difficult discrimination in case of the double same stimuli. (B) Inactivation effects on signal detection variables for the difficult discrimination, with data separately shown for each monkey, with single sessions and overall means displayed. (C) Illustration of the two alternative hypotheses for the easy discrimination in case of the double same stimuli. (D) Inactivation effects on signal detection variables for the easy discrimination. Abbreviation: T – target, D – distractor, contra – contralesional, ipsi – ipsilesional.

The effect of inactivation for double different stimuli

Similar to the double same stimuli, the double different stimuli condition also comprises a high spatial competition between hemifields. Furthermore, might be influenced by the possibility of directly comparing the simultaneously presented target and distractor in the opposite hemifields. Notably, the central fixation is always an incorrect response option in this condition (**Suppl. Figure 2.4**).

During difficult discrimination, for the spatial selection bias hypothesis we expect the same effects as for the double same stimuli (**Figure 2.6A**). But for the perceptual discrimination deficit hypothesis and assuming the "go" bias, in contrast to double same stimuli here we expect the decrease in contralesional d-prime to be necessarily linked to the *decrease* in ipsilesional d-prime. This is because selecting less targets on the contralesional side would lead to selecting *more* distractors on the ipsilesional side, and selecting more contralesional distractors – to *less* ipsilesional targets (**Figure 2.6A**).

During difficult discrimination, the contralesional hit rate decreased significantly in both monkeys (independent t-test; M1: $t(1,12) = -2.8$, $p = .02$; M2: $t(1,12) = -2.98$, $p = .01$) and ipsilesional hit rate increased for M1 (M1: $t(1,12)= 2.92$, $p = .01$; M2: $t(1,12) = 1.49$, $p = .16$; **Figure 2.6B**). The contralesional and ipsilesional false alarm rate significantly decreased only for M1 (contra: M1: $t(1,12) = -2.9$, $p = .01$; M2: $t(1,12) = -0.65$, $p = .53$; ipsi: M1: $t(1,12) = -2.9$, $p = .01$; M2: $t(1,12) = -1.8$, $p = .09$). Consequently, we observed for the criterion a significant main effect of "Perturbation" in M1 ($F(1,12) = 6.47$, $p = .026$) and an interaction of "Perturbation" × "Hemifield" in M2 (M2: $F(1,12) = 6.88$, $p = .022$; **Suppl. Table S2.5**). In line with the response bias hypothesis, M1 showed a significant shift for the contralesional and ipsilesional criterion towards "less contra" (contra: $t(1,12) = 2.4$, $p = .03$, ipsi: $t(1,12) = 2.72$, $p = .02$) and no effect for contralesional or ipsilesional d-prime (contra: $t(1,12) = -1.42$, $p = .18$, ipsi: $t(1,12) = -2.03$, $p = .06$). Likewise, M2 showed a significant shift for the contralesional criterion towards "less contra" (M2: $t(1,12) = 2.42$, $p = .03$). But, in accordance with a significant main effect of "Perturbation" for the d-prime in M2 ($F(1,12) = 10.73$, $p = .007$), M2 also exhibited a significant decrease in contralesional and ipsilesional d-prime (contra: $t(1,12) = -3.14$, $p = .01$; ipsi: $t(1,12) = -3.32$, $p = .006$).

During easy discrimination in the presence of a yellow distractor, for the spatial selection bias hypothesis, we expect a decrease in a contralesional hit without the decrease in false alarm rate due to the "ceiling effect". We also expect no increase in the ipsilesional hit rate because it is already very high and no increase in the ipsilesional false alarm rate because of the easy discriminability of the yellow distractor (**Figure 2.6C**). For contralesional perceptual

discrimination deficit, similarly to the double same stimuli, we expect a decrease in contralesional d-prime but no effect on ipsilesional d-prime (**Figure 2.6C**).

For easy discrimination (**Figure 2.6D**), the false alarm rate was already near zero, so there was no room to exhibit any inactivation-induced contralesional decrease (independent t-test; M1: $t(1,12) = 0.8$, $p = .47$; M2: $t(1,12) = -1.87$, $p = .09$). The ipsilesional false alarm rate did not increase (M1: $t(1,12) = 0.98$, $p = .35$; M2: $t(1,12) = 1.66$, $p = .12$). The contralesional hit rate decreased for M2 (M1: $t(1,12) = -1.2$, $p = .25$; M2: $t(1,12) = -4.22$, $p < .001$). In the ANOVA, for the criterion we found a significant interaction of “Perturbation” × “Hemifield”, and the main effect of “Perturbation” in M2 but not M1 ($F(1,12) = 9.52$, $p = .009$; $F(1,12) = 22.96$, $p < .001$; **Suppl. Table S2.6**). Accordingly, only M2 showed a significant shift for the contralesional criterion towards “less contra” (M1: $t(1,12) = 0.82$, $p = .25$; M2: $t(1,12) = 4.75$, $p < .001$). Furthermore, in M2 there was a significant main effect of “Perturbation” for the d-prime ($F(1,12) = 13.49$, $p = .003$) and a corresponding decrease in contralesional and ipsilesional d-prime (contra M1: $t(1,12) = -0.82$, $p = .43$; M2: $t(1,12) = -5.16$, $p < .001$; ipsi: M1: $t(1,12) = -2.03$, $p = .07$; M2: $t(1,12) = -2.19$, $p = .049$). This decrease in d-prime was due to the “ceiling effect” of already very low false alarm rate.

To sum up these results, the inactivation effects for M1 during difficult discrimination fully matched the predictions of the spatial selection bias hypothesis (shift of both contralesional and ipsilesional criteria towards less contra). In contrast, in M2, only the contralesional criterion, for both difficulty levels, shifted towards less contra. For M2, we also observed a decrease in contralesional d-prime for both difficulty levels and a decrease in ipsilesional d-prime for the difficult discrimination. The contralesional d-prime decline can be accounted for by the “ceiling effect” on the already very low false alarm rate (for both difficulty levels), as in the single stimuli and double same stimuli conditions for easy discrimination. But the ipsilesional d-prime decrease, which only manifested in the double different stimuli condition, can be related to the compromised ability of this monkey to utilize the information from the contralesional hemifield for the direct comparison with the ipsilesional stimulus – the strategy that the monkey successfully relied on in the control sessions (*cf.* **Figure 2.3**). We further address this proposition in the Discussion.

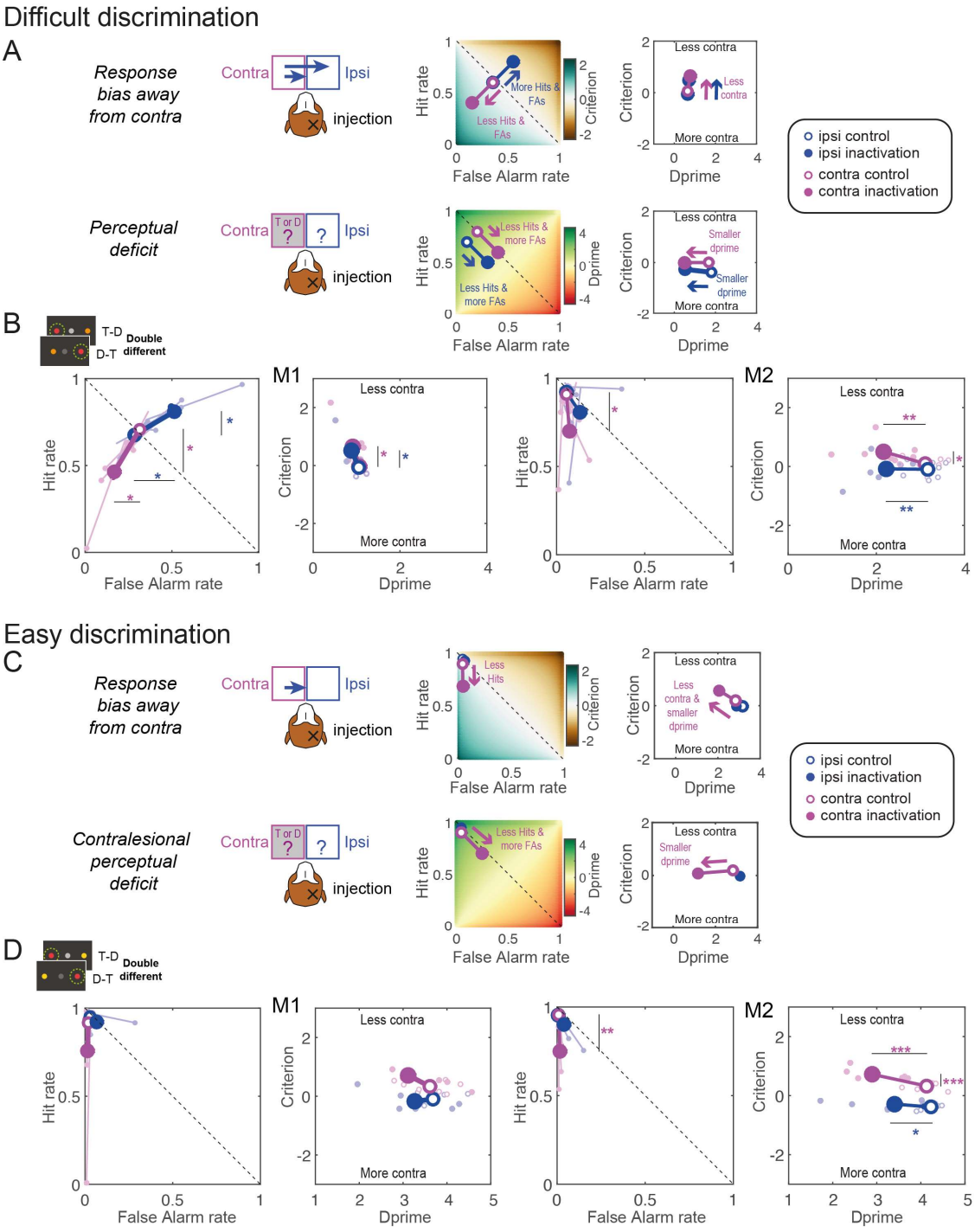

Figure 2.6. Predictions and results for double different stimuli. Same format and notations as in Figure 4. (A) Illustration of the two alternative hypotheses for the difficult discrimination in case of the double different stimuli. (B) Inactivation effects on signal detection variables for the difficult discrimination, with data separately shown for each monkey, with single sessions and overall means displayed. (C) Illustration of the two alternative hypotheses for the easy discrimination in case of the double different stimuli. (D) Inactivation effects on signal detection variables for the easy discrimination. Abbreviation: T – target, D – distractor, contra – contralesional, ipsi – ipsilesional.

Table 2.3. Summary of inactivation effects for the criterion and d-prime using independent t-tests. Significant effects are in bold font, consistent effects across the two monkeys are highlighted with gray background. **Suppl. Figures S2.5** and **S2.6** plot the summary of the corresponding data, and **Suppl. Table S2.8** for nonparametric tests.

Stimulus type	Difficulty	Measure	Hemifield	Monkey 1			Monkey 2		
				t-value	p-value	Direction of the effect	t-value	p-value	Direction of the effect
Single stimuli	difficult	criterion	contra	1.21	.25	-	**3.07**	**.01**	**Less contra**
			ipsi	-0.99	.34	-	0.15	.88	-
		d-prime	contra	-0.36	.73	-	-1.26	.23	-
			ipsi	-0.41	.69	-	-1.98	.07	-
	easy	criterion	contra	0.85	.41	-	**2.63**	**.02**	**Less contra**
			ipsi	-0.12	.91	-	-0.74	.47	-
		d-prime	contra	-1.49	.16	-	**-2.27**	**.04**	**Decrease**
			ipsi	-1.08	.30	-	-0.83	.42	-
Double same stimuli	difficult	**criterion**	**contra**	**2.68**	**.02**	**Less contra**	**2.87**	**.01**	**Less contra**
			ipsi	**3.74**	**.003**	**Less contra**	**3.80**	**.003**	**Less contra**
		d-prime	contra	-1.28	.23	-	-1.39	.18	-
			ipsi	1.89	.08	-	1.04	.32	-
	easy	**criterion**	**contra**	**2.83**	**.02**	**Less contra**	**3.60**	**.004**	**Less contra**
			ipsi	**2.66**	**.02**	**Less contra**	**7.66**	**.001**	**Less contra**
		d-prime	**contra**	**-2.32**	**.04**	**Decrease**	**-2.30**	**.04**	**Decrease**
			ipsi	**3.31**	**.006**	**Increase**	0.38	.71	-
Double different stimuli	difficult	**criterion**	**contra**	**2.40**	**.03**	**Less contra**	**2.42**	**.03**	**Less contra**
			ipsi	2.72	.02	Less contra	0.07	.95	-
		d-prime	contra	-1.42	.18	-	**-3.14**	**.009**	**Decrease**
			ipsi	-2.03	.07	-	**-3.32**	**.006**	**Decrease**
	easy	criterion	contra	1.20	.25	-	**4.75**	**.001**	**Less contra**
			ipsi	-0.58	.57	-	1.84	.09	-
		d-prime	contra	-0.82	.43	-	**-5.16**	**.001**	**Decrease**
			ipsi	-1.23	.24	-	**-2.19**	**.049**	**Decrease**

Discussion

This study used task demands such as fast perceptual color discrimination between target and distractor, spatially competing stimuli, and stimulus-congruent saccade responses to investigate whether the impairments in contralesional perceptual discrimination, as opposed to more general response bias, might contribute to visuospatial deficits after dorsal pulvinar inactivation. Following the inactivation, we primarily observed slowing of contralesional saccades and criterion shifts away from contralesional stimuli, especially when two peripheral stimuli elicited high spatial competition between hemifields (**Table 2.3**). These effects were present at both perceptual difficulty levels. Notably, the d-prime and the overall accuracy remained largely unaffected. We conclude that the contralesional visuospatial deficits observed after inactivating the dorsal pulvinar are not caused by a contralesional perceptual deficiency but by a spatial selection bias.

We adopted the Signal Detection Theory approach to differentiate between the spatial selection bias and discrimination sensitivity by calculating the response criterion and d-prime

(Luo and Maunsell, 2015). After inactivation, a shift in criterion manifested as reluctance to select stimuli in the contralesional hemifield, regardless of whether a target or distractor was presented there. This spatial selection bias and delays in making a saccade to contralesional stimuli were observed for all three stimulus conditions (single, double same, and double different). As in our previous studies (Wilke et al., 2010, 2013), we found a pronounced selection bias “away from contra” for the double same stimulus condition most similar to the free-choice between two identical targets. For single stimuli, the shift of the criterion “away from contra” was significant for one monkey and similar but not significant for the other monkey.

In contrast to the current results, Wilke et al. (2010, 2013) did not find a decrease in the correct selection of contralesional single instructed targets. In these studies, the instructed condition differed from the current single stimulus condition because monkeys invariably had to saccade to the target. Here we included a second response option, central fixation, as the correct response for the distractor trials. The presence of two options and the perceptual discrimination task context created a low level of spatial competition between the fixation and the peripheral option for single stimuli - sufficient to engender an effect from pulvinar inactivation. Hence, the dorsal pulvinar inactivation influenced the competition not only between the hemifields but also the competition between the foveal and the contralesional options. Our findings suggest that the dorsal pulvinar is involved in biasing such competition during perceptual discrimination (Desimone and Duncan, 1995; Cisek, 2006), likely via its extensive connectivity to the frontoparietal cortical network in the same hemisphere.

Support for the importance of spatial competition also comes from a pilot study by Desimone and colleagues, who inactivated the lateral pulvinar in one macaque during a color rule task that required responding with a manual lever to a briefly flashed colored target and not to a distractor (Desimone et al., 1990). The target was defined as the stimulus appearing at the same location as the briefly flashed cue. The error rate increased when the cue and the target were in contralesional hemifield while the conflicting distractor was in the ipsilesional hemifield. However, when both the target and the distractor were located within the same hemifield - thereby obviating spatial competition between hemifields - pulvinar inactivation did not yield any significant impact on performance.

Notably, in the present study the inactivation-induced selection bias occurred even in the context where only one response option is correct and rewarded. Placing a target in the contralesional hemifield when it was the only rewarded option (i.e. single target or target-distractor conditions) did not alleviate the spatial selection bias “away from contra”. Both monkeys selected the contralesional target less and instead chose the ipsilesional distractor or the fixation option, receiving no reward in these trials. Again, this contrasts with the observed alleviation of the selection bias in the value-based saccade choice task where a color cue

explicitly and unambiguously signaled a large reward (Wilke et al., 2013). Another difference to the present study was that in Wilke et al. there was a memory delay that monkeys could have used for making a deliberate value-based choice. The present results emphasize the contribution of dPul to fast decisions between conflicting options under uncertainty, in agreement with the previous inactivation study in the lateral pulvinar (Desimone et al., 1990), and in agreement with a microstimulation study from our group which showed a strong microstimulation-induced choice bias in the immediate visually-guided saccade task but not in the delayed memory-guided task (Dominguez-Vargas et al., 2017).

A hypothetical inactivation-induced contralesional perceptual discrimination deficit should cause a confusion between targets and distractors in the contralesional hemifield. This would lead to an increased false alarm rate alongside a decreased hit rate, resulting in a decreased contralesional d-prime. After inactivation, we did not observe a pattern that would be consistent with a contralesional perceptual discrimination deficit in any of the three stimulus type conditions. Previous pulvinar lesion studies in non-human primates showed unimpaired visual discrimination learning (Ungerleider and Christensen, 1977; Bender and Butter, 1987) and unimpaired contralesional visual motion discrimination performance without spatially-competing distractors (Komura et al., 2013). These studies however used manual responses that were spatially dissociated from the visual stimuli. Our study extends these findings to situations where saccadic responses are spatially-contingent on the stimuli, and where there is a competition between spatial locations. But even under these conditions, where the contribution of the pulvinar might be more crucial, the perceptual sensitivity was largely unaffected after pulvinar inactivation.

One possible strategy to accurately discriminate targets from distractors in our task is to compare the presently visible stimuli with a learned and memorized representation of the target and the distractors. This strategy could be used for all three stimulus types. For the double different condition, however, an additional strategy could be employed. The visual appearance of the two stimuli, one target, and another distractor, could be directly compared across hemifields without relying on, or in addition to, memorized representations. Indeed, both monkeys had significantly higher accuracy in the target-distractor condition than in the single or double same stimuli conditions for the difficult discrimination. Furthermore, the accuracy for easy and difficult target-distractor trials was very high and did not significantly differ during control sessions in M2. Hence, the strategy based on the direct comparison improved discrimination performance for the target-distractor condition.

After dorsal pulvinar inactivation, M2's accuracy decreased substantially for the difficult target-distractor condition, driven by a significant drop in both, contralesional and ipsilesional d-prime. We argue that this is not an indication of a specific contralesional perceptual discrimination

deficit but a consequence of a direct across-hemifield comparison strategy, and its partial failure. In this interpretation, M2 avoided going to the contralesional hemifield (due to the criterion shift), but still could utilize the information from the ipsilateral hemifield to correctly reject contralesional distractors, as demonstrated by a very low contralesional false alarm rate even after the inactivation. The resulting contralesional sensitivity decrease is thus similar to the case of easy discrimination but the ipsilesional hit rate did not increase (on the contrary, it decreased non-significantly). Instead, the contralesional hit rate decrease was compensated by more frequent central fixations. Furthermore, the ipsilesional false alarm rate increased non-significantly. We suggest that the ipsilesional sensitivity decreased because the inactivation disrupted the access to information from contralesional hemifield for comparing it to the stimulus in the ipsilesional hemifield.

Pulvinar lesions in humans (Karnath et al., 2002; Arend et al., 2008a; Snow et al., 2009) and monkeys (Petersen et al., 1987; Desimone et al., 1990; Robinson and Petersen, 1992; Zhou et al., 2016) lead to deficits in spatial attention tasks. Prior work also showed that subjects may shift either their criterion or sensitivity at the attended location relative to the unattended location (Wyart et al., 2012; Luo and Maunsell, 2015). These studies raise the possibility of relating our findings to visual spatial attention. Experiments investigating spatial attention typically use a valid or invalid cue indicating where to attend to an upcoming target without making an eye movement (Posner et al., 1980; Petersen et al., 1987; Lovejoy and Krauzlis, 2010; Luo and Maunsell, 2015; Fiebelkorn et al., 2019). Our task was not designed to investigate covert spatial attentional processes or shifts of attention, as it lacked an attentional cue. Nevertheless, our main finding of the spatial selection bias after dorsal pulvinar inactivation generally fits well with the previous work emphasizing the role of the pulvinar in selective spatial attention (Kastner and Pinsk, 2004; Halassa and Kastner, 2017).

Indeed, spatial choice bias is often considered a component, or a manifestation of attentional processing, because it captures the competition between spatial locations (Krauzlis et al., 2014; Jaramillo et al., 2019). Desimone and Duncan proposed interpreting the findings after unilateral pulvinar inactivation as formulated in the biased competition theory (Desimone and Duncan, 1995). In this framework, unilateral dorsal pulvinar inactivation puts the contralesional hemifield at a disadvantage for selection by biasing the ongoing competition for the neuronal representation of multiple stimuli, and leading to the observed bias “away from contra”. When various stimuli compete for attention, attending to one option biases the competition by enhancing the neuronal activity representing this response option within their receptive field. We speculate that the activity in the pulvinar – and/or in the connected cortical regions – in response to a salient yellow distractor will be suppressed compared to the target or a difficult distractor – as has been found in V4 during visual search in the presence of a salient pop-out

color distractor (Klink et al., 2023). After pulvinar inactivation, we expect a decrease in the saliency of the contralesional stimuli, which might also lead to altered confidence in choosing the correct response (Fetsch et al., 2014). Our task did not involve confidence judgments. It is plausible however that decreased contralesional confidence in choosing the correct response, operationalized as the increased frequency of opt-out choices (Komura et al., 2013), might result in a spatial selection bias 'away from contra' that we have observed. Conversely, the diminished confidence about contralesional stimuli may be a consequence of the observed criterion change. Further studies need to investigate the interplay between response and choice bias, sensitivity, bottom-up or/and top-down saliency of a stimulus and confidence, utilizing tasks designed to dissociate between the contributing factors (Wyart et al., 2012; Luo and Maunsell, 2015; Linares et al., 2019).

While in the present study we focused on the dorsal pulvinar, the ventral pulvinar is also associated with visual attention and salience (Saalmann et al., 2012; Saalmann and Kastner, 2015; Zhou et al., 2016). It can be considered a more perceptually-relevant visual nucleus due to extensive connectivity to the primary visual cortex and the ventral visual stream (Kaas and Lyon, 2007; Bridge et al., 2016; Kaas and Baldwin, 2020; Kagan et al., 2021). Given its connectivity, visual response properties, visual target-related microstimulation effects (Dominguez-Vargas et al., 2017), and strong perceptual modulation (Wilke et al., 2009), it would be interesting to investigate if the ventral pulvinar inactivation shows a more substantial perceptual deficit than the dorsal pulvinar.

Finally, the function of the pulvinar is often described as distractor filtering (Fischer and Whitney, 2012; Lucas et al., 2019). For instance, LaBerge and Buchsbaum (1990) investigated the contribution of the pulvinar to visual distractor processing using positron emission tomography in healthy subjects. Increased pulvinar activation was found when the target in the contralateral visual field was surrounded by distractors relative to no distractors. The authors concluded that identifying an object in a cluttered visual scene might involve the pulvinar through a filtering mechanism. Similarly, several fMRI studies also showed increased activation during more demanding distractor conditions – but these effects could have been driven by task difficulty and response competition rather than specific contralateral filtering processing (Kastner et al., 2004; Strumpf et al., 2013). Likewise, very few patient studies support the notion that the pulvinar participates in filtering out distracting visuospatial inputs in the contralateral hemifield. A study by Van der Stigchel, Arend, van Koningsbruggen, and Rafal (2010) on oculomotor capture found that patients with unilateral pulvinar lesion made slightly more errors when the target was ipsilesional and the distractor was contralesional, compared to the reverse configuration – although the effect was very small (3% error rate difference). Another study

in patients with ventral pulvinar lesions showed impaired contralateral perceptual discrimination in the presence of flanking distractors (Snow et al., 2009).

One interpretation of the distractor filtering hypothesis is that unilateral pulvinar inactivation should disrupt monitoring and filtering out the distractors in the *contralesional* hemifield. If so, we should observe an increased selection of contralesional distractors. We however found no inactivation-induced increase in false alarm rate when an easy or a difficult distractor was presented in the contralesional hemifield. An additional counterargument against the contralateral distractor filtering hypothesis can be derived from cued spatial attention tasks. The inactivation of the lateral pulvinar decreased the error rate due to contralesional distractors – i.e. decreased contralesional false alarm rate (Desimone et al., 1990). Similarly, dorsal lateral pulvinar inactivation caused faster reaction times, compared to control, when the distracting invalid cue was contralesional and the target ipsilesional (Petersen et al., 1987). Collectively, these observations, in conjunction with our findings, challenge the role of the pulvinar in filtering out contralesional distractors, particularly under conditions where stimuli are isolated and not subject to crowding. Instead, the pulvinar might be crucial for the contralateral spatial orienting and selective attention, as was also suggested in a number of patient studies that typically combined dorsal and ventral pulvinar lesions due to stroke etiology (Danziger et al., 2001, 2004; Ward and Danziger, 2005; Ward and Arend, 2007).

Outside the pulvinar, an ipsilesional selection bias and/or increased contralesional saccade latencies also occur after inactivating parietal area LIP in a visual search task (Wardak et al., 2002, 2004), or memory saccade task (Li et al., 1999; Wilke et al., 2012), and as well as after inactivating FEF in a visual search task (Wardak et al., 2006). This is in line with dorsal pulvinar's reciprocal anatomical (Blatt et al., 1990; Hardy and Lynch, 1992; Romanski et al., 1997; Gutierrez et al., 2000) and functional connections (Arcaro et al., 2018; Fiebelkorn et al., 2019; Kagan et al., 2021) with the frontoparietal cortex. In addition to the frontoparietal connectivity, recent studies also emphasize the role of the superior temporal regions – that are also interconnected with the pulvinar – in the visuospatial processing (Bogadhi et al., 2019). Of course, the specifics of impairments differ between the regions and the paradigms. For instance, the reaction time deficits in visual search target detection depended on the perceptual task difficulty after LIP but not after FEF inactivation (Wardak et al., 2006). The major challenge for the future research is to systematically characterize the degree of the involvement and the specific contribution of the interconnected subcortical and cortical circuitry to visuospatial processing.

In conclusion, this study demonstrates that dorsal pulvinar is involved in contralateral spatial orienting and resolving spatial competition, rather than in perceptual discrimination, even during a demanding perceptual decision task. Future work should further investigate the

neuronal basis of these effects in the pulvinar and in the connected cortical areas, and compare the role of the pulvinar to other subcortical structures such as the superior colliculus, known to mediate target selection and selective attention via thalamo-cortical pathways (Zenon and Krauzlis, 2012; Lovejoy and Krauzlis, 2017; Sridharan et al., 2017, 2017; Bogadhi et al., 2019; Klink et al., 2021).

Authors contributions

Conceptualization: KK, MW, IK. Data curation: KK. Formal analysis: KK, IK. Funding acquisition: MW, IK. Project Administration: IK. Supervision: MW, IK. Visualization: KK, IK. Writing—Original draft preparation: KK, IK. Writing—Review & editing: KK, MW, IK.

Acknowledgments

We thank Lydia Gibson and Uwe Zimmermann for developing the color discrimination task, Lukas Schneider for help with the monkeypsych experimental task software, and Daniela Lazzarini, Sina Plümer, Klaus Heisig, and Dirk Prüße for technical support. We also thank Stefan Treue, Alexander Gail, the Decision and Awareness Group, the Sensorimotor Group, and the Cognitive Neuroscience Laboratory for helpful discussions. Supported by the Hermann and Lilly Schilling Foundation, German Research Foundation (DFG) grants WI 4046/1-1 and Research Unit GA1475-B4, KA 3726/2-1, CNMPB Primate Platform, and funding from the Cognitive Neuroscience Laboratory.

Conflict of interest

The authors declare no competing financial interests.

Data availability statement

The datasets generated and analyzed for the current study are available from the corresponding author on reasonable request.

Supplementary Information

Dorsal pulvinar inactivation leads to spatial selection bias without perceptual deficit

Kristin Kaduk, Melanie Wilke, Igor Kagan

6 Supplementary Figures

8 Supplementary Tables

Supplementary Figures

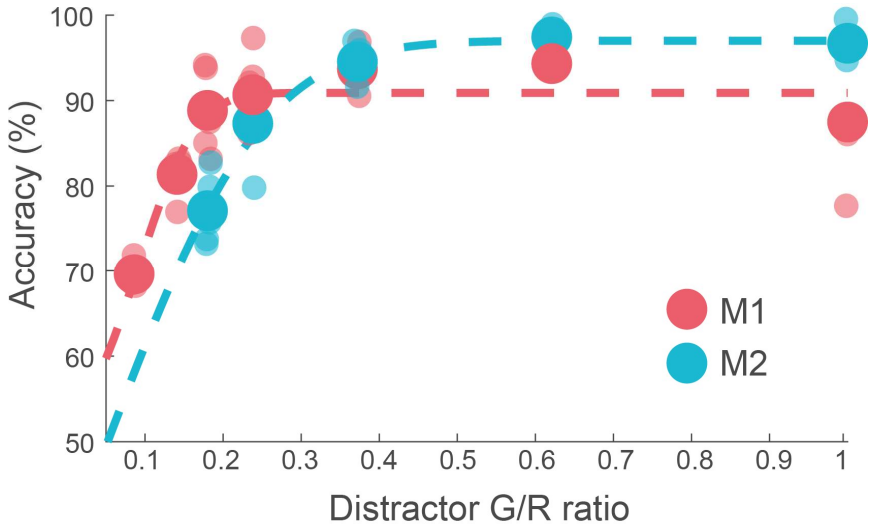

Supplementary Figure S2.1. Accuracy per distractor color. The monkeys performed a color discrimination paradigm with five distractor colors of different perceptual difficulty ranging from yellow (easy, G/R ratio: 1, RGB [60 60 0]) to red-orange (difficult, G/R ratio M1: 0.09, M2: 0.18, [M1: 128 11 0; M2: 128 23 0]). We calculated how accurate the target was discriminated from a distractor in the opposite hemifield. The large dots display the mean accuracy across sessions for the different applied G/R ratios separated for each monkey. To these accuracy values, the cumulative normal function was fitted. The small transparent dots display the accuracy per session. The goal of the assessment was to determine a distractor color that could be correctly discriminated from the target with 70 - 80% accuracy, for the difficult perceptual condition.

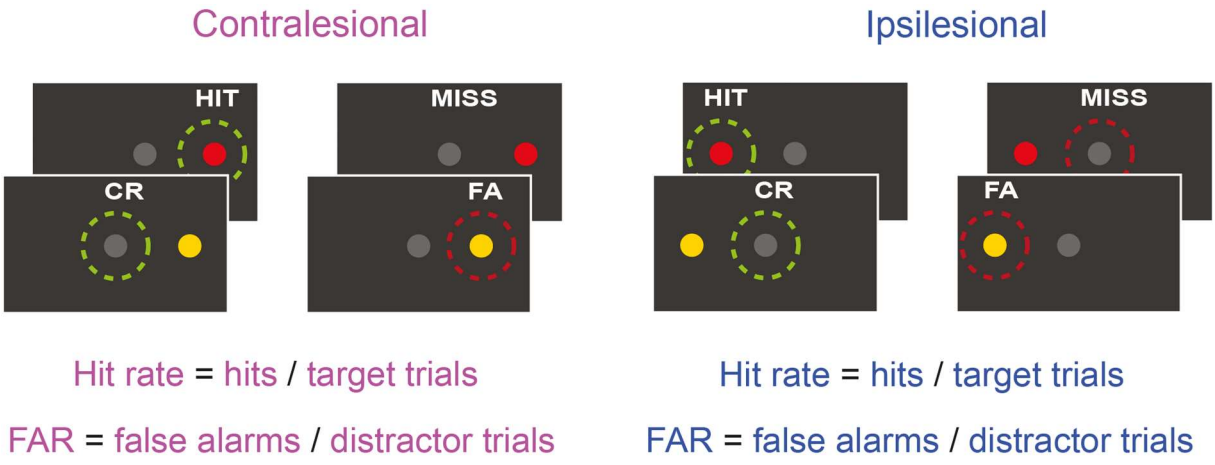

Supplementary Figure S2.2. Calculation of the signal detection theory variables for single stimuli related to the results in Figure 4. Here we describe, firstly, how trials were classified in relation to the monkey's responses and secondly, the calculations. Hits are trials where a saccade was made to a target (correct response, green dashed circle). Misses are trials where the monkey fixated the dot in the middle of the screen while a single target was displayed (incorrect response, dark red dashed circle). Correct rejections are trials where the monkey fixated the dot in the middle of the screen when a single distractor was displayed in the periphery (correct response, green dashed circle). False alarms are trials where the monkey made a saccade to the distractor (incorrect response, dark red dashed circle). We calculated the hit rate and false alarm rate (FAR) according to Hit rate = Hits / contralesional target trials and False alarm rate = False alarms / contralesional distractor trials. We used the standard calculations for the d-prime (d' = z (Hit) –z(FAR)) and criterion (c = -0.5*(z(Hit) + z(FAR))). All variables were calculated separately for stimuli presented in the ipsilesional and contralesional hemifield to compare the changes in d-prime and criterion for each hemifield.

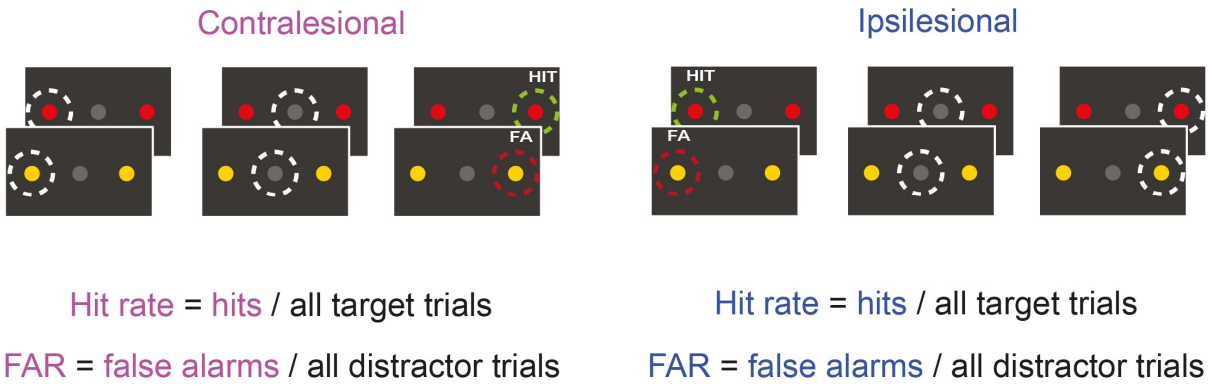

Supplementary Figure S2.3. Calculation of the signal detection theory variables for double same stimuli related to the results in Figure 5. Notations are the same as in **Suppl. Figure 2**. All variables were calculated separately for stimuli presented in the ipsilesional or contralesional hemifield, which allows us to compare the changes in d-prime and criterion for each hemifield. In the following, the examples are given for the contralesional hemifield. Contralesional hits are trials where a saccade was made to the contralesional target when a target was presented in each hemifield. Contralesional false alarms are trials where a saccade was made to the contralesional distractor when a distractor was presented in each hemifield. Hit rate is computed as all contralesional hits divided by all double same target trials. False alarm rate is computed as all contralesional false alarms divided by all double same distractor trials. We used the standard calculations for the d-prime (d' = z(Hit) –z(FAR)) and criterion (c = -0.5*(z(Hit) + z(FAR))).

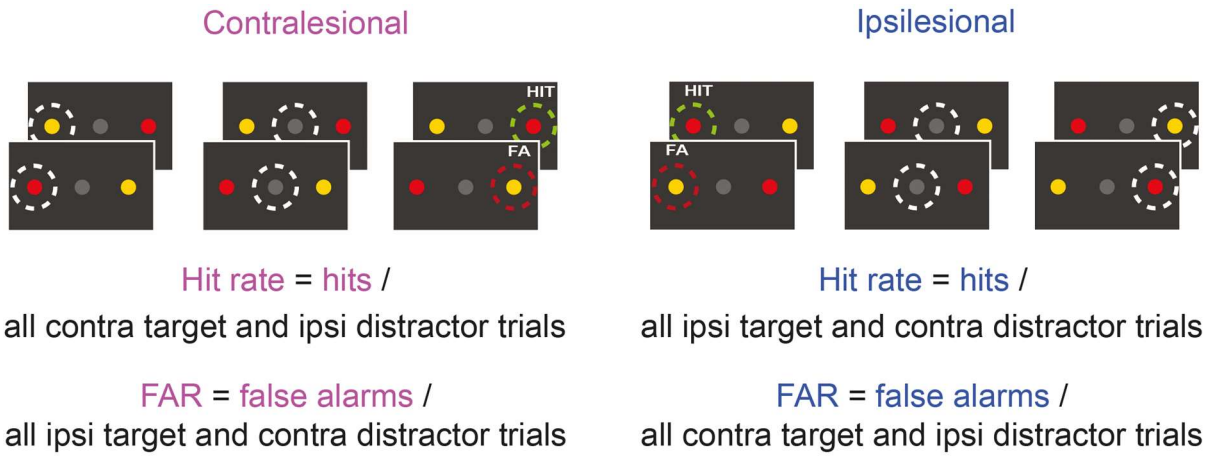

Supplementary Figure S2.4. Calculation of the signal detection theory variables for double different stimuli related to the results in Figure 6. Notations are the same as in **Suppl. Figure 2**. All variables were calculated separately for stimuli presented in the ipsilesional or contralesional hemifield, which allows us to compare the changes in d-prime and criterion for each hemifield. In the following, examples are given for the ipsilesional hemifield. Ipsilesional hits are trials where a saccade was made to the ipsilesional target. Ipsilesional false alarms are trials where a saccade was made to the ipsilesional distractor. The hit rate is computed as all ipsilesional hits divided by all double different trials where a target was presented in the ipsilesional hemifield (including all response options, i.e. fixation and saccades to either ipsi- or contralesional stimulus). Likewise, false alarm rate (FAR) is computed as all ipsilesional false alarms divided by all double different trials where a distractor was presented in the ipsilesional hemifield. We used the standard calculations for the d-prime (d' = z(Hit) –z(FAR)) and criterion (c = -0.5*(z(Hit) + z(FAR)).

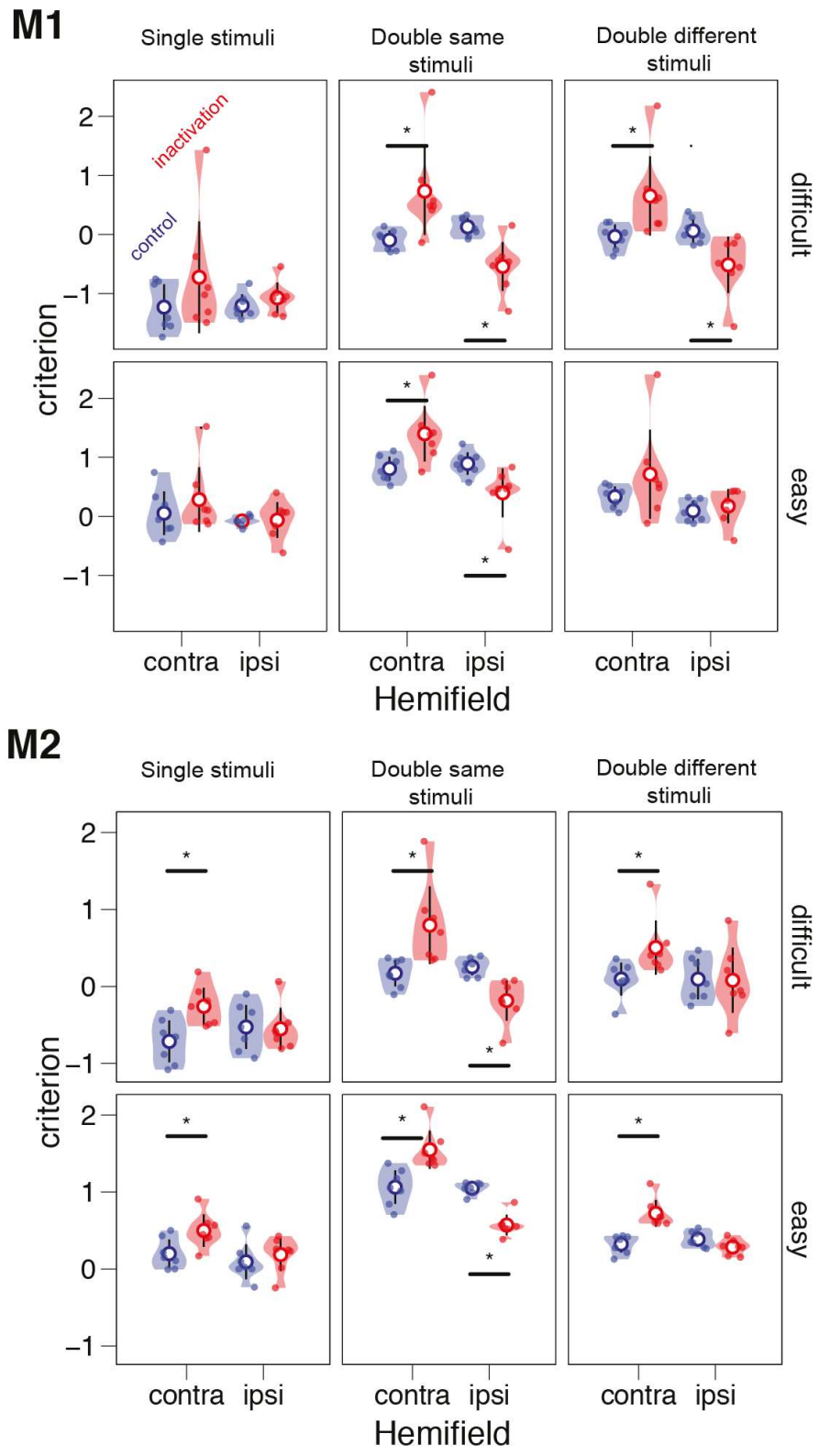

Supplementary Figure S2.5. Summary of the inactivation results for the criterion. The violin plots display the distribution of the computed values for the criterion for the two difficulty levels (difficult and easy), stimulus types (single / double same / double different stimuli), and hemifield (contra-/ipsilesional) for control (blue) and inactivation (red) sessions. The mean is displayed with an empty circle and 95% confidence intervals are shown. Each small colored dot represents a session. The stars display the significance of the t-test at the p-value < 0.05.

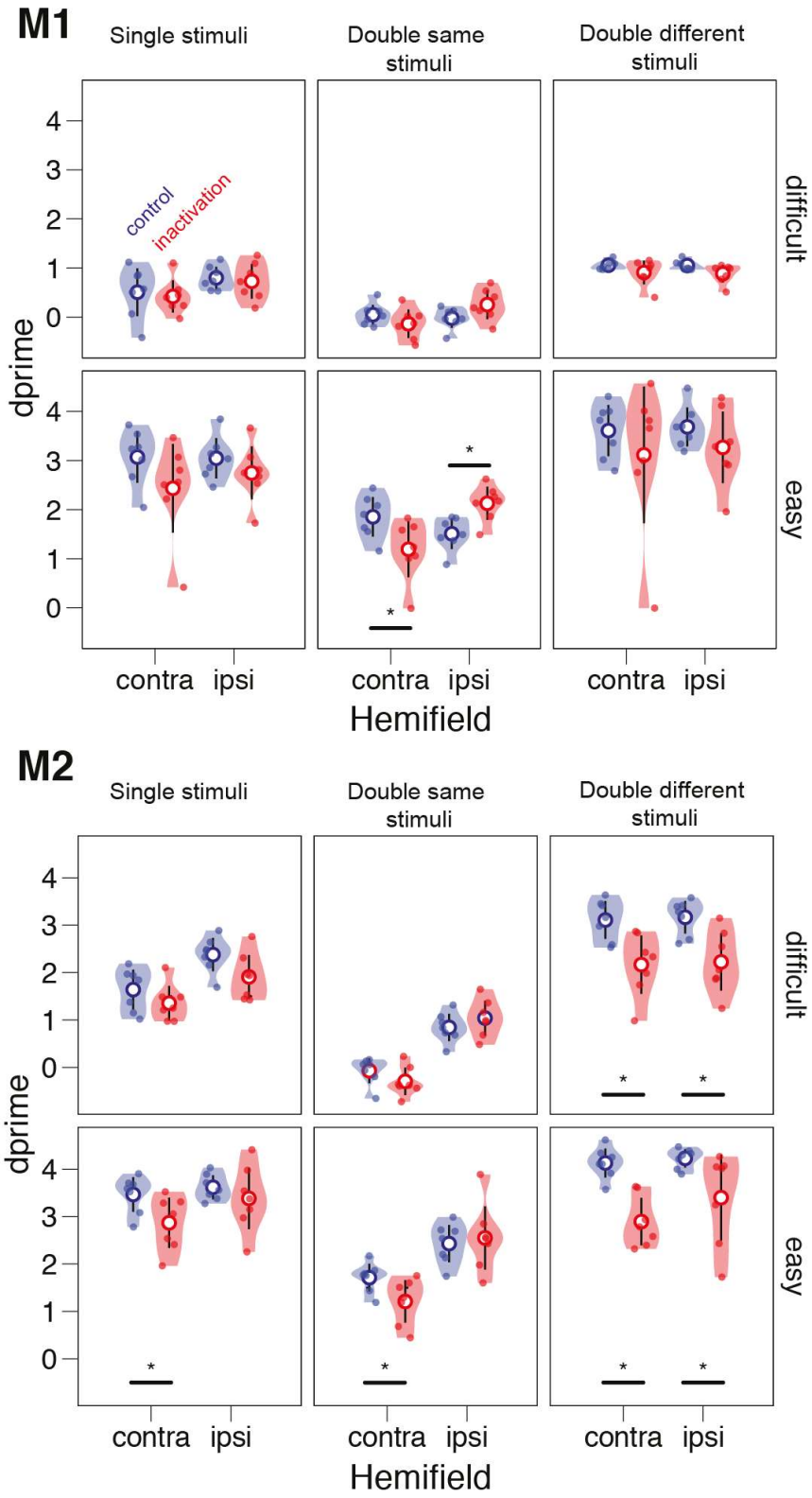

Supplementary Figure S2.6. Summary of the inactivation results for the d-prime. The violin plots display the distribution of the computed values for the criterion for the two difficulty levels (difficult and easy), stimulus types (single / double same / double different stimuli), and hemifield (contra-/ipsilesional) for control (blue) and inactivation (red) sessions. The mean is displayed with an empty circle and 95% confidence intervals are shown. Each small colored dot represents a session. The stars display the significance of the t-test at the p-value < 0.05.

Supplementary Tables

Supplementary Table S2.1. Three-way mixed ANOVA on saccade latency, with within-factors "Stimulus Type" (single / double same / double different) and "Hemifield" (contralesional/ipsilesional) and between-factor "Perturbation" (control/inactivation sessions); ges - generalized eta squared. Significant effects are shown in bold font.

Factor	DFn	DFd	F	p-value	p<.05	ges	Monkey
Perturbation	**1**	**11**	**5.96**	**0.033**	*	**0.24**	M1
Hemifield	**1**	**11**	**20.08**	**0.001**	*	**0.18**	
Stimulus Type	**2**	**22**	**25.29**	**< .001**	*	**0.20**	
Perturbation × Hemifield	**1**	**11**	**21.81**	**0.001**	*	**0.20**	
Perturbation × Stimulus Type	**2**	**22**	**5.25**	**0.014**	*	**0.05**	
Hemifield × Stimulus Type	2	22	1.12	0.344		0.02	
Perturbation × Hemifield × Stimulus Type	**2**	**22**	**4.64**	**0.021**	*	**0.07**	
Perturbation	**1**	**12**	**7.48**	**0.018**	*	**0.26**	M2
Hemifield	**1**	**12**	**6.72**	**0.024**	*	**0.15**	
Stimulus Type	**2**	**24**	**14.19**	**< .001**	*	**0.08**	
Perturbation × Hemifield	1	12	3.47	0.087		0.08	
Perturbation × Stimulus Type	2	24	1.27	0.299		0.01	
Hemifield × Stimulus Type	**2**	**24**	**11.44**	**< .001**	*	**0.05**	
Perturbation × Hemifield × Stimulus Type	**2**	**24**	**3.74**	**0.039**	*	**0.02**	

Supplementary Table S2.2. Pairwise t-tests comparing the accuracy in the different stimulus type conditions for the control sessions, separately within each perceptual difficulty (difficult/easy discrimination). Significant effects are shown in bold font.

Comparison	Difficulty	95% Confidence Intervals	t-value	p-value	p<.05	Monkey
Single Stimuli vs. Double Same Stimuli	difficult	**7.85, 21.97**	**14.91**	**< .001**	*	M1
Single Stimuli vs. Double Different Stimuli	difficult	**-20.54, -6.41**	**-13.47**	**< .001**	*	
Double Same Stimuli vs. Double Different	difficult	**-35.45, -21.30**	**-28.39**	**< .001**	*	
Single Stimuli vs. Double Same Stimuli	easy	-3.66, 0.93	-1.36	.4		
Single Stimuli vs. Double Different Stimuli	easy	-2.63, 1.94	-0.34	.9		
Double Same Stimuli vs. Double Different	easy	-1.28, 3.31	1.02	.7		
Single Stimuli vs. Double Same Stimuli	difficult	**1.92, 8.17**	**5.05**	**.001**	*	M2
Single Stimuli vs. Double Different Stimuli	difficult	**-16.91, -10.65**	**-13.79**	**< .001**	*	
Double Same Stimuli vs. Double Different	difficult	**-21.96, -15.71**	**-18.83**	**< .001**	*	
Single Stimuli vs. Double Same Stimuli	easy	-5.96, 2.35	-1.81	.8		
Single Stimuli vs. Double Different Stimuli	easy	-5.36, 2.96	-1.20	.9		
Double Same Stimuli vs. Double Different	easy	-3.56, 4.77	0.60	.9		

Supplementary Table S2.3. Three-way mixed ANOVA on accuracy, with within-factors “Stimulus Type” (single / double same / double different and “Difficulty” (difficult/easy discrimination) and between-factor “Perturbation” (control/inactivation sessions); ges - generalized eta squared. Significant effects are shown in bold font.

Factor	DFn	DFd	F	p-value	p<.05	ges	Monkey
Perturbation	1	12	1.46	0.250		0.06	
Difficulty	**1**	**12**	**349.71**	**< .001**	*	**0.87**	
Stimulus Type	**2**	**24**	**6.09**	**.007**	*	**0.11**	
Perturbation × Difficulty	1	12	1.36	.275		0.03	M1
Perturbation × Stimulus Type	2	24	3.17	.060		0.06	
Difficulty × Stimulus Type	**2**	**24**	**124.01**	**< .001**	*	**0.29**	
Perturbation × Difficulty × Stimulus Type	2	24	1.88	.175		0.01	
Perturbation	**1**	**12**	**9.42**	**.010**	*	**0.22**	
Difficulty	**1**	**12**	**421.89**	**< .001**	*	**0.72**	
Stimulus Type	**2**	**24**	**8.12**	**.002**	*	**0.24**	
Perturbation × Difficulty	1	12	0.07	.798		0.0004	M2
Perturbation × Stimulus Type	**2**	**24**	**6.40**	**.006**	*	**0.20**	
Difficulty × Stimulus Type	**2**	**24**	**104.36**	**< .001**	*	**0.48**	
Perturbation × Difficulty × Stimulus Type	2	24	1.12	.342		0.01	

Supplementary Table S2.4. Four-way mixed ANOVA on d-prime and criterion with within-factor "Stimulus type" (single / double same / double different), "Difficulty" (easy / difficult), and "Hemifield" (contralesional / ipsilesional) and between-factor "Perturbation" (control / inactivation sessions), separately for each stimulus type, for the difficult discrimination; ges - generalized eta squared. Significant effects are shown in bold font, effects involving perturbation factor are highlighted with gray background.

Factor	DFn	DFd	F	p-value	p<.05	ges	DV	Monkey
Perturbation	1	12	3.62	.081		0.18	criterion	M1
Hemifield	1	12	1.28	.281		0.01		
Difficulty	1	12	0.56	.467		0.00		
Stimulus Type	**2**	**24**	**7.14**	**.004**	*	**0.02**		
Perturbation × Hemifield	1	12	2.70	.127		0.03		
Perturbation × Difficulty	**1**	**12**	**17.86**	**.001**	*	**0.02**		
Perturbation × Stimulus Type	**2**	**24**	**17.30**	**< .001**	*	**0.05**		
Hemifield × Difficulty	**1**	**12**	**611.37**	**< .001**	*	**0.43**		
Hemifield × Stimulus Type	**2**	**24**	**220.56**	**< .001**	*	**0.48**		
Difficulty × Stimulus Type	2	24	2.71	.087		0.00		
Perturbation × Hemifield × Difficulty	1	12	0.09	.767		0.00		
Perturbation × Hemifield × Stimulus Type	2	24	1.35	.279		0.01		
Perturbation × Difficulty × Stimulus Type	**2**	**24**	**8.69**	**.001**	*	**0.01**		
Hemifield × Difficulty × Stimulus Type	**2**	**24**	**47.64**	**< .001**	*	**0.14**		
Perturbation × Hemifield × Difficulty × Stimulus Type	2	24	8.69	.116		0.01		
Perturbation	1	12	1.42	.257		0.03	d-prime	
Hemifield	1	12	3.98	.069		0.03		
Difficulty	**1**	**12**	**227.69**	**< .001**	*	**0.81**		
Stimulus Type	**2**	**24**	**105.16**	**< .001**	*	**0.55**		
Perturbation × Hemifield	1	12	4.61	.053		0.03		
Perturbation × Difficulty	1	12	0.82	.383		0.02		
Perturbation × Stimulus Type	2	24	1.75	.196		0.02		
Hemifield × Difficulty	1	12	0.07	.796		0.00		
Hemifield × Stimulus Type	2	24	0.82	.452		0.01		
Difficulty × Stimulus Type	**2**	**24**	**19.85**	**< .001**	*	**0.10**		
Perturbation × Hemifield × Difficulty	1	12	2.26	.159		0.01		
Perturbation × Hemifield × Stimulus Type	**2**	**24**	**3.99**	**.032**	*	**0.03**		
Perturbation × Difficulty × Stimulus Type	2	24	0.81	.459		0.01		
Hemifield × Difficulty × Stimulus Type	2	24	3.13	.062		0.01		

Perturbation × Hemifield × Difficulty × Stimulus Type	**2**	**24**	**3.87**	**.035**	*	**0.01**		
Perturbation	**1**	**12**	**12.14**	**.005**	*	**0.28**	criterion	M2
Hemifield	**1**	**12**	**102.84**	**< .001**	*	**0.57**		
Difficulty	1	12	0.56	.469		< 0.01		
Stimulus Type	**2**	**24**	**7.99**	**.002**	*	**0.08**		
Perturbation × Hemifield	**1**	**12**	**6.71**	**.024**	*	**0.08**		
Perturbation × Difficulty	1	12	0.39	.547		**<** 0.01		
Perturbation × Stimulus Type	**2**	**24**	**7.82**	**.002**	*	**0.08**		
Hemifield × Difficulty	**1**	**12**	**542.18**	**< .001**	*	**0.60**		
Hemifield × Stimulus Type	**2**	**24**	**202.10**	**< .001**	*	**0.64**		
Difficulty × Stimulus Type	**2**	**24**	0.82	.454		0.01		
Perturbation × Hemifield × Difficulty	1	12	1.03	.330		**<** 0.01		
Perturbation × Hemifield × Stimulus Type	2	24	2.22	.130		0.02		
Perturbation × Difficulty × Stimulus Type	2	24	0.74	.486		0.01		
Hemifield × Difficulty × Stimulus Type	**2**	**24**	**104.88**	**< .001**	*	**0.22**		
Perturbation × Hemifield × Difficulty × Stimulus Type	2	24	0.33	.723		**<** 0.01		
Perturbation	**1**	**12**	**10.00**	**.008**	*	**0.29**	d-prime	
Hemifield	**1**	**12**	**41.40**	**< .001**	*	**0.69**		
Difficulty	**1**	**12**	**591.40**	**< .001**	*	**0.77**		
Stimulus Type	**2**	**24**	**179.90**	**< .001**	*	**0.02**		
Perturbation × Hemifield	1	12	2.24	.160		0.01		
Perturbation × Difficulty	1	12	0.82	.382		0.14		
Perturbation × Stimulus Type	**2**	**24**	**8.76**	**.001**	*	**0.01**		
Hemifield × Difficulty	1	12	0.19	.674		0.14		
Hemifield × Stimulus Type	**2**	**24**	**18.44**	**< .001**	*	**0.08**		
Difficulty × Stimulus Type	**2**	**24**	**21.91**	**< .001**	*	**0.01**		
Perturbation × Hemifield × Difficulty	1	12	2.33	.153		0.01		
Perturbation × Hemifield × Stimulus Type	2	24	1.11	.346		0.01		
Perturbation × Difficulty × Stimulus Type	2	24	0.26	.774		**<** 0.01		
Hemifield × Difficulty × Stimulus Type	**2**	**24**	**3.48**	**.047**	*	**0.02**		
Perturbation × Hemifield × Difficulty × Stimulus Type	2	24	0.33	.721		**<** 0.01		

Supplementary Table S2.5. Two-way mixed ANOVA on d-prime and criterion with within-factor "Hemifield" (contralesional/ipsilesional) and between-factor "Perturbation" (control/inactivation sessions), separately for each stimulus type, **for the difficult discrimination**; ges - generalized eta squared. Significant effects are shown in bold font.

Factor	DFn	DFd	F	p-value	p<.05	ges	DV	Monkey	Stimulus type
Perturbation	1	12	0.70	.42		0.03	criterion	M1	Single
Hemifield	**1**	**12**	**98.70**	**< .001**	*	**0.80**			
Perturbation × Hemifield	1	12	2.23	.161		0.08			
Perturbation	1	12	0.31	.588		0.01	d-prime		
Hemifield	1	12	3.77	.076		0.15			
Perturbation × Hemifield	1	12	0.003	.96		< .001			
Perturbation	**1**	**12**	**6.40**	**.026**	*	**0.17**	criterion	M2	
Hemifield	**1**	**12**	**69.56**	**< .001**	*	**0.78**			
Perturbation × Hemifield	1	12	3.09	.104		0.14			
Perturbation	1	12	3.46	.087		0.18	d-prime		
Hemifield	**1**	**12**	**33.58**	**< .001**	*	**0.39**			
Perturbation × Hemifield	1	12	0.68	.425		0.013			
Perturbation	**1**	**12**	**9.65**	**.009**	*	**0.42**	criterion	M1	Double Same
Hemifield	1	12	2.19	.165		0.02			
Perturbation × Hemifield	1	12	1.11	.313		0.01			
Perturbation	1	12	0.76	.401		0.01	d-prime		
Hemifield	1	12	1.42	.256		0.09			
Perturbation × Hemifield	1	12	2.89	.115		0.17			
Perturbation	**1**	**12**	**10.43**	**.007**	*	**0.44**	criterion	M2	
Hemifield	**1**	**12**	**82.07**	**< .001**	*	**0.43**			
Perturbation × Hemifield	1	12	2.62	.132		0.02			
Perturbation	1	12	0.02	.888		0.00	d-prime		
Hemifield	**1**	**12**	**55.80**	**< .001**	*	**0.77**			
Perturbation × Hemifield	1	12	1.95	.188		0.11			
Perturbation	**1**	**12**	**6.47**	**.026**	*	**0.34**	criterion	M1	Double Different
Hemifield	1	12	4.04	.067		0.01			
Perturbation × Hemifield	1	12	1.86	.198		0.00			
Perturbation	1	12	2.91	.114		0.19	d-prime		
Hemifield	1	12	0.90	.361		0.00			
Perturbation × Hemifield	1	12	0.32	.582		0.00			
Perturbation	1	12	1.53	.24		0.10	criterion	M2	
Hemifield	**1**	**12**	**26.77**	**< .001**	*	**0.27**			
Perturbation × Hemifield	**1**	**12**	**6.88**	**.022**	*	**0.09**			
Perturbation	**1**	**12**	**10.73**	**.007**	*	**0.46**	d-prime		
Hemifield	1	12	1.23	.289		< 0.01			
Perturbation × Hemifield	1	12	< 0.01	.993		< 0.01			

Supplementary Table S2.6. Two-way mixed ANOVA on d-prime and criterion with within-factor "Hemifield" (contralesional/ipsilesional) and between-factor "Perturbation" (control/inactivation sessions), separately for each stimulus type, **for the easy discrimination**; ges - generalized eta squared. Significant effects are shown in bold font.

Factor	DFn	DFd	F	p-value	p<.05	ges	DV	Monkey	Stimulus type
Perturbation	1	12	0.37	.557		0.02	criterion	M1	Single
Hemifield	1	12	0.74	.405		0.02			
Perturbation × Hemifield	1	12	1.14	.306		0.03			
Perturbation	1	12	2.09	.174		0.12	d-prime		
Hemifield	1	12	0.84	.378		0.01			
Perturbation × Hemifield	1	12	1.16	.302		0.02			
Perturbation	1	12	1.73	.213		0.06	criterion	M2	
Hemifield	**1**	**12**	**28.33**	**< .001**	*	**0.58**			
Perturbation × Hemifield	1	12	4.59	.053		0.18			
Perturbation	1	12	3.50	.086		0.16	d-prime		
Hemifield	1	12	4.34	.059		0.11			
Perturbation × Hemifield	1	12	1.28	.279		0.04			
Perturbation	**1**	**12**	**8.30**	**.014**	*	**0.39**	criterion	M1	Double Same
Hemifield	**1**	**12**	**832.64**	**< .001**	*	**0.87**			
Perturbation × Hemifield	1	12	0.62	.445		0.01			
Perturbation	1	12	0.02	.899		0.001	d-prime		
Hemifield	1	12	2.56	.135		0.11			
Perturbation × Hemifield	**1**	**12**	**11.99**	**.005**	*	**0.37**			
Perturbation	**1**	**12**	**31.20**	**< .001**	*	**0.64**	criterion	M2	
Hemifield	**1**	**12**	**1252.30**	**< .001**	*	**0.97**			
Perturbation × Hemifield	1	12	0.004	.949		< 0.01			
Perturbation	1	12	2.052	.178		0.04	d-prime		
Hemifield	**1**	**12**	**18.84**	**< .001**	*	**0.54**			
Perturbation × Hemifield	1	12	1.72	.215		0.09			
Perturbation	1	12	0.49	.498		0.03	criterion	M1	Double Different
Hemifield	**1**	**12**	**32.22**	**< .001**	*	**0.38**			
Perturbation × Hemifield	1	12	3.93	071		0.07			
Perturbation	1	12	0.98	.342		0.07	d-prime		
Hemifield	1	12	0.46	.511		< 0.01			
Perturbation × Hemifield	1	12	0.05	.823		< 0.01			
Perturbation	**1**	**12**	**22.96**	**< .001**	*	**0.51**	criterion	M2	
Hemifield	**1**	**12**	**318.79**	**< .001**	*	**0.92**			
Perturbation × Hemifield	**1**	**12**	**9.52**	**.009**	*	**0.27**			
Perturbation	**1**	**12**	**13.49**	**.003**	*	**0.47**	d-prime		
Hemifield	1	12	4.24	.062		0.07			
Perturbation × Hemifield	1	12	1.94	.189		0.03			

Supplementary Table S2.7. Non-hemifield-specific bias ("stay" – central fixation option, vs. "go" – saccade to a peripheral stimulus) in control and inactivation sessions. The negative criterion indicated a "go" bias. The table shows the results of the two-sided t-test against zero.

Monkey	Difficulty	Session type	Stimulus type	Criterion	t-value	p-value	Bias
M1	difficult	control	single stimuli	-1.21	-11.16	< .001	Go
		inactivation		-0.89	-4.73	.003	Go
	easy	control		0.01	0.13	.903	Neutral
		inactivation		0.10	1.46	.196	Neutral
	difficult	control	double same stimuli	-2.25	-27.63	< .001	Go
		inactivation		-2.17	-14.83	< .001	Go
	easy	control		-0.54	-10.33	< .001	Go
		inactivation		-0.49	-7.05	< .001	Go
	difficult	control	double different stimuli	0.01	2.64	.039	Stay
		inactivation		0.02	2.93	.026	Stay
	easy	control		0.23	8.4	< .001	Stay
		inactivation		0.41	5.37	.002	Stay
M2	difficult	control	single stimuli	-0.65	-5.8	.001	Go
		inactivation		-0.38	-6.5	.001	Go
	easy	control		0.15	2.25	.065	Neutral
		inactivation		0.50	6.39	.001	Stay
	difficult	control	double same stimuli	-1.36	-19.69	< .001	Go
		inactivation		-1.04	-9.96	< .001	Go
	easy	control		-0.18	-2.14	.076	Neutral
		inactivation		0.09	1.04	.340	Neutral
	difficult	control	double different stimuli	0.08	2.79	.032	Stay
		inactivation		0.27	3.91	.008	Stay
	easy	control		0.41	11.35	< .001	Stay
		inactivation		0.61	9.5	< .001	Stay

Supplementary Table S2.8. Nonparametric tests (Wilcoxon rank sum test) on d-prime and criterion separately for each stimulus type, hemifield and difficulty level. Same as **Table 3**, but nonparametric. Significant effects are in bold font, consistent effects across the two monkeys are highlighted with gray background.

Stimulus type	Difficulty	Measure	Hemifield	Monkey 1			Monkey 2		
				Wilcoxon rank sum	p-value	Direction of the effect	Wilcoxon rank sum	p-value	Direction of the effect
Single stimuli	difficult	criterion	contra	44	.318	-	**34**	**.017**	**Less contra**
			ipsi	45	.383	-	53	.999	-
		d-prime	contra	59	.456	-	61	.318	-
			ipsi	57	.620	-	67	.073	-
	easy	criterion	contra	47	.535	-	**36**	**.038**	**Less contra**
			ipsi	48	.620	-	44	.318	-
		d-prime	contra	64	.165	-	**70**	**.026**	**Decrease**
			ipsi	61	.318	-	60	.383	-
Double same stimuli	difficult	**criterion**	**contra**	**73**	**.007**	**Less contra**	**74**	**.004**	**Less contra**
			ipsi	**32**	**.007**	**Less contra**	**28**	**.001**	**Less contra**
		d-prime	contra	61	.318	-	63	.209	-
			ipsi	39	.097	-	44	.318	-
	easy	**criterion**	**contra**	**72**	**.011**	**Less contra**	**75**	**.002**	**Less contra**
			ipsi	**32**	**.007**	**Less contra**	**28**	**.001**	**Less contra**
		d-prime	contra	68	.053	-	**69**	**.038**	**Decrease**
			ipsi	**32**	**.007**	**Increase**	52	.999	-
Double different stimuli	difficult	**criterion**	**contra**	**34**	**.017**	**Less contra**	**74**	**.004**	**Less contra**
			ipsi	**73**	**.007**	Less contra	**52**	.999	-
		d-prime	contra	58	.535	-	**73**	**.007**	**Decrease**
			ipsi	62	.259	-	**73**	**.007**	**Decrease**
	easy	criterion	contra	44	.318	-	**75**	**.002**	**Less contra**
			ipsi	44	.318	-	63	.209	-
		d-prime	contra	57	.259	-	**75**	**.002**	**Decrease**
			ipsi	62	.620	-	68	.053	-

3. Chapter

The effects of pulvinar microstimulation during perceptual decision-making

Kristin Kaduk, Lydia Gibson, Uwe Zimmerman, Melanie Wilke, Igor Kagan

Manuscript in preparation

Authors Contributions

LG, KK, MW, and IK designed the experiments, KK, LG, and UZ collected data and performed analyses; LG, KK, MW, and IK wrote the paper.

Acknowledgments

I acknowledge that Lydia Gibson originally developed and started this study with a different research question. Preliminary results for one monkey with a different focus of the analyses had been described previously in her doctoral thesis (Gibson, 2018). This previous work has been extended by adding the data of the second monkey and completely re-analyzing the data using the Signal Detection Theory, similar to the inactivation study.

We thank Lukas Schneider for help with the visually-guided saccade task as a control experiment, Ira Panolias, Daniela Lazzarini, Sina Plümer, Klaus Heisig, and Dirk Prüße for technical support. We also thank Stefan Treue, Alexander Gail, Decision and Awareness Group members, the Sensorimotor Group, and the Cognitive Neuroscience Laboratory for helpful discussions. Supported by the Hermann and Lilly Schilling Foundation, German Research Foundation (DFG) grants WI 4046/1-1 and Research Unit GA1475-B4, KA 3726/2-1, CNMPB Primate Platform, and funding from the Cognitive Neuroscience Laboratory.

Summary of the chapter

Microstimulation of the dorsal pulvinar after target onset (“late”) but before saccade increased the contraversive target selection in free-choice trials (Dominguez-Vargas et al., 2017). We expected that microstimulation starting after the stimulus onset but before the saccade would potentiate the function of the pulvinar. It is an open question if the enhancement of the visuospatial representation is the same for distractors and targets and how the microstimulation-induced contraversive drive interacts with the task difficulty. Here, we electrically microstimulated the dorsal pulvinar while two macaque monkeys performed a color discrimination task with varying perceptual difficulty. We used Signal Detection Theory to dissociate perceptual discrimination (dprime) and spatial selection (response criterion) effects. In the single stimuli condition with late microstimulation, the contraversive criterion or dprime remained unaffected by microstimulation, regardless of the difficulty level. For the double same stimuli condition, we observed no significant change in contraversive hit rate, criterion and dprime after late microstimulation, except for an increased contraversive dprime during easy discrimination for M2. For the double different stimuli condition, M2 showed a significant shift towards “more contra” for the difficult discrimination, whereas M1 showed a decrease in contraversive dprime. However, we primarily observed criterion shifts away from ipsiversive stimuli after late microstimulation for both difficulty levels and most stimulus conditions, manifesting as reluctance to select stimuli in the ipsiversive hemifields after late microstimulation. In addition, we also observed similar effects after early microstimulation compared to the previously reported inactivation study. In conclusion, late microstimulation of the dorsal pulvinar influenced spatial selection criteria with a consistent bias way from ipsiversive stimuli, and the contraversive dprime was mainly unaffected, suggesting that perceptual discrimination remains largely unaltered, the spatial selection is notably adapted by microstimulation.

Introduction

Several sensory, cognitive, and motor processes are ongoing as we look at or select many times in a day one out of many objects placed at different locations. The temporal integration of these underlying processes, including perception, discrimination of objects in space, and prioritizing their sensory input by selecting a location and acting towards it, determines visuospatial cognition and behavior.

Casual perturbation studies could show that a shift in bias towards ipsilaterally presented stimuli occurred due to lesions or interferences in pulvinar, superior colliculus, parietal, cingulate, and frontal brain structures. A large-scale network is involved in visuospatial cognition and selection-guided actions, including the three cortical nodes: parietal, frontal, and cingulate cortices. They are directly interconnected with one another and are additionally interconnected through participating subcortical hubs. Wardak and colleagues (2011) showed that the lateral bank of the intraparietal sulcus (LIP), located in the parietal cortex, is mainly involved in salience representation and orienting visual-spatial attention underlies saccade guidance in the presence of a competing stimulus. In contrast, the frontal eye fields (FEF), located in the frontal cortex, are implicated more in coding the location of attention or shifting the attention (Moore & Fallah, 2004) and in generating saccadic eye movements (Schall & Hanes, 1993). The specific functional roles of these brain areas are still debated (Murd et al., 2020), and additional current research emphasizes the crucial role of subcortical regions, in particular the superior colliculus, striatum, and pulvinar nucleus of the thalamus (Nobre & Mesulam, 2014) in spatial cognition.

Similar to findings of lesions and interference studies in the frontal-parietal network, patients with unilateral thalamic lesions encompassing the pulvinar have deficits in orienting or responding to visually or behaviorally relevant stimuli in the contralesional hemifield (Arend, Machado, et al., 2008; Arend, Rafal, et al., 2008; Danziger et al., 2001; Karnath et al., 2002; Lucas et al., 2019). These findings partially agree with monkey studies that can explicitly perturb the neural activity of distinct pulvinar subnuclei (Desimone et al., 1990; Komura et al., 2013; Wilke et al., 2010, 2013; Zhou et al., 2016), showing a contralateral visuospatial deficit. These deficits manifest behaviorally as contralateral attentional orienting deficit (Desimone et al., 1990), in a decrease of contralateral confidence about difficult perceptual discrimination (Komura et al., 2013) and a selection bias towards (microstimulation) or away from “contra” hemifield (inactivation) when two stimuli were presented (Dominguez-Vargas et al., 2017; Wilke et al., 2010, 2013). Such inactivation-induced bias could be alleviated by presenting only a single target or increasing the reward for contraversive targets but less so by perceptual saliency manipulations (Wilke et al., 2013). In the context of perceptual decisions, the selection

bias occurred after unilateral dorsal pulvinar inactivation regardless of whether the target or distractor was shown in the presence of a competing stimulus. Still, the ability of perceptual discrimination in the contralateral hemifield remains (see Chapter 2 of this dissertation as Kaduk et al. in prep).

Although inactivation studies provide strong evidence that normal pulvinar functioning is crucial for visuospatial cognition, particularly in the presence of competing stimuli, the limitation of inactivation studies is their long timescale (several hours) and a very strong pharmacological effect that nearly abolishes the neural activity in the inactivated region. Consequently, inactivation and lesion studies cannot employ trial-based and epoch-specific design and resolve at which processing stage a brain region exerts its impact on visuospatial cognition. A more nuanced conclusion might be drawn using temporally and spatially more selective techniques, such as electrical stimulation or optogenetics. To our knowledge, two studies investigated the temporal effects on saccade generation and target selection by applying unilateral electrical microstimulation to the dorsal pulvinar in rhesus monkeys during visually-guided and memory-guided saccades (Dominguez-Vargas et al., 2017; Kagan et al., 2021). At the stimulation site, microstimulation tended to enhance the initial task-related cue/delay period activity before a memory saccade to an ipsiversive or contraversive single target additively by a similar amount. Induced enhancements of neural activity by microstimulation were also present in different regions of the network related to spatial cognition in both hemispheres (Kagan et al., 2021). The prolonged stimulation (ten 200 ms trains during 10 s memory delay, with the last train ending ~1 s before the saccade onset) induced minimal behavioral consequences. However, a single 200 ms stimulation train applied around the time of the visually-guided saccade had a more profound behavioral effect. When microstimulation started before and overlapped with the target onset, it increased the selection of the ipsiversive targets in free-choice trials where a competing target was present in the opposite hemifield.

In contrast, microstimulation starting after the target onset increased the contraversive target selection in free-choice trials (Dominguez-Vargas et al., 2017). The authors interpreted the bidirectional effects of stimulation before (early) and after (late) stimulus onset as different manifestations of the same stimulation-induced mechanism, specifically the contraversive drive. Neither of these studies could address questions about microstimulation's specific time-dependent effects during a task involving perceptual discrimination. Therefore, this study addresses the question of how dorsal pulvinar stimulation at different time points before and during the formation and execution of a decision influences the selection behavior and saccade latencies during a perceptual discrimination task.

To test this question, unilateral, high-current stimulation was applied to the dorsal pulvinar before and during the saccadic decision, as in the previous microstimulation study. We used the same

color discrimination saccade selection task as in the inactivation study (see Chapter 2 of this dissertation), with two essential features. The perceptual difficulty with easy and difficult (i.e., perceptually similar to a target) behaviorally relevant stimuli that a saccade should not select. They are called distractors in the following for easy reference. Secondly, we introduced an option to maintain central fixation as a correct response when only distractor(s) were presented. The task involved three different stimulus types – single stimuli, double "same" stimuli (target-target or distractor-distractor), and double "different" stimuli (distractor-target). Single stimuli included a peripheral target or a distractor and a central fixation option, resulting in low spatial competition. The double stimuli had left and right peripheral stimuli and a fixation option, adding competition between hemifields. We investigated the time-dependent effect of unilateral dPul microstimulation on perceptual decision-making in the presence of competing stimuli.

We expected that microstimulation starting after the stimulus onset but before the saccade potentiates the function of the pulvinar. It is an open question if the enhancement of the visuospatial representation is the same for distractors and targets and how the microstimulation-induced contraversive drive interacts with the task difficulty. Suppose dorsal pulvinar is enhancing the visuospatial representations of distractors and targets of the contraversive hemifield in the presence of a competing stimulus in the opposite hemifield. In the case of a spatial selection bias acting as a general orienting or a contraversive drive, we expect for late microstimulation an increase in contraversive hit and false alarm rate resulting in a shift in the criterion "away from ipsi" regardless of whether an easy distractor, difficult distractor or target was presented in the opposite hemifield. On the contrary, suppose dorsal pulvinar improves the sensitivity by enhancing the discriminability of targets and distractors in the contraversive hemifield. In that case, we expect for late microstimulation an increase in contraversive hit rate and a decrease in false alarm rate resulting in increased dprime corresponding to contraversive perceptual improvement.

Furthermore, given the previous findings from the lab, we expected microstimulation of the dorsal pulvinar starting before stimulus onset, where the task required to maintain central eye fixation, biases the selection towards ipsiversive stimuli by shifting the criterion away from contra regardless of a distractor or a target is presented. In other words, we assumed that the early microstimulation in the dorsal pulvinar influences selection behavior similarly to unilateral pharmacological inactivation. i.e., inducing the ipsilateral bias, away from "contra" (although the underlying mechanism can differ). To test our hypotheses, we used the Signal Detection Theory to compute dprime, defined as the ability to discriminate between target and distractors, and the criterion, defined as selection regardless if it is a target or distractor, for each hemifield, difficulty level, and stimulus type. For unilateral microstimulation before stimulus onset, we

observed a shift in criterion away from contraversive selection regardless of the task context. Microstimulation around and after stimulus onset increased the saccade latency for contralateral saccades, and we observed a shift in criterion away from ipsiversive selection.

Methods

All experimental procedures complied with the ARRIVE guidelines (https://arriveguidelines.org) and were conducted in accordance with the European Directive 2010/63/EU, the corresponding German law governing animal welfare, and German Primate Center institutional guidelines. The procedures were approved by the responsible government agency (Niedersaechsisches Landesamt fuer Verbraucherschutz und Lebensmittelsicherheit (LAVES), Oldenburg, Germany).

Two adult male rhesus monkeys (*Macaca mulatta*), weighing 9 kg and 10.5 kg, respectively, served as subjects. For both monkeys, the surgical procedures for implanting an MRI-compatible head post and chambers including the craniotomies were the same as described in (Dominguez-Vargas et al., 2017)). MR visible markers were embedded in the head cap to aid the planning of the chamber in stereotaxic space allowing access to the right pulvinar (Monkey 1: center at 0.5 A/14.5 R mm, tilted -11 P/27 R degrees, Monkey 2: center at 4 A/21 L mm, tilted 7 P/19 L degrees) with the MR-guided stereotaxic navigation software Planner (Ohayon & Tsao, 2012). A separate surgery was performed in each animal to implant a PEEK MRI-compatible chamber (inside diameter 22 mm). After confirming chamber positioning with postsurgical MRI measurements, a partial craniotomy was made inside the chamber of each animal.

Electrical microstimulation

The microstimulation locations in the dorsal pulvinar were estimated based on anatomical MRI as described in more detail in previous work (Dominguez-Vargas et al., 2017; Kagan et al., 2021). Based on the MRI images, we planned where to target the dorsal pulvinar (the grid hole and depth) based on the anatomical MR image using the Planner (Ohayon & Tsao, 2012) and BrainVoyager (Version 2.4.2, 64-bit; Brain Innovation). To confirm the microstimulation location, we performed another anatomical MRI scan for each monkey where a platinum-iridium electrode (FHC) was placed in the corresponding grid hole and estimated depth as in the

following microstimulation experiment **(Figure 3.1 A**). A custom-made MR-compatible polyetherimide (Ultem) grid (0.8 mm hole spacing, 0.45 mm hole diameter) and a customized plastic XYZ manipulator drive (Moeller et al., 2008) were used to position platinum-iridium electrodes (FHC) in the corresponding grid hole and estimated depth. During penetration, the electrode was protected by a custom-made stainless-steel guide tube (450 µm outer diameter, 27 gauge Spinocan, Braun Melsungen). A stopper (530 µm inner diameter, 665 µm outer diameter, 23 gauge MicroFil; World Precision Instruments) ensured that the guide tube only penetrated the dura and minimally the cortex below. Before penetration, the electrode tip was aligned to the guide tube tip and was held in place by a drop of melted petroleum jelly.

An S88X dual output square pulse stimulator (Grass Products, Natus Neurology, USA) triggered by a MATLAB-based task controller software (https://github.com/dagdpz/monkeypsych) generated 200 ms trains of twin pulses at 300 Hz, which in turn started a constant current stimulus isolator A365 (World Precision Instruments, USA) to produce 60 biphasic pulses. The current (200-250 µA) was delivered to the target structure using single monopolar electrodes (platinum-iridium, 100 mm length, 125 µm thick core, initial 2 cm glass coating with an exposed tip of 40 µm, total thickness of 230 µm including polyamide tubing coating, customer part ID: UEIK1, FHC Inc., USA). A reference tungsten rod was placed in the chamber filled with saline. Voltage drop was monitored as the difference between voltage measured before and after a 10 k resistor in series with the electrode using a 4 channel 1GS/s Tektronix TDS2004C oscilloscope. The manufacturer-specified impedance of the electrodes was 300-336 kΩ. The initial impedance measured before the experiment was around 200-650 kΩ. Since the impedance dropped dramatically after a few stimulation trains were applied before each session 20-30 pulse trains were delivered to the electrode immersed in saline using 250 µA current to bring the electrode impedance to a more stable regime. Following this procedure, the impedance ranged from 20 kΩ to 70 kΩ.

Pre-test for microstimulation time windows

The stimulation time windows for the experiment were determined using a visually-guided saccade task and stimulating at different time points before and after the visual stimulus presentation. According to the findings from Dominguez-Vargas and colleagues (2017), who tested different stimulation time windows using a visually-guided saccade task, we expected that stimulation starting early before the go-signal led to a decrease in the proportion of contraversive target selection. In contrast, stimulation starting late after the go-signal resulted in an increased proportion of contraversive target choices.

Accordingly, the stimulation time windows were determined in separate sessions (15 sessions in Monkey 2, 6 sessions in Monkey 1) using a visually-guided saccade task with two different trial types (target-target, single target) task while stimulating at different time points (monkey 1: -250ms to 150 ms stimulus onset times in steps of 50 ms relative to the go-signal; stimulation onsets for monkey 2: -120 to 120 ms stimulus onset times in steps of 40ms relative to the go-signal). We tested a broader range of stimulation time windows for monkey 1 because both stimulation timings (-80 as early, +80 as late) used for monkey 2 resulted in an increase in contraversive selection for target-target trials in the color discrimination task for monkey 1 (**Figure 3.2**). We computed the mean and standard error for the percentage of contraversive selection as a function of the stimulation time window for the target-target trials across sessions to determine the target selection for each stimulation time window. Each stimulation time window was tested against the control using a paired Friedman test with post hoc Wilcoxon signed-rank tests. In the experiment, electrical microstimulation of the dorsal pulvinar was applied either at an early, intermediate, or late period relative to the go-signal (**Figure 3.1 B**), Monkey 1: 250 ms, 100 ms, or 50 ms before the go-signal, Monkey 2: 80 ms before the go-signal, simultaneously with the go-signal, or 80 ms after the go-signal).

Target selection equalization in the visually-guided saccade task

Both monkeys had a selection bias to the right side of space in choice trials during the training. To be able to assess potential target selection changes in both directions due to stimulation, we used for monkey 1 a method established by Dominquez and colleagues (2017) and which was adapted from Scherberger et al., 2003 to equalize the target selection in control trials by shifting the entire stimulus array horizontally toward the preferred right hemifield without modifying the 20-degree eccentricity from the fixation spot to the targets. The offset of the stimulus array was determined mainly during sessions where the microstimulation window was also determined using a visually-guided saccade task as described in Dominquez and colleagues (2017). Before every experimental session, the previous session's offset was re-evaluated and adjusted using the stimulus positions of the color discrimination task.

A

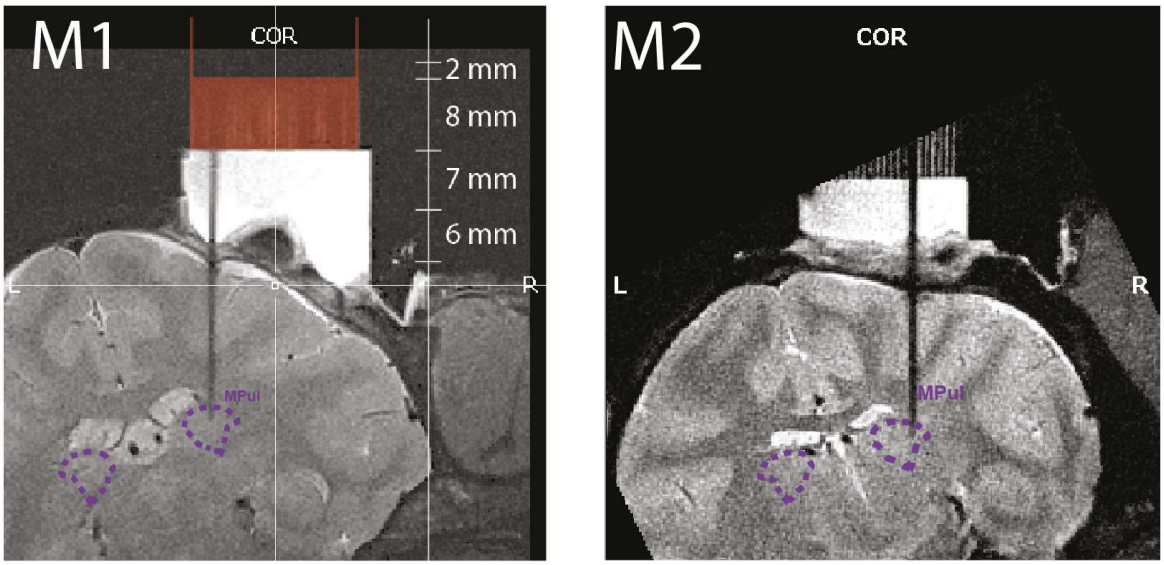

B

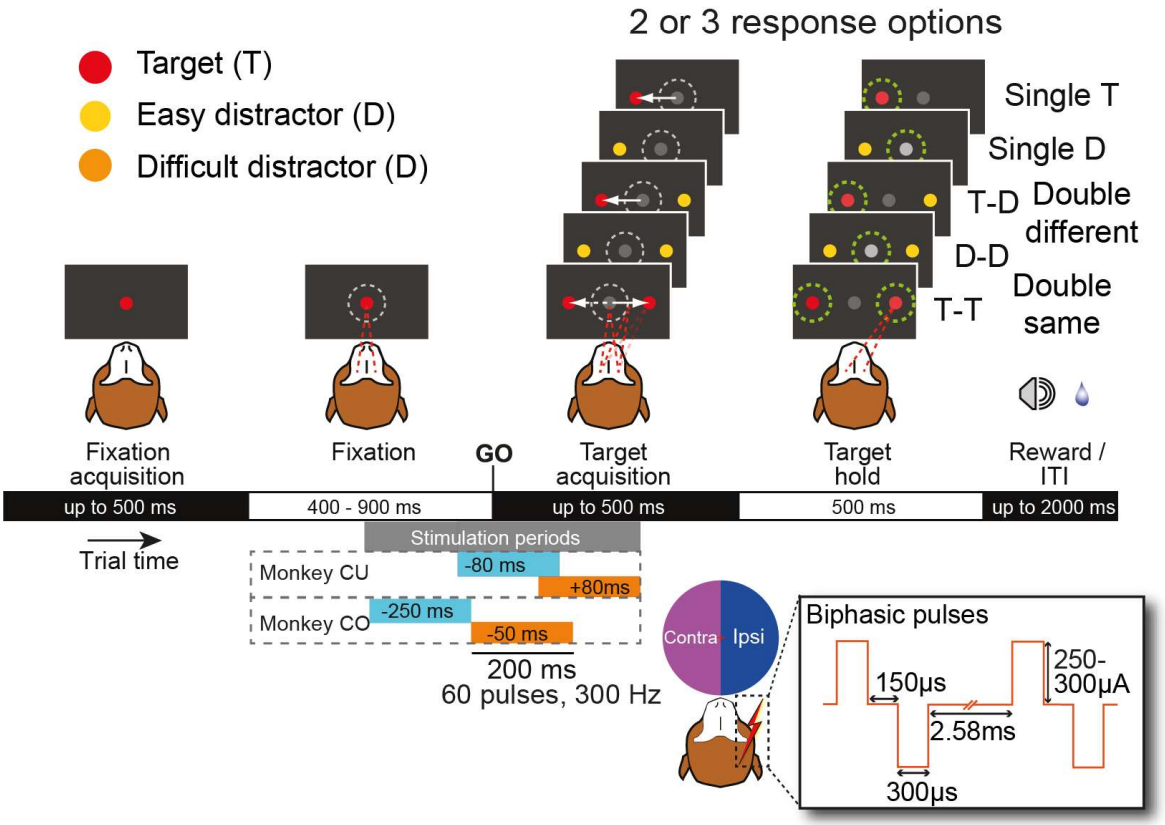

Figure 3.1. Microstimulation sites and task design. (A) MR images show the microstimulation sites. The tip of electrodes is in the medial pulvinar visualized with the overlayed borders of the medial pulvinar (MPul). (B) Two monkeys performed a color discrimination task where the perceptual difficulty was determined by the color similarity of the target (T, red) vs. distractor (D, easy - yellow, difficult - orange). Target or distractor was presented alone or with a second stimulus (distractor or target) in the opposite hemifield. Monkeys had to saccade to the target and continue fixating when only distractor(s) were

presented. Stimulation was delivered in two different periods (M1: -250ms and -50 ms before the stimulus presentation; M2: -80ms before and 80ms after the stimulus presentation).

Behavioral paradigm

The monkeys were sitting in a dark room in a custom-made primate chair with the head restrained 30 cm away from a 27" LED display (60 Hz refresh rate, model HN274H, Acer Inc. USA). The gaze position of the right eye was monitored at 220 Hz using an MCU02 ViewPoint infrared eye tracker (Arrington Research Inc. USA). The monkey's face and body were monitored with infrared cameras to ensure that microstimulation did not elicit abrupt movements or signs of discomfort. A MATLAB-based task controller (https://github.com/dagdpz/monkeypsych, MATLAB version R2012b, The MathWorks, Inc., USA) and the Psychophysics Toolbox (Brainard, 1997) were used to controlling stimulus presentation.

Fixation task

At the beginning of each stimulation session, the monkey performed an eye fixation task to determine the optimal current strength and electrode position for subthreshold microstimulation that did not evoke saccades. We first placed the electrode at the estimated location in the center of the dPul. In several blocks of 20 trials, the animals were presented with a dark grey central fixation spot (0.5° diameter) that turned light grey as soon as the animal acquired eye fixation. The monkey was required to maintain eye fixation for 2000 ms within a radial window of 5° around the fixation spot. The inter-trial interval (ITI) was 2000 ms and 1000 ms long for successful and aborted trials, respectively. In half of the trials, 500 ms after eye fixation was acquired, one current-pulse train was delivered, and the online, MATLAB-based representation of the eye position and the infrared camera images were carefully monitored to detect eye movements, including eye blinks. For monkey 2, the current strength started at 50 µA and was increased in steps of 50 µA after each block without apparent stimulation-induced eye movements until the final current strength of 200 or 250 µA was reached. For monkey 1, the current strength of 200 or 250 µA was directly tested. As soon as noticeable eye movements time-locked to the delivery of the pulse train were observed, the electrode was retrieved by approximately 0.25 mm, and the respective block was repeated. This procedure was repeated until an electrode position was found that allowed stimulation with a current strength of at least 200 µA without evoking eye movements.

Color discrimination task

Two monkeys performed a color discrimination task (**Figure 3.1 B**) where the perceptual difficulty was determined by the color similarity of the target (T, red) vs. distractor (D, easy – yellow, difficult - orange). Target or distractor was either presented alone or with a second stimulus (distractor or target) in the opposite hemifield, determining the level of spatial competition. Monkeys had to saccade to the target or continue fixating when only distractor (s) were presented. Each trial started with the presentation of a red fixation spot. The monkey initiated each trial by acquiring eye fixation by entering the 5° radial window around the fixation spot within 500 ms after the onset of the fixation spot. After maintaining fixation for 500-900 ms, the fixation spot turned gray, and one or two peripheral dots simultaneously appeared (go-signal). Red dots represented targets, whereas yellow and orange dots represented distractors. In conditions with a single peripheral stimulus, one target or distractor was presented in the left or right hemifield. The monkey was shown two dots in opposite hemifields in conditions with two peripheral stimuli. In double-target trials, two equally-rewarded targets were presented, and the monkey could choose either as a saccade target. In double-distractor trials, two distractors were shown, which had to be ignored by maintaining central fixation. In target-distractor trials, a target was presented with a distractor in the opposite hemifield. The monkey had to make a saccade towards the target while ignoring the distractor. The monkey had to choose within 500 ms (target acquisition epoch). As soon as the eye position entered the 5° radial window around one of the stimuli, the stimulus was selected, and the monkey was not allowed to reverse his decision. The chosen stimulus, either the selected peripheral dot for saccade responses or the fixation spot for maintaining eye fixation, turned bright to confirm the monkey's selection. After fixating the selected stimulus for another 500 ms, (target hold epoch), correct responses were followed by the reward tone, a fluid reward, and an intertrial interval (ITI) of 2000 ms. Incorrect answers were followed by the error tone, no fluid reward, and an ITI of 2000 ms. A trial was completed as soon as the animal either selected one of the peripheral stimuli or the fixation spot.

All stimuli were matched in luminance (dim stimuli: 11 cd/m^2, bright stimuli: 35 cd/m^2) and size (1° diameter). Targets and distractors were displayed at one of three locations per hemifield (six locations in total) with an eccentricity of 20° of visual angle. Stimulus locations were arranged concentrically around the fixation spot at 0° (mid-left), 20° (up left), 160° (upright), 180° (mid-right), 200° (down right), and 340° (down left). They were presented on a horizontal or a diagonal axis in conditions with two peripheral stimuli. All experimental conditions (stimulus type, difficulty level, spatial location) were pseudorandomized. Trials aborted before the monkey selected a stimulus returned to the pool of trials from which the next trial was chosen

randomly. Distractor colors were determined in the initial sessions of psychophysical assessment.

After initial training of the task with a yellow distractor, we determined the two distractor colors (yellow and dark orange) for the experiment based on the results of a psychophysical assessment (Monkey 1: four sessions, Monkey 2: seven sessions). In these sessions, the monkeys performed target-distractor and double-distractor trials of the color discrimination paradigm with five distractor colors of different perceptual difficulty ranging from yellow (very easy, [60 60 0]) to dark orange (very difficult, [M1:128 11 0; M2:128 23 0]). All trial conditions were presented in a pseudorandomized order. The perceptual difficulty was defined as the RGB color-coded ratio between green (G) and red (R). A stimulus with a G/R ratio of 1 is a yellow distractor (60 60 0) which is perceptually very different from the target color ([128 0 0]) with a G/R ratio of 0. Based on the psychophysical assessment of the hit rate of the contraversive and ipsiversive targets, we chose a dark orange color (M1: G/R ratio = 0.09, M2: G/R ratio = 0.18), aiming for performance above the chance level for the difficult distractor.

Data analysis

We analyzed the behavioral data for the post-testing period from two monkeys, with seven injections and seven control sessions for each monkey. Data analysis and statistical tests were performed using MATLAB R2015a. The research focuses on the saccade latencies, accuracy, and the Signal Detection Theory variables to evaluate whether there is a significant statistical difference between control and inactivation sessions. Accuracy was defined as the proportion of correct and rewarded trials among all trials in a specific condition (e.g., correct hits and rejections for all single stimuli trials, regardless of the hemifield). For calculating the saccade latencies, we used all saccades, i.e., correct target selection and erroneous distractor selection.

Saccade definition

All eye movements with a minimum velocity of 200 °/s and a minimum duration of 30 ms were considered saccades. To detect a saccade, the instantaneous saccade velocity was calculated sample by sample as the square root of the sum of squared interpolated (220 Hz to 1 kHz) and smoothed (12 ms moving average rectangular window) horizontal and vertical eye position traces. These data were smoothed again (12 ms moving average rectangular window). Saccade onset was defined as the first eye position change after the go-signal that exceeded

a velocity threshold of 200°/s. Saccade offset was the first point when eye velocity dropped below 50°/s after saccade onset.

Signal detection theory

To address our two alternative hypotheses, whether the contraversive visuospatial deficit is a consequence of a contraversive perceptual discrimination deficit or spatial selection bias, we used the Signal Detection Theory to assess changes in perceptual sensitivity index (dprime) and response criterion after unilateral reversible dorsal pulvinar microstimulation. We divided trials into hits, misses, correct rejections, and false alarms separately for stimuli presented in the contraversive (hemifield opposite to the side of microstimulation) or ipsiversive side to calculate the hit rate, false alarm rate, dprime, and criterion for each hemifield (see **Suppl. Figure S1 – S3 for chapter 2**). Dprime (d') measures how well the monkeys discriminate targets from distractors in units of d' using the hit rate and false alarm rate values. Dprime is the difference between the z-transformed hit rate and false alarm rate (Eq. 1). The response criterion indicates the tendency to select a stimulus in a specific hemifield regardless if it is a target or distractor. The response criterion was defined as the sum of the z-transformed hit and false alarm rates divided by -2 (Eq. 2).

$$d' = z(False\ alarm\ rate) - z\ (Hit\ rate) \quad (1)$$

$$c = -0.5 * z(Hit\ rate) + z\ (False\ alarm\ rate) \quad (2)$$

The data were analyzed separately for each monkey (M1 and M2), for each difficulty level (yellow and orange distractor), and stimulus type (single, double same, and double different stimuli). To compare the effect of microstimulation per hemifield, we calculated the signal detection variables separately for the contraversive and ipsiversive hemifield relative to the side of microstimulation (see the details in Supplementary Information, **Suppl. Figure S1 – S3 for chapter 2**).

Statistical analysis

To evaluate how stimulating the dorsal pulvinar before and during the formation and execution of a decision causes a spatial selection bias or a change in perceptual discrimination, we assessed the time-dependent microstimulation effects on saccade latency, response criterion, and perceptual discrimination (dprime). The data were separated for each monkey, for stimulus presentation (contraversive vs. ipsiversive), stimulus type (single, double same, and double different), and difficulty level (easy vs. difficult). The dprime and response criterion was

analyzed using a non-parametric test, the two-sided Wilcoxon rank-sum test for the equal median.

For accuracy, we compared the means of groups using three-way ANOVAs by including the within-sessions factors: “Stimulus type” with the three levels of single stimuli, double same, and double different stimuli, “Experiment” with the levels early, late, and no stimulation, “Difficulty” with the levels easy and difficult. This procedure was repeated to analyze the means of groups for the saccade latencies, adding a fourth factor, the within-sessions factor “hemifield” which involved the levels making either a saccade to the contraversive and ipsiversive hemifield. This analysis was complemented with post hoc tests to evaluate significant contrasts displayed in the stimulations related to our hypotheses.

Results

We investigated how electrically stimulating the dorsal pulvinar before and during the formation and execution of a perceptual decision influences the selection behavior and saccade latencies in a perceptual discrimination task. Electrical microstimulation in the dorsal pulvinar (**Figure 3.1 A**) was applied while two monkeys performed the color discrimination task between red targets and distractors (orange stimuli as difficult distractors and yellow stimuli as easy distractors) in three stimulus type conditions (single stimuli, double same stimuli, double different stimuli) (**Figure 3.1 B**). We expected that unilateral, high-current microstimulation during stimulus presentation but stopping before the saccade, referred to as late microstimulation in the following, potentiates the function of the pulvinar causing a general orienting (spatial selection) or an enhancement of sensitivity by enhancing the contraversive discriminability of targets and distractors (perceptual improvement). On the contrary, we expect that microstimulation starting before the stimulus onset causes a spatial selection bias “away from contra” or a deficit in sensitivity by disrupting the contraversive discrimination of targets and distractors. We analyze the following dependent variables: saccade latency, accuracy, dprime, and response criterion. To test these hypotheses, the statistical analysis focuses on the main comparison between control vs. microstimulation trials, including the following additional factors: perceptual difficulty, stimulus type, and hemifield.

Individually adjusted microstimulation windows related to selection behavior in a visually-guided saccade task

The stimulation time windows for the experiment were determined using a visually-guided saccade task and stimulating at different time points before and after the visual stimulus presentation. According to the findings from Dominguez-Vargas and colleagues (2017), who tested different stimulation time windows using a visually-guided saccade task, we expected that stimulation starting early before the go-signal led to a decrease in the proportion of contraversive target selection. In contrast, stimulation starting late after the go-signal resulted in an increased proportion of contraversive target choices.

To investigate the effects of pulvinar stimulation on visuospatial decision-making in the context of a color discrimination task, we aimed to have for each monkey one stimulation time window where the contraversive target selection decreases and a different stimulation time window where the contraversive target selection in the target-target trials significantly increased in the visually-guided saccade task. In Monkey 2, we chose 80 ms after stimulus onset as the stimulation onset time for the late stimulation window. This onset time resulted in the most

substantial increase in contraversive target selection in the free-choice task ($p < 0.01$, Wilcoxon signed-rank test, Bonferroni corrected). We chose 80 ms before the stimulus onset as the stimulation onset time for the early stimulation window as this onset time led to a significant decrease in contraversive target selection ($p < 0.05$, Wilcoxon signed-rank test, Bonferroni corrected) and, at the same time, provided symmetrical stimulation timing relative to the go-signal (Figure 3.2, Monkey 1). To reproduce the aimed pattern of saccade target selection in Monkey 1, stimulation time windows had to be shifted towards earlier stimulation onset times (Figure 2.2., Monkey 2). In Monkey 2, we chose 250 ms before the stimulus onset as the stimulation onset time for the early stimulation window because this onset time led to a significant decrease in contraversive target selection in the visually-guided saccade task ($p < 0.01$, Wilcoxon signed-rank test, Bonferroni corrected). For monkey 2, the stimulation time windows from 50ms to 50ms after the stimulus onset show a significant increase in contraversive target selection ($p < 0.05$, Wilcoxon signed-rank test, Bonferroni corrected). In the following, we choose 50 ms before the stimulus onset as the stimulation onset time for the late stimulation window for monkey 2.

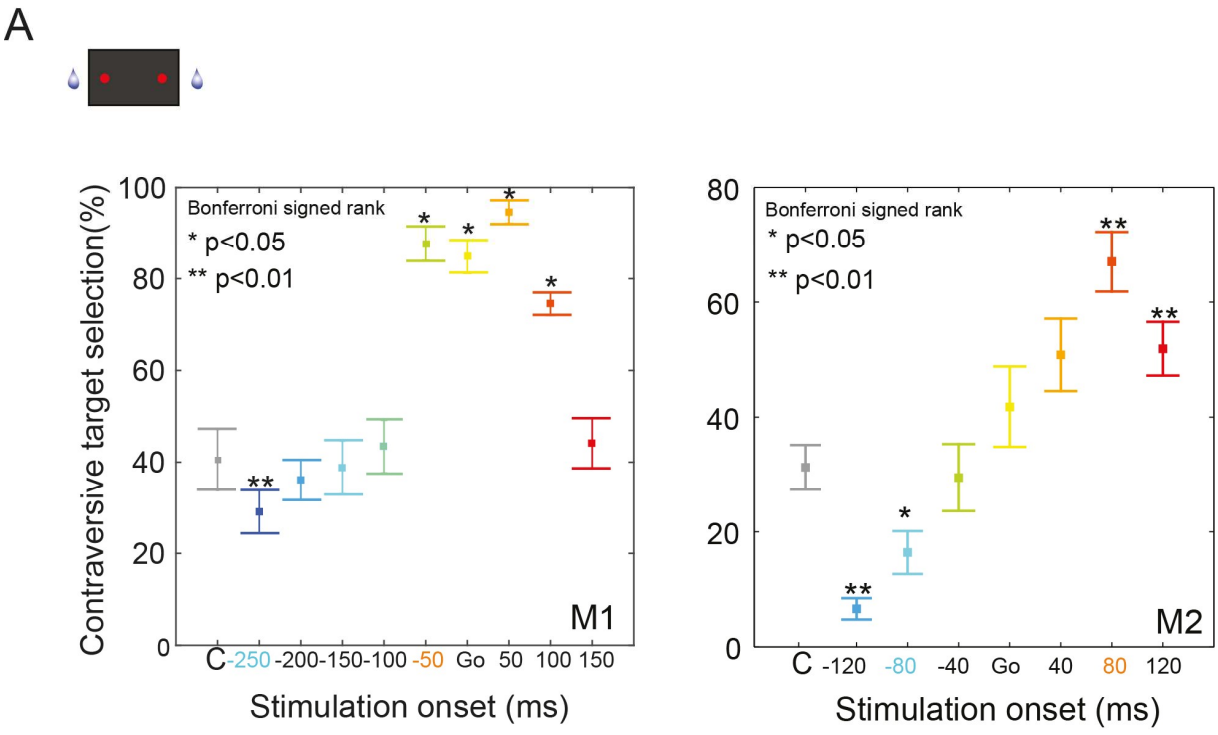

Figure 3.2. Effect of different stimulation windows on target selection in visually-guided saccade task. (A) Percentage of contraversive target selection as a function of stimulation periods. In control trials (marked as "C"), both monkeys show an ipsiversive (right) target selection bias. In stimulation trials, the current applied before the go-signal further decreased the selection of contraversive targets. Late stimulation periods increase contraversive target selection. The square represents the mean in the

graph, and the error bars show the standard error across sessions. The p-values are computed with a Friedman test followed by Wilcoxon signed-rank test, Bonferroni corrected (* p< 0.05, ** p< 0.01).

The effect of microstimulation on saccade latency

The saccade latency is a sensitive measure for the effect of dorsal pulvinar microstimulation. According to previous work, we expected slower ipsiversive and contraversive saccades after late microstimulation and faster ipsiversive saccades after early microstimulation (Dominguez-Vargas et al., 2017). Here, the saccades latency includes all responses (correct and incorrect) to a stimulus. To evaluate the microstimulation effects on saccade latencies in the color discrimination task, we compared the means of the group using a 4-way repeated measure ANOVAs (the four within factors: Experiment, Hemifield, StimulusType, Difficulty). We found for both monkeys a significant 3-way interaction of “Experiment x Hemifield x StimulusType” (4-way repeated measure ANOVAs, M1: $F(2,14) = 6.75$, $p = 0.009$, M2: $F(4,60) = 5.01$, $p = 0.001$,**Table 1**) and 3-way interaction of “Experiment x Hemifield x Difficulty” (4-way repeated measure ANOVAs, M1: $F(4,28) = 2.9$, $p = 0.04$, M2: $F(2,30) = 10.38$, $p = .001$,**Table 1**). We wanted further to evaluate the effect of microstimulation on saccade latency to compare with the previous work using dependent t-tests. The saccade latency increased for early and late microstimulation for M2 (dependent t-test, **Table 2, Figure 3.3**). Also, M2 significantly slowed down after late microstimulation of the dorsal pulvinar during contraversive and ipsiversive stimulus selection for both difficulty levels in all three stimulus types (dependent t-test, **Table 2, Figure 3.3**). After early microstimulation, M2 had faster saccade latency for ipsiversive and contraversive stimulus selection.

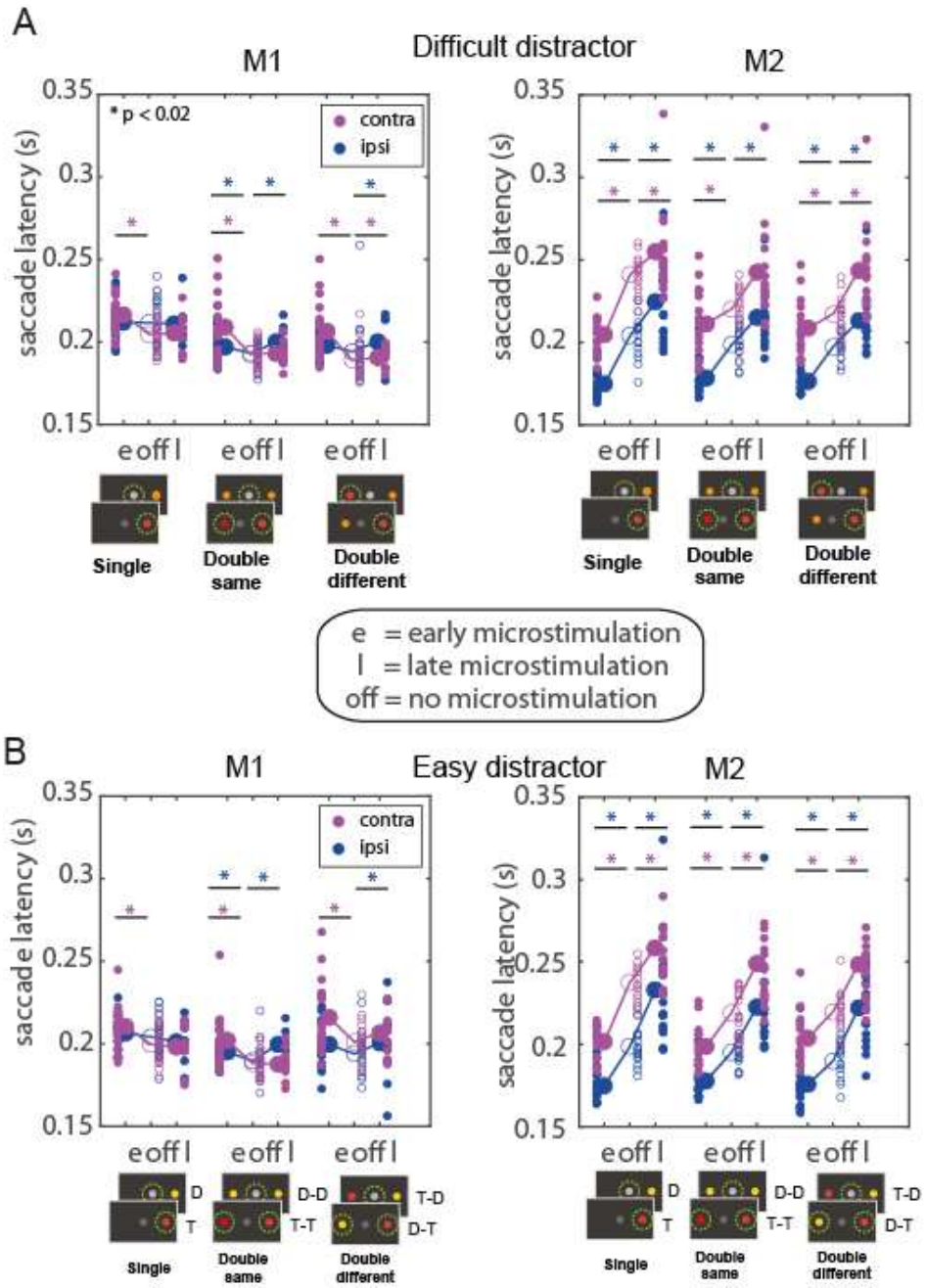

Figure 3.3 Microstimulation effects on saccade latency. The saccade latency is displayed separately for control (empty circles, Ctr) and microstimulation (filled circles, Ina) trials for each stimulus type and difficulty level. Small circles display the average of one session, and large circles indicate the mean across sessions. We tested the difference between control and microstimulation on saccade latency of either contraversive (magenta) or ipsiversive (blue) stimuli (dependent t-test, $p \leq .05$) for difficult (A) and easy (B) distractors.

Table 1. Results of the 4-way repeated ANOVAs for saccade latency

Monkey	Effect	DFn	DFd	F	p	p<.05
M1	Experiment	2	14	5.912	.014	*
	DisDifficulty	1	7	0.163	.698	
	Hemifield	1	7	0.049	.832	
	StimulusType	2	14	34.670	<.001	*
	Experiment x DisDifficulty	2	14	1.406	.278	
	Experiment x Hemifield	2	14	14.667	<.001	*
	DisDifficulty x Hemifield	1	7	9.253	.019	*
	Experiment x StimulusType	4	28	1.747	.168	
	DisDifficulty x StimulusType	2	14	37.103	<.001	*
	Hemifield x StimulusType	2	14	1.690	.220	
	Experiment x DisDifficulty x Hemifield	2	14	1.306	.302	
	Experiment x DisDifficulty x StimulusType	4	28	2.902	.040	*
	Experiment x Hemifield x StimulusType	4	28	0.765	.557	
	DisDifficulty x Hemifield x StimulusType	2	14	6.714	.009	*
	Experiment x DisDifficulty x Hemifield x StimulusType	4	28	0.199	.937	

Monkey	Effect	DFn	DFd	F	p	p<.05
	Experiment	2	30	55.582	<.001	*
M2	DisDifficulty	1	15	0.004	.949	
	Hemifield	1	15	153.021	<.001	*
	StimulusType	2	30	25.475	<.001	*
	Experiment x DisDifficulty	2	30	24.715	<.001	*
	Experiment x Hemifield	2	30	0.056	.946	
	DisDifficulty x Hemifield	1	15	1.730	.208	
	Experiment x StimulusType	4	60	15.643	<.001	*
	DisDifficulty x StimulusType	2	30	0.271	.764	
	Hemifield x StimulusType	2	30	2.567	.094	
	Experiment x DisDifficulty x Hemifield	2	30	10.382	<.001	*
	Experiment x DisDifficulty x StimulusType	4	60	1.515	.209	
	Experiment x Hemifield x StimulusType	4	60	5.012	.001	*
	DisDifficulty x Hemifield x StimulusType	2	30	0.720	.495	
	Experiment x DisDifficulty x Hemifield x StimulusType	4	60	1.535	.204	

Table 1. Results of the dependent t-test for the saccade latency.

Control compared to	Stimulus type	Difficulty	Hemifield	Monkey 1			Monkey 2		
				t-value	p-value	Direction of the effect	t-value	p-value	Direction of the effect
Late Micro-stimulation	Single stimuli	difficult	contra	0.93	.38	-	4.05	.001	slower
			ipsi	2.06	.07	-	4.84	< .001	slower
		easy	contra	2.05	.08	-	3.35	.004	slower
			ipsi	1.77	.12	-	4.60	< .001	slower
	Double same stimuli	difficult	contra	0.46	.66	-	5.48	.002	slower
			ipsi	4.37	.003	slower	3.70	.002	slower
		easy	contra	1.31	.23	-	3.70	.002	slower
			ipsi	4.23	.004	slower	3.75	.001	slower
	Double different stimuli	difficult	contra	3.34	.01	slower	4.31	.002	slower
			ipsi	3.83	.006	slower	3.79	< .001	slower
		easy	contra	0.39	.71	-	4.42	.002	slower
			ipsi	3.19	.015	slower	3.70	.002	slower
Early micro-stimulation	Single stimuli	difficult	contra	3.62	.002	slower	-18.91	< .001	faster
			ipsi	0.20	.84	-	-10.47	< .001	faster
		easy	contra	3.84	.001	slower	-14.47	< .001	faster
			ipsi	0.88	.38	-	-11.28	< .001	faster
	Double same stimuli	difficult	contra	5.09	< .001	slower	-1.68	.11	-
			ipsi	2.81	.01	slower	-6.58	< .001	faster
		easy	contra	4.72	< .001	slower	-4.26	.001	faster
			ipsi	2.48	.02	slower	-5.71	< .001	faster
	Double different stimuli	difficult	contra	4.81	< .001	slower	-2.35	.033	faster
			ipsi	1.15	.26	-	-9.70	< .001	faster
		easy	contra	2.87	.01	slower	-7.87	< .001	faster
			ipsi	1.54	.14	-	-3.28	.005	faster

The effect of microstimulation on accuracy

Here, we verified the difference in accuracy for the two difficulty levels and the three stimulus types (single stimuli, double same, and double different stimuli) as in Chapter 2. We next analyzed the effects of microstimulation on accuracy for each stimulus type and difficulty level (**Figure 3.4**) by comparing the means of groups using a 3-way repeated measure ANOVAs by including the within-sessions factors: “StimulusType” with the three levels of single stimuli, double same and double different stimuli, “Experiment” with the levels early, late and no stimulation, “Difficulty” with the levels easy and difficult perceptual similarity between target and distractor. We found for monkeys one a significant interaction of “Experiment x Difficulty x StimulusType” (3-way repeated measure ANOVAs, M1: $F(2,14) = 6.75$, $p = .009$, M2: $F(4,60) = 5.01$, $p = .001$). For monkey M1 the following 2-way interactions were significant “StimulusType x Difficulty” (3-way repeated measure ANOVAs, M1: $F(2,14) = 194.62$, $p < .001$, M2: $F(4,60) = 5.01$, $p = .001$) and “StimulusType x Experiment” (3-way repeated measure ANOVAs, M1: $F(4,28) = 5.62$, $p = .002$, see all main effects and interactions in Supplementary Tables).

Table 3. Results of the 3-way repeated measure Anova.

Monkey	Factor	DFn	DFd	F	p	p<.05
M1	Experiment	2	14	2.52	.11	
	DisDifficulty	1	7	1187.88	<.001	*
	StimulusType	2	14	47.48	<.001	*
	Experiment:DisDifficulty	2	14	2.25	.14	
	Experiment x StimulusType	4	28	5.61	.002	*
	DisDifficulty x StimulusType	2	14	194.61	<.001	*
	Experiment x DisDifficulty x StimulusType	4	28	1.44	.24	

Monkey	Factor	DFn	DFd	F	P	p<.05
M2	Experiment	2	30	79.551	<.001	*
	DisDifficulty	1	15	5717.406	<.001	*
	StimulusType	2	30	111.144	<.001	*
	Experiment x DisDifficulty	2	30	3.083	.061	
	Experiment x StimulusType	4	60	0.898	.471	
	DisDifficulty x StimulusType	2	30	61.192	<.001	*
	Experiment x DisDifficulty x StimulusType	4	60	14.69	<.001	*

To follow up on the significant interaction, we analyzed all possible contrasts with a dependent t-test. In the next step, we apply the signal detection theory to identify if the decrease in accuracy is related to a shift in response criterion or a reduction in dprime, in a hemifield-specific manner.

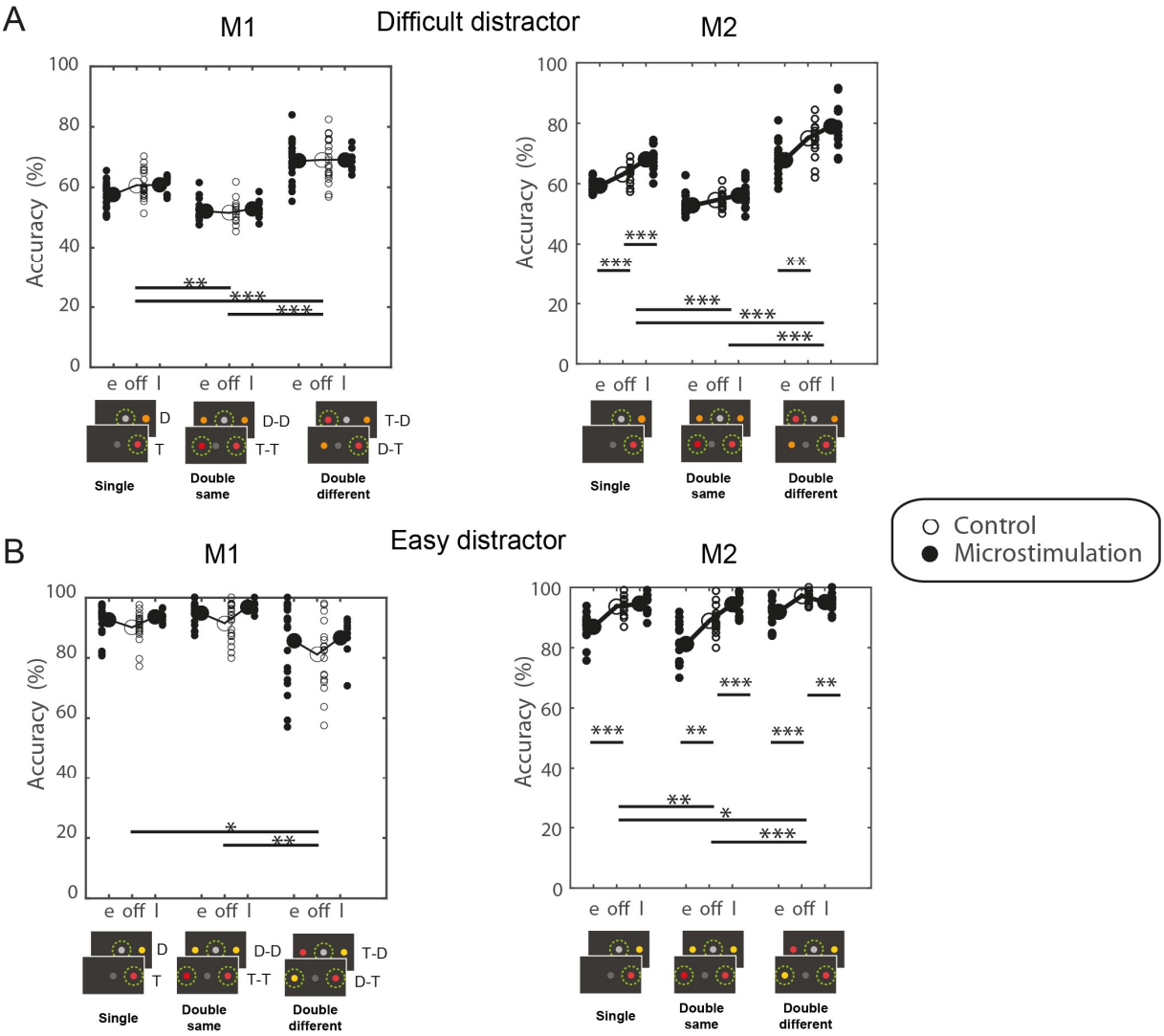

Figure 3.4 Microstimulation effects on accuracy. The accuracy is displayed separately for control (off, non-filled circles), early and late microstimulation (filled circles) trials for each stimulus type, and difficulty level. Small circles depict single sessions, and large circles indicate the mean across sessions. Here are two statistical analyses presented. We tested the difference between control and microstimulation trials and the accuracy difference between stimulus types (single, double same, double different) for the control trials. (A) Difficult distractor. The microstimulation did not affect the accuracy for M1, but the accuracy decreased for M2 after early microstimulation and increased or decreased after late microstimulation. Considering only the control sessions per stimulus type, the accuracy significantly varied between stimulus types. (B) Easy distractor. The microstimulation affected accuracy for M2 for single and double different conditions. The accuracy of the control condition was very high and did not vary between stimulus types.

The early microstimulation shifts the criterion “away from contra”

We investigate how high-current stimulation at different time points during the formation and execution of a decision influences the selection behavior and saccade latencies before or while discriminating targets from distractors in a color discrimination task. In particular, electrical

microstimulation starting before the stimulus presentation ("early microstimulation") already perturbs the neural activity in the dorsal pulvinar before the formation and execution of a decision. Microstimulation starting before the stimulus onset causes either a spatial selection bias "away from contra" (spatial selection hypothesis) or and deficit in sensitivity by disrupting the contraversive discrimination of targets and distractors (perceptual deficit hypothesis). We explain, illustrate, and quantitative hypotheses and our predictions for the different stimulus types in the corresponding results sections using simulated data and then the actual data.

Single stimuli

The single stimuli condition involves a perceptual judgment between making a saccade to a peripheral target or continuing fixating as the correct response to a peripheral distractor (low spatial competition between hemifields). To evaluate an improvement in discrimination versus a spatial selection bias, we divided trials into hits, misses, correct rejections, and false alarms separately for stimuli presented in the contraversive (hemifield opposite to the side of microstimulation) or ipsiversive side to calculate the hit rate, false alarm rate, dprime and criterion for each hemifield (**Suppl. Figure S1**). Since we used two different distractors, one distractor (yellow) being perceptually clearly different from the red target while the other (orange) requiring a difficult perceptual discrimination, we analyzed these two distractor conditions separately, contrasting them to target trials.

During difficult discrimination, if early microstimulation causes a spatial selection, we expect a similar decrease both in contraversive hit rate and false alarm rate, resulting in a shift of criterion towards "less contra" (**Figure 3.5 A**). If the early microstimulation causes a contraversive perceptual discrimination deficit, we expect a decrease in contraversive hit rate and an increase in false alarm rate, resulting in decreased contraversive dprime (**Figure 3.5 A**). We did not expect changes to the ipsiversive criterion and dprime.

In the target trials, the contraversive hit rate did not change after the early microstimulation (dependent t-test; M1: $t(1,20) = 0.5$, $p = .57$; M2: $t(1,15) = 2.0$, $p = .06$). For difficult discrimination (**Figure 3.5 B**), the contraversive false alarm rate, dprime, criterion was not affected after microstimulation ($p>.05$). Against our predictions, both monkeys showed significant decrease in ipsiversive false alarm rate (M1: $t(1,20) = -0.86$, $p = .039$, M2: $t(1,15) = -4.22$, $p = .001$) and a decrease in dprime (M1: $p = .039$; M2: $p = .039$). For M2, the criterion shifts towards "less contra" (M1: $p = .38$; M2: $p = .005$).

During easy discrimination, if dorsal pulvinar microstimulation causes a spatial selection bias, we expect a decrease in contraversive hit rate but no change in false alarm rate due to a "ceiling effect" (already very low false alarm rate in control). This will result in a shift of criterion

towards “less contra” combined with a decrease in contraversive dprime (**Figure 3.5 C**). For completeness, if the microstimulation causes a contraversive perceptual discrimination deficit, one expects a decrease in contraversive hit rate and an increase in false alarm rate (although, given the easy discriminability of the yellow distractor, we do not expect such an increase in the actual behavior). This would result in decreased contraversive dprime but no change in criterion (**Figure 3.5 C**).

For both monkeys during easy discrimination (**Figure 3.5 D**), the contraversive false alarm rate significantly decreased for M1 (dependent t-test; M1: $t(1,12) = 3.33$, $p = .003$; M2: $t(1,15) = 1.98$, $p = .06$) and the ipsiversive false alarm rate increased significantly for M2 (dependent t-test; M1: $t(1,12) = -0.4$, $p = .8$; M2: $t(1,15) = 5.23$, $p < 0.001$). No change for the contraversive criterion was seen but the contraversive dprime increased for M1 and decreased for M2 (Wilcoxon rank sum test; criterion: M1: $p = .1$; M2: $p = .5$, dprime: M1: $p = .02$; M2: $p = .04$). In addition, M2 showed a significant shift for the ipsiversive criterion towards “less contra” (Wilcoxon rank sum test; M1: $p = .9$; M2: $p = .001$), but also a decrease in ipsiversive dprime (M1: $p = .1$; M2: $p = .004$).

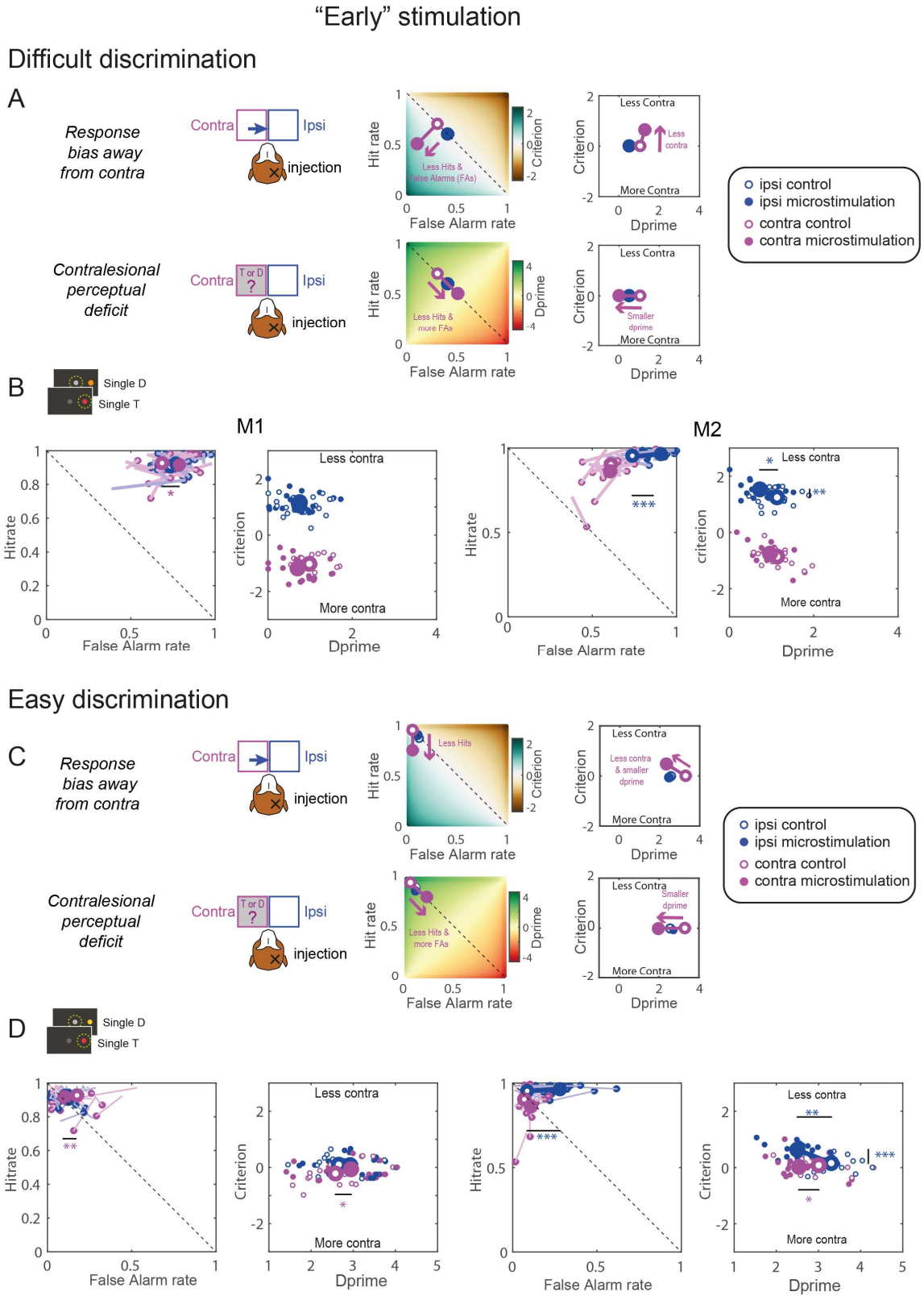

Figure 3.5. Predictions and results for single stimuli. (A) Illustration of the two alternative hypotheses for the difficult discrimination using simulated data showing the expected changes in hit rate, false alarm rate, dprime, and criterion after unilateral dPul microstimulation starting before stimulus onset. (B) Microstimulation effects on signal detection variables are displayed separately for each monkey for the difficult discrimination (orange distractor). For each monkey, the first column shows the ipsiversive (blue) and contraversive (magenta) false alarm rate and hit rate. The second column shows the ipsiversive and contraversive criterion and dprime. Small circles display single sessions, and large circles display

the mean across sessions. (C) Illustration of the two alternative hypotheses for the easy discrimination. (D) Microstimulation effects on signal detection variables for the easy discrimination (yellow distractor).

Double same stimuli

Previous studies suggested that dorsal pulvinar becomes most relevant in the case of spatial competition between hemifields. Two equally rewarded targets or two distractors were presented in the periphery during the double same stimuli condition, eliciting a high competition between hemifields for visual representation and response selection. The monkeys choose between fixating or making a saccade to one of the two peripheral stimuli (**Suppl. Figure 2 of chapter 2**).

The prediction for early microstimulation for the double same stimulus condition is identical to the predictions for this condition outlined in chapter 2 for inactivation. For the difficult discrimination, we expected a shift for both contraversive and ipsiversive criteria towards “less contra” (**Figure 3.6A**). Suppose early microstimulation causes a contraversive perceptual discrimination deficit. In that case, we expect a decrease in contraversive hit rate and an increase in contraversive false alarm rate resulting in a reduction of contraversive dprime (**Figure 3.6A**).

The contraversive hit rate decreased significantly for both monkeys (dependent t-test; M1: $t(1,20) = -5.34$, $p < .001$; M2: $t(1,15) = -5.09$, $p < .003$), and ipsiversive hit rate increased significantly (M1: $t(1,29) = 5.48$, $p < .001$ M2: $t(1,15) = 5.63$, $p < .001$). For **difficult discrimination** displayed in **Figure 3.6B**, the contraversive false alarm rate significantly decreased (M1: $t(1,20) = -4.33$, $p < 0.001$; M2: $t(1,15) = -2.61$, $p = .003$) and the ipsiversive false alarm rate significantly increased for both monkeys (M1: $t(1,20) = 3.71$, $p < .001$; M2: $t(1,20) = 3.30$, $p = .001$). Both monkeys showed a significant shift for the contraversive and ipsiversive criterion towards “less contra” (Wilcoxon rank sum test; M1 contra: $p < 0.001$, ipsi: $p < 0.001$; M2 contra: $p = .003$; ipsi: $p = .001$). Neither monkey showed a significant change in contraversive dprime (Wilcoxon rank sum test; M1: $p = .48$; M2: $p = .16$).

For easy discrimination (**Figure 3.6D**), the false alarm rate was low but not close to zero. There was some room to exhibit any microstimulation-induced decrease that was expected according to the spatial selection bias hypothesis. Hence, the contraversive false alarm rate showed a decrease for both monkeys (dependent t-test; M1: $t(1, 20) = -4.01$, $p < .001$; M2: $t(1,15) = -1.99$, $p < .003$). M2 showed also a significant increase in ipsiversive false alarm rate (M1: $t(1, 20) = 5.33$, $p = .001$; M2: $t(1,15) = 0.85$, $p < .001$). Consequently, both monkeys showed a significant shift for the contraversive and ipsiversive criterion towards “less contra” (Wilcoxon rank-sum test; M1 contra: $p < .001$, ipsi: $p = .002$; M2 contra: $p = .002$, ipsi: $p < .001$). M2 showed a significant decrease in contraversive dprime (M1: $p = .87$; M2: $p = .049$) which was

not due to an increase in contraversive false alarm rate, indicating that distractors were correctly rejected. Both monkeys showed an opposite effect for the ipsiversive dprime. M2 showed a decrease in ipsiversive dprime. M1 showed an increase in ipsiversive dprime (M1: $p = .006$, M2: $p = .008$) due to an increase in ipsiversive hit rate but without a corresponding increase in ipsiversive false alarm rate. All in all, the data support the spatial selection bias hypothesis in the case of early microstimulation.

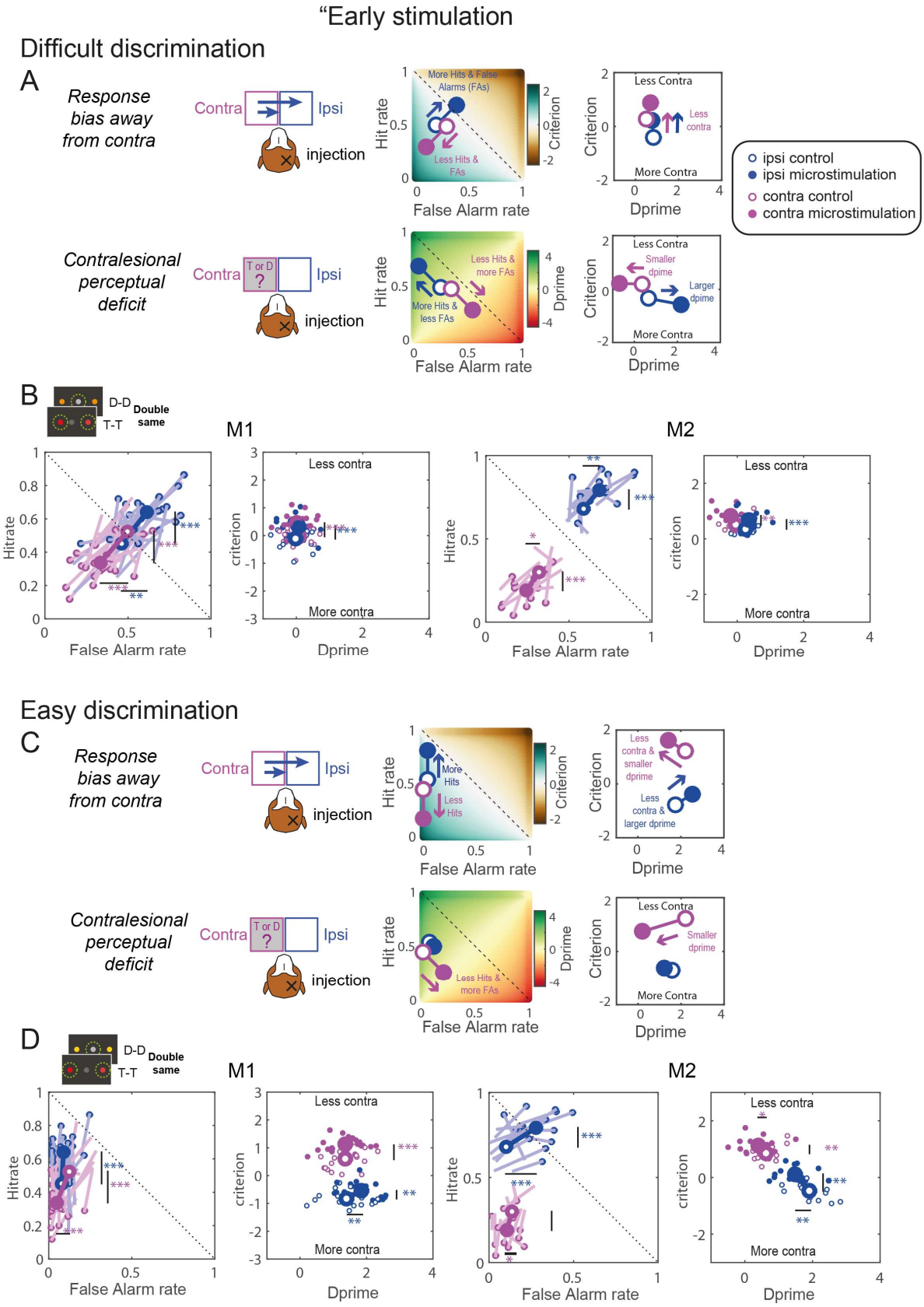

Figure 3.6. Predictions and results for double same stimuli. Same format and notations as in Figure 3.5.

Double different stimuli

The double different stimuli condition also includes a high spatial competition between hemifields. Furthermore, it is influenced by the possibility of directly comparing the simultaneously presented target and distractor in the opposite hemifields. Notably, the central fixation is always an incorrect response option (**Suppl. Figure 3**).

During difficult discrimination, for the spatial selection bias hypothesis, we expect the same effect as in the double same stimuli (**Figure 3.7A**). But for the discrimination deficit hypothesis, in contrast, to double same stimuli, assuming the "go" bias, here we expect the decrease in contraversive dprime to be necessarily linked to the *decrease* in ipsiversive dprime because selecting fewer targets on the contraversive side would lead to selecting more distractors in the ipsiversive side, and choosing more contraversive distractors – to less ipsiversive targets (**Figure 3.7A**).

The contraversive hit rate decreased significantly (dependent t-test; M1: $t(1,20) = 5.1$, $p < .001$; M2: $t(1,15) = 3.88$ $p = .001$) and ipsiversive hit rate increased for M1 (M1: $t(1,20)= 4.63$, $p < .001$; M2: $t(1,15) = 0.4$, $p = .7$; **Figure 3.7B**). The contraversive and ipsiversive false alarm rate significantly decreased only for M1 (contra: M1: $t(1,20) = -5.01$, $p < .001$; M2: $t(1,15) = 0.01$, $p = .9$; ipsi: M1: $t(1,20) = 5.01$, $p < .001$; M2: $t(1,15) = 3.71$, $p = .002$). Consequently, both monkeys showed a significant shift for the contraversive and ipsiversive criterion towards "less contra" (Wilcoxon rank sum test; M1 contra: $p < .001$, ipsi: $p < .001$, M2: contra: $p = .02$, ipsi: $p = .02$). M1 shows an increase in contraversive dprime (M1 contra: $p = .046$, ipsi: $p = .3$). In contrary, M2 showed a decrease in contraversive and ipsiversive criterion (M1 contra: $p = .03$, ipsi: $p = .034$).

During easy discrimination in the presence of a yellow distractor, for the spatial selection bias hypothesis, we expect a decrease in a contraversive hit without the reduction of false alarm rate due to the "ceiling effect". We expect no increase in the ipsiversive hit rate because it is already very high and no increase in the ipsiversive false alarm rate because of the easy discriminability of the yellow distractor (**Figure 3.7C**). For contraversive perceptual discrimination deficit, similarly to the double same stimuli, we expect a decrease in contraversive dprime but no effect on ipsiversive dprime (**Figure 3.7 C**).

For easy discrimination (**Figure 3.7D**), the contraversive false alarm rate decreased for M1 and the ipsiversive false alrm rate increases for M2 (dependent t-test; contra: M1: $t(1,20) = -2.61$, $p = .02$; M2: $t(1,15) = 1.39$, $p = .2$; ipsi: M1: $t(1,20) = 1.5$, $p = .1$; M2: $t(1,15) = 6.30$, $p = <.001$). Both monkey showed a shift of the contraversive and ipsiversive criterion towards "less contra" (Wilcoxon rank sum test, contra: M1: $p = .03$, M2: $p = .003$, ipsi: M1: $p = .002$, M2: $p = .001$). M1 showed a significant increase in ipsiversive dprime and M2 a decrease for

contraversive and ipsiversive dprime (contra: M1: p = .08, M2: p < .001; ipsi: M1: p = .02, M2: p = .001).

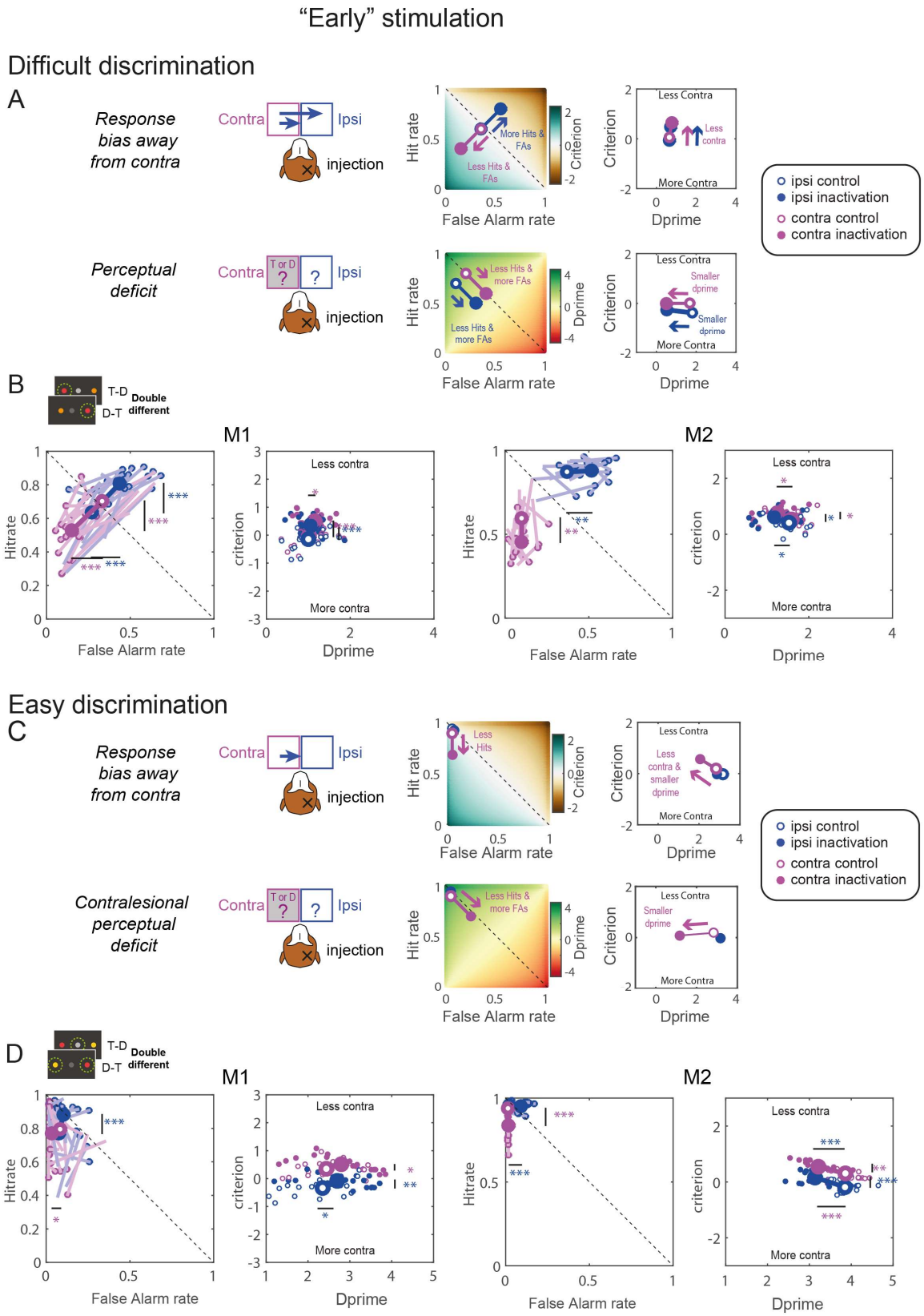

Figure 3.7. Predictions and results for double different stimuli after "early" microstimulation. Same format and notations as in Figure 3.5.

Late microstimulation shifts the criterion “away from ipsi”

We investigate how high-current stimulation at different time points during the formation and execution of a decision influences the selection behavior and saccade latencies while discriminating targets from distractors in a color discrimination task. In particular, electrical microstimulation starting around and after the stimulus presentation (“late microstimulation”) perturbs the neural activity in the dorsal pulvinar during the formation but before the execution of a decision. We expect that unilateral microstimulation starting around the stimulus onset potentiates the functions of the dorsal pulvinar, causing either a spatial selection bias “away from ipsi” (spatial selection hypothesis) or an improvement in sensitivity by improving the contraversive discrimination of targets and distractors (perceptual improvement hypothesis). We explain, illustrate, and quantitative both hypotheses and our predictions for the different stimulus types in the corresponding results sections using simulated and actual data.

Single stimuli

The single stimuli condition involves a perceptual judgment between making a saccade to a peripheral target or continuing fixating as the correct response to a peripheral distractor (low spatial competition between a central “stay” and peripheral “go” options). To evaluate an improvement in perceptual sensitivity versus a spatial selection bias, we divided trials into hits, misses, correct rejections, and false alarms separately for stimuli presented in the contraversive (hemifield opposite to the side of stimulation) or ipsiversive side to calculate the hit rate, false alarm rate, dprime and criterion for each hemifield as we have done it in Chapter 2 (see the **Suppl. Figure S1** of chapter 2). Since we used two different distractors, one easy distractor (yellow) being perceptually clearly different from the red target while the other (orange) requires a difficult perceptual discrimination, we analyzed these two distractor conditions separately, contrasting them to target trials. Here and in the following sections, we first describe quantitative predictions using simulated data and then the actual data.

During difficult discrimination, if late microstimulation causes a spatial selection bias, we expect a similar increase in contraversive hit rate and false alarm rate, resulting in a shift of criterion towards “more contra” (**Figure 3.8 A**). If late the microstimulation causes a contraversive perceptual improvement, we expect an increase in contraversive hit rate and a decrease in false alarm rate, resulting in increased contraversive dprime (**Figure 3.8A**). We did not expect changes to the ipsiversive criterion and dprime.

Both monkeys showed no significant effects on the contraversive hit rate ($p > .05$). However, for difficult discrimination (**Figure 3.8B**), the contraversive false alarm rate decreased only for M2 (M1: $t(1,8) = 0.9$, $p = .2$; M2: $t(1,15) = -2.6$, $p = .02$). Consequently, neither monkey showed a decrease in contraversive dprime or a shift for the contraversive criterion after late microstimulation (Wilcoxon rank sum test; $p > .05$). Against our predictions, M2 showed significant decrease in ipsiversive false alarm rate (M1: $t(1,8) = 0.8$, $p = .5$,M2: $t(1,15) = 4.4$, $p < .001$) and hit rate (M1: $t(1,8) = 2.9$, $p < .5$, M2: $t(1,15) = 4.7$, $p < .001$) resulting into a shift of the ipsiversive criterion towards “more contra” (criterion M1: $p = .09$; M2: $p = .001$, dprime M1: $p = .30$; M2: $p = .87$).

During easy discrimination, if late microstimulation causes a spatial selection, bias we expect an increase in contraversive hit rate and no change in false alarm rate, given that the easy yellow distractor acts more like a “stop-signal”. This will result in a shift of criterion towards “more contra” combined with an increase in contraversive dprime (**Figure 3.8C**). For completeness, if the microstimulation causes a contraversive perceptual improvement, one expects an increase in contraversive hit rate and a decrease in false alarm rate. This would result in increased contraversive dprime but no change in criterion (**Figure 3.8C**).

For both monkeys during easy discrimination (**Figure 3.8D**), the contraversive criterion or dprime were not affected after late microstimulation (Wilcoxon rank sum test; $p > .05$). Against our predictions, M2 showed significant decrease in ipsiversive false alarm rate (M1: $t(1,8) = 0.38$, $p = .5$, M2: $t(1,8) = 3.25$, $p = .005$) and hit rate (M1: $t(1,8) = 2.9$, $p < .5$, M2: $t(1,15) = 4.7$, $p < .001$) resulting into a shift in the ipsiversive criterion towards “more contra” (criterion M1: $p = .13$; M2: $p < .001$) but no change in dprime (M1: $p = .46$; M2: $p = .19$). To sum up, the data do not support the perceptual improvement hypotheses and the evidence is sparse for the spatial selection bias hypotheses.

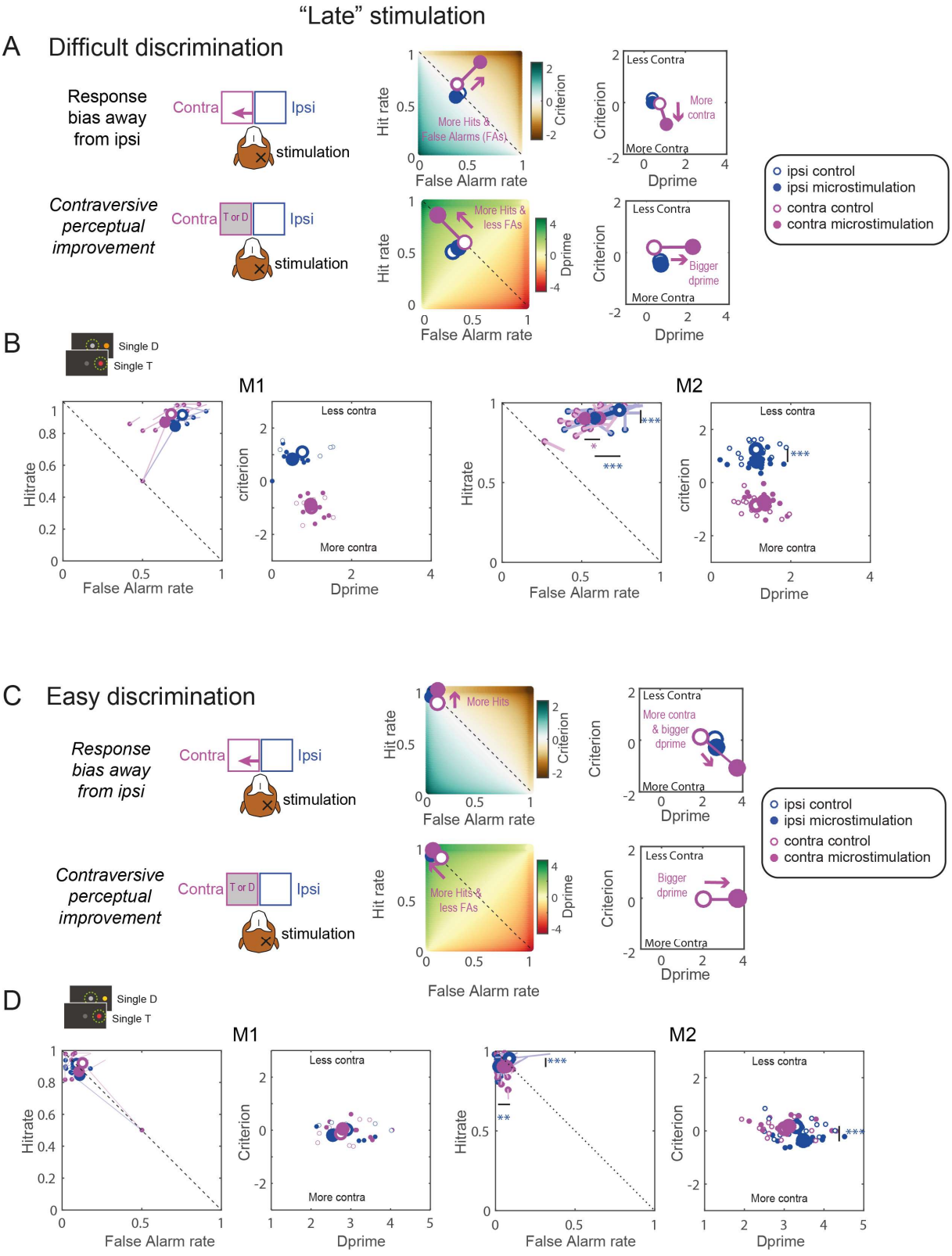

Figure 3.8. Predictions and results for single stimuli. (A) Illustration of the two alternative hypotheses for the difficult discrimination using simulated data showing the expected changes in hit rate, false alarm rate, dprime, and criterion after unilateral dPul microstimulation starting around or after stimulus onset. (B) Microstimulation effects on signal detection variables are displayed separately for each monkey for the difficult discrimination (orange distractor). The first column shows each monkey's ipsiversive (blue) and contraversive (magenta) false alarm rate and hit rate. The second column shows the ipsiversive and contraversive criterion and dprime. Small circles display single sessions, and large circles display

the mean across sessions. (C) Illustration of the two alternative hypotheses for the easy discrimination. (D) Microstimulation effects on signal detection variables for the easy discrimination (yellow distractor).

Double same stimuli

Previous studies suggested that dorsal pulvinar becomes most relevant in the case of spatial competition between hemifields (Desimone et al., 1990; Dominguez-Vargas et al., 2017; Wilke et al., 2013). Here, two equally rewarded targets or two distractors were presented in the periphery during the same stimuli condition, eliciting a high competition between hemifields for visual representation and response selection. The monkeys chose between continuing fixating or making a saccade to one of the two peripheral stimuli.

As for the single stimuli, if late microstimulation causes a spatial selection bias during inter-hemifield competition, we expect a similar increase in contraversive hit and false alarm rates. Necessarily, such a decrease has to result in (i) a corresponding decrease in ipsiversive hit rate and false alarm rate or (ii) a decrease of central fixation selection. We expected a shift for contraversive and ipsiversive criteria towards “more contra” (**Figure 3.9A**). Suppose late stimulation potentiates the functions of the dorsal pulvinar resulting in a contraversive perceptual improvement. In that case, we expect an increase in contraversive hit rate and a decrease in contraversive false alarm rate resulting in a reduction of contraversive dprime (**Figure 3.9A**). We do not have strong predictions for the ipsiversive discrimination: it might remain unaffected as for single stimuli (instead, only fixation responses will be affected), or it might deteriorate due to ipsiversive hit rate decrease and ipsiversive false alarm rate increase. To illustrate a case similar to single stimuli conditions, we simulated the first case.

The ipsiversive hit rate decreased for M1 (M1: $t(1,8) = 3.8$, $p = .004$; M2: $t(1,15) = 0.9$, $p = .15$). For difficult discrimination, contraversive false alarm rate significantly increased for M2 (M1: $t(1,8) = 1.8$, $p = .07$; M2: $t(1,15) = 2.83$, $p = .002$) and the ipsiversive false alarm rate significantly decreased for both monkeys (M1: $t(1,8) = -4.29$, $p = .004$, M2: $t(1,15) = -2.82$, $p = .015$). Both monkeys showed a significant shift for ipsiversive criterion towards “more contra” (Wilcoxon rank sum test; M1: $p = .004$; M2: $p = .01$) and an increase in ipsiversive dprime for M2 (Wilcoxon rank sum test; M1: $p = .91$; M2: $p = .008$). Both monkeys showed no significant effects on the contraversive hit rate, contraversive criterion and dprime ($p > .05$).

During easy discrimination (**Figure 3.9B**), if late microstimulation causes a spatial selection bias, we expect an increase in contraversive hit rate and no change in false alarm rate, given that the easy yellow distractor acts more like a “stop-signal” and a corresponding decrease in ipsiversive hit rate and no change for ipsiversive false alarm rate due to ceiling effect on already

very low false alarm rate for the spatial selection bias hypothesis. This will result in a shift of both criteria towards “more contra” combined with a change in both dprime (**Figure 3.9C**).For the contraversive perceptual improvement hypothesis, we expect an increase in contraversive hit rate but no change in the false alarm rate due to the ceiling effect on the already very low false alarm rate increasing contraversive dprime (**Figure 3.9C**).

For easy discrimination (**Figure 3.9D**)., the contraversive false alarm rate significantly decreased for M2 and the ipsiversive false alarm rate decreased for both monkeys (dependent t-test; M1 contra: t (1,8) = -0.4, p =0.7; ipsi: t(1,8) = -0.013, p = 0.004, M2 contra: t(1,15) = 2.32, p < .05; ipsi: t(1,15) =, p =.015). For M2, the contraversive dprime increased, the ipsiversive criterion shifted towards “more contra” (criterion: M1: p =.12; M2: p = .005, dprime: M1: p =.2; M2: p = .02,) and the ipsiversive dprime increased (Wilcoxon rank sum test; M1: p =.16, M2: p < 0.01) but no significant effects are observed for M2 (p > .05).

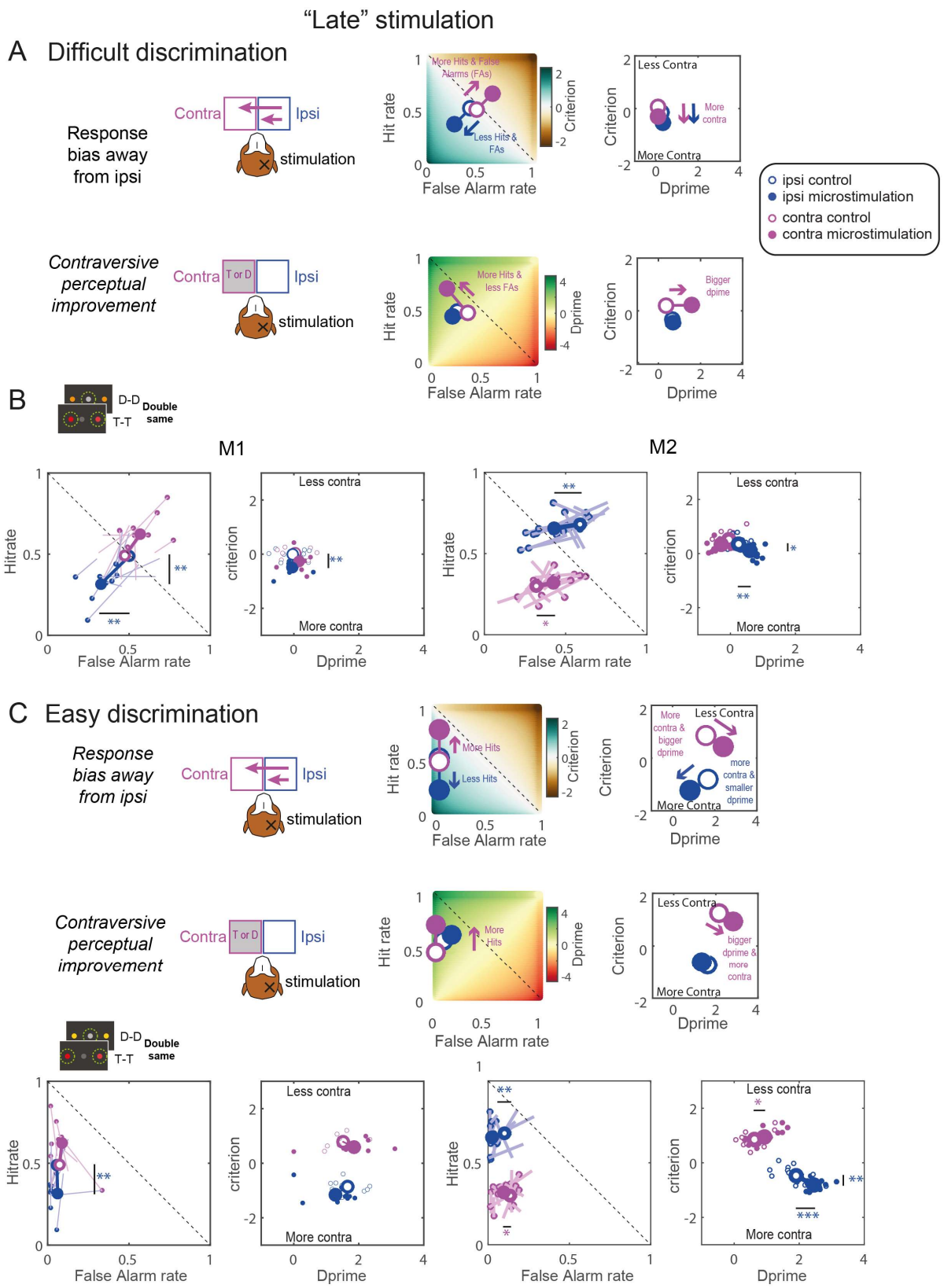

Figure 3.9. Predictions and results for double same stimuli. Same format and notations as in Figure 3.8.

Double different stimuli

The double different stimuli condition also includes a high spatial competition between hemifields. Furthermore, it is influenced by the possibility of directly comparing the simultaneously presented target and distractor in the opposite hemifields. Notably, the central fixation is always an incorrect response option.

During difficult discrimination, for the spatial selection bias hypothesis, we expect the same effect as in the double same stimuli (**Figure 3.10A**). But for the perceptual improvement hypothesis, in contrast, to double the same stimuli, we expect the increase in contraversive dprime to be necessarily linked to the increase in ipsiversive dprime because selecting more targets on the contraversive side would lead to selecting less distractors on the ipsiversive side and selecting less contraversive distractors – to more ipsiversive targets (**Figure 3.10A**).

The contraversive hit rate increased significantly for M2 (dependent t-test; M1: $t(1,8) = 0.3$, $p= .8$; M2: $t(1,15) = 2.7$ $p = .02$) and ipsiversive hit rate decreased for both monkeys (M1: $t(1,8)=6.3$, $p < .001$; M2: $t(1,15) = 2.7$, $p = .016$; **Figure 3.10B**). The contraversive false alarm rate increased for both monkeys and the ipsiversive false alarm rate significantly decreased for M2 (contra: M1: $t(1,8) = 4.32$, $p =.003$.; M2: $t(1,15) = 2.41$, $p = .03$; ipsi: M1: $t(1,8) = 1.4$, $p = .2$; M2: $t(1,15) = 3.49$, $p = .003$). Consequently, M2 showed a significant shift for the contraversive and ipsiversive criterion towards “more contra” (Wilcoxon rank sum test; M2 contra: $p = .003$, ipsi: $p = .003$) and no change in dprime ($p > .5$). M1 showed an ipsiversive criterion shift towards “more contra” (M1 contra: $p = .055$, ipsi: $p = .008$) and a decrease in contraversive or ipsiversive dprime (contra: M1: $p = .02$, ipsi: $p = .01$).

During easy discrimination in the presence of a yellow distractor in case of the late microstimulation, we expect an increase in a contraversive hit, but because of the “stop-signal” of the easy distractor, no change in the contraversive false alarm rate for the spatial selection bias hypothesis (**Figure 3.10C**). For contraversive perceptual improvement, similar to the double same stimuli, we expect an increase in contraversive dprime but no effect on ipsiversive dprime (**Figure 3.10C**).

For easy discrimination (**Figure 3.10D**), the false alarm rate was already near zero, so there was no room to exhibit any microstimulation-induced changes. Hence, the contraversive and ipsiversive false alarm rate and criterion did not show an effect ($p > .5$) The ipsiversive hit rate decreased for M2 (ipsi M1: $t(1,8) = 1.5$, $p = .6$; M2: $t(1,15) =3,15$ $p = .007$, contra: M1: $t(1,8) = 0.5$, $p = .6$; M2: $t(1,15) = 0.5$, $p < .6$). Both monkey (M2) showed a significant shift for the ipsiversive criterion towards “more contra” (Wilcoxon rank sum test, M1: $p = .04$, M2: $p <.02$). Only M2 showed also a significant decrease in contraversive and ipsiversive dprime (contra: M1: $p = .7$, M2: $p < .49$; ipsi: M1: $p = .9$, M2: $p = .03$).

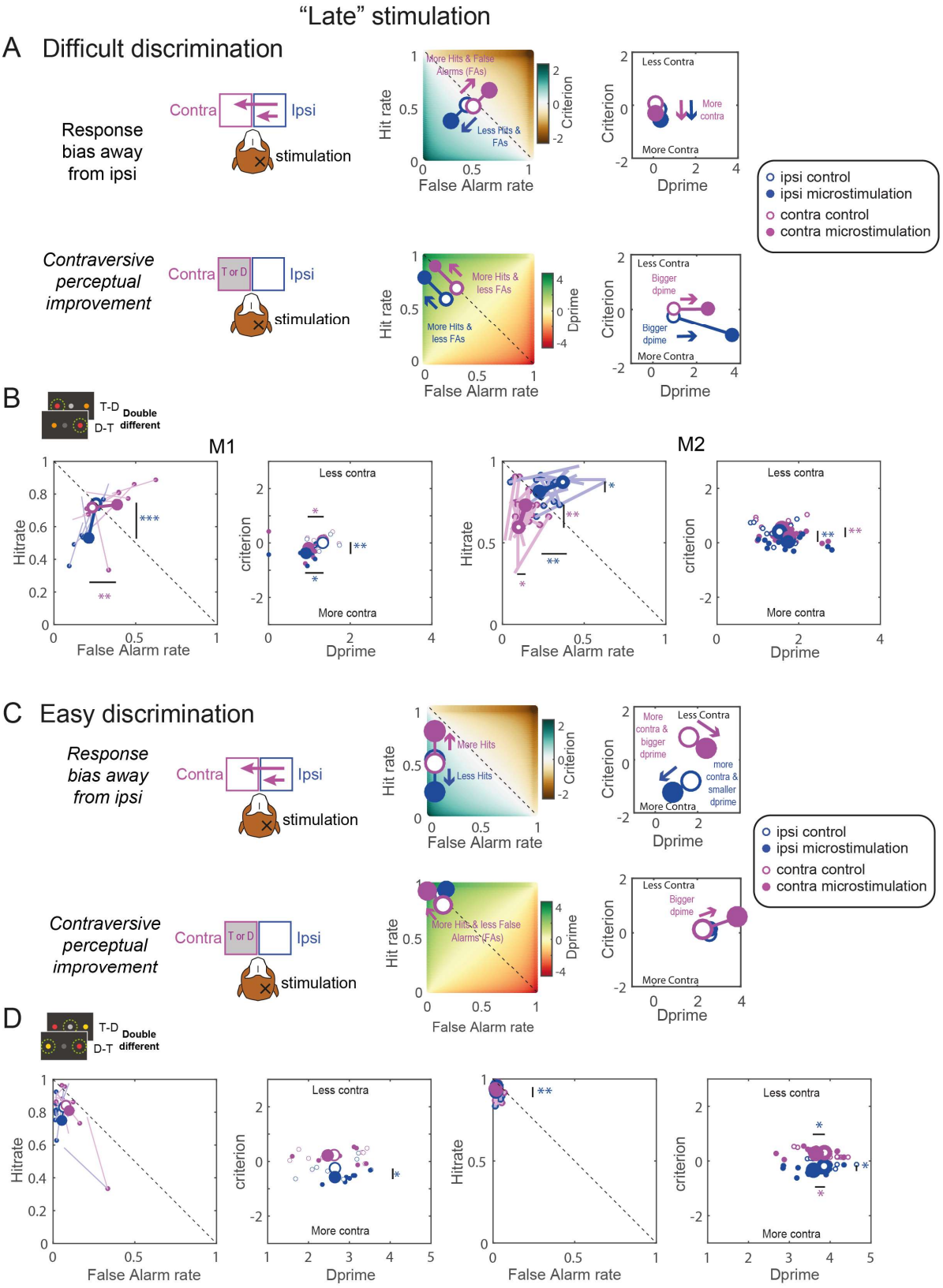

Figure 3.10. Predictions and results for double different stimuli. Same format and notations as in Figure 3.8.

Discussion

This study investigated how dorsal pulvinar stimulation before and during the formation and execution of a perceptual decision influences the selection behavior and saccade latencies in spatial competition and perceptual uncertainty conditions. Two monkeys performed a color discrimination task in including task demands such as fast perceptual color discrimination between target and distractor, spatially competing stimuli, and stimulus-congruent saccade responses to investigate the selection behavior in a spatially and time-dependent manner by electrically stimulating in two periods of the trial timeline (indicated by “early” and “late” microstimulation). Early microstimulation perturbs the neural activity in the dorsal pulvinar already before the formation and execution of a decision (the monkey is fixating a red spot in the center of the screen), and late microstimulation perturbs the neural activity in the dorsal pulvinar during the formation but before the execution of a decision. In addition, we adopted the signal detection theory approach to differentiate between the spatial selection bias by calculating the response criterion and the discrimination between stimuli by calculating dprime.

Following early microstimulation, we primarily observed criterion shifts away from contraversive stimuli when two peripheral stimuli elicited high spatial competition between hemifields. This shift in criterion manifested as reluctance to select stimuli in the contraversive hemifield, regardless of whether a target or distractor was presented there. The high-current early microstimulation for M1 started 250ms before stimulus onset and ended 50ms before stimulus onset had a lasting effect on the selection behavior of M1, for which the initiation of the saccade for selection occurred on average 260 ms after stimulation offset (M1’s saccade latency: ~200 ms). Early microstimulation seems to bias the contralateral neuronal tuning of neurons in the pulvinar in M1, resulting in a spatial selection “away from contra” for double stimulus conditions combined with a consistent contraversive effect of slowing down after early microstimulation. The dprime and the overall accuracy remained largely unaffected for M1. On contrary, the accuracy and dprime significantly decreased for M2 for both difficulty levels after early microstimulation because M2 was selected systematically for all stimulus conditions the ipsiversive distractor, and even the easy “stop-signal” like distractor. We observed a substantial decrease in saccade latency for M2 where the microstimulation started 50ms before the stimulus onset but lasted until 150 ms after stimulus onset, which is closer to the saccade initiation (M2 = ~210 ms initiation of the saccade).

Following late microstimulation, we primarily observed criterion shifts away from ipsiversive stimuli for both difficulty levels manifesting as reluctance to select stimuli in the ipsiversive hemifields. The decrease of selection of ipsiversive stimuli was consistently present but not

equal to the increase of selection for the contraversive stimuli, leading mainly to effects on the ipsiversive criterion. The dprime and the overall accuracy remained largely unaffected for M1. M2 showed a decrease in accuracy for the easy perceptual difficulty for both double stimuli conditions, driven by a reduction in ipsiversive false alarm rate. Still, on neither side the hit rate improves. The saccade latency consistently slowed down for the contraversive and ipsiversive selection for M2, which was similar in M1 but less consistent. Although the data fit better the quantified predictions of the selection bias hypothesis, accuracy and dprime significantly change but inconsistently between monkeys, stimulus timings, and the different stimulus conditions. However, the contraversive perceptual discrimination performance largely remained unaffected, indicating more of an interaction effect between the spatial response bias and the dprime.

As in our previous microstimulation study, we found a selection bias “away from contra” for early microstimulation for the double same stimulus condition most similar to the free-choice between two identical targets in the visually-guided saccade task (Dominguez-Vargas et al., 2017). We did not find more contraversive target selections after late microstimulation for the perceptual discrimination task, but a significant decrease in ipsiversive target selection for all three stimulus conditions combined with an increase in “staying” at the fixation spot. Possible reasons could be that the visually guided saccade task differed from our stimulus conditions because monkeys invariably had to saccade to a target, and there was no option to stay. Domingues-Vargas et al. (2017) also describe two distinct modes of the reaction time distributions after stimulating at the Go-signal or later, indicating that saccades are made either during the stimulation train or after the stimulation offset. Does the previously reported first mode in the reaction time distribution correspond in the color discrimination task to the trials where the monkeys stayed? As the current analysis does not analyze the reaction time distributions, it might also be a follow-up analysis by differentiating the saccades made to a distractor and a target.

For the single stimulus, we observed a significant increase in fixating for one monkey and similar but not significant for the other after late microstimulation. The effects after early microstimulation were somewhat puzzling for the single stimuli and did not align with our predictions. In contrast, Domingues-Vargas et al. (2017) did not find an effect of stimulation on the hit rate of the single instructed targets. Their guided condition differed from our single stimulus condition because monkeys invariably had to saccade to the target. Here we included a second response option, central fixation, as the correct response for the distractor trials. The presence of two options and the perceptual discrimination context created a low spatial competition between the fixation option and peripheral option for single stimuli. During action selection, multiple response options compete against each other. At the same time, information

is collected to bias this competition between representations at different levels of neuronal processing until one option is selected (Cisek, 2006). Previous studies suggested that dorsal pulvinar becomes most relevant in the case of spatial competition between hemifields (Desimone et al., 1990; Dominguez-Vargas et al., 2017; Wilke et al., 2013). Hence, the low spatial competition between the fixation option and peripheral option for single stimuli might be a condition where the task-evoked activity of the pulvinar is less pronounced, resulting in less effect of the perturbation of the neural activity of the pulvinar compared to the double stimuli condition that elicits a high competition between hemifields for visual representation and response selection.

Notably, the microstimulation-induced selection bias occurs even in the context where only one response option is correct and rewarded. Both monkeys selected the ipsiversive target less and chose the ipsiversive distractor or fixation option after late microstimulation and vice versa by selecting less the ipsiversive target after early microstimulation. Therefore, presenting a correct target in the contraversive hemifield for early microstimulation and an ipsiversive target for late microstimulation was the only rewarded option (single target or target-distractor condition) that did not alleviate the spatial selection bias. We also found the same selection behavior after early microstimulation for the target-distractor condition. This selection behavior was even stronger manifested in M2 after microstimulation. M2 selected more often the ipsiversive easy distractor for all three stimulus types after early microstimulation but not the contraversive easy distractor. Selecting the so-called “stop-signal” distractor is puzzling, particularly for the target-distractor trials. M2 chose instead of the simultaneously presented contraversive target, the ipsiversive presented easy distractor resulting in a significant decrease in contraversive hit rate and a significant increase of the ipsiversive false alarm rate for the easy distractor-target condition. This selection behavior seems to be the reason for the decrease in dprime after early microstimulation. However, we do not observe an increase in selecting more contraversive distractors, which is expected for a perceptual discrimination deficit. Further analyses are needed for this chapter to understand better the interaction of the criterion and dprime, and possibility exclude the possibility of evoked saccade due to microstimulation.

4. Chapter

Relationship between cardiac, respiratory and neural activity in the dorsal pulvinar and other thalamic nuclei

Kristin Kaduk, Lukas Schneider, Melanie Wilke, Igor Kagan

Manuscript in preparation

Authors Contributions

KK, MW, and IK designed the experiments, and KK collected the data. IK designed the preprocessing pipeline for ECG data, KK and LS performed the analysis, and KK, MW, and IK wrote the paper.

Acknowledgments

We thank Daniela Lazzarini, Sina Plümer, and Klaus Heisig for technical support. We also thank Mathias Bähr, Stefan Treue, Alexander Gail, the Cognitive Neurology Group members, the Decision and Awareness Group members, the Sensorimotor Group, and the Cognitive Neuroscience Laboratory for helpful discussions. We are supported by the Hermann and Lilly Schilling Foundation, German Research Foundation (DFG), and the Else Kröner-Fresenius Foundation (to M.W.).

Summary of the chapter

As outlined in the introduction, the dorsal pulvinar is a unique hub region that had been suggested to be involved in multisensory integration and arousal-related emotional processing. Here, we investigate the role of the pulvinar and other thalamic nuclei in autonomic control and cardiovascular function. The chapter includes two experiments where ECG and respiration data from behaving rhesus monkeys were recorded and combined with either targeted pharmacological inactivation of the pulvinar or extracellular recordings in the dorsal pulvinar and two other thalamic nuclei. Pharmacological inactivation resulted in a change in the heart rate of two monkeys. Particularly promising were the findings on the relationship of the neural activity with the cardiac activity indicating a high percent of thalamic nuclei showing a cardiac-related effect with spiking activity.

Introduction

Cardio- and neurovascular diseases, such as heart attack or stroke, are the leading cause of death in the Western world. Although the effects of cardiovascular disease on the nervous system have been widely studied, the impact of neurological disorders on the cardiovascular system has been poorly understood (Palma & Benarroch, 2014; Tahsili-Fahadan & Geocadin, 2017; van der Wall & van Gilst, 2013), like cardiac arrhythmias that are a possible cause of stroke and heart failure in humans (e.g. Koppikar et al., 2013). Increasing evidence suggests the critical involvement of the autonomic nervous system as a trigger and predisposing factor of arrhythmias. It seems that cardiac dysfunctions rely on structural and functional alterations in brain regions belonging to the central autonomic network (Chen et al., 2007; Franciosi et al., 2017; Lakkireddy, 2020), but the interactions of the central autonomic network with the cardiovascular system need to be further investigated to improve therapeutic interventions for cardiovascular diseases.

The central autonomic network (CAN) is a critical component of an internal regulation system for controlling visceromotor, neuroendocrine, cardiovascular, and behavioral responses to changing emotional, cognitive, and physical demands (e.g. Galosy et al., 1981; Gordan et al., 2015; Sklerov et al., 2019; Talman, 1985). The CAN modulates the hypothalamus-pituitary-adrenal axis and the autonomic nervous system to maintain homeostasis (Benarroch, 1993; Edlow et al., 2016; Silvani et al., 2016). The CAN consists of an extensive network of interconnected regions of the brain stem to cortical and subcortical brain areas, including the insula, ventromedial prefrontal cortex, anterior cingulate, and amygdala. The role of those major brain regions engaged in autonomic control was established by a combination of anatomical tracing studies, electrical stimulation, and lesion studies in rats, rabbits, cats, monkeys, and humans. So far, the following brain regions have been related to heart rate regulation identified by direct electrical stimulation. Electrical stimulation of the midbrain (Benedetti et al., 2004; Thornton et al., 2002), insula (Chouchou et al., 2019; S. M. Oppenheimer et al., 1992; S. M. Oppenheimer & Cechetto, 1990), cingulate (Parvizi et al., 2013; Pool & Ransohoff, 1949; Talairach et al., 1973), mediodorsal thalamus (Buchanan & Powell, 1986) and superior colliculus (Keay et al., 1988) changes the heart rate and partially the blood pressure or respiration rate. This suggests that some ongoing fluctuations in neural firing rate might be directly related to the heart rate. Indeed, cardiac-related neuronal activity was shown in the human amygdala, mid-to-anterior cingulate, and the anterior parahippocampal gyrus (Frysinger & Harper, 1989, 1990; M. J. Kim et al., 2011), which play a significant role for the homeostatic control of internal bodily states, the heart-brain axis (Manea et al., 2015; S. Oppenheimer & Cechetto, 2016; Verberne & Owens, 1998) and perception, cognition and emotion (Azzalini et al., 2019; Critchley & Harrison, 2013).

The integrated homeostatic afferent information from the parabrachial nucleus reaches the anterior cingulate and insular cortices through the medial thalamic nuclei and the basal ventral medial nucleus of the thalamus (Craig, 2002, 2003; Nieuwenhuys, 2012; Zhang & Oppenheimer, 2000). Cardiac-related neural activity was identified with extracellular recordings in the ventral posterior lateral nucleus of epileptic patients (Oppenheimer et al., 1998) and the cat (Massimini et al., 2000). And functional magnetic resonance studies mentioned the mediodorsal thalamus (MD) in association with autonomic control (Critchley et al., 2003; Napadow et al., 2008). Available magnetic resonance studies emphasized that higher-order thalamic nuclei, such as pulvinar or mediodorsal thalamus, should be explored directly and in more detail to understand better their potential role in interacting with the autonomic network (Barber et al., 2020; Beissner et al., 2013; Ojemann & Van Buren, 1967).

The current study targets this research gap with two experimental studies on the dorsal pulvinar. The dorsal pulvinar has reciprocal connections with all major notes of the central autonomic network (amygdala, insula, cingulate, and prefrontal cortex) and integrates multisensory information (Froesel et al., 2021; Gattass et al., 1978; Vittek et al., 2022). Evidence converges on the conclusion that the dorsal pulvinar appears to be critical for the emotional processing of threatening information (Almeida et al., 2015; Bertini et al., 2018; Kragel et al., 2021; Maior et al., 2010; Soares et al., 2017; Van Le et al., 2013; Ward et al., 2005, 2007). These identify the dorsal pulvinar as a well-suited candidate hub region to integrate neuronal signals from and to the autonomic nervous system. However, whether the dorsal pulvinar is directly related to the cardiovascular system beyond this specific emotional content remains largely unknown. Poirier and Schulmann (1954) electrically stimulated the pulvinar posterior part, leading to respiratory arrest and blood pressure alteration (Poirier & Shulman, 1954). Additional to this limited evidence, some patient studies reported relationships between pulvinar damage and impaired oxygen regulation or a reduction of gray matter volume of the pulvinar in patients with a high risk for sudden cardiac death compared to low risk and healthy controls (Rosenberg et al., 2006; Wandschneider et al., 2015; Woo et al., 2003). Since disentangling the contribution of a specific brain region to cardiac activity is difficult in human patients, we here asked if and how local reversible pharmacological inactivation of dorsal pulvinar affects cardiac and respiratory activity in awake monkeys.

In the first experiment, we recorded the electrocardiogram (ECG) and respiration of three monkeys continuously before and after suppressing the neural activity of the dorsal pulvinar. We utilized two levels of task engagement by interleaving blocks where the monkeys were engaged in an effortful cognitive task or were passively sitting in their primate chair (rest). We analyzed the difference in heart rate, respiration rate, and heart rate variability between

injection and control sessions for these two task engagement levels. Suppressing the neural activity of the dorsal pulvinar pharmacologically led to an inactivation-induced decrease in the heart rate in two monkeys coupled with a reduction in respiration rate or an increase in heart rate variability. In an electrophysiology experiment with a similar study design, we investigated the relationship between cardiac activity and neural spiking activity of three thalamic nuclei: the dorsal pulvinar, another higher-order thalamic nucleus mediodorsal thalamus (MD), and a first-order ventral posterolateral nucleus (VPL) as controls.

Methods

This study was conducted in accordance with the European Directive 2010/63/EU, the corresponding German law governing animal welfare, and the German Primate Center institutional guidelines. The responsible government agency approved the procedures (Niedersaechsisches Landesamt fuer Verbraucherschutz und Lebensmittelsicherheit (LAVES), Oldenburg, Germany).

Four healthy male rhesus monkeys participated in the study (*Macaca mulatta*, monkey 1: 10.5 kg, 12 years old, monkey 2: 8.8 kg, 13 years old, monkey 3: 12.3 kg, 14 years old, monkey 4: 9.5 kg, 16 years old). The animals had free access to food. They were maintained on a water regulation schedule with primate food supplemented by fruits and vegetables. During the experiment, the monkeys sat in a primate chair with their heads restrained via implanted head posts. The surgical procedures for the MRI-compatible polyetheretherketone (PEEK) head post and chamber implantations were conducted as described in chapter 2 of this dissertation and the recent publications from the lab (Dominguez-Vargas et al., 2017; Schneider et al., 2019).

Study design with an inactivation and electrophysiology experiment

Three monkeys participated in the inactivation experiment (**Figure 4.1A**). We conducted inactivation sessions interleaved with control (no injection) sessions for each monkey. The control sessions were performed with the same occurrence and timing of events. Every experimental session started with a pre-injection testing period, followed by the injection, a 30-40 min waiting period, and ended with the post-injection testing period (**Figure 4.1B**).

For the electrophysiology experiment (**Figure 4.1C**), data were collected from monkey 4 in 36 recording sessions. Extracellular recordings were simultaneously performed in different thalamic nuclei in both hemispheres. In the left hemisphere, recordings were mainly performed in the dorsal pulvinar (dPul) and one session in the mediodorsal thalamus (MD). In the right hemisphere, recordings were conducted in MD, ventral posterior lateral nucleus (VPL), and dPul.

Monkeys were seated in a primate chair during the experiments, facing a monitor (viewing distance: ~ 30-35 cm). Stimulus presentation, reward delivery, and behavioral data acquisition were implemented in MATLAB R2011 (The MathWorks Inc., USA) combined with the Psychophysics Toolbox extensions (Brainard, 1997). During the experiments, monkeys either engaged in a cognitively demanding task or sat passively in their primate chair (rest). Monkey 1, monkey 2, and monkey 4 performed a saccade color discrimination task, and monkey 3 performed a direct (visually-guided) reaching task with cued hand usage. The color discrimination task is outlined in detail in Chapters 1 and Chapter 2.

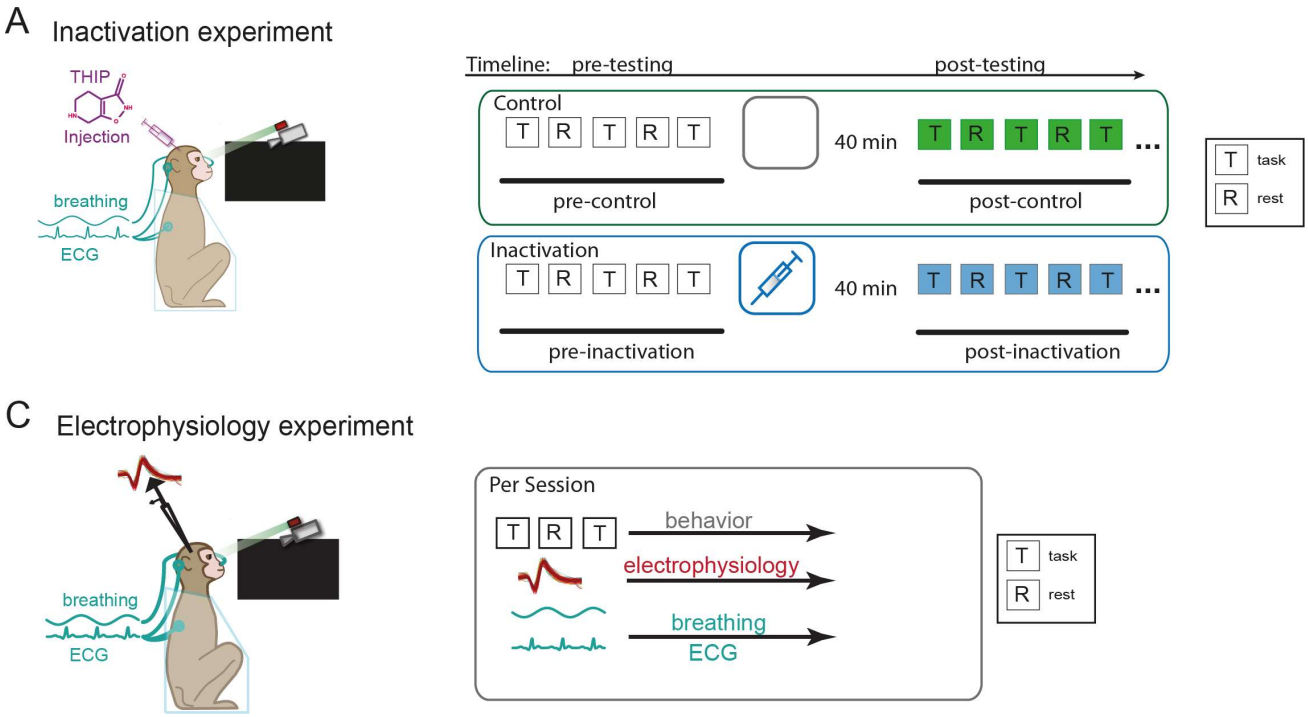

Figure 4.1. Study design and timeline of the experiments. For both experiments, blocks where the monkey was passively sitting in the primate chair (R stands for rest) were interleaved with performing a task (T stands for the task). (A) Illustrates the main features of the inactivation experiment where the neural activity of the dorsal pulvinar was suppressed by the GABA-A agonist (THIP). Additionally, respiratory and cardiac activity was continuously recorded. Every session had the same sequence of events as outlined here: pre-injection (or pre-"sham injection") periods followed by post-injection (or post-"sham injection) periods. The timeline was identical for control (no injection) and inactivation sessions (local THIP injection in the dorsal pulvinar). (B) Illustrates the main features of the electrophysiological experiment where the neural activity of three thalamic nuclei (VPL, MD, dPul), the

electrocardiogram, and breathing were continuously recorded during interleaved task (~30 min) and rest (~10 min) periods.

Recording of the electrocardiogram and respiration

The heart's electrical activity (electrocardiogram) was continuously recorded in the awake state while the monkeys sat in the primate chair. All monkeys were accustomed to shaving and placing the electrodes using positive reinforcement training. Three disposable adhesive disk surface electrodes were used, including an Ag/AgCl sensor and a conductive gel via a modified lead-3 placement (Technomed, Germany). After shaving and cleaning the skin with water, the bipolar recordings consisted of two electrodes placed left and right on the back of the monkey below the scapula. The third electrode was the reference set on the back of the head below the head cap implant, on the right side. The exact position of these electrodes was individually adjusted for each monkey to record a stable signal with a full QRS-complex of the ECG activity. The ECG signal was amplified using the RA 4PA Medusa preamplifier with a connection to a low impedance RA4LI headstage via a standard 25-pin connector (Tucker-Davis Technologies, USA), digitized with a sampling rate of 2034.5 Hz, and sent via fiber optics to an RZ2 BioAmp Processor as acquisition system (Tucker-Davis Technologies, USA) for online filtering (2^{nd} order low pass Butterworth filter (band gain = 1, center filter frequency = 20, bandwidth = 5).

The respiration was continuously recorded by measuring breath by breath the exhaled levels of carbon dioxide from the nostrils of the monkey using a capnograph (Medlab, Germany). The capnography had an interface module for data transmission to the RZ2 BioAmp Processor. The ECG and respiration signals were displayed online and stored on a hard drive, together with the behavioral and timing data streams.

Reversible pharmacological inactivation of the dorsal pulvinar

The neural activity in the dorsal pulvinar was reversibly inactivated using the GABA-A agonist 4,5,6,7-tetrahydro isoxazole [5,4-c]-pyridine-3-ol (THIP hydrochloride; Tocris). The THIP was dissolved in phosphate-buffered saline (PBS). The solution (pH 7.0-7.5) was sterile and filtered with a hydrophobic PTFE membrane filter (pore size: 0.2 µm, Sartorius) before injection via a sterile 31-gauge sharp-tip steel cannula (31 gauge, 50 mm length). The volume was delivered at a 0.25 µl/min rate using a 0.1 ml glass-tight Hamilton syringe driven by a digital infusion pump (Harvard Apparatus Holliston, MA). The inactivation location in the dorsal pulvinar was estimated based on anatomical MRI applying the traditional segregation of the

pulvinar nucleus into medial, lateral, and inferior pulvinar as currently available and downloadable atlases (Calabrese et al., 2015; Rohlfing et al., 2012). Based on the MRI images, we planned where to target the dorsal pulvinar to determine the grid hole based on the anatomical MR image using the Planner (Ohayon & Tsao, 2012) and BrainVoyager (Version 2.4.2.2070, 64-bit; Brain Innovation BV). To plan and confirm the injection locations, we performed gadolinium injections combined with structural MRI (**Figure 4.2 A**).

In the experimental sessions, the inactivation of the dorsal pulvinar was performed in the left and right hemispheres on separate days for monkey 1 and monkey 3 and in the right dorsal pulvinar for monkey 2. The optimal volume for injection was determined separately for each monkey in pilot sessions to find the dose where the monkey is continuously working without nystagmus after the inactivation. The injection volume per session was 4.5-5 µl of 10 mg/ml of THIP for monkey 1, 1.5 µl of 10 mg/ml of THIP for monkey 2, and 3-3.5 µl of 10 mg/ml of THIP for monkey 3. The success of the inactivation procedure was evaluated based on the previously described findings of an ipsilesional selection bias for free choice target-target stimuli (Wilke et al., 2010, 2013).

A

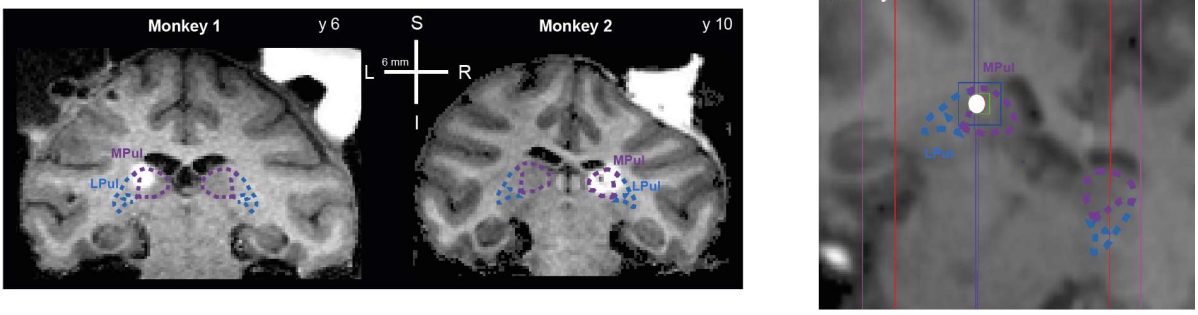

Figure 4.2. Inactivation sites. (A) MR images show the inactivation sites visualized with co-injection of gadolinium MR contrast (ratio: 1:200) agent ~20 min following the injection (for M1: 2µl, for M2: 3 µl planner) and the overlaid borders of dorsal pulvinar (dPul) and lateral pulvinar (lPul.

Electrophysiological recordings

Neuronal activity was recorded with up to four individually-movable single platinum-tungsten (95%-5%) quartz glass insulated electrodes using a chamber-mounted 5-channel Mini Matrix Microdrive (Thomas Recording, Germany). Before the recording, the dura at the estimated grid location was marked. It was penetrated using a single custom-made stainless steel guide tube (27 gauge) made from a Spinocan spinal needle (B. Braun Meldungen AG, Germany). For the recording, two types of guide tubes were used: a similar 27-gauge custom-made stainless steel guide tube with a metal funnel attached to the microdrive nozzle or four individual electrodes concentrically-arranged thinner guide tubes (Thomas Recording,

Germany). Guide tubes were filled with silicone oil and protected electrodes during dura penetration. A reference tungsten rod or a silver wire was placed in the chamber filled with saline and connected to the drive's chassis. Neuronal signals were amplified (x20 headstage, Thomas Recording, x5, 32 channel PZ2 preamplifier, Tucker-Davis Technologies, USA), digitized at 24 kHz and 16-bit resolution, and sent via a fiber optics to an RZ2 BioAmp Processor (Tucker-Davis Technologies, USA) for online filtering (300 - 5000 Hz bandpass), display and storage on a hard drive together with behavioral and timing data streams.

Notably, to stabilize the position of the recording electrodes relative to the brain tissue after driving them deep (15 to 19 mm) until the thalamus, a non-recording time (waiting time for the monkey) of one hour was necessary before searching actively for neurons. This procedure was crucial to record stable single and multi-units for 2 to 3 hours across the interleaved rest blocks (10 min) and task (30-40 min).

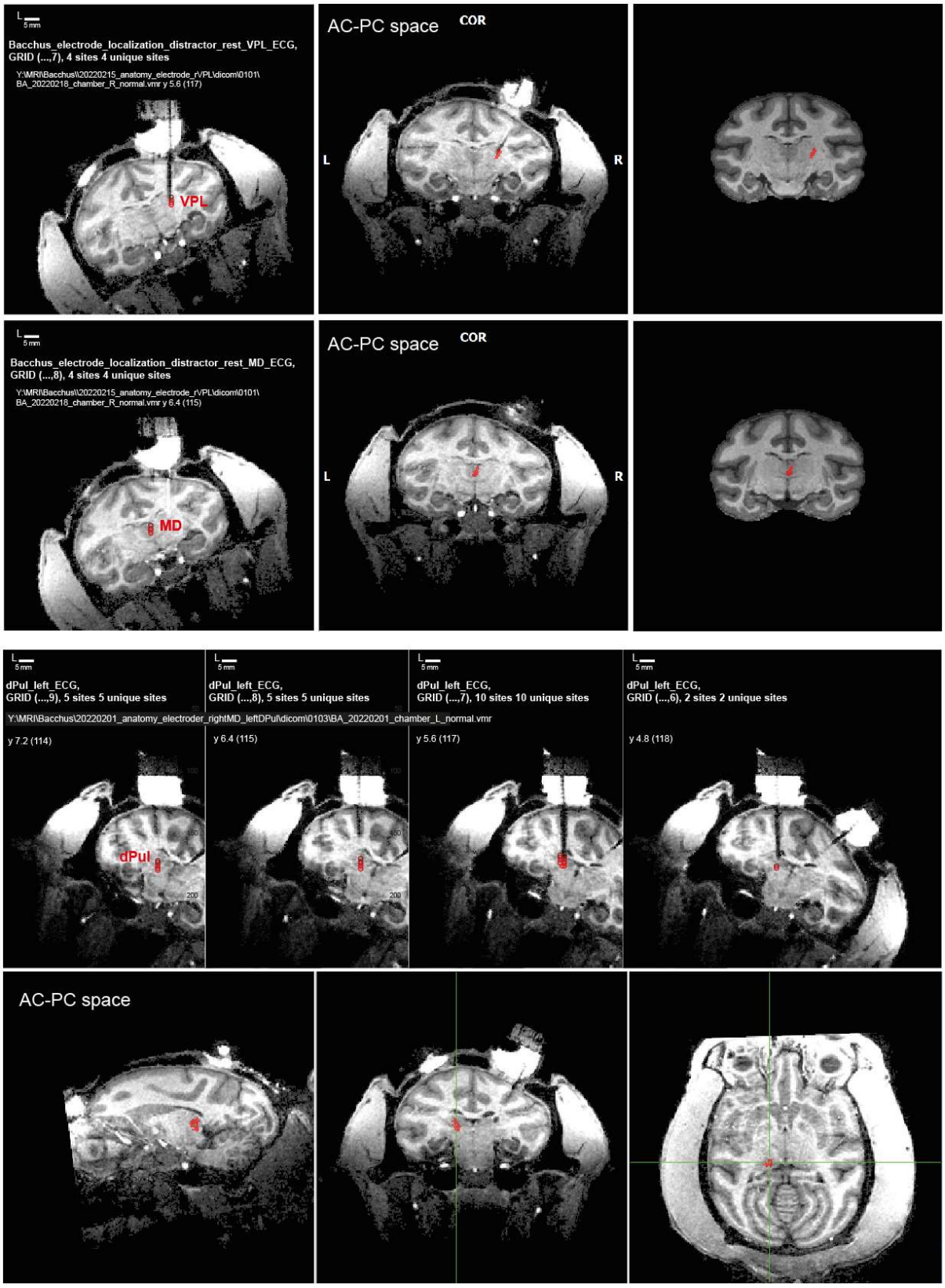

Figure 4.3 Recording sites for all three thalamic nuclei.

Data analysis

Data were preprocessed and analyzed using MATLAB R2011 (The MathWorks, Inc., USA), and statistical tests were performed using the R software (version 4.1.2, R Core Team, 2022). For the inactivation experiment, we analyzed the data from three monkeys separately for rest and task periods. Monkey 1 participated in ten inactivation sessions and ten control sessions. Monkey 2 participated in nine inactivation and nine control sessions, and monkey 3 participated in seven inactivation sessions and four control sessions.

Preprocessing of electrocardiogram & respiration

We detected the R-peaks of the QRS wave offline from the electrocardiogram, and we detected the exhaling peaks of the signal from capnography (**Figure 4.4**). For peak detection, we first detrended and digitally filtered the signal with a low-frequency cutoff to eliminate baseline drifts between 1 and 5 Hz. As a filter, we applied a 20^{th} order Butterworth filter with a cut-off frequency of 0.041 Hz, which is based on a Nyquist frequency (Fn) of 1017.3 Hz, a normalized bandpass frequency of 0.039 Hz (40/Fn), and a normalized stopband frequency of 0.098 Hz (100/Fn) having a passband ripple of 1 dB and stopband ripple of 150 dB. These parameters were chosen based on the frequency components of the baseline drifts in the first sessions, where we recorded the ECG in Monkey 1.

The ECG signal was decomposed from 1Hz to 12 Hz to obtain different time-frequency components using Continuous Wavelet Transformation given the Morlet waveform (spacing between scales of 1/32 Hz and the scale number 178). Afterward, the signal was segmented into n * 300 s segments with an overlap of 50 s for faster processing to compute the energy of the second derivative, and afterward, these were concatenated.

The peaks (R-peaks and exhaling peaks) were detected given the following parameter: minimum distance between peaks: 0.25s; and a minimum height of the peak as 0.5 of the proportion of the median of the energy profile. Afterward, outliers were removed using, at first, the median of the absolute difference between the amplitude of peaks (M1 = 2, M2 = 3), where a larger value indicates removing less outlier. Then, the R-R interval time series is computed and checked for outliers. Invalid R-R intervals have a deviation from x * minimum (M1: x = 0.66, M2: x = 0.43) and x * maximum (M1: x = 1.5, M2: x = 2) of the mode of R-R intervals of the session. We applied the Hampel filter, a moving window nonlinear data cleaning filter that defines an outlier if the data point lies some number of t of MAD scale estimates (M1: t = 4, M2: t = 15) as an alternative measure for distance from the median of its neighboring observations. All detected outliers and their consecutive R-R intervals were deleted from the signal. To determine the exhaling peaks of the respiration signal, we used the same procedure

for R-peak detection, adjusting the parameters to the respiration signal by visually inspecting the successful detection of exhaling peaks from several sessions.

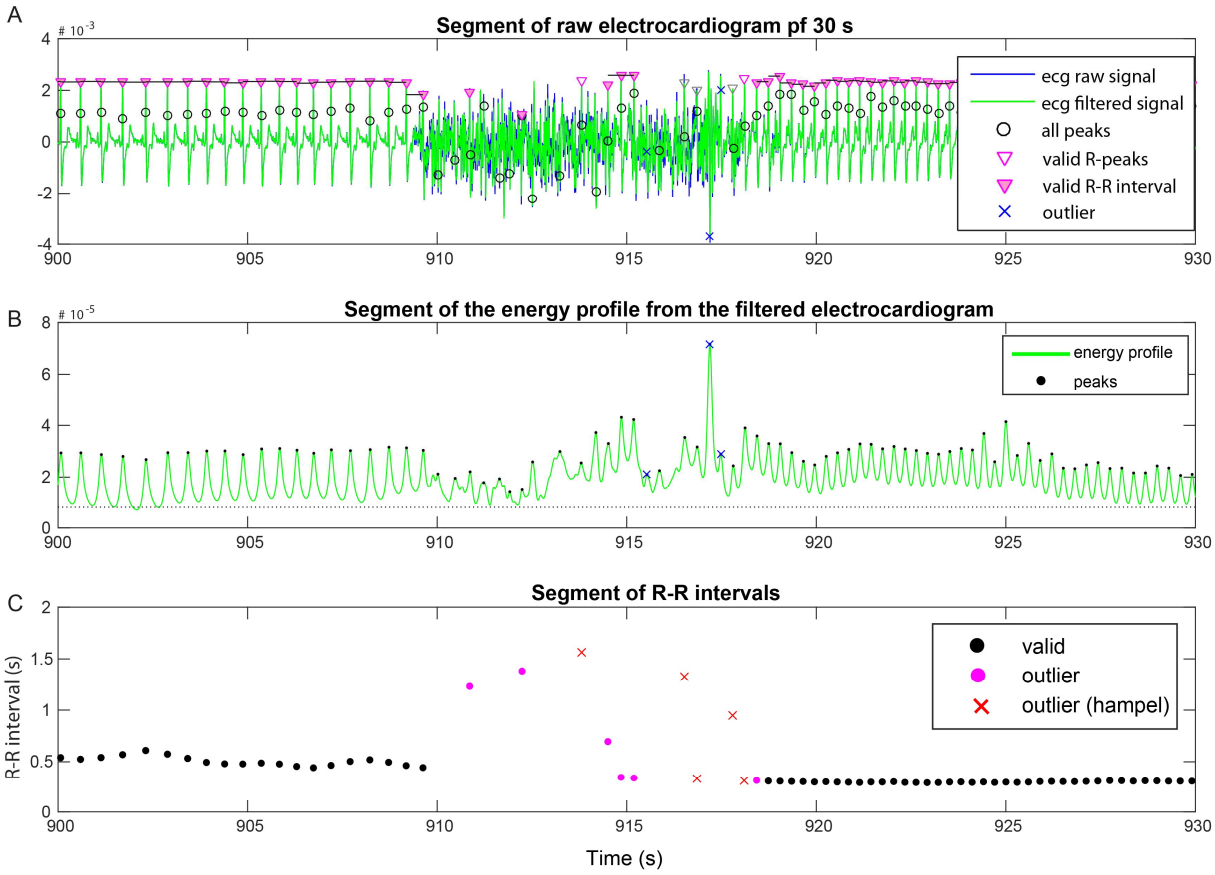

Figure 4.4. Illustration of a segment of ECG signal for the R-peak detection. A segment of the raw electrocardiogram (Monkey4, Session: 20220310, rest block) is presented here to display the quality of peak detection in case of movement artifacts. (A) The graph shows the raw (blue) and filtered (green) signal of the 30s from the electrocardiogram. The symbols show where a peak was detected (unfilled circle), marked as a valid peak or valid peak-to-peak interval. (B) The energy profile is shown here from the filtered electrocardiogram. (C) The R-R intervals were computed from the electrocardiogram. The black-filled circle represents the valid R-R intervals used for further analyses. The pre-processing procedure worked well to identify and remove outliers related to movement artifacts.

Heart- and respiration rate, heart rate variability

The statistical analysis focuses on changes in average heart and respiration rate, the heart rate variability (HRV) indices, the standard deviation of heart rate, and the root mean square of successive differences in the R-R interval. The heart rate is defined by the number of heart contractions (R-peaks) per minute. The respiration rate is the number of exhalations per minute. The heart rate variability is rhythmic fluctuations in the time intervals between consecutive heartbeats. We calculated two heart rate variability measures belonging to the time-domain indices. Firstly, the R-R-intervals (SD) standard deviation was computed in beats per minute for a block of 10 minutes for rest and a maximum of 30 minutes for the task,

displaying a general trend in the electrocardiogram. Secondly, the root means square of successive differences of adjacent heartbeats (RMSSD) was obtained by calculating each successive time difference between heartbeats in milliseconds of each block. These values are squared, and their result is averaged before the square root of the total is obtained for each block. The RMSSD reflects the beat-to-beat variance in heart rate, which is more sensitive to local changes. The RMSSD is well validated as a metric of HRV and represents vagally mediated changes but is less affected by respiration rate (Shaffer & Ginsberg, 2017). The RMSSD value correlates strongly with the high-frequency power as an HRV metric and should be preferred with records having ectopic beats that reset the cardiac rhythm. These dependent variables were calculated for each block and then averaged for every condition (level of engagement (rest vs. task), time (pre vs. post)) separately per session and monkey.

The two levels of cognitive engagement included either performing a task or resting while sitting in the primate chair (no explicit task demand, no control of eye movement). As the state of rest is characterized by spontaneous neural activity that differs from the task-evoked activity, and we also expect a different physiological level between these states, we analyzed the data separately for rest and task.

To evaluate our hypothesis whether local reversible pharmacological inactivation of dorsal pulvinar affects heart rate, respiration rate, or/and heart rate variability in awake monkeys compared to control sessions without injections, we compared the means of groups using three-way mixed measure ANOVAs by including as within-session factors “timeline” with the levels pre-injection and post-injection testing period per session (“pre” and “post”), “TaskType” with the levels “rest” and “task”, and as a between-session factor “experiment” with the level control sessions and inactivation sessions. This analysis was complemented with post hoc tests to evaluate three crucial contrasts related to our hypothesis: (1) difference between pre- vs.- post-injection period for control and inactivation, (2) difference between the post-testing periods of control and inactivation sessions, (3) difference between the pre-testing periods of control and inactivation sessions. The resulting p-values were corrected for multiple comparisons using Bonferroni correction.

Spike detection and unit selection criteria

The raw data were recorded as full broadband and “snippets” (33 samples, 1.375 ms) around the threshold crossing. For the current analysis, we only used “snippets”. An online visually determined threshold generated the snippets so that all recorded voltage drops surpassed this threshold were defined as potential spikes. Spike detection and waveform sorting were performed with the semiautomatic procedure implemented in the Plexon Offline Sorter v. 3.3.5 (Plexon, USA). After defining templates by manually clustering in principle component space

using the first three principal components and the recording time axis, the waveform template algorithm was used. Based on visual inspection of spike shapes, cluster shapes, and inter-spike intervals, clusters were categorized as single units, multi-units, and rejected “noise”. Typically, one to three clusters were isolated from each microelectrode where spikes had been identified.

In total, 616 single and multi-units were recorded in the dorsal pulvinar (right hemisphere: n = 163, left hemisphere: n = 453), 74 single and multi-units were recorded in the ventral posterior lateral nucleus, and 172 single and multi-units were recorded in the mediodorsal thalamus (right hemisphere MD: n = 161, left hemisphere MD: n= 11). The units for MD are combined in further analyses. We applied two selection criteria to this dataset. First, we discarded units (left dPul: n=51, right dPul: n=25, MD: n=9, VPL: n=5) with very low firing rate (< 2 spike/s). Second, we discarded units that were recorded for less than 600 heartbeats (left dPul: n=48, right dPul: n=20, MD: n=2, VPL: n=5). All remaining units were considered valid, resulting in 494 units (left dPul: n= 376, right dPul: n = 118) in the dorsal pulvinar and 161 units in the mediodorsal thalamus, and 64 units in the ventral posterior lateral nucleus. Notably, not all units remained stable over the time recorded in a sequence of the rest and task periods, leading to different numbers of recorded units for rest and task of the further analysis.

We computed a signal-to-noise ratio for each unit to estimate the quality of the recorded signal. The signal-to-noise ratio for each unit was computed by calculating the amplitude difference from peak to trough of the average waveform divided by the averaged standard deviation for each bin of the individual spike waveforms. A homogenous waveform cluster with a high amplitude of the waveform compared to the noise level would correspond to a high signal-to-noise ratio, while a small noisy multiunit that barely crosses the threshold would correspond to a low signal-to-noise ratio (**Figure 4.5**). This signal-to-noise ratio was used to evaluate the potential confounding effects of heart activity-related brain pulsation on spike detection. The underlying assumption is that mechanical instability could lead to increased variability between recorded spike waveforms of the same unit and therefore an unstable detection of units with an amplitude close to the spike detection threshold (Mosher et al., 2020).

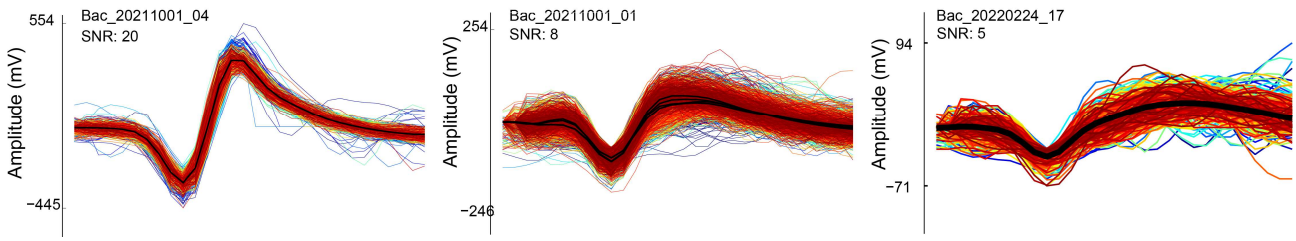

Figure 4.5. Example units covering the range of signal-to-noise (SNR) ratios.

Firing rate and ECG-triggered averages

We analyzed the recorded units separately for task and rest periods. Data analysis and statistical tests were performed using MATLAB R2015a. The analysis focuses on the timing of spikes to assess if the neural activity of a neuron is related to the cardiac cycle. The firing rate of a single unit was computed by summing the number of spikes per time interval (spike count rate) divided by the time interval. This continuous estimate of instantaneous firing rate (spike density) was computed at a bin size of 10 ms by convolving the spike density time series with a Gaussian kernel (σ = 20 ms). Averaging the spike density locked to the R-peak across multiple trials leads to the peri-“stimulus” (peri-event) time histogram (PSTH). Here, an event is defined as one instance of a heartbeat because the spike density time series was used to identify time-locked transient changes in firing rate in relationship to heartbeats.

The existence of significant transient increases or decreases in firing rate in the spike-density time series was assessed by comparison to surrogate data. The coarse-temporal structure in the cardiac activity reflected in the R-R intervals is taken into account by using a jitter-based resampling method to create the surrogate data, adapted from the approaches tested on spiking activity (Amarasingham et al., 2012). For each surrogate dataset, each R-R interval was contracted or expanded by a small amount, randomly drawn from a normal distribution with a standard deviation based on the measured distribution of R-R intervals in this particular recording. Note that this is different from jittering the R-peaks themselves because several subsequent intervals can be expanded (or contracted), resulting in accumulated R-peak offset. Because the movements of the animals caused artifacts that rendered R-peak detection impossible in specific periods, those recording periods were treated as invalid. For computing the standard deviation for jittering, only R-R intervals that fell into valid periods were considered for computing the standard deviation for jittering. Additionally, the R-peaks that fell into invalid time periods after jittering were removed similar to the measured R-R intervals. One thousand surrogate datasets were computed for each unit using normally distributed random jitters of intervals, but the inherent distribution of R-R intervals was mainly preserved.

Each time point of the observed spike-density time series was compared to the respective time point of the surrogate data and marked as significant if it was outside the surrogate dataset's 95% confidence interval. The 95% confidence interval was derived from the sorted surrogates by taking the 25^{th} and 975^{th} values as the borders of the confidence interval. This procedure potentially leads to several significant modulation intervals in the firing rate per unit. In this case, only the interval with the highest significant firing rate modulation lasting at least 40 ms (4 consecutive bins) was labeled a “significant modulation” and used to group the units

into units with and without a significant heart rate relationship for further analysis. To compare units with different average firing rates, each unit normalized spike density function was calculated by subtracting the average of the surrogate data from the actual R-peak-triggered time course for each bin across all trials and dividing by the average of the surrogate data, resulting in a percent firing rate change after multiplication by 100. In addition, we also performed a simple subtractive normalization (actual – surrogate time course). For population PSTHs, the average normalized spike density and standard error across units were calculated separately for task and rest periods.

To quantify the heart rate-related modulation strength (modulation index), we computed the difference between the maximum and a minimum of the normalized signal (either as % signal change from the ongoing (surrogate) firing rate or a difference between an actual R-peak-triggered average and a surrogate) separately for rest and task for each unit in the time window of 0.25 s before and after the R-peak. As an indicator for the potential mechanical waveform instability confound, we assessed the relationship between the signal-to-noise ratio of a unit and its cardiac modulation index. For this purpose, we calculated Pearson's correlation coefficient between the signal-to-noise ratio of a unit and the modulation index for each brain region with and without the non-significant units.

Results of the inactivation experiment

We investigated whether local unilateral injections of THIP disrupt the dorsal pulvinar neuronal activity influencing cardiac and respiratory signals. To address this question, the continuous electrocardiogram and respiration were recorded by two monkeys before and after inactivating the dorsal pulvinar. Heart rate, respiration rate, and heart rate variability were computed to analyze the difference between pre-and post-injection periods in inactivation and control sessions. The animals were either engaged in a cognitively demanding task performing color discrimination or passively sitting in their primate chair during rest. We expected a lower heart rate and respiration rate for rest periods before the injection due to different behavioral activity (perceptual decisions and goal-directed saccades vs. passively sitting) and psychological states (cognitive effortful vs. no mental stimulation). Our prediction about the heart rate was confirmed by a statistical significant main effect "TaskType" for all three monkeys (three-way mixed measure ANOVAs, M1: $F(1,18) = 20.75$, $p< 0.001$, M2: $F(1,16) = 100.01$, $p< 0.001$, M3: $F(1,9) = 50.17$, $p< 0.001$; see the details in Supplementary Information, **Suppl. Tables S4.1-S4.3,** with additional information for the respiration rate).

Verification of the pharmacological effect of inactivation

The success of the inactivation procedure was evaluated based on the previously described findings of an ipsilesional selection bias for target-target stimuli (Wilke et al., 2010, 2013). The mixed measure ANOVAs indicate that the contralateral target selection differed significantly for monkeys 1 and 2 for the interaction “Experiment x Timeline” (2-way mixed measure ANOVAs, M1: $F(1,20) = 14.37$, $p= 0.001$, M2: $F(1,16) = 14.78$, $p= 0.001$) and the main effects “Timeline” (2-way mixed measure ANOVAs, M1: $F(1,20) = 11.44$, $p= 0.003$, M2: $F(1,16) = 23.43$, $p< 0.001$) and the main effect “Experiment” (2-way mixed measure ANOVAs, M1: $F(1,20) = 5.58$, $p= 0.028$). The latter main effect was not significant for M2: $F(1,16) = 2.97$, $p< 0.1$). Both monkeys show a significant decrease in contralateral target selection for the target-target trials after dPul inactivation (Ina, post) compared to pre-injection periods (Ina, pre) and post-control periods (Ctr, post), indicating a spatial selection bias and a successful inactivation procedure.

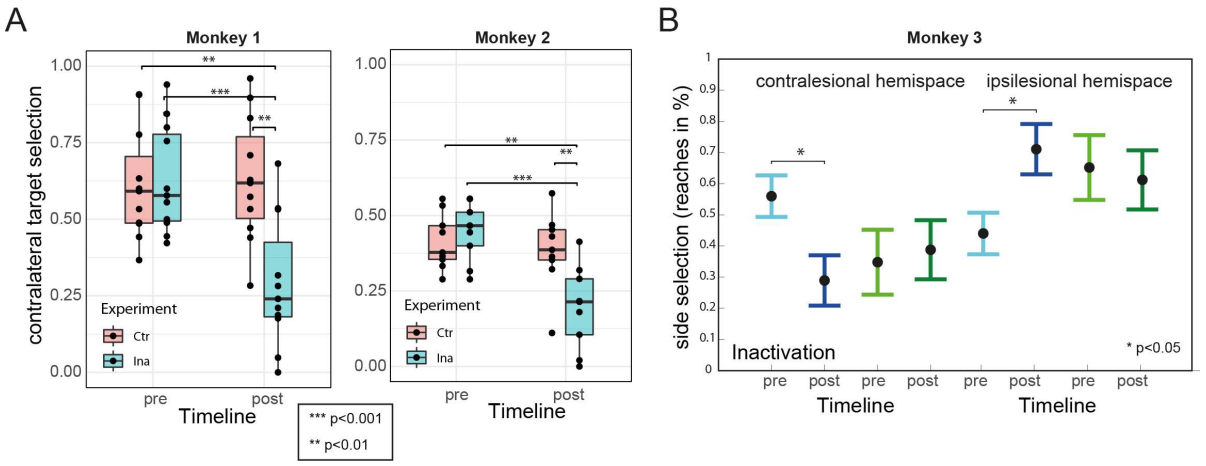

Figure 4.6. Behavioral effects to confirm the success of the inactivation procedure. (A) Monkeys 1 and 2 performed the color discrimination task where a free-choice target-target condition was included in determining the inactivation-induced change in selection behavior. The selection behavior is displayed here in a box and whisker plot where the minimum, maximum, and as a box the first quartile, median and third quartile are displayed. The additional black dots represent the mean contralateral target selection per session. The change in contralateral target selection in control compared to inactivation sessions at pre vs. post periods of a session was statistically evaluated using a two-way mixed ANOVA followed by Bonferroni-corrected post hoc tests. The post-doc tests are depicted as follows: *** shows $p_{Bonferroni}$ values ≤ 0.001, ** $p_{Bonferroni}$ values ≤ 0.01, and * $p_{Bonferroni}$ value ≤ 0.05). Both monkeys show a significant decrease in contralateral target selection for the target-target trials after dPul inactivation (Ina) compared to pre-injection periods (Ina, pre) and post-control periods (Ctr, post), indicating a spatial selection bias and a successful inactivation procedure. (B) Monkey 3 performed a direct reach task with cued hand usage where also a free choice target-target condition was included in determining the validity of the inactivation procedure. After unilateral inactivation, monkey 3 selected significantly less the contralesional target with the contralesional hand (blue for the contralesional hand) in the post-inactivation periods compared to pre-inactivation periods.

The effect of dPul inactivation on heart rate and respiration rate

To evaluate our hypothesis whether local reversible pharmacological inactivation of dorsal pulvinar affects heart and respiration rate, we compared the means of groups using three-way mixed measure ANOVAs by including as within-sessions factors “timeline” with the levels pre- and post-testing periods per session and “TaskType” with the levels “rest” and “task”, as well as one between-session factor “experiment” with the levels control and inactivation sessions and their interaction. This analysis was complemented with post hoc tests to evaluate two essential contrasts to discriminate the effect of inactivation from an effect over time: (1) difference between pre- vs.- post-injection period for control and inactivation, (2) difference between the post-testing periods of control and inactivation sessions.

We analyzed the effect of dPul inactivation on the average heart rate, defined by the number of heart contractions (R-peaks) per minute. The three-way mixed measure ANOVAs for heart rate indicates significant main effects for “Experiment” (M1: $F(1,18) = 18.39$, $p < .001$) and “Timeline” ($F(1,18) = 20.03$, $p < .001$) for M1 but no significant interaction effects. The other monkeys showed only a main effect of “Timeline” (M2: $F(1,16) = 50.77$, $p < .001$, M3: $F(1,9) = 8.11$, $p = .02$) on heart rate and also here, no significant interaction effects (see the details in Supplementary Information, **Suppl. Tables S4.1-S4.3**). We further analyzed the effect of dPul inactivation on the average heart rate separately for the two level of task engagements (**Figure 4.7 A**). In all three monkeys, dPul inactivation significantly slowed down the average heart rate during post-injection periods at rest compared to pre-injection periods by ~22 bpm for M1, ~12 bpm for M2 and ~7 bpm for M3 (three-way mixed measure ANOVA followed by Bonferroni-corrected post-hoc tests, M1: $t(1,18) = -4.02$, $p = .005$; M2: $t(1,16) = -5.49$, $p = .0003$; M3: $t(1,9) = -3.45$, $p = .043$). We compared the post-injection periods to the post-control periods to differentiate between effect of inactivation and changes over the time course of a session. For M1, the inactivation-induced effect of post-injection periods was significant different to the post-control periods by ~31 bpm for M1 (three-way mixed measure ANOVA followed by Bonferroni-corrected post-hoc tests, M1: $t(1,18) = -4.06$, $p = .002$; M2: $t(1,16) = .88$, $p = 1$; M3: $t(1,9) = -0.23$, $p = 1$). When the monkeys were engaged in the task, the average heart rate slowed down during post-injection periods for two monkeys compared to pre-injection periods by ~18 bpm for M1 and ~8 bpm for M2 (three-way mixed measure ANOVA followed by Bonferroni-corrected post-hoc tests, M1: $t(1,18) = -4.22$, $p = .003$; M2: $t(1,16) = -4.59$, $p = .002$; M3: $t(1,9) = 1.22$, $p = 1$;). For M1, the inactivation-induced effect of post-injection periods was significantly different to the post-control periods by ~27 bpm (two-way mixed measure ANOVA followed by Bonferroni-corrected post-hoc tests, M1: $t(1,18) = -4.67$, $p = .0004$; M2: $t(1,16) = 0.07$, $p = 1$; M3: $t(12) = -0.61$, $p = 1$).

We measured the exhaling peaks from the nose of monkey to calculate the respiration rate, defined by the number of exhaling peaks per minute. The three-way mixed measure ANOVAs for respiration rate indicates significant interaction effect for “Experiment x Timeline” (M3: $F(1,9) = 11.94$, $p= 0.007$) for M3. M2 showed a main effect of “Timeline” (M2: $F(1,16) = 10.59$, $p< 0.001$) and M1 no significant effect (see the details in Supplementary Information, **Suppl. Tables S4.1-S4.3**). We further analyzed the effect of dPul inactivation on the average respiration rate separately for the two level of task engagements (**Figure 4.7B**). In one of three monkeys, the respiration rate significantly decreased after dorsal pulvinar inactivation at rest during post-injection periods compared to pre-injection periods by ~2 bpm for M3 (M1: $t(1,18) = 1.58$, $p= .79$; M2: $t(1,16) = 2.89$, $p= .065$; M3: $t(1,9) = -4.00$, $p= .016$) but no significant difference was found to post-control periods (M1: $t(1,18) = 2.05$, $p= .3$; M2: $t(1,16) = 0.66$, $p= 1$; M3: $t(1,9) = 1.37$, $p= 1$). When the monkeys were engaged in the task, the respiration rate of two monkeys significantly decreased after dorsal pulvinar inactivation during post-injection periods compared to pre-injection periods by ~3 bpm for M3 (M1: $t(1,18) = 2.09$, $p= .3$; M2: $t(1,16) = 2.52$, $p= .14$; M3: $t(1,9) = 5.5$, $p= .002$). No significant difference was found to post-control periods (M1: $t(1,18) = 2.1$, $p= .27$; M2: $t(1,16) = .31$, $p= 1$; M3: $t(1,9) = 2.67$, $p= .1$).

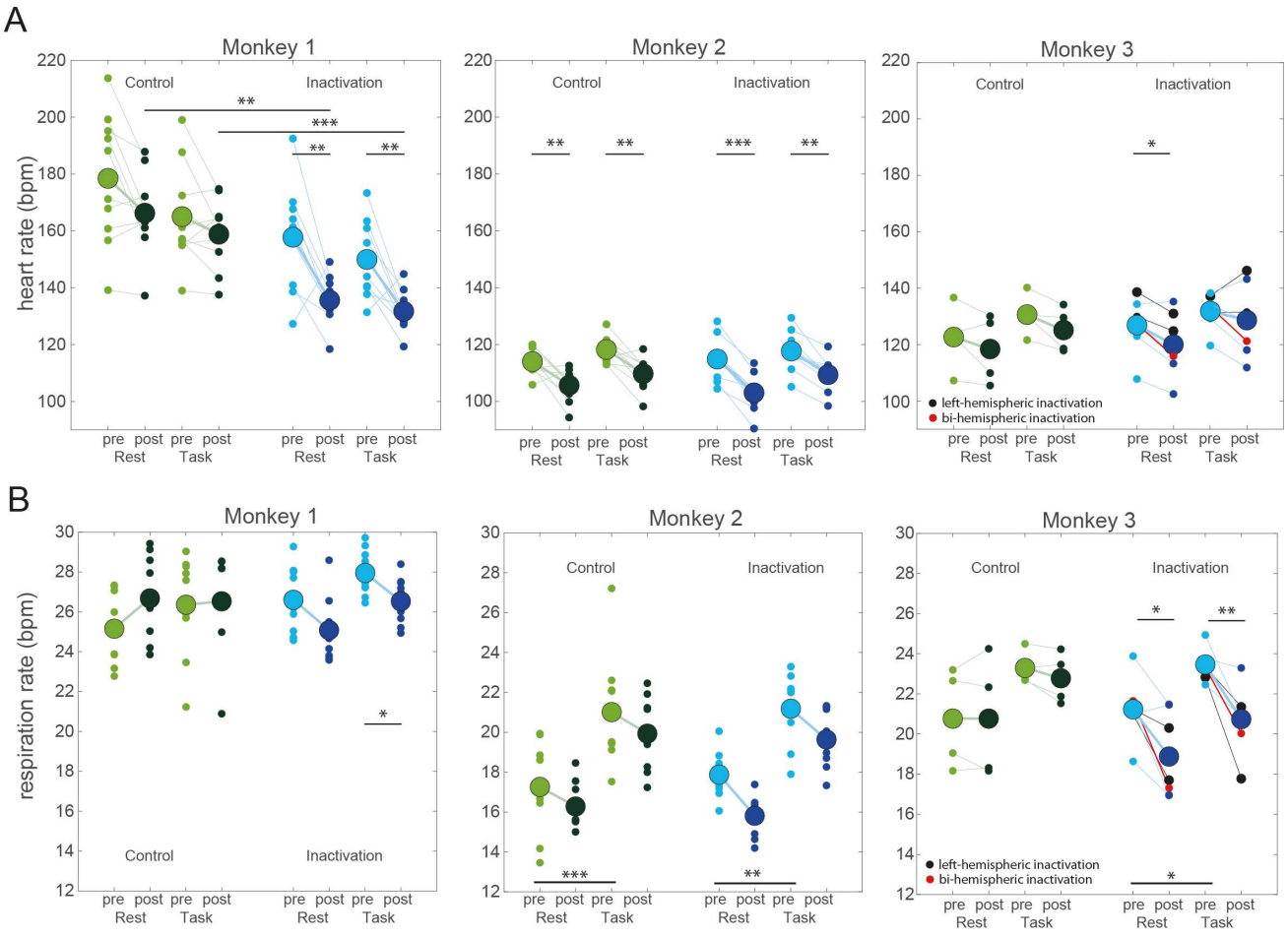

Figure 4.7. Inactivation effects on heart rate and respiration rate. Each monkey's heart and respiration rates are displayed for the two engagement levels (rest vs. task) and control and inactivation sessions. Small circles indicate single sessions, and large circles display the mean across sessions. The significant statistical results of the corrected post-hoc tests are depicted as follows: *** shows $p_{Bonferroni}$ values ≤ 0.001, ** $p_{Bonferroni}$ values ≤ 0.01, and * $p_{Bonferroni}$ value ≤ 0.05) (A) For all three monkeys, the heart rate decreases at post-injection compared to pre-injection. For one of these three monkeys, the heart rate decreased post-injection compared to post-control periods for rest and task. (B) For one of three monkeys, the respiration rate decreased post-injection compared to pre-injection periods.

The effect of dPul inactivation on heart rate variability

Normal rhythmic fluctuations between heartbeats were analyzed using two different heart rate variability measures. Well-established is that heart rate variability depends on heart rate, but it's still debated how to adjust for these dependency (de Geus et al., 2019; Gąsior et al., 2016; Kazmi et al., 2016; Sacha, Barabach, et al., 2013; Sacha, Sobon, et al., 2013). Here, we adjusted for the effect of heart rate for both variables as in the approach from Monfredi and colleagues (Monfredi et al., 2014), but still, we display adjusted and non-adjusted heart rate variability.

We computed the adjusted root mean square of successive differences (RMSSD) that measures the fast changes in heart rate and is the primary time-domain measurement to estimate the vagally-mediated changes reflected in HRV (**Figure 4.8A**). The three-way mixed measure ANOVAs for the adjusted RMMSSD indicates significant interaction effect for "Experiment x Timeline" (M1: $F(1,18) = 12.27$, $p= .003$) and the main effects for "Experiment" (M1: $F(1,18) = 23.09$, $p< .001$) and "Timeline" for M1 (M1: $F(1,18) = 18.23$, $p< .001$). M2 and M3 showed a main effect of "Timeline" (M2: $F(1,16) = 10.12$, $p= .006$, M3: $F(1,9) = 5.75$, $p= .04$). Further details on the ANOVAs and the statistical analysis for the non-adjusted RMSSD are included in Supplementary Information, **Suppl. Tables S4.4-S4.6**.

We further analyzed the effect of dPul inactivation on the RMSSD separately for the two level of engagements (**Figure 4.8B**). For two out of three monkey, the adjusted root mean square of differences of the adjacent peaks (RMSSD) increased significantly after dorsal pulvinar inactivation at rest during post-injection periods compared to pre-injection periods by ~ 3.9 ms for M1 and ~ 22 ms for M2 (three-way mixed measure ANOVA followed by Bonferroni-corrected post-hoc tests, M1: $t(1,18) = 4.92$, $p= .001$; M2: $t(1,16) = 4.1$, $p= .005$; M3: $t(1,9) = 0.09$, $p= 1$) and compared to post-control periods by ~ 3.7 ms (three-way mixed measure ANOVA followed by Bonferroni-corrected post-hoc tests, M1: $t(1,18) = 3.1$, $p= .026$; M2: $t(1,16) = 0.52$, $p= 1$; M3: $t(1,9) = -2.22$, $p= .31$). While the monkey was engaged in the task, the adjusted RMSSD increased during post-injection periods for the same monkey compared to pre-injection periods by ~4.2 ms for M1 (three-way mixed measure ANOVA followed by

Bonferroni-corrected post-hoc tests, M1: t(1,18) = 6.84, p < .001; M2: t(1,16) = 1.99, p= .38; M3: t(1,9) = -1.46, p= 1) and compared to post-control periods by ~3.3 for M1 ((two-way mixed measure ANOVA followed by Bonferroni-corrected post-hoc tests, M1: t(1,18) = 3.94, p= .003; M2: t(1,16) = -0.52, p= 1; M3: t(1,9) = -1.86, p= .52).

We also computed the standard deviation of the R-R-intervals to assess the slow changes in heart rate (**Figure 4.8B**). For the adjusted standard deviation of the R-R-interval, the three-way mixed measure ANOVAs indicates significant main effects for “Experiment” (M1: F(1,18) = 12.81 , p= .002) and for “Timeline” (M1: F(1,18) = 6.98 , p< .017) for M1, a significant three-way interaction for M2 (M2: F(1,16) = 4.65 , p= .047) as well as significant interaction of “Experiment x Timeline” (M2: F(1,16) = 4.58 , p= .044). No significant effect was found for M3 (see the details of the ANOVAs in Supplementary Information, **Suppl. Tables S4.4-S4.6**).

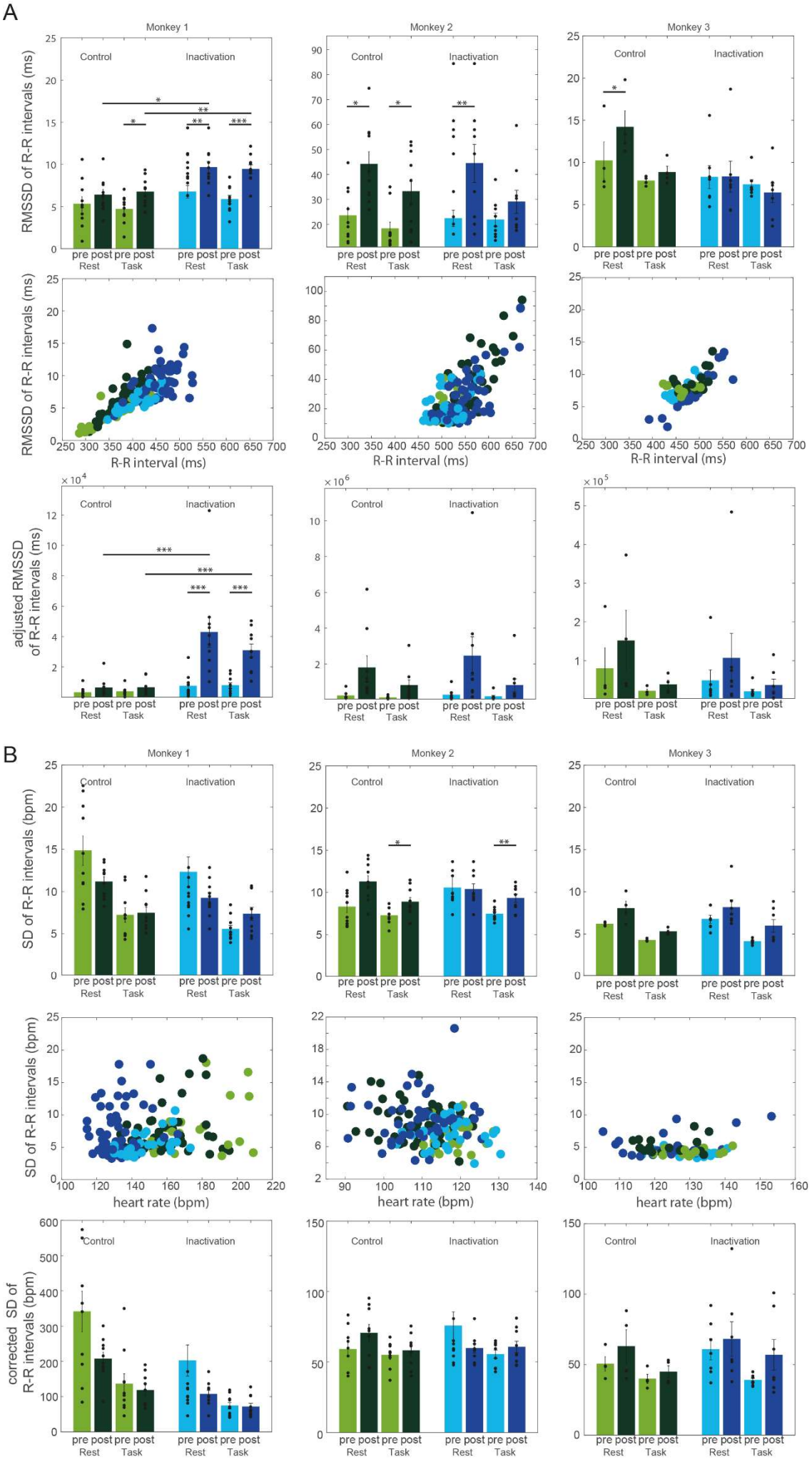
A
Monkey 1
Monkey 2
Monkey 3
Control
Inactivation
RMSSD of R-R intervals (ms)
pre post pre post
Rest Task
R-R interval (ms)
adjusted RMSSD of R-R intervals (ms)
B
SD of R-R intervals (bpm)
heart rate (bpm)
corrected SD of R-R intervals (bpm)

Figure 4.8. Inactivation effects on heart rate variability. Two heart rate variability indices of the time domain are displayed for each monkey for the engagement levels (rest vs. task) and control (green), and inactivation sessions (blue). The bar graphs display the mean and standard error of the specific heart rate variability indices, and small black circles show single sessions. Since heart rate variability depends on heart rate, their relationship is plotted. Each circle displays the average heart rate and variability for a block of 10-min recorded data. The significant statistical results of the corrected post-hoc tests are as follows: *** shows $p_{Bonferroni}$ values ≤ 0.001, ** $p_{Bonferroni}$ values ≤ 0.01, and * $p_{Bonferroni}$ value ≤ 0.05). (A) At first, the results of the root mean square of successive differences (RMSSD) in ms as a local index for the heart rate variability are plotted for all conditions for each monkey. The positive relationship between the R-R interval (ms) and the RMSSD (ms) is displayed. Finally, the bar graph shows the RMSSD, adjusted for the universal exponential relationship between RMSSD and R-R intervals. (B) The standard deviation of the R-R interval in bpm as a global index for the heart rate variability is plotted for all conditions for each monkey. The negative relationship between heart rate and the standard deviation of the R-R interval is displayed for each monkey. The final bar graph shows the R-R interval's standard deviation, adjusted for the universal decay-like exponential relationship between the standard deviation of the R-R interval and heart rate.

Two control experiments for the inactivation-induced effect in monkey 1: targeting ventral pulvinar and the opposite (right) dorsal pulvinar

The experimental procedure was repeated for M1 to investigate whether unilateral pharmacological inactivation of the ventral pulvinar or the opposite dorsal pulvinar in the right hemisphere showed the cardiac effects as in the left dorsal pulvinar for this monkey (**Figure 4.9**). For the ventral pulvinar, the 3-way mixed measure ANOVAs for heart rate shows a significant main effect for “Experiment” (M1: $F(1,4) = 17.56$, $p < .01$), indicating a difference in heart rate between control and inactivation sessions. No main effect or interaction for the sessions in the right hemisphere of the dorsal pulvinar got significant. To conclude, we saw a significant change in heart or respiration rate after post-inactivation for neither of the two injection locations (ventral pulvinar, right dorsal pulvinar).

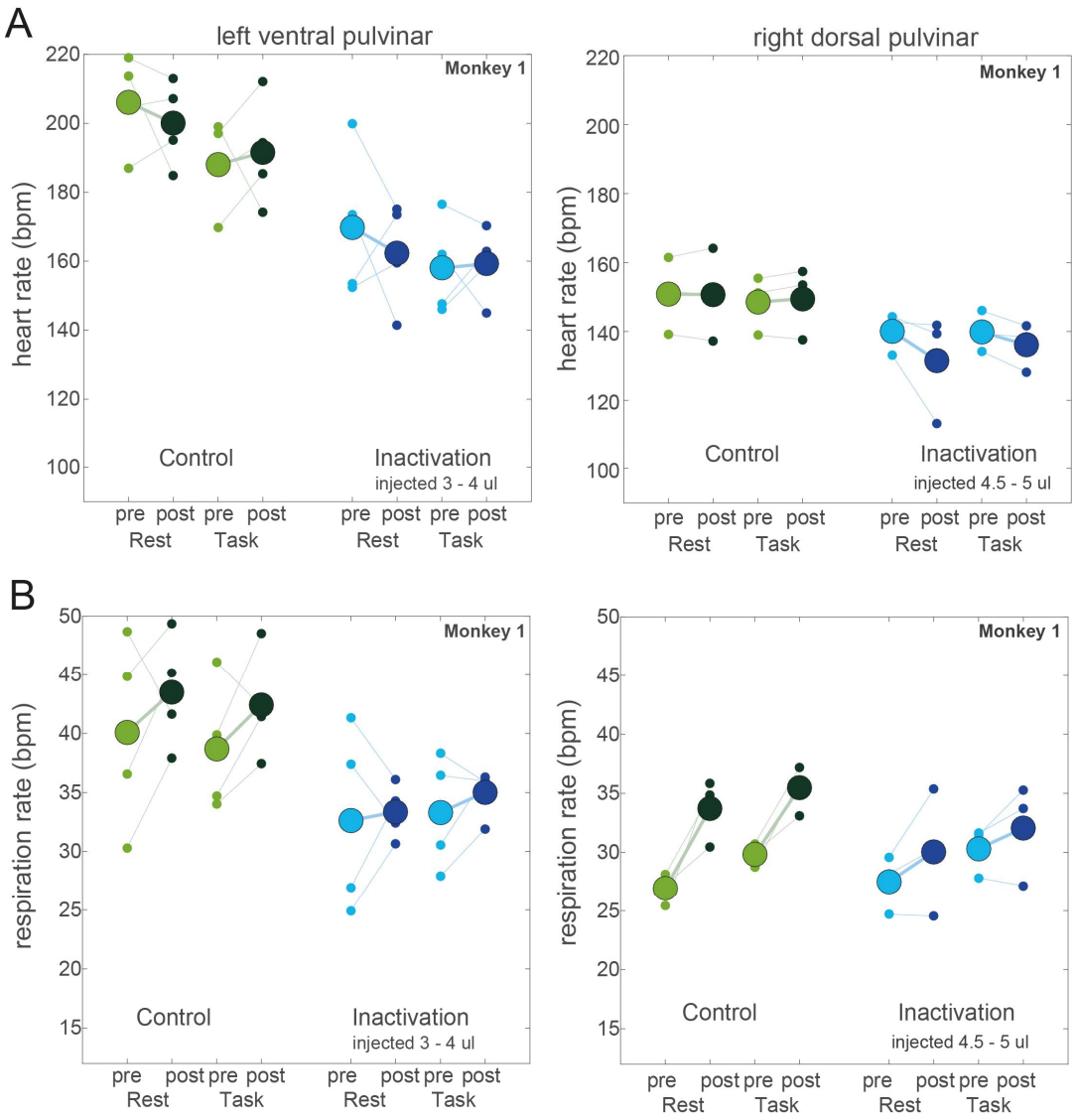

Figure 4.9. Ventral pulvinar and right dorsal pulvinar inactivation effects on heart rate and respiration rate. Each monkey's heart and respiration rates are displayed separately for each engagement level (rest vs. task) and according to control and inactivation sessions. Small circles indicate single sessions, and large circles display the mean across sessions. The significant statistical results of the corrected post-hoc tests are as follows: *** shows $p_{Bonferroni}$ values ≤ 0.001, ** $p_{Bonferroni}$ values ≤ 0.01, and * $p_{Bonferroni}$ value ≤ 0.05). No significant effect was observed for the (A) heart rate or (B) respiration rate nor for the ventral pulvinar or the dorsal pulvinar in the right hemisphere.

Results of the electrophysiology experiment

We investigated the relationship between the R-peak from the electrocardiogram (ECG) and the neural firing rate of thalamic neurons. The neural and cardiac activity was continuously recorded in one monkey performing the color discrimination saccade task or sitting in the primate chair (rest without explicit task demand, no control of eye movements). As the state of rest is characterized by spontaneous neural activity that differs from the task-evoked activity, we analyzed all data separately for rest and task. The coupling between heartbeats

and spiking activity was assessed for each unit in three thalamic nuclei, the dorsal pulvinar (dPul), the mediodorsal thalamus (MD), and the ventral posterior lateral nucleus (VPL) separately for rest and task periods.

Heart rate variability between and across sessions

The R-R intervals (cardiac cycles) derived from the electrocardiogram vary spontaneously. We assessed the average heart rate (**Figure 4.10A**) and the root means square of successive differences (RMSSD) as a measure of heart rate variability for each session. The RMSSD reflects the beat-to-beat variance in heart rate. The heart rate for monkey 4 varies between two successive beats by an average of 20 ms **Figure 4.10B**). In addition, it is crucial to examine the variability of the R-R intervals displayed for three example sessions as a histogram of the distribution of R-R intervals (**Figure 4.10C**) to analyze the relationship between spiking activity and heart rate. Another presentation of the variability between R-R intervals is the R-peak triggered ECG (see example in **Figure 4.10A**). Here, the standard deviation of the R-peak aligned electrocardiogram is small in the time window of analysis.

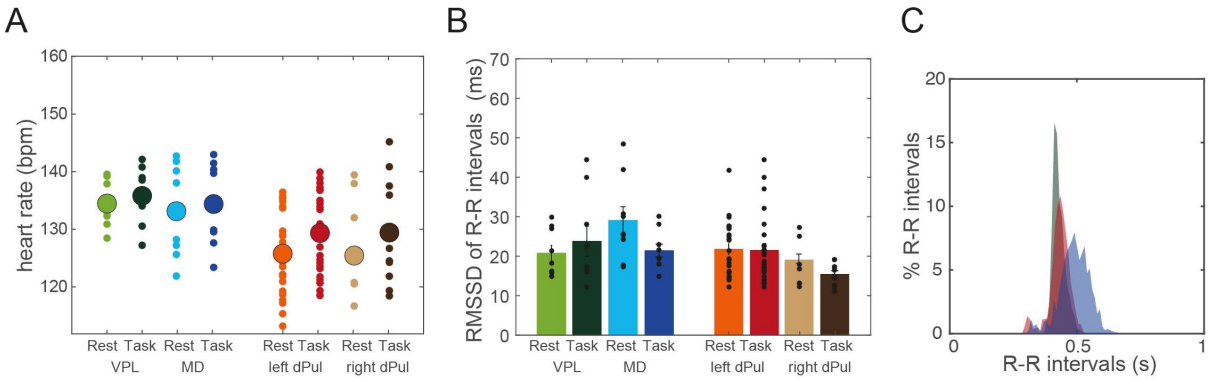

Figure 4.10. The variability of the heart rate between and within sessions. The average heart rate and its variability are grouped according to the recording locations of these sessions. (A) Each session's average heart rate is displayed separately for each brain region for the two engagement levels (rest vs. task). Small circles indicate single sessions and large circles show the mean across sessions. (B) The bar graphs show the mean and the standard error of the root mean square of successive differences (RMSSD) of R-R intervals in milliseconds across sessions, and small black circles show the RMSSD of R-R intervals of each session. (C) Histogram of distribution of R-R intervals of 3 example sessions from the (VPL, MD, dPul).

The relationship between the R-peak of the ECG and the firing rate

We investigated the spike timing relative to the R-peak (see examples in **Figure 4.11A**) and the ongoing firing rate of a unit by computing the average firing rate time-locking to the R-peaks resulting in the R-peak-triggered average for each unit (see examples in **Figure 4.11B**). We observed units showing a significant relationship between the R-peak of the ECG and the firing rate for all three thalamic regions (see typical example units in **Figure 4.11C**).

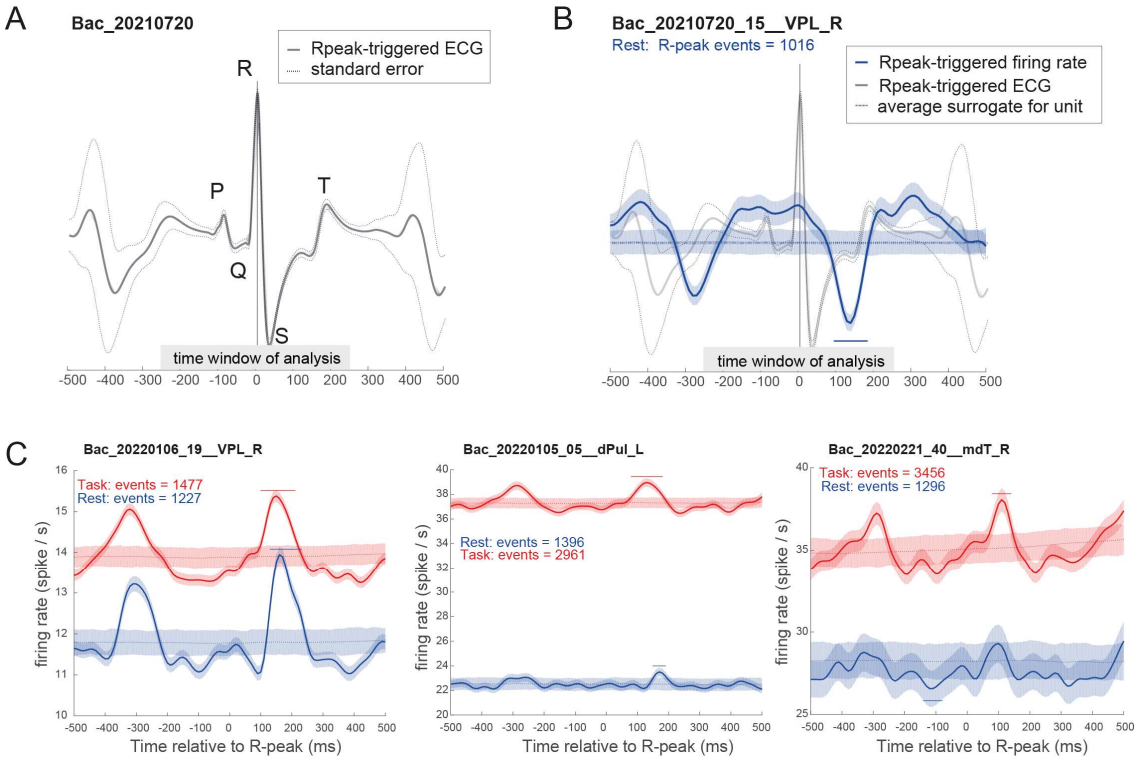

Figure 4.11. One example of R-peak triggered ECG of one session the R-peak triggered firing rate of three example units. (A) Displayed is the average electrocardiogram time-locked to the R-peak of one session and its standard deviation. The letters indicate the waves of the QRS-complex of the electrocardiogram. (B) Displayed are the averaged firing rates time-locked to the R-peaks and their surrogates of three units (from left to right: VPL, dPul left, MD), where the signal was averaged for periods of task and rest separately. The number of events represents the number of R-peaks for which the firing rate modulation was calculated.

Units were categorized into units with and without a significant heart rate relationship (R-peak-triggered modulation of firing rate) according to whether the observed spike density time series was outside the surrogate dataset's 95% confidence interval at a respective time point (see Methods). Note that not all units remained stable over the time to record the rest and task periods in a sequence leading to different numbers of recorded units for each engagement level. When the monkey was sitting in the chair without task demands (rest), we found in total 142 units (out of 336; 42%, left dPul: 132/278; 47%; right dPul: 10/ 58; 17%) in the dorsal pulvinar and 62 (out of 116; 53 %) units in the mediodorsal thalamus that showed a significant modulation of the firing rate about the cardiac cycle (**Figure 4.12 A**). At rest, the dorsal pulvinar had the lowest number of cardiac-related neurons with 42% compared to 53 % of cardiac-related units in MD and 84% (46/55; 84%) in VPL that showed significant coupling between spiking activity and cardiac cycle.

When the monkey was performing the task, we found in total 260 units (out of 388; 67%, left dPul: 206/299; 69%; right dPul: 54/89; 61%) in the dorsal pulvinar and 104 units (out of 152;

68%) in the mediodorsal thalamus that showed a significant modulation of the firing rate with the cardiac cycle (**Figure 4.12B**). Both higher-order thalamic nuclei had a similar percentage of around 67- 68% of cardiac-related units. In VPL, 49 units (out of 56; 88 %) showed significant coupling between spiking activity and cardiac cycle at the task.

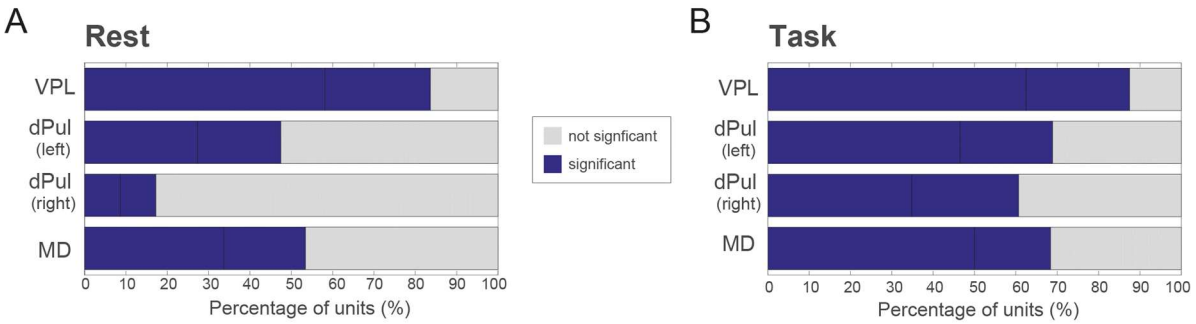

Figure 4.12. Percentage of units with significant R-peak locked neural activity. The proportion of non- and significant units for each brain region are presented separately for rest (A) and task (B).

The period after the R-peak is related to the systole, where the blood is pumped from the heart's two ventricles through the body, followed by the diastole, where the heart's chambers are re-filled with blood. To address the question of how the firing is changing in systole or diastole, we grouped the maximal significant transient firing rate changes according to when the change happened relative to the R-peak (before the R-peak and after the R-peak) and the direction of firing rate change (increase vs. decrease). The corresponding time course of each group is shown as the average normalized spike density time series (%signal change, %sc) separately for rest and task (**Figure 4.13**). The number of units and the average modulation index per group is displayed in **Table 4.1**. Although the time course after grouping looks very similar between different thalamic nuclei, the modulation index appeared on average higher for VPL compared to the other thalamic nuclei, suggesting that the units in VPL exhibited a stronger modulation in the normalized firing rate (average in %sc; VPL: Rest = 10.88, Task = 10.38; dPul (left): Rest = 8.65, Task = 6.44; dPul (right): Rest = 10.78, Task = 6.73; MD: Rest = 8.31, Task = 6.51). Compared to the dorsal pulvinar and MD, the spike density of the VPL units grouped exhibited strong average modulations for both periods, with one exception for the period before the R-peak in the Rest-period (before the R-peak during the diastole, average in %sc; VPL: Rest = 9.67, Task = 10.11; dPul (left): Rest = 7.88, Task = 5.62; dPul (right): Rest = 10.13, Task = 5.53; MD: Rest = 9.10, Task = 4.74; and after the R-peak during the systole, average in %sc; VPL: Rest = 12.09, Task = 10.64; dPul (left): Rest = 9.41, Task = 7.26; dPul (right): Rest = 11.11, Task = 7.94; MD: Rest = 7.52, Task = 8.29).

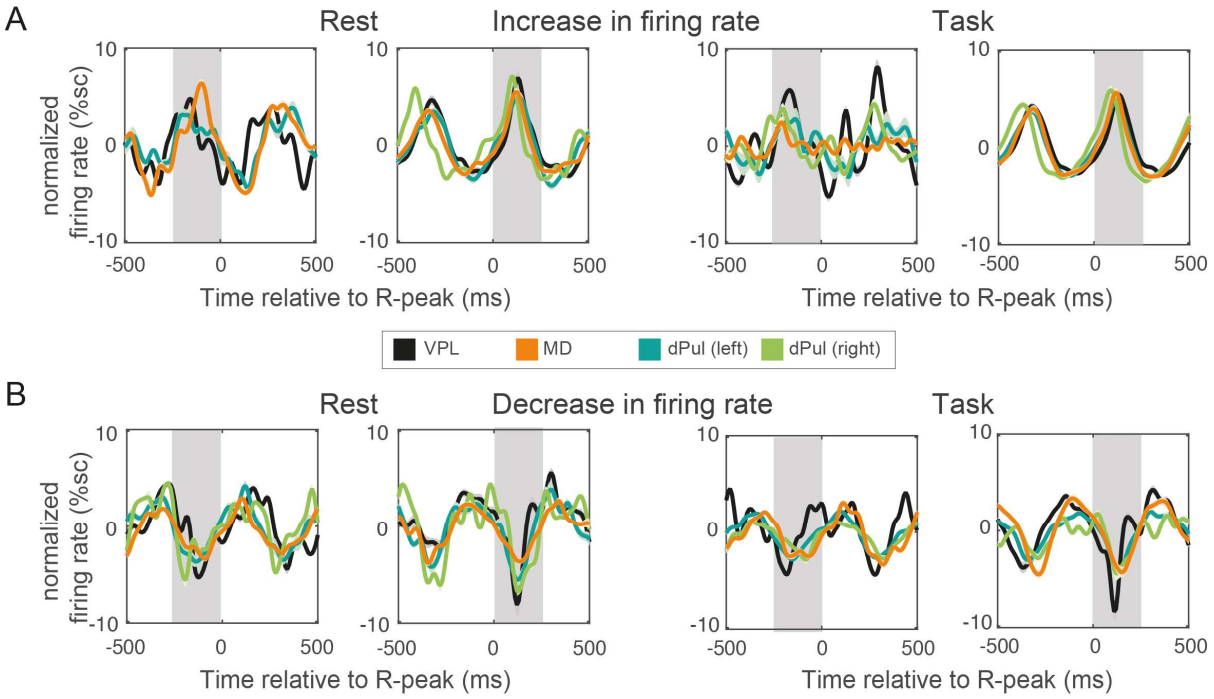

Figure 4.13. Time course of the transient changes in firing rate is time-locked to the R-peak. The significant average transient change in firing rate aligned to the R-peak for each brain region (VPL, dPul right and left, MD) is displayed. The cardiac-related changes in the firing rate are grouped according to the direction of change (increase vs. decrease) and when does this change happen relative to the R-peak (marked in gray is the duration of grouping interval: starting before the R-peak or after the R-peak related to a time window for analysis of -250 ms to 250 ms around the R-peak). The line displays each group's mean normalized firing rate (percent signal change), and the shading is the standard error, separated for rest and task. The increase (A) and decrease (B) in firing rate for the periods before or after the R-peak is displayed. See **Table 4.1** for the number of units in each panel.

Table 4.1. The number of units and average modulation strength (modulation index) per group.

Firing rate	Brain region	Relative to R-peak	MI (%sc)	N units	Relative to R-peak	MI (%sc)	N units
		Rest			Task		
Increase	VPL	Before	9.48	1	Before	11.16	2
	dPul (left)	Before	7.72	8	Before	6.13	6
	dPul (right)	Before	-	0	Before	6.92	3
	MD	Before	11.77	4	Before	3.8	7
	VPL	After	10.26	31	After	8.45	33
	dPul (left)	After	9.28	67	After	7.91	133
	dPul (right)	After	10.79	5	After	9.54	28
	MD	After	8.62	35	After	8.76	69
Decrease	VPL	Before	9.86	2	Before	9.07	1
	dPul (left)	Before	8.04	36	Before	5.11	36
	dPul (right)	Before	10.13	2	Before	4.13	13
	MD	Before	6.43	15	Before	5.68	19

	VPL	After	13.92	12	After	12.83	13
	dPul (left)	After	9.55	19	After	6.61	31
	dPul (right)	After	11.42	3	After	6.34	10
	MD	After	6.43	8	After	7.83	19

The control for potential mechanical cardiac-related effects leading to spike waveform instability.

We tested the relationship between signal-to-noise ratio and modulation index to evaluate cardiac-related recording instability due to the electrode's potential movements, as Mosher et al. (2020) proposed. We calculated the Pearson correlation coefficient between the signal-to-noise ratio of the spike waveform and the cardiac-related modulation strength of each recorded unit. In the case of a mechanical confound, we expect a negative correlation (less SNR → more modulation) because small noisy units with an amplitude close to the threshold might be un-proportionally “affected” by the cardiac activity. Such correlation, although indirectly, would suggest a confound due to the mechanical cardiac-related effect on recorded waveform stability and detection. The data did not show a negative correlation. Instead, the modulation index based on percent signal change and the signal-to-noise ratio showed either no significant correlation or a positive correlation for all recorded units in the dorsal pulvinar (**Figure 4.14A**). The positive direction of the correlation indicates that, on average, units with a higher signal-to-noise ratio also tend to have a higher modulation index.

This relationship, however, might be because a multiunit activity typically has a low signal-to-noise ratio compared to well-isolated single units. At the same time, multiunit activity usually has a high firing rate, leading to a potentially lower modulation index because of the divisive normalization if the presumed heart cycle-related modulation amplitude is below the multiplicative effect. Indeed, on average, units with a higher signal-to-noise ratio had a lower firing rate for all thalamic nuclei (**Figure 4.14 B**). Two examples of the relationship between modulation index and signal-to-noise ratio related to firing rates of the VPL and right dorsal pulvinar during rest are shown (**Figure 4.14 C**). Thus, the division in the normalization procedure to generate the percent signal change disadvantages units with a high firing rate and a low signal-to-noise ratio that might be more likely affected by the potential mechanical cardiac-related effects. Consequently, a possible negative correlation between SNR and cardiac modulation (that would be indicative of a spike detection confound) might be counteracted, and even overridden, by an opposite trend: a positive correlation between the SNR and the modulation (high SNR → low firing rate → high modulation).

Indeed, the modulation indexes derived from a subtractive “normalization” (a simple difference between the actual R-peak-triggered modulation of the firing and the (typically flat) surrogate reflecting mean ongoing firing rate) show a significant negative correlation with SNR for dPul and MD – but not VPL, This relationship indicates that in higher-order thalamus, on average, units with a higher signal-to-noise ratio and lower firing rate have a lower heart-related modulation of firing, when the modulation is expressed as a difference to the ongoing firing rate (**Figure 4.15**). The negative correlation is, however, expected in such analysis if a putative cardiac influence is manifested not as merely adding (or subtracting) a certain amount of spikes around the R-peak independently of the unit firing rate but is scaled in some way by the firing rate. Therefore, a negative correlation is not a definitive indication of the mechanical instability confound.

The scatter plot showing the two types of modulation indices, and the normalized firing rate indicated that the relationship between these variables is systematic but not very tight: while there are indeed units with low firing rate, low subtractive modulation, and high %sc modulation, and vice versa, high firing rate units with high subtractive modulation and low %sc modulation, there were also units in between these cases, with intermediate values (**Figure 4.16**).

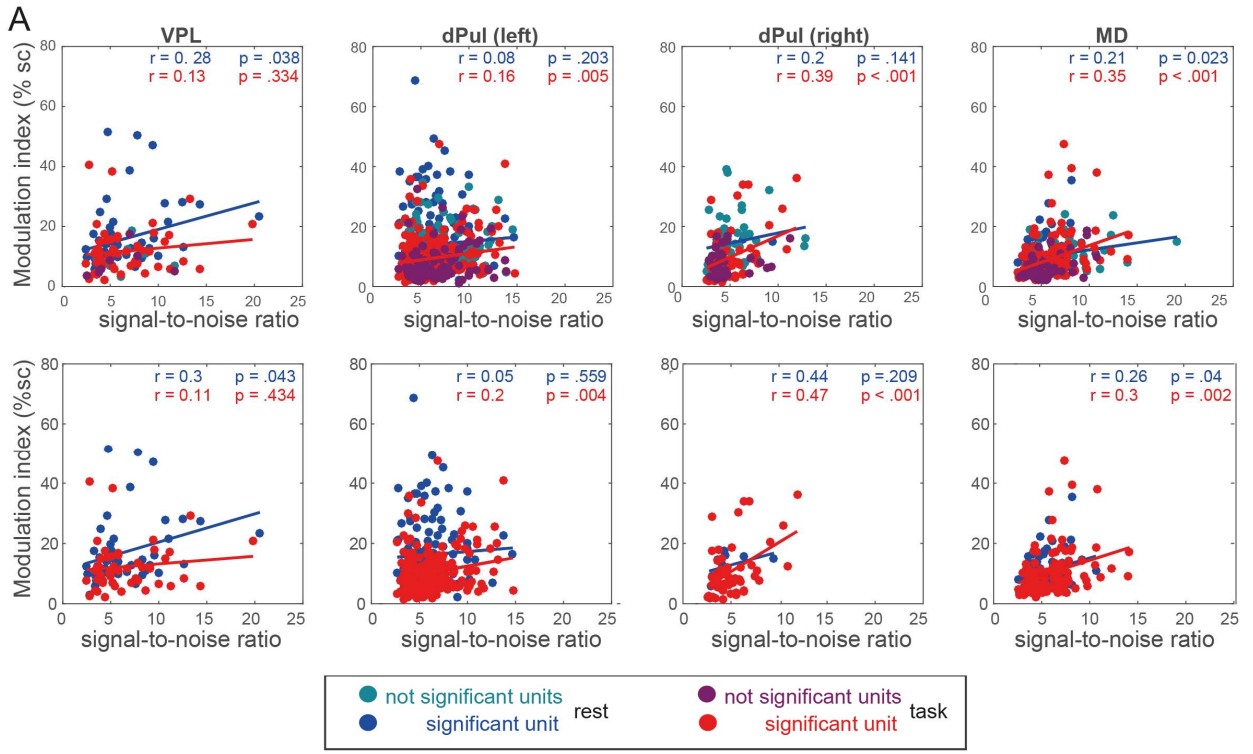
A
VPL
dPul (left)
dPul (right)
MD
Modulation index (% sc)
Modulation index (%sc)
signal-to-noise ratio
r = 0. 28 p = .038
r = 0.13 p = .334
r = 0.08 p = .203
r = 0.16 p = .005
r = 0.2 p = .141
r = 0.39 p < .001
r = 0.21 p = 0.023
r = 0.35 p < .001
r = 0.3 p = .043
r = 0.11 p = .434
r = 0.05 p = .559
r = 0.2 p = .004
r = 0.44 p =.209
r = 0.47 p < .001
r = 0.26 p = .04
r = 0.3 p = .002
not significant units
significant unit
rest
not significant units
significant unit
task

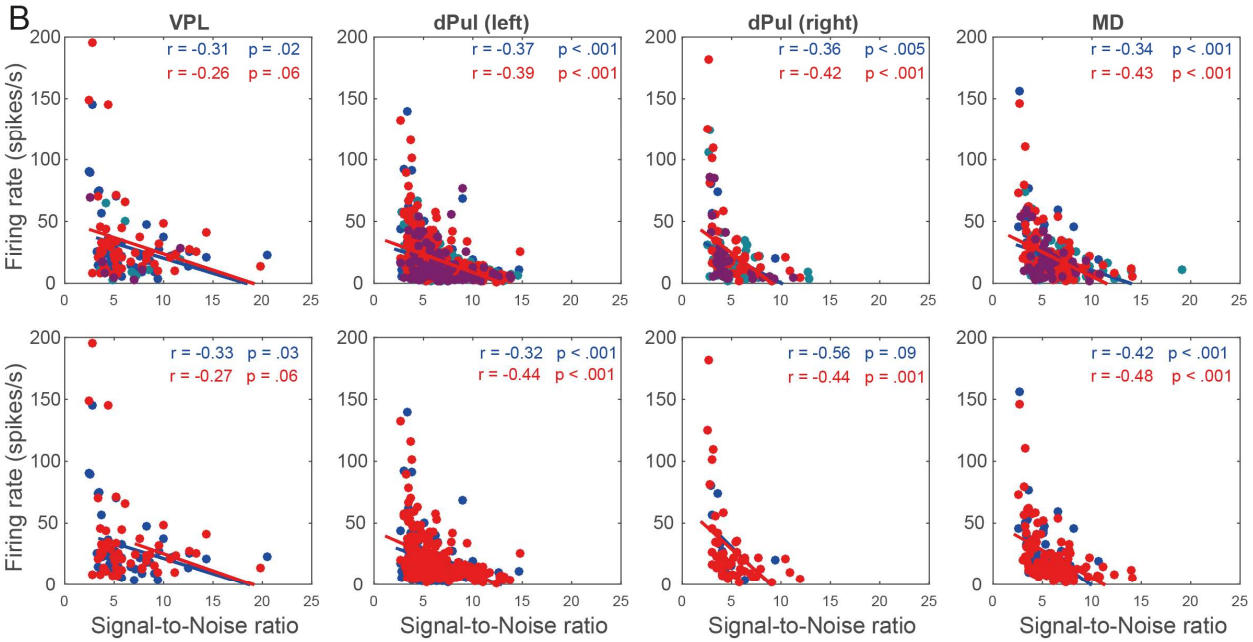
B
VPL
dPul (left)
dPul (right)
MD
Firing rate (spikes/s)
Signal-to-Noise ratio
r = -0.31 p = .02
r = -0.26 p = .06
r = -0.37 p < .001
r = -0.39 p < .001
r = -0.36 p < .005
r = -0.42 p < .001
r = -0.34 p < .001
r = -0.43 p < .001
r = -0.33 p = .03
r = -0.27 p = .06
r = -0.32 p < .001
r = -0.44 p < .001
r = -0.56 p = .09
r = -0.44 p = .001
r = -0.42 p < .001
r = -0.48 p < .001

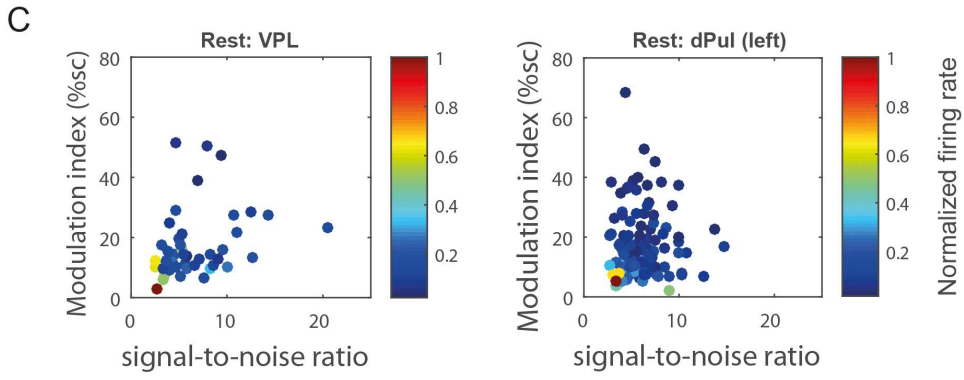
C
Rest: VPL
Rest: dPul (left)
Modulation index (%sc)
signal-to-noise ratio
Normalized firing rate

Figure 4.14. Correlations of the modulation index (%sc) or the firing rate with the signal-to-noise ratio. (A) The modulation index (%sc) is plotted as a function of the signal-to-noise ratio. Each dot represents a recorded unit either during rest (blue) or task (red). The slope of the lines shows the correlation coefficient separately for rest and task for the units shown in each graph. The related statistical parameter of the Pearson correlation (r, p-value) is displayed respectively for rest and task. The modulation index is plotted as a function of the signal-to-noise ratio (upper panel) and without the non-significant cardiac-related units (lower panel). Units are shown with no significant cardiac-related effect for rest (cyan) and task (purple), and units showing a significant cardiac-related impact for rest (blue) and task (red). (B) The firing rate is plotted as a function of the signal-to-noise ratio. (C) Examples of the relationship between signal-to-noise ratio and modulation index (%sc) together with the normalized firing rate (color scale) for two thalamic nuclei (VPL, dPul left) during rest periods.

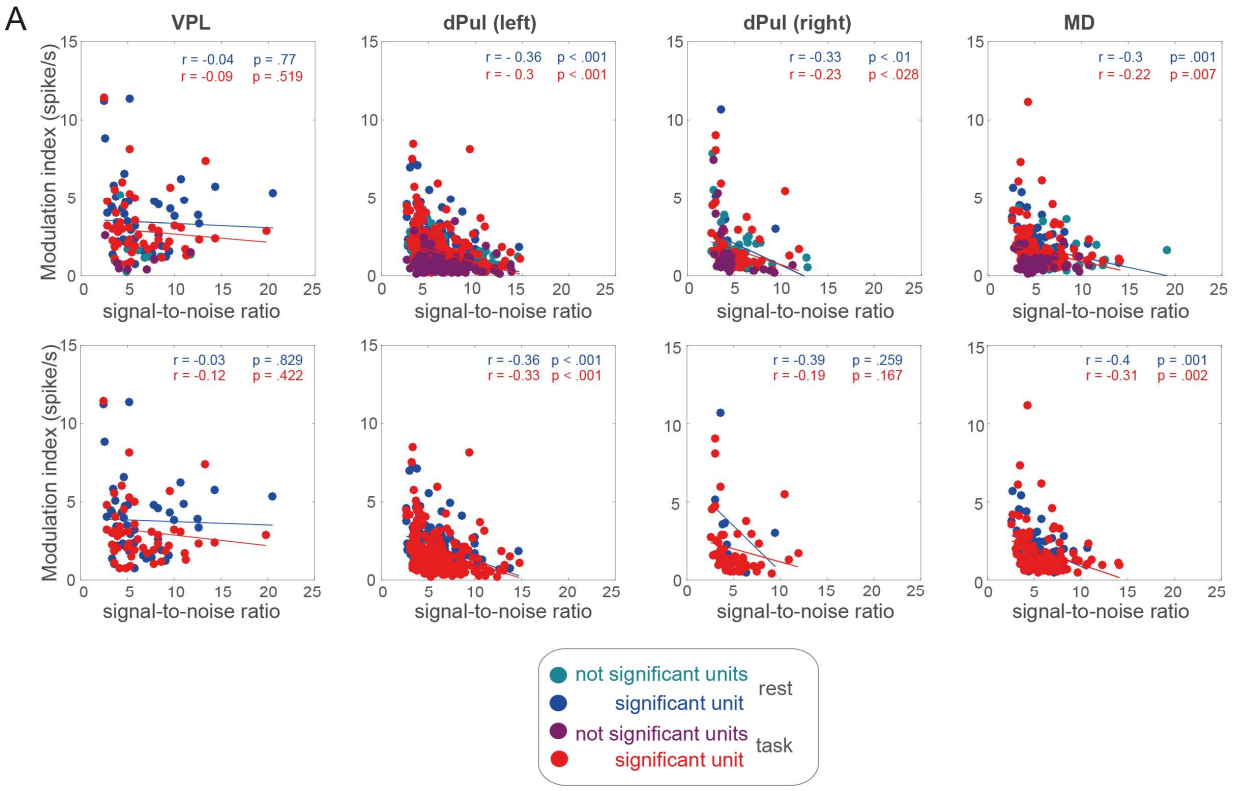

Figure 4.15. Correlations of the signal-to-noise ratio with the modulation index derived from subtractive normalization (spikes/s). Each dot represents a recorded unit either during rest (blue) or task (red). The slope of the lines shows the correlation coefficient separately for the rest and task for the units shown in each graph. The related statistical parameter (r, p-value) are displayed respectively for rest and task. (A) Here, the modulation index based on the subtractive normalization approach is plotted as a function of the signal-to-noise ratio with (upper panel) and without (lower panel) the non-significant cardiac-related units. Here, units are displayed for no significant cardiac relationship for rest (cyan) and task (purple) and units showing a significant cardiac-related effect for rest (blue) and task (red). The Pearson correlation coefficient and the p-value are displayed for computed correlation for rest and task, respectively.

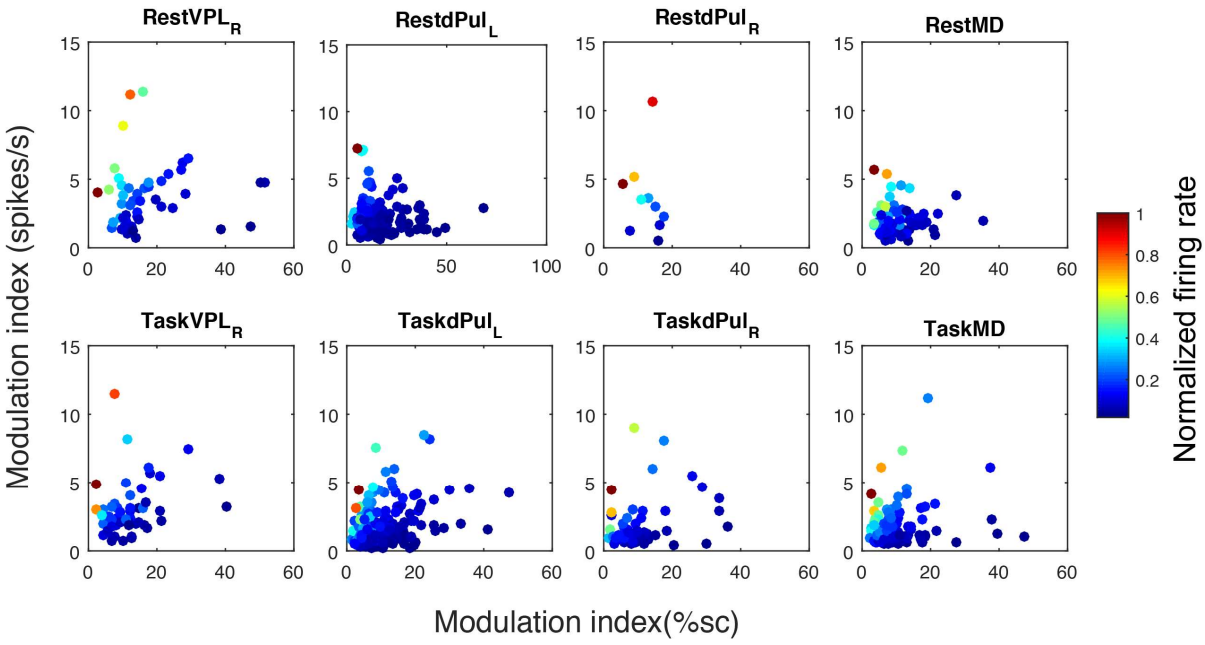

Figure 4.16. Relationship between modulation indices based on % signal change normalization (%sc) and subtractive normalization (spikes/s) and the firing rate, normalized separately in each dataset across units.

Discussion

We investigated whether neural activity in the dorsal pulvinar is related to the cardiac cycle and whether a pharmacologically induced suppression of neural activity in the dorsal pulvinar influences cardiac- or respiratory activity. These are plausible hypotheses because of the dorsal pulvinar's extensive and reciprocal connection to the primary nodes of the central autonomic network, such as the insula, prefrontal cortex, anterior cingulate, and amygdala, and its involvement in multisensory integration (Froesel et al., 2021; Gattass et al., 1978; Vittek et al., 2022) and arousal-related emotional processing (Almeida et al., 2015; Bertini et al., 2018; Kragel et al., 2021; Maior et al., 2010; Van Le et al., 2013; Ward et al., 2005, 2007).

Inactivation experiment

Suppressing neural activity in dPul affects cardiac- and respiration activity. After pharmacological reversible dorsal pulvinar inactivation, two out of three monkeys showed a decrease in heart rate and respiration rate. Specifically, for one monkey, it was a consistent inactivation-induced change compared to control sessions (post-control vs. post-injection). This monkey also had an inactivation-induced increase in RMSSD. These inactivation-induced changes in cardiac- and respiration activity were reproducible across sessions. The other monkey showed a time-dependent change in heart rate, heart rate variability, and respiration rate that was similar for control and inactivation sessions. Although the inactivation-induced

change in cardiac- and respiration activity was observed only in two monkeys, the dPul inactivation was also effective for the third monkey, as evidenced by task-related performance changes and the pulvinar inactivation locations overlapped across monkeys.

Minor differences occurred in the experimental procedure, such as injection volume and hemisphere. We do not think these differences can entirely explain the inactivation-induced change in the cardiac- and respiratory activity of M1 and M3. First, M1 received a larger volume of THIP injection, which might affect nearby brain regions, such as the ventral pulvinar and the superior colliculus. However, inactivating the left ventral pulvinar in M1 using a similar volume (3.5 - 4 μl) did not change heart rate, variability, or respiration rate. Secondly, the injections were conducted for M1 in the left and M2 in the right hemispheres. We repeated the same injection procedure (4.5 - 5μl) in the right hemisphere of M1; the results do not show a tendency for an inactivation-induced change in heart rate across the three sessions. These sessions indicate that the inactivation-induced effects in dorsal pulvinar might depend on the hemisphere. However, the procedure was repeated in a third monkey with the possibility of inactivating either the right or left dorsal pulvinar and bi-hemispherical. For M3, we observed an inactivation-induced decrease in heart rate for the rest period and a decrease in respiration rate in case of combining all injection sessions.

To sum up, perturbations of the neural activity in the dorsal pulvinar affect the cardiac- and respiratory activity to some extent. After dPul inactivation, the decrease in respiration rate indicates a slower exchange of oxygen and carbon dioxide with the blood. Combined with a reduced heart rate, the heart pumps less oxygen-rich blood through the body. In contrast, the increased heart rate variability (RMSSD) after dPul inactivation marks a “better” cardiovascular state because low heart rate variability indicates current or future health problems. Together, slower heart rate and increased heart rate variability (RMSSD) characterize the autonomic nervous system's parasympathetic tonus and a decrease in arousal level. Indeed, pulvinar was highlighted as a brain region showing arousal-related activity in three different tasks in an fMRI study (Barber et al., 2020). Furthermore, several studies showed that the neural activity of the pulvinar is related to arousal (Gattass et al., 1978, 1979, 2018; Stitt et al., 2018), and suppressing the neural activity of the dorsal pulvinar is related to sleepiness (Wilke et al., 2010).

Considering the extensive and polysynaptic connectivity profile, the pulvinar may be functionally involved in autonomic processing via the central autonomic network. We know that causal perturbation affecting the neural activity in the amygdala, insula, or superior colliculus triggers either a decrease or increase in the heart rate (Cechetto & Gelb, 2001; Chouchou et al., 2019; Healy & Peck, 1997; Iwata et al., 1987; M. J. Kim et al., 2011; S. M. Oppenheimer et al., 1992; S. M. Oppenheimer & Cechetto, 1990; Pool & Ransohoff, 1949;

Verberne & Owens, 1998). However, these brain regions have direct anatomical connections to the autonomic network. I am unaware of a comparable study investigating the link between the thalamus and cardiovascular system by perturbing the neural activity of the pulvinar or other thalamic nuclei having polysynaptic contacts to interact with cardiac- or respiratory activity via the central autonomic network.

To put the reported cardiac and respiratory effects into perspective, the superior colliculus, also part of the network involved in spatial attention, seems suitable to compare with cardiac effects in the pulvinar. After electrical stimulation or injection of the GABA-antagonist bicuculline in the deep layers of the superior colliculus, an increase in heart rate occurred in anesthetized rats (Keay et al., 1988). This finding has been discussed regarding the critical implications of the superior colliculus in generating and controlling spatially coordinated movements, including motor responses of orienting to salient environmental stimuli or defensive actions, such as avoidance or flight. Spatial orienting can trigger autonomic and respiratory changes related to the sudden emergency to act (Dean et al., 1989; Isa et al., 2020; Lynch et al., 2021). Like dorsal pulvinar, neurons in the deeper layer of the superior colliculus respond to auditory, visual, and somatosensory stimuli, integrate multisensory inputs, and have active descending projections to premotor pathways responsible for orienting and attention (Holmes & Spence, 2005; Wallace et al., 1998). These findings suggested a functional link between subcortical nuclei involved in multisensory integration, such as the superior colliculus and the pulvinar, and cross-modality attentive and orienting behaviors.

Although dorsal pulvinar has the essential reciprocal connections to the CAN, the mixed results between the monkeys hint that the extensive connections with the CAN regions are insufficient for a brain region to interact with the cardiac- or respiratory circuitry. While dorsal pulvinar has a causal effect on heart rate and its variability in one monkey, there seem to be factors determining such an effect. Here, we explore two aspects: the apparent difference in the average heart rate and respiration rate between monkeys and the impact of inactivation on two different behavioral states.

The most apparent difference between the two monkeys in our study lies in their average heart rate (HR) and respiration rate (BR) during the pre-testing phase (monkey 1: HR: ~170 bpm, BR: ~25 bpm; monkey 2: HR ~110 bpm, BR: ~ 19 bpm). The heart rate is affected by environmental (stress, emotion), health, and individual (body size, age) factors (Schmidt-Nielsen, 1997). Individual factors cannot explain this difference in heart rate between monkeys because both monkeys were relatively similar in age, size, and body weight. Monkey (M1), which showed an inactivation-induced decrease in heart rate and increased heart rate variability (RMSSD), had the highest heart rate of all tested monkeys. We measured the heart rate of four monkeys (additional monkey 3: ~ 125 bpm, monkey 4: ~ 150 bpm) under the same

physiological and environmental conditions. Considering all individual recorded sessions, the recorded heart rate ranged from 90 bpm to 200 bpm. We can exclude artifacts while measuring or recording the ECG for all tested animals. Placing two surface electrodes for recording the ECG on the back of the monkey provided stable, non-invasive ECG acquisition in the behaving monkey for at least 4 - 5 hours while applying neural perturbation methods.

The measured heart rates in our study follow previously reported values of heart rate for rhesus monkeys ranging from 100 to 250 bpm when sitting in a primate chair (Clarke et al., 1994; Froesel et al., 2020; Grandi & Ishida, 2015; Tatsumi et al., 1990; Unakafov et al., 2018). The closest comparable conditions used in another study reported a range of heart rate from 115 bpm to 155 bpm for the two male rhesus monkeys (aged 4 and 5 years and weighing 4 and 4.7 kg) that were also sitting in a primate chair performing a fixation task and at the same time, the ECG was recorded from two surface electrodes attached to the back of the monkey (Grandi & Ishida, 2015). Accordingly, the average heart rate of M1 seems to be in the normal range for rhesus monkeys. Nevertheless, it is essential to consider the individual health status of the monkey because an elevated heart rate is a major risk for cardiovascular diseases. Monkey 1 received daily and extensive yearly veterinarian check-ups with an assessment of blood parameters. No abnormalities during the time of the experiment were observed for monkey 1. One year after the investigation, the veterinarians of the institute diagnosed spondylosis. In this regard, an x-ray was performed on the body, which showed no abnormalities in the heart. However, heart rate is a good indicator of the physiological state of an animal with relevance in diverse contexts, from health checks to experimental studies of emotional and cognitive states. We suggest that the difference in baseline heart rate might be due to the monkeys' different physiological, behavioral, or psychological conditions during the experiment.

Heart rate and heart rate variability are non-invasive indicators of physiological, behavioral, and psychological states related to health and welfare (e.g., H.-G. Kim et al., 2018; Thayer et al., 2012; von Borell et al., 2007). A moderate increase in arousal leads to increased heart rate and blood pressure, and sensory alertness, desire, mobility, readiness to respond, and better performance. However, a substantial increase in arousal leads to stress reactions. The difference in heart rate and respiration rate between M1 and M2 indicates that the animals experienced different physiological states in the experiment despite the identical environmental settings (same room, experimenter, etc.). The interaction of the dorsal pulvinar with the autonomic nervous system might depend on the monkey's physiological state or/and arousal level. Could the state explain the difference in the inactivation-induced effect in M1 compared to an intermediate effect in M3, and no effect in M2. It is a scientifically likely

explanation for our results because the central autonomic control is state-dependent (Benarroch, 1993).

The current experimental design involved two cognitively engaging states induced by the rest and task. The color discrimination task, with its two difficulty levels, needs a continuous high cognitive engagement to be correctly performed compared to the periods of rest where the monkeys were sitting in their primate chair with no task demands. While performing the effortful cognitive task, the monkeys continuously initiated trials indicating a sustained level of attention and accurately performed the task to earn rewards, leading to a physiological state with a higher arousal level than passively sitting in the primate chair. We expected a higher heart rate for the task than for rest periods. Indeed, we found a significant main effect for all three monkeys' engagement levels (“TaskType”). We observed a higher heart rate for the task indicating a higher arousal level than rest periods for monkey 2. Despite the possible higher arousal level during the task, we did not observe any inactivation-induced effects on the cardiac or respiration activity for the task period for monkey 2. Although the heart rate significantly increased while performing the task, it was a small effect.

In the end, the heart rate during the task of monkey 2 (~ 4 - 6 bpm) was not increased equivalently to the average heart rate of monkey 1 (~ 170 bpm). These leads to two equally likely conclusions; the arousal level is not a crucial mediator and, therefore, cannot explain the strength of the inactivation-induced effects of monkey 1 or the increase of the heart rate due to performing a task in monkey 2 did not reach an appropriate level of arousal to involve the dorsal pulvinar. Further studies are needed to investigate whether the relationship between the dorsal pulvinar and the cardiac- and respiratory activity depends on the level of arousal—several lines of research about dorsal pulvinar support this hypothesis. Firstly, several studies showed that the neural activity of the pulvinar is related to arousal (Barber et al., 2020; Gattass et al., 1978, 1979, 2018; Stitt et al., 2018). Secondly, recent evidence supports that the pulvinar is relaying threat-related visual information (Maior et al., 2010; Rafal et al., 2015; Ward et al., 2005, 2007) and hemianopic patients with pulvinar lesions show a deficit in orienting to threat compared to hemianopic patients without a pulvinar lesion (Bertini et al., 2018) suggesting a crucial role of dorsal pulvinar in arousal-related processing.

Electrophysiological experiment

The electrophysiology experiment aimed to investigate whether the neural firing rate of neurons in the thalamic nuclei, particularly the dorsal pulvinar, is related to the cardiac cycle. To address this question, we recorded single-unit and multiunit activity in three different thalamic nuclei in the awake monkey. The recordings in the VPL and MD serve as controls. Previous studies in humans and cats identified cardiac-related neural activity in VPL

(Massimini et al., 2000; S. M. Oppenheimer et al., 1992). The MD also serves as a broader control because MD is a higher-order thalamic nuclei (Mitchell, 2015) as the pulvinar. Electrical stimulation of MD changes the heart rate (Buchanan & Powell, 1986), and its relationship to autonomic control is mentioned in studies using functional magnetic resonance imaging (Critchley et al., 2003; Napadow et al., 2008). The neural and cardiac activity was continuously recorded in one monkey performing either the color discrimination saccade task or sitting in the primate chair (rest demand, no eye movement control). As the state of rest is characterized by spontaneous neural activity that differs from the task-evoked activity, we analyzed all data separately for rest and task.

The neural firing rate is directly related to the cardiac cycle in more than forty percent of neurons in the dorsal pulvinar (rest: 42%, 142 of 336 units, task: 67%, 260 of 388 units) and mediodorsal thalamus (rest: 53%, 62 of 116 units, task: 68%, 104 of 152 units). In the present study, we confirm the existence of cardiac-related activity in the ventral posterior nucleus (rest: 84%, 46 of 55 units, task: 88%, 49 of 56 units) and extend these findings by comparing the VPL where we found the highest percentage of cardiac-related units to the pulvinar or mediodorsal thalamus in our study. This study is the first to report the relationship between heart rate and spiking activity of neurons in the dorsal pulvinar and the mediodorsal thalamus. According to our expectation, we found fewer cardiac-related neurons in MD and pulvinar compared to the VPL that has direct interconnection with the brain stem (Craig, 2004). Oppenheimer and colleagues report that 65% (17 of 26 neurons) of cardiac-related VPL neurons exhibited an increase in firing rate within 50ms at the peak of the systolic pressure, and 35% (9 of 26 neurons) showed an increase in firing rate either 50 - 100ms before or 150ms after the systolic pressure peak in humans. The systolic peak of a photoplethysmogram (PPG) signal corresponds to the R-peak of an ECG signal, both reflecting the ventricular contraction.

Although the existence of thalamic cardiovascular-related neurons is anticipated from tracer studies that have previously demonstrated thalamic connectivity with other known sites of cardiovascular control, such as the brain stem, insula, cingulate, or amygdala, the high percentage of pulvinar neurons whose neuronal activity is related to the R-peak of the electrocardiogram is unexpected. We found a higher proportion of cardiac-related neurons in dPul and MD as reported for the amygdala (20% & 36%, Frysinger & Harper, 1989; Kim et al., 2019).

Limitations

Physiological noises that are time-locked to the heartbeat, such as pulse artifacts, can confound our results, as mentioned in previous work (Frysinger & Harper, 1989; K. Kim et al., 2019; Mosher et al., 2020). The cardiac-related activity of the three examined thalamic units

might result from the effect of the neurons by underlying arteries or transmitted pulsations of cerebrospinal fluid. The dorsal pulvinar lies below the ventricular surface, a major CSF-containing space. Neurons that are closer to the ventricle should exhibit a stronger cardiac-related relationship. For the dorsal pulvinar lying directly below the ventricle, we expect all units to show a cardiac-related relationship. Only a sample of the total neurons recorded in this study showed pulse-related activity. In addition, we tried to verify that the relationship between spiking activity and R-peak of the cardiac cycle was not due to the mechanical cardiac-related confounds on recorded waveform stability and spike detection due to potential movement of the electrode, as proposed by Mosher et al. (2020).

We found no or a positive correlation between spike waveform (signal-to-noise ratio) and the cardiac-related modulation strength (modulation index in %sc) on the population level, suggesting that small noisy units with an amplitude close to the threshold are not un-proportionally “affected” by the cardiac activity. Modulation index and signal to noise ratio were not correlated in VPL but we found a positive correlation between signal-to-noise ratio and modulation index including also the non-significant units was found for VPL ($r = 0.28$, $p = .038$) and MD ($r = 0.21$, $p = .023$) for rest, while these conditions were not significant for right and left dorsal pulvinar. Dorsal pulvinar shows a positive correlation (left: $r = 0.16$, $p = .005$; right: $r = 0.39$, $p < .001$) for units recorded during task, similar to MD (right: $r = 0.35$, $p < .001$). This analysis cannot fully clarify whether pulsations artifacts lead to the high number of cardiac-related neurons in our population of thalamic nuclei.

In the current analysis, the spiking activity of a neuron is time-locked to the R-peak of the electrocardiogram. This is also a standard procedure to compute the heartbeat-evoked potentials (HEP). This ERP component marks characteristic changes in neural activity caused by evoked potentials due to changes in cardiac activity, often measured with EEG and MEG (see review Park & Blanke, 2019). The HEP is computed like visual-evoked potentials that can be obtained by averaging the firing rate of neurons (or averaging the EEG signals) time-locked to the presentation of a visual stimulus. The alignment to the R-peak of the electrocardiogram also has a disadvantage. The electrocardiogram is the electrical manifestation of the heart muscle activity where the rhythms of its pacemaker cells determine each cycle. The heart's contraction is displayed in the ECG as the highest peak, called R-peak. The R-peak is the strongest electrical signal that denotes ventricular depolarization and muscular contraction that initiates the cardiac cycle as the R-peak is a bigger problem related to strong cardiac field artifacts for computing the HEP. Some studies restrict the time of interest for the HEP analysis to the period that is known to be less affected by the cardiac field artifact, such as the time period from the decay of the ECG T-wave to the beginning of the next R-wave (Gray et al., 2007; Park et al., 2014).

Assuming that with the alignment to the T-wave, the level of distortion from electrical discharge originating from the myocardium is lower, and the electrode also might move less, it might serve as an additional control. On the contrary, Mosher et al. (2020) report that some units exhibited an increase in the amplitude of the extracellular action potentials towards the end of the cardiac cycle with a concomitant decrease in the half-width of the waveform, while others exhibited the inverse response. Accordingly, all recorded neurons should show a cardiac-related effect due to the systematic movement of the electrode. Still, we found that only half of the recorded units show cardiac-related effects. In addition, the ratio of cardiac-related neurons in higher-order thalamic nuclei (dPul, MD) and lower-order-thalamic nuclei (VPL) is according to our expectations.

Significant transient increases or decreases in firing rate in the spike-density time series were assessed using surrogate R-peaks in a permutations procedure also utilized for the HEP analysis (Babo-Rebelo et al., 2016; Park et al., 2014). Our results are only considered statistically significant if the data point was outside the surrogate dataset's 95%-confidence interval and lasted at least 40 ms. However, it results in the problem that units exhibiting a very sharp change in firing rate were marked as non-significant leading to a more conservative estimation of significant units. Using 4 consecutive bins reduces the possibility of having single spurious time points with significance by chance because the significant interval needs to be significant for several bins in a row. The current statistical analysis might have overestimated the number of significant units because the analysis neglects the multiple comparison problem related to the spatiotemporal structure of the data. Here, units are sampled from the brain region of one monkey recording from a nearby position on different days. In addition, multiple time points were evaluated for the signal of one unit. To correct for multiple comparisons, a cluster-based permutation test needs to be implemented where the result is considered statistically significant if a data point of the spike density time series lies below $\alpha = 0.05$ of the null distribution based on the shuffled data.

Cardiac-related neurons in the dorsal pulvinar

Surprisingly, we found a higher percentage of cardiac-related neurons in dPul and MD as reported for the amygdala (20% & 36%, Frysinger & Harper, 1989; Kim et al., 2019). The amygdala is a connector region between sensory and limbic areas of the cortex and subcortical brain regions. The Amygdala receives projections from the nucleus of the solitary tract or ventral posterior lateral nucleus and projects to autonomic nuclei (Critchley & Harrison, 2013; McDonald, 1998; Ricardo & Tongju Koh, 1978). The amygdala projects directly to the vagal nuclei in the medulla, the nucleus ambiguous, and the dorsal motor nucleus of the vagus nerve (Hopkins & Holstege, 1978; Spyer, 1994). The anterior region of the lateral nucleus of the amygdala receives afferent input from the medial part of the medial pulvinar, but it does

not project to the medial pulvinar (Jones & Burton, 1976; Romanski et al., 1997). This leads to how the amygdala receives information about the ongoing cardiovascular processes to integrate them for emotional behavior and motivation. Could also the pulvinar relay crucial cardiovascular information to the amygdala?

Evidence is accumulating that the dorsal pulvinar belongs to a putative multi-synaptic subcortical pathway for processing arousal-related emotional stimuli that could quickly convey visual and perhaps the related autonomic information to the amygdala. Although the existence of an anatomical path to rapidly transferring information from the retina to the amygdala without interference has been heavily criticized (Pessoa & Adolphs, 2010, 2011), evidence is converging from tracer studies in non-human primates (Baldwin et al., 2011; Benevento & Fallon, 1975; Elorette et al., 2018) and diffusion-weighted imaging in human (Kragel et al., 2021; McFadyen et al., 2019; Rafal et al., 2015) about overlapping anatomical connections between the superior colliculus, pulvinar, and amygdala. In addition, evidence from single-unit activation in medial and lateral pulvinar (Maior et al., 2010) supported findings from patients (Ward et al., 2005, 2007) that neural activity in the pulvinar is related to recognizing fearful faces. In hemianopia patients with pulvinar lesions, the implicit visual processing of threatening stimuli was disrupted compared to those without a pulvinar lesion recent studies (Bertini et al., 2018). The dorsal pulvinar is linked to arousal-related emotional processing and multisensory integration (Froesel et al., 2021; Gattass et al., 1978; Vittek et al., 2022), suggesting a potential role in autonomic control. How dorsal pulvinar interacts with the central autonomic network and which role it has remains unclear.

Supplementary Information

6 Supplementary Tables

Table S4.1: Three-way mixed ANOVAs for inactivation experiment for heart rate and respiration rate, monkey 1.

Table S4.2: Three-way mixed ANOVAs for inactivation experiment for heart rate and respiration rate, monkey 2.

Table S4.3: Three-way mixed ANOVAs for inactivation experiment for heart rate and respiration rate, monkey 3.

Table S4.4: Three-way mixed ANOVAs for inactivation experiment for heart rate variability, monkey 1.

Table S4.5: Three-way mixed ANOVAs for inactivation experiment for heart rate variability, monkey 2.

Table S4.6: Three-way mixed ANOVAs for inactivation experiment for heart rate variability, monkey 3.

Table S4.1: Three-way mixed ANOVAs for inactivation experiment for heart rate and respiration rate, monkey 1.

Monkey	Variable	Source of Variance	F	df	p	p<.0
M1 - Cornelius (dPul left)	heart rate	Experiment (control/injection)	18.39	(1,18)	<2e-16	*
		Timeline (pre/post)	20.03	(1,18)	<2e-16	*
		TaskType (rest/task)	20.76	(1,18)	<2e-16	*
		Experiment x Injection	2.84	(1,18)	0.11	
		Experiment x TaskType	1.64	(1,18)	0.22	
		Injection x TaskType	4.11	(1,18)	0.06	
		Experiment x Injection:TaskType	0.17	(1,18)	0.69	
	respiration rate	Experiment (control/injection)	2.99	(1,18)	0.10	
		Timeline (pre/post)	0.81	(1,18)	0.38	
		TaskType (rest/task)	21.96	(1,18)	<2e-16	*
		Experiment x Injection	3.13	(1,18)	0.09	
		Experiment x TaskType	0.03	(1,18)	0.88	
		Injection x TaskType	<0.005	(1,18)	0.98	
		Experiment x Injection:TaskType	0.03	(1,18)	0.86	

Table S4.2: Three-way mixed ANOVAs for inactivation experiment for heart rate and respiration rate, monkey 2.

Monkey	Variable	Source of Variance	F	df	p	p<.
M2 - Curius (dPul right)	heart rate	Experiment (control/injection)	0.07	(1,16)	0.80	
		Timeline (pre/post)	50.77	(1,16)	<2e-16	*
		TaskType (rest/task)	100.01	(1,16)	<2e-16	*
		Experiment x Injection	0.34	(1,16)	0.57	
		Experiment x TaskType	0.27	(1,16)	0.61	
		Injection x TaskType	2.91	(1,16)	0.11	
		Experiment x Injection:TaskType	3.61	(1,16)	0.08	
	respiration rate	Experiment (control/injection)	<0.005	(1,16)	1.00	
		Timeline (pre/post)	10.59	(1,16)	<2e-16	*
		TaskType (rest/task)	81.81	(1,16)	<2e-16	*
		Experiment x Injection	0.82	(1,16)	0.38	
		Experiment x TaskType	0.03	(1,16)	0.86	
		Injection x TaskType	0.21	(1,16)	0.65	
		Experiment x Injection:TaskType	0.4	(1,16)	0.54	

Table S4.3: Three-way mixed ANOVAs for inactivation experiment for heart rate and respiration rate, monkey 3.

Monkey	Variable	Source of Variance	F	df	p	p<.05
M3 - Magnus (dPul left, right, bilateral)	heart rate	Experiment (control/injection)	0.19	(1,9)	0.67	
		Timeline (pre/post)	8.11	(1,9)	0.02	*
		TaskType (rest/task)	50.17	(1,9)	<2e-16	*
		Experiment x Injection	<0.005	(1,9)	0.96	
		Experiment x TaskType	0.06	(1,9)	0.81	
		Injection x TaskType	0.55	(1,9)	0.48	
		Experiment x Injection:TaskType	1.95	(1,9)	0.20	
	respiration rate	Experiment (control/injection)	0.8	(1,9)	0.40	
		Timeline (pre/post)	18.01	(1,9)	<2e-16	*
		TaskType (rest/task)	25.53	(1,9)	<2e-16	*
		Experiment x Injection	11.95	(1,9)	0.01	*
		Experiment x TaskType	0.07	(1,9)	0.80	
		Injection x TaskType	0.57	(1,9)	0.47	
		Experiment x Injection:TaskType	0.01	(1,9)	0.91	

Table S4.4: Three-way mixed ANOVAs for inactivation experiment for heart rate variability, monkey 1.

Table S4.4: Three-way mixed ANOVAs for inactivation experiment for heart rate variability, monkey 2.

Monkey	Variable	Source of Variance	F	df	p	p<.05
M2 - Curius (dPul right)	RMSSD	Experiment (control/injection)	0.02	(1,16)	0.89	
		Timeline (pre/post)	23.98	(1,16)	<2e-16	*
		TaskType (rest/task)	12.78	(1,16)	<2e-16	*
		Experiment x Injection	0.02	(1,16)	0.89	
		Experiment x TaskType	0.07	(1,16)	0.80	
		Injection x TaskType	18.23	(1,16)	<2e-16	*
		Experiment x Injection:TaskType	6.42	(1,16)	0.02	*
	adjusted RMSSD	Experiment (control/injection)	0.17	(1,16)	0.69	
		Timeline (pre/post)	10.13	(1,16)	0.01	*
		TaskType (rest/task)	10.58	(1,16)	<2e-16	*
		Experiment x Injection	0.12	(1,16)	0.73	
		Experiment x TaskType	0.53	(1,16)	0.48	
		Injection x TaskType	8.71	(1,16)	0.01	*
		Experiment x Injection:TaskType	0.66	(1,16)	0.43	
	SD R2R interval	Experiment (control/injection)	0.3	(1,16)	0.59	
		Timeline (pre/post)	20.6	(1,16)	<2e-16	*
		TaskType (rest/task)	14.15	(1,16)	<2e-16	*
		Experiment x Injection	4.36	(1,16)	0.05	
		Experiment x TaskType	0.09	(1,16)	0.76	
		Injection x TaskType	0.27	(1,16)	0.61	
		Experiment x Injection:TaskType	3.8	(1,16)	0.07	
	adjusted SD R2R interval	Experiment (control/injection)	0.2	(1,16)	0.66	
		Timeline (pre/post)	0.11	(1,16)	0.75	
		TaskType (rest/task)	6.65	(1,16)	0.02	*
		Experiment x Injection	4.58	(1,16)	0.05	*
		Experiment x TaskType	0.04	(1,16)	0.85	
		Injection x TaskType	0.88	(1,16)	0.36	
		Experiment x Injection:TaskType	4.65	(1,16)	0.05	*

Table S4.6: Three-way mixed ANOVAs for inactivation experiment for heart rate variability, monkey 3.

Monkey	Variable	Source of Variance	F	df	p	p<.05
M3 - Magnus (dPul left, right, bilateral)	RMSSD	Experiment (control/injection)	2.08	(1,9)	0.18	
		Timeline (pre/post)	5.21	(1,9)	0.05	*
		TaskType (rest/task)	10.98	(1,9)	0.01	*
		Experiment x Injection	10.99	(1,9)	0.01	*
		Experiment x TaskType	2.42	(1,9)	0.15	
		Injection x TaskType	10.41	(1,9)	0.01	*
		Experiment x Injection:TaskType	2.42	(1,9)	0.15	
	adjusted RMSSD	Experiment (control/injection)	0.18	(1,9)	0.68	
		Timeline (pre/post)	5.76	(1,9)	0.04	*
		TaskType (rest/task)	4.49	(1,9)	0.06	
		Experiment x Injection	0.04	(1,9)	0.84	
		Experiment x TaskType	0.34	(1,9)	0.58	
		Injection x TaskType	4.95	(1,9)	0.05	
		Experiment x Injection:TaskType	0.09	(1,9)	0.77	
	SD R2R interval	Experiment (control/injection)	0.24	(1,9)	0.63	
		Timeline (pre/post)	8.44	(1,9)	0.02	*
		TaskType (rest/task)	46.92	(1,9)	<2e-16	*
		Experiment x Injection	0.04	(1,9)	0.86	
		Experiment x TaskType	0.01	(1,9)	0.91	
		Injection x TaskType	0.18	(1,9)	0.68	
		Experiment x Injection:TaskType	1.94	(1,9)	0.20	
	adjusted SD R2R interval	Experiment (control/injection)	0.4	(1,9)	0.54	
		Timeline (pre/post)	2.74	(1,9)	0.13	
		TaskType (rest/task)	16.5	(1,9)	<2e-16	*
		Experiment x Injection	0.09	(1,9)	0.77	
		Experiment x TaskType	0.1	(1,9)	0.76	
		Injection x TaskType	0.07	(1,9)	0.79	
		Experiment x Injection:TaskType	2.11	(1,9)	0.18	

5. General discussion

The view of the higher-order thalamic nuclei as a passive relay of sensory information to and across the cortex has been replaced by a more complex understanding of their role. However, further evidence is still necessary to demonstrate that thalamic nuclei, such as the dorsal pulvinar, actively integrate and regulate cognition- and arousal-related signal transmission. This dissertation aims to shed light on the function of the dorsal pulvinar through the outcome of three experimental studies. These investigations specifically focus on the higher-order thalamic nucleus, the dorsal pulvinar, to better understand its role in diverse cognitive processes, including visuospatial cognition, perceptual-decision making, and arousal-related processing. The methodological design of these studies is multifaceted. The results of the electrophysiology experiment focused on the relationship between the spiking activity of the dorsal pulvinar to cardiac activity (ECG). Crucially, the identified relationship between the dPul neurons' activity and the heart's rhythm hint that the dorsal pulvinar might not only receive, integrate, and modulate information from the senses and various cortical brain regions but also plays a role in integrating or conveying information about the body's internal state. This experiment is complemented with two additional techniques: pharmacological inactivation and electrical microstimulation to draw more definite causal inferences. Pharmacological inactivation of the dorsal pulvinar decreased the heart and respiration rates in two out of three monkeys and reduced the heart rate variability (RMSSD) in one monkey. The discovery of a functional link between the dorsal pulvinar and the autonomic nervous system emphasizes our understanding of the dorsal pulvinar's role in cardiac-cortical interactions. In all experiments, monkeys performed the color discrimination task, including the following task demands: fast perceptual color discrimination between target and distractor, spatially competing stimuli, and stimulus-congruent saccade responses to investigate whether perceptual factors contribute to visuospatial deficits after dorsal pulvinar perturbations in conditions of spatial competition. The results confirm the crucial contribution of the dorsal pulvinar in contralateral spatial orienting while correctly discriminating against competing stimuli in the context of perceptual uncertainty. Together, these studies set the foundation for future research into how attentive perception intertwines with arousal, emphasizing the potential mechanisms related to oscillatory and neuromodulator dynamics.

The following section summarize and discuss the main results. It discusses the two main research questions of the dissertation. It points out limitations and possible future directions to provide the reader with general conclusions of the presented work in this dissertation and finally concludes with an outlook.

5.1 Visuospatial effects of dorsal pulvinar perturbations during different levels of spatial competition and perceptual uncertainty

The first overarching goal of this thesis was to investigate the role of dorsal pulvinar (dPul) in spatial orienting and perceptual discrimination (cognition). The ability to correctly discriminate spatially competing for stimuli and initiate contextually appropriate behaviors was investigated after perturbating the neural activity of the dorsal pulvinar. Two monkeys performed the *perceptual color discrimination task*. This task consists of the following task demands: fast perceptual color discrimination between target and distractor, spatially competing stimuli, and stimulus-congruent saccade responses to investigate whether perceptual factors contribute to visuospatial deficits after dorsal pulvinar perturbations in conditions of spatial competition. The results of the inactivation study outlined in Chapter 2 and the microstimulation study summarized in Chapter 3 demonstrate the critical involvement of the dorsal pulvinar in contralateral spatial orienting and resolving the spatial competition, rather than in perceptual discrimination, even in the context of perceptual uncertainty.

The results presented in Chapter 2 are mainly consistent with the hypothesis that unilateral dorsal pulvinar inactivation causes a spatial selection bias (spatial selection bias hypothesis). While the perceptual discrimination in the contralateral hemifield remained unaffected after pharmacologically suppressing the neural activity in the dorsal pulvinar, we observed a shift in response criterion away from contralesional stimuli in the context of perceptual decisions for both difficulty levels compared to control sessions. This selection bias occurred regardless of whether a target or a distractor was shown in the presence of a competing stimulus after dorsal pulvinar inactivation, especially when two competing peripheral stimuli were present. Notably, the inactivation-induced selection bias occurs even when only one response option is correct and rewarded. Presenting a valid target in the contralesional hemifield that was the only rewarded option (single target or target-distractor condition) didn't alleviate the spatial selection bias "away from contra". Both monkeys selected the contralesional target less and chose the ipsilesional distractor or fixation option, receiving no reward in these trials. The saccade latency for the contralesional selection increased for all conditions.

The local reversible inactivation method relies on local injections of a pharmacological non-neurotoxic GABA-A agonist to temporally suppress local neural activity. The advantage is that the neuronal effects are short-term, no long-term reorganization in the brain appears, and repeatable with interleaved recovery periods (A. H. Bell & Bultitude, 2018). Thus, injection and control sessions are interleaved and repeated on consecutive days. The limitation of inactivation studies is their long timescale (several hours) and strong pharmacological effect that nearly abolishes the neural activity in the inactivated region. Consequently, inactivation cannot

employ trial-based and epoch-specific design and resolve at which processing stage the dorsal pulvinar impacts visuospatial cognition. More nuanced conclusions might be drawn using temporally and spatially more selective techniques like electrical stimulation.

In Chapter 3, the microstimulation study investigated how dorsal pulvinar stimulation before and during the formation and execution of a perceptual decision influences the selection behavior and saccade latencies in the conditions of spatial competition and perceptual uncertainty by electrically stimulating in two periods of the trial timeline (indicated by “early” and “late” microstimulation). Early microstimulation perturbs the neural activity in the dorsal pulvinar before the formation and execution of a decision (the monkey is fixating on a red spot in the center of the screen). In contrast, late microstimulation perturbs the neural activity in the dorsal pulvinar during the formation but before the execution of a decision. In agreement with previously reported findings of dorsal pulvinar indicating an opposite direction effect on target selection after early and late microstimulation (Dominguez-Vargas et al., 2017), we found that early microstimulation was primarily shifting the criterion away from contraversive stimuli when two peripheral stimuli elicited high spatial competition between hemifields. This shift in criterion manifested as reluctance to select stimuli in the contraversive hemifield, regardless of whether a target or distractor was presented there. We expected that microstimulation starting after the stimulus onset but before the saccade (“late”) would potentiate the function of the pulvinar. It is an open question if the enhancement of the visuospatial representation is the same for distractors and targets and how the microstimulation-induced contraversive drive interacts with the task difficulty. In the single stimuli condition with late microstimulation, the contraversive criterion or dprime remained unaffected by microstimulation, regardless of the difficult level. For the double same stimuli condition, we observed no significant change in contraversive hit rate, criterion, and dprime after late microstimulation, except for an increased contraversive dprime during easy discrimination for M2. For the double different stimuli condition, M2 showed a significant shift towards “more contra” for the difficult discrimination, whereas M1 showed a decrease in contraversive dprime. However, we primarily observed criterion shifts away from ipsiversive stimuli after late microstimulation for both difficulty levels and most stimulus conditions, manifesting as reluctance to select stimuli in the ipsiversive hemifields after late microstimulation. In conclusion, late microstimulation of the dorsal pulvinar influenced spatial selection criteria with a consistent bias way from ipsiversive stimuli, and the contraversive dprime was mainly unaffected, suggesting that perceptual discrimination remains largely unaltered, the spatial selection is notably adapted by microstimulation.

The results of the inactivation and microstimulation study point in the same direction: After perturbing the neural activity of the dorsal pulvinar, the response criterion was mainly affected,

and the ability to discriminate between target and distractor in the contralateral hemisphere remained intact. The effect on the saccade latency varies between the pharmacological inactivation and early microstimulation for the color discrimination task. Inactivation of the dorsal pulvinar leads to delays in making a saccade to contralateral stimuli. Microstimulation before stimulus onset leads to consistent speeding up of contraversive and ipsiversive saccades for M2 but not M1. However, faster ipsiversive saccades were previously observed after pharmacological inactivation (Wilke et al. 2010).

Microstimulation effects are less pronounced compared to the pharmacological effects of inactivation. The latter methodology profoundly impacts neural activity, often resulting in an "all-or-none" effect that nearly abolishes the neural activity of mostly contralaterally tuned neurons in the inactivated dorsal pulvinar. In contrast, electrical microstimulation affects only a localized subset of neurons temporarily (Cohen & Newsome, 2004; Histed et al., 2013). While most neurons in the dorsal pulvinar are contralaterally tuned, some dorsal pulvinar neurons react to stimuli in the ipsilateral and contralateral visual hemifields. Interestingly, their responses to spatially presented stimuli, whether in the ipsilateral or contralateral visual hemifield, exhibit a broad range of diversity. For example, during the memory-guided saccade task, the firing rate of certain pulvinar neurons increased after presenting a contralateral saccade target and decreased with an ipsilateral one (Dominguez-Vargas et al., 2017).

Extracellular recordings are invaluable to understanding the varied contributions of neuronal subpopulations in specific brain regions. In this thesis, an electrophysiology dataset was collected from one monkey performing the color discrimination task. Neural activity from three thalamic nuclei, including the dorsal pulvinar, was recorded to investigate how different dorsal pulvinar neurons might respond to varying spatial competition, whether from a distractor or target. This data might help to understand whether neurons exhibit increased firing rates in the presence of targets compared to distractors, indicating their potential role in selective attention. It can also reveal how these neurons handle different types of spatial competition between stimuli when the second stimulus is presented in the same or opposite hemifield. Other analyses could focus on the local field potential and the changes in brain oscillations related to the selective enhancement or sensory suppression mechanism related to spatially presented distractors and targets. The preliminary PSTH's including only the units recorded in the right dorsal pulvinar indicated that the firing rate of spatially tuned neurons increases with the number of competing stimuli, with the highest firing rate when two stimuli are presented in the same visual hemifield (visual inspection). These indicated that neural activity of the dorsal pulvinar encodes spatial competition within and between hemifields. The neural activity did not differ when a distractor or target was shown in the same hemifield. Moreover, further analyses might also focus on questions such as: How responsive are neurons in the mediodorsal thalamus to perceptual

uncertainty in the color discrimination task? How does the task-related neural activity (spikes, LFP) differ between the mediodorsal thalamus and dPul? In conclusion, examining the firing rates of dorsal pulvinar neurons and the local field potential during the color discrimination task deepens our understanding of the dorsal pulvinar's contributions to selective attention and spatial orienting under spatial competition while expanding our knowledge about the underlying neural mechanism of spatial cognition.

5.2 Dorsal Pulvinar's Role in Brain-Heart Interactions: Exploring the interplay between neural and cardiac activity.

The second overarching goal of this thesis was to gain new insights into the dorsal pulvinar's interaction with physiological processes by investigating the relationship between the neural activity of the dorsal pulvinar and cardiac activity. This goal is particularly interesting as it aims to explore the role of the thalamus, focusing mainly on the dorsal pulvinar, in brain-heart interactions, which also increases our understanding of the underlying neural processes related to arousal (non-specific activation of the cerebral cortex associated with sleep-wake states, high arousal is related to tonic LC activity, (Aston-Jones & Cohen, 2005; Oken et al., 2006)).

The results from both experiments (inactivation, electrophysiology in combination with ECG and capnography) have identified a compelling link between cardiac activity, partly respiration rate, and the neural activity of the dorsal pulvinar. Specifically, the pharmacological inactivation of the dorsal pulvinar decreased the heart and respiration rates in two out of three monkeys and reduced the heart rate variability (RMSSD) in one monkey. We conclude that the dorsal pulvinar interacts via polysynaptic connections with physiological processes via the central autonomic network, expanding the established role of the dorsal pulvinar towards integrating information from and to the body and a putative role of the dorsal pulvinar in arousal. Subsequent electrophysiological testing revealed a significant coupling between the thalamic neuronal spiking activity and the cardiac cycle for the dorsal pulvinar, mediodorsal thalamus (around 68% of neurons), and the VPL (88% of neurons) in one monkey. We found no evidence that potential mechanical influences from the heart confounded the neuronal recordings, strengthening the argument for a functional link. This study is the first to compare the relationship between the cardiac cycle and the spiking activity of neurons in three thalamic nuclei, dorsal pulvinar, mediodorsal thalamus, and ventral posterior lateral nucleus. Notably, VPL units exhibited greater changes in their normalized firing rates to the cardiac cycle, suggesting a stronger influence from heart-related activity. Surprisingly, we found a substantial number of cardiac-related neurons dorsal pulvinar, and mediodorsal thalamus, which are both

not traditionally seen as primary centers for cardiac- & respiratory control. These high numbers of cardiac-related neurons were surprising because other studies reported fewer cardiac-related neurons for the amygdala (20% & 36%, Frysinger & Harper, 1989; Kim et al., 2019). As traditionally expected, the substantial neural-cardiac coupling observed in these higher-order thalamic nuclei implies a stronger involvement in neuro-cardiological processes. This research points to a broader role of the thalamus in heart-brain interactions and regulations related to the autonomic nervous system, which expands and challenges our understanding of the thalamus and its functions.

While the dorsal pulvinar is not traditionally seen as a primary center for cardiac- & respiratory control, this thalamic hub region has been mainly associated with selective attention and spatial orienting by modulating and integrating various visual signals to form a coherent percept (Petersen et al., 1987; Robinson et al., 1986). Additionally, the dorsal pulvinar plays a role in multisensory integration (Froesel et al., 2021; Gattass et al., 1978; Vittek et al., 2022) and arousal-related emotional processing (Barber et al., 2020; Gattass et al., 1979, 2018a; Maior et al., 2010; Rafal et al., 2015; Stitt et al., 2018; Ward et al., 2005, 2007). Several studies established a connection between the pulvinar and arousal (Coull et al., 2004; Gattass et al., 2018b; Stitt et al., 2018). This relationship concerning arousal is also emphasized in a sleep study in humans, where pulvinar deactivation precedes cortical deactivation at the onset of sleep (Magnin et al., 2010). Moreover, when the neural activity of the dorsal pulvinar is suppressed in non-human primates, it leads to sleepiness (Wilke et al., 2010). These observations, combined with our new findings about the connection between the dorsal pulvinar and cardiac activity, propose that the dorsal pulvinar might be processing and integrating arousal-related information from the body. This idea is further reinforced by the reciprocal connections of the dorsal pulvinar with all major nodes of the central autonomic network, including the amygdala, insula, cingulate, and prefrontal cortex (Rosenberg et al., 2009). In conclusion, the dorsal pulvinar is involved in arousal-related processing. It is a promising candidate for integrating internal signals about the body's state from and to the autonomic nervous system to modulate behavior.

Future perspectives of the presented work focus first on further and more elaborated analyses of the collected data. The dPul inactivation study consisted of ECG and respiration rate recordings while monkeys performed the perceptual color discrimination task.

To analyze how the dPul inactivation affects the cardio-respiratory coupling, the respiratory sinus arrhythmias will be analyzed in more detail. The modulation of the heart rate by respiration, also called respiratory sinus arrhythmias, is the number of heartbeats per breath changing according to the respiration cycle, with the heart rate increasing during inspiration and decreasing during expiration. The cardio-respiratory coupling is calculated as the phase

ratio between heartbeat and respiration. The underlying origin and neural mechanism of cardio-respiratory coupling is still subject to scientific discussion. As we found inactivation-induced changes in breathing in one monkey and stronger inactivation-induced changes in heart rate for the other monkey, it would be essential to investigate if pharmacological inactivation has a specific influence on the cardio-respiratory coupling to explain the dynamic of the inactivation effect.

To investigate whether the cardiac and respiratory rate interaction with the selection behavior in the color discrimination task changes after dorsal pulvinar inactivation, I planned to analyze the proportion of hits, false alarms, and response behaviors over the cardiac cycle. Previous studies reported different cardiac effects on risky decision-making, the decision threshold in somatosensory perception, and reinforcement learning (Al et al., 2020; Kimura et al., 2022, 2023; Skora et al., 2022), suggesting a potential interplay between decision-making and cardiac cycle.

By suppressing the neural activity of the dorsal pulvinar using a $GABA_A$ agonist, the heart rate strongly decreased in one monkey and was less consistent in the second monkey but not in the third monkey. The variety of the neural effects between the monkeys leaves us with unresolved questions: Does the dorsal pulvinar play a role in overall arousal and/ or autonomic regulation, or is its function more restricted or context-dependent? And which signals from the body reach the dorsal pulvinar? Given the polysynaptic contacts of the dorsal pulvinar to interact with cardiac activity via the central autonomic network, future studies should focus on potential modulatory inputs to the dorsal pulvinar to determine which bodily signal influence its activity in which context.

The electrophysiology study resulted in a unique and rich dataset, including recorded neurons in three thalamic nuclei in one monkey combined with continuous recordings of respiration and ECG while the monkey was passively sitting in his primate chair (rest) or performing the perceptual color discrimination task. Further analyses should investigate the heart-brain interactions in more detail. To quantify the amount of information that flows from the heart to the thalamus and vice versa, I planned to compute the transfer entropy. Transfer entropy is a non-parametric statistic measuring the amount of directed (time-asymmetric) transfer of information between two random processes, such as spikes and heartbeats. For this purpose, various datasets were simulated with pre-defined parameters describing the coupling between R-peak and spikes (see examples in Fig. 5.1 A for a spike train with and without a time-locked relationship with the R-peak). Given a fixed baseline firing rate of a neuron, these simulated datasets enable the evaluation of the potential range of expected values for the transfer entropy. This is a work in progress to analyze further the relationship between R-peaks in the cardiac cycle and spiking activity.

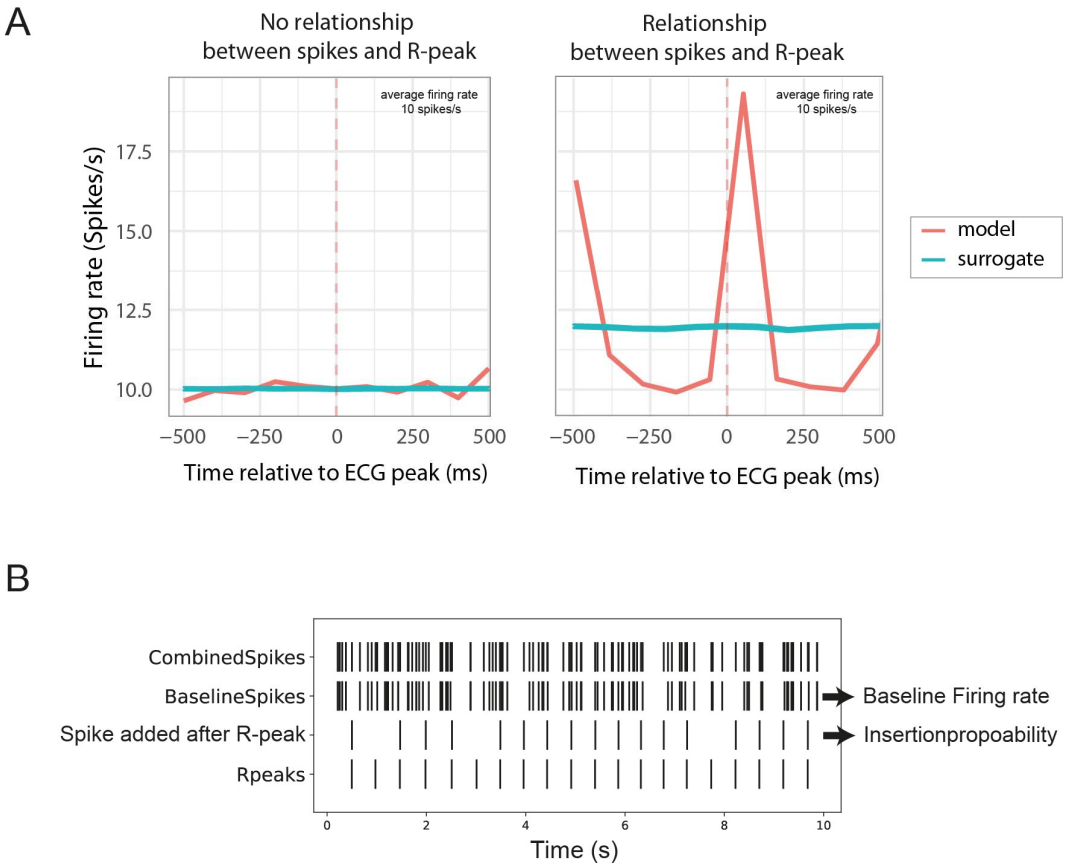

5.1. Simulation to ECG-triggered averages (A) Example of a spike train with and without a time-locked relationship with the R-peak (B) Displayed are the Poisson-distributed spikes train, the R-R intervals, and that with a given insertion probability, a spike is added to the spike train 100 ms after the R-peak.

Moreover, several studies suggested that the involvement of dorsal pulvinar can integrate processed complex sensory inputs from the cortex with limbic influences and transmit this information to the amygdala (Maior et al., 2010; Rafal et al., 2015; Van Le et al., 2013) and the cortex. The electrophysiology dataset also allows for investigating questions, such as whether cardiac-related neurons and visually responsive neurons encompass two separate co-localized populations in the dorsal pulvinar or whether this information is encoded in the same neuron.

So far, the results from the electrophysiology experiment could neither clarify the precise role of the pulvinar in heart-brain interaction nor the nature of the relationship. This leaves us with unresolved questions, for instance: Is the pulvinar responding to changes in cardiac activity?, or Is the pulvinar neural activity in some way influencing the heart? Or are both being influenced by some other variables? Notably, the inactivation study complemented the results from the R-peak-triggered averages by exploring one direction of the link between dPul neural activity and heart rate. Another interesting experiment is to increase the heart rate through an

autonomic challenge, such as high-calorie food intake, to investigate related changes in neural activity.

5.3 Limitations

The experiments have limitations from a methodological, empirical, and analytical perspective. The inactivation approach, using THIP, offers benefits like being non-neurotoxic and spatially specific. However, its effects persist for a considerable duration (several hours) and profoundly suppress nearly all neural activity within the targeted area. This duration poses a challenge in determining the precise temporal window during which dorsal pulvinar affects visuospatial cognition in the color discrimination task (see Chapter 2). We employed microstimulation in the same task in response to these challenges, aiming for more trial-specific and epoch-focused analyses. The electrical microstimulation study enabled more detailed conclusions regarding the dorsal pulvinar's role in visuospatial decision-making.

Notably, the timing of the electrical stimulation relative to stimulus presentation varied between the monkeys. M1 received stimulation at -250 ms ("early") and -50 ms ("late") before the stimulus presentation, while M2 received stimulation -80 ms ("early") before and 80 ms ("late") after the stimulus presentation. Notably, "early" but also "late" stimulations led to consistent selection patterns between the monkeys for the double same stimuli condition. However, it also suggests profound variations between the two monkeys' readiness, decision-making, and response execution times, in stimulating "early" before stimulus onset or stimulating "late" resulted in similar selection behavior in the double same stimuli for the two monkeys. This indicates different timings between the monkeys in preparing, deciding, and executing the response, which needs to be more considered by interpreting the results of the selection behavior and saccade latencies after microstimulation.

A main question arises in the color discrimination task: Should the yellow dot, perceptually distinct from the red target, be classified as a distractor? While the yellow stimulus might not be as distracting as other potential distractors, it stands out – almost like a 'NoGo' signal. There is speculation that the pulvinar's neural activity could be suppressed in response to this yellow distractor. This hypothesis needs further exploration by analyzing the electrophysiology dataset related to the color discrimination task. Given the distinct characteristics of the two types of distractors, it is essential to analyze the shifts in criterion and dprime separately based on difficulty levels (yellow and orange distractors). This approach aligned with the methodology presented in Chapter 2.

The color discrimination task was designed with three trial-type conditions (single stimuli, double same stimuli, double different stimuli) to explore the pulvinar's role in resolving the spatial competition, particularly in the case of a competing stimulus in each hemifield. Therefore, the included trial-type conditions vary in the level of spatial competition (spatial competition between one hemifield and fixation (single stimuli) or two hemifields (double same and double different stimuli)). To assess the impact of the interhemispheric competition between the same and different stimuli, future analyses should evaluate and compare the strength of the inactivation effect on the criterion considering the different stimulus types. Moreover, an additional control condition would be necessary to evaluate better the pulvinar's role in the interhemispheric competition between visual representations, where both stimuli appear within the same hemifield. Introducing a trial-type condition where both stimuli are in the same hemifield ensures that the visual context is uniform to identify whether the pulvinar's response is influenced by the complexity and nature of the visual context or purely spatial competition. Moreover, this control condition would provide a clearer picture of whether the pulvinar's role is specifically interhemispheric or if it is also involved in resolving competitions within a single hemisphere.

The R-peak/ECG Triggered Average method offers valuable insights but has inherent limitations. The method assumes a consistent temporal relationship between R-peaks and neuronal firing, which might not always account for dynamic changes in this relationship. As this method is noise-sensitive, we excluded periods of movement in the ECG and neuronal data to analyze stationary periods. However, the exclusion of periods can introduce gaps in the continuous data, which inadvertently omit important dynamic neuronal-cardiac interactions or could introduce biases by focusing solely on stationary periods, which do not capture the complete range of neuronal responses to cardiac activity. Moreover, by focusing on the R-peak, the R-peak Triggered Average method could oversimplify scenarios where multiple cardiac phases or other non-cardiac influences modulate neuronal firing. Also the innovative adaption of combining jitter-based and bootstrap resampling to generate surrogate data presents unique challenges. The approach can introduce cumulative timing shifts of expanding or contracting several subsequent intervals by altering several subsequent R-R intervals. This potential drift in timing can distort the authentic relationship between R-peaks and neuronal activity, influencing the derived confidence intervals and the detection of significant modulations. Finally, the RTA method, by its nature, remains descriptive and does not directly infer causality between cardiac activity and the firing rate of the neurons. Exploring methodologies that neither rely on stationary periods nor utilize this specific resampling approach could provide alternative insights and potentially mitigate some inherent biases in the current approach.

5.4 Outlook: Integration of bodily and multisensory signals in the dorsal pulvinar

The integration and modulation of various subcortical and cortical signals are crucial neural processes performed by the dorsal pulvinar, and understanding the neural computations underpinning this multi-faceted integration process is vital to gain more insights into the dorsal pulvinar's role in cognition and behavior. Neural integration, in its simplest terms, is the process by which neurons combine information from diverse sources to form a comprehensive understanding of the body's environments (Stein et al., 2014). While neural integration is a common function across all brain regions, the dorsal pulvinar exhibits several unique characteristics that set it apart as a potential hub for integrating internal bodily and sensory information. As part of the thalamus, the dorsal pulvinar is centrally positioned topologically to facilitate integrative functions across multiple functional networks. It is extensively interconnected with several brain areas involved in sensory, cognitive, emotional, and interoceptive processing (Rosenberg et al., 2009), enabling the dorsal pulvinar to receive and integrate a wide range of signals. Moreover, the dorsal pulvinar, along with anterior, mediodorsal ventrolateral, and ventroposterior nuclei, exhibits strong connector hub properties, which were found to be stronger than in cortical hubs (P. T. Bell & Shine, 2016; Hwang et al., 2017). With its newly discovered association with the heart, the integration of signal from the autonomic nervous system by the dorsal pulvinar is particularly crucial, as it enriches its signal processing capacity, providing a more comprehensive understanding of the body's internal state, which is essential for effective decision-making and adaptive behavioral responses to varying environmental conditions.

While there has been some research on how the dorsal pulvinar integrates diverse neural signals from various brain regions, the precise neural mechanism underlying this integration remains an open question. A notable gap in our understanding lies in how neuronal computations with the dorsal pulvinar achieves the integration and modulation of signal from various sources to coordinate cortical information flow. Given the crucial roles of brain oscillations in the dorsal pulvinar in coordinating interaction both with and across brain regions, modulating attention mechanism and influencing sensory representations, and a high density of alpha-1 and alpha-2 receptors, it might be important to explore their potential interaction in depth.

The pulvinar is critical for efficiently transmitting sensory information within and between cortical regions (Jaramillo et al., 2019; Kastner et al., 2020; Stitt et al., 2018). Moreover, during

specific periods where visual target detection is less efficient, alpha-band activity synchronization increases, especially between the parietal cortex and the mediodorsal pulvinar (Fiebelkorn et al., 2019). In addition, the input from the pulvinar, like other thalamic nuclei, seems crucial in maintaining the cortex in an active state. When the pulvinar is deactivated, there's a significant decrease in low-frequency LFP power in the affected cortex (Zhou et al., 2016), suggesting that the intact pulvinar prevents the cortex from descending into a slow-wave sleep-like state (low arousal), characterized by slow oscillations, diminished sensory responsiveness, and reduced attentional influence.

Moreover, the medial pulvinar is characterized by a high density of alpha-1 and alpha-2 receptors (Pérez-Santos et al., 2021), indicating a strong influence of noradrenaline in modulating dorsal pulvinar's processing. So far, we know that noradrenergic neurons increase their discharge during arousal and high vigilance and in response to stimuli perceived as salient (Foote et al., 1980). However, studies on thalamic modulation by noradrenaline are sparse, particularly in primates. In humans, Coull et al. (2004) showed that the performance of a target detection task was decreased under dexmedetomidine treatment (Alpha-2 adrenergic receptor agonist) and that this detrimental effect was reversed by exposure to white noise involving the selective activation of higher-order thalamic nuclei, such as the pulvinar. Notably, the dorsal pulvinar's role in integrating and regulating diverse signals related to spatial cognition and arousal would go hand in hand by utilizing different signal transmission modes. On the microscopic level, each electrical and chemical signal impacts the neuron differently, modifying its state and influencing whether it will fire an action potential. Integrating these diverse signals related to an event requires spatial and temporal summation, where multiple signals converge on a single neuron either from the same neuron over a short period or from different neurons. This summation can lead to the neuron reaching its firing threshold and emitting an activation potential. Simultaneously, neuromodulators can influence this process by adjusting the neuron's responsivity. The effect of these neuromodulators is typically mediated through binding to specific receptors on the neurons. Neurons release neuromodulators at their target sites, which can modify the activity mode of the brain region – altering their excitability and responsivity without necessarily causing them to fire an action potential (Salinas & Sejnowski, 2001; Shine et al., 2021). Consequently, even minor shifts in neuromodulator levels can dramatically change the dynamics of the target regions, leading to a nonlinear effect on the coordinated patterns of activity.

The neurotransmitter noradrenaline plays a dual role within the central nervous system. Tonic activity of the locus coeruleus, coupled with sustained noradrenergic presence, underpins the maintenance of arousal, ensuring vigilance. Conversely, phasic NA activity enhances attention processes by modulating neural response to salient stimuli (Berridge & Waterhouse, 2003;

Poe et al., 2020). It is important to note the interdependency of these two modalities; the attentional enhancement via phasic activity is contingent upon the concurrent arousal state (tonic activity) within the pulvinar (Coull et al., 2004).

In the state of relaxed, inattentive wakefulness and the transitioning from waking to sleeping, when the ability to respond to external stimuli decreases, the human electroencephalogram (EEG) shows a range of distinctive waves progressively increasing in amplitude and decreasing in frequency, the most prominent of which are the alpha rhythm, sleep spindles, and delta waves (Berger, 1934; Klimesch, 1999). Specifically, increased alpha oscillations are seen in low-vigilance state-dependent activities (low arousal) and attentive perception. The mechanism underlying these behavioral states' alpha waves might differ from their generation to propagation through the brain (Bonnefond et al., 2017; Brüers & VanRullen, 2018; Crunelli et al., 2018; Foxe & Snyder, 2011). Dahl et al. (2022) showed that locus coeruleus activations temporarily enhance important information processing by adjusting cortical activity through thalamocortical alpha synchronization. This implicates NA in potentially modulating arousal and spatial attentional processing via alpha power adjustments. This integrated neural mechanism, modulated by NA levels, offers a cohesive rationale for signal convergence within the dorsal pulvinar of diverse signals from internal bodily to sensory signals. Future experiments are essential to validate and further elucidate this potential relationship between levels of noradrenaline and alpha oscillations in the dorsal pulvinar. Key areas should be the noradrenergic influence within the dorsal pulvinar, complemented by pupillometry and low-frequency neural power modulation assessments during visual-spatial tasks, aiming to discern their combined impacts on arousal and spatial selection. Moreover, future studies must investigate whether signals related to cardiac-related arousal are linked to spatial cognition, indicating a potential base on how energy resources are considered for attentive perception and decision-making. Additionally, a broader network perspective that examines the interactions between the dorsal pulvinar and other brain regions, such as the prefrontal cortex, involved in attention and perception could provide a holistic understanding of the neurocircuitry underpinning of these processes.

5.5 Conclusions

In this dissertation, the crucial contribution of the dorsal pulvinar in spatial orienting was confirmed while correctly discriminating competing stimuli in the context of perceptual uncertainty. Crucially, the identified relationship between the dPul neuronal activity and the cardiac rhythms indicates dPul’s multifaceted functionality. Beyond its traditionally recognized role to receive, integrate, and modulate information from the senses and various cortical brain regions, the dPul appears instrumental in integrating and conveying information about the

body’s internal physiological state. The emergent link between the dorsal pulvinar and the autonomic nervous system enriches our comprehension of the dPul’s intricate functionality. This discovery not only refines our understanding but also prompts a reevaluation of the dorsal pulvinar’s role in cardiac-cerebral interactions. From a forward-looking perspective, this study paves the way for exploring the nuanced mechanism underlying the attentive perception signals with arousal indicators, particularly emphasizing the oscillatory and neuromodulatory dynamics in future studies.

6. References

Acuna, C., Cudeiro, J., Gonzalez, F., Alonso, J. M., & Perez, R. (1990). Lateral-posterior and pulvinar reaching cells—Comparison with parietal area 5a: A study in behaving Macaca nemestrina monkeys. *Exp Brain Res*, *82*(1), 158–166.

Acuna, C., Gonzalez, F., & Dominguez, R. (1983). Sensorimotor Unit Activity Related to Intention in the Pulvinar of Behaving Cebus Apella Monkeys. *Exp Brain Res*, *52*, 411–422.

Adam, R., Johnston, K., Menon, R. S., & Everling, S. (2020). Functional reorganization during the recovery of contralesional target selection deficits after prefrontal cortex lesions in macaque monkeys. *NeuroImage*, *207*, 116339. https://doi.org/10/gg3c6r

Adams, M. M., Hof, P. R., Gattass, R., Webster, M. J., & Ungerleider, L. G. (2000). Visual cortical projections and chemoarchitecture of macaque monkey pulvinar. *The Journal of Comparative Neurology*, *419*(3), 377–393.

Aggleton, J. P., Burton, M. J., & Passingham, R. E. (1980). Cortical and subcortical afferents to the amygdala of the rhesus monkey (Macaca mulatta). *Brain Research*, *190*(2), 347–368. https://doi.org/10.1016/0006-8993(80)90279-6

Al, E., Iliopoulos, F., Forschack, N., Nierhaus, T., Grund, M., Motyka, P., Gaebler, M., Nikulin, V. V., & Villringer, A. (2020). Heart–brain interactions shape somatosensory perception and evoked potentials. *Proceedings of the National Academy of Sciences*, *117*(19), 10575–10584. https://doi.org/10.1073/pnas.1915629117

Almeida, I., Soares, S. C., & Castelo-Branco, M. (2015). The Distinct Role of the Amygdala, Superior Colliculus and Pulvinar in Processing of Central and Peripheral Snakes. *PLOS ONE*, *10*(6), e0129949. https://doi.org/10.1371/journal.pone.0129949

Arcaro, M. J., Pinsk, M. A., Chen, J., & Kastner, S. (2018). Organizing principles of pulvino-cortical functional coupling in humans. *Nature Communications*, *9*(1), 5382. https://doi.org/10.1038/s41467-018-07725-6

Arcaro, M. J., Pinsk, M. A., & Kastner, S. (2015). The Anatomical and Functional Organization of the Human Visual Pulvinar. *Journal of Neuroscience*, *35*(27), 9848–9871. https://doi.org/10.1523/JNEUROSCI.1575-14.2015

Arend, I., Machado, L., Ward, R., McGrath, M., Ro, T., & Rafal, R. D. (2008). The role of the human pulvinar in visual attention and action: Evidence from temporal-order judgment, saccade decision, and antisaccade tasks. *Prog Brain Res*, *171*, 475–483.

Arend, I., Rafal, R., & Ward, R. (2008). Spatial and temporal deficits are regionally dissociable in patients with pulvinar lesions. *Brain*, *131*(8), 2140–2152. https://doi.org/10.1093/brain/awn135

Asanuma, C., Andersen, R. A., & Cowan, W. M. (1985). The thalamic relations of the caudal inferior parietal lobule and the lateral prefrontal cortex in monkeys: Divergent cortical projections from cell clusters in the medial pulvinar nucleus. *J Comp Neurol*, *241*(3), 357–381. https://doi.org/10.1002/cne.902410309

Aston-Jones, G., & Cohen, J. D. (2005). AN INTEGRATIVE THEORY OF LOCUS COERULEUS-NOREPINEPHRINE FUNCTION: Adaptive Gain and Optimal Performance. *Annual Review of Neuroscience*, *28*(1), 403–450. https://doi.org/10.1146/annurev.neuro.28.061604.135709

Baldwin, M. K. L., & Bourne, J. A. (2017). The Evolution of Subcortical Pathways to the Extrastriate Cortex. In *Evolution of Nervous Systems* (pp. 165–185). Elsevier. https://doi.org/10.1016/B978-0-12-804042-3.00081-6

Baldwin, M. K. L., Wong, P., Reed, J. L., & Kaas, J. H. (2011). Superior Colliculus Connections With Visual Thalamus in Gray Squirrels (Sciurus carolinensis): Evidence for Four Subdivisions Within the Pulvinar Complex. *The Journal of Comparative Neurology*, *519*(6), 1071–1094. https://doi.org/10.1002/cne.22552

Barber, A. D., John, M., DeRosse, P., Birnbaum, M. L., Lencz, T., & Malhotra, A. K. (2020). Parasympathetic arousal-related cortical activity is associated with attention during cognitive task performance. *NeuroImage*, *208*, 116469. https://doi.org/10.1016/j.neuroimage.2019.116469

Beck, D. M., & Kastner, S. (2009). Top-down and bottom-up mechanisms in biasing competition in the human brain. *Vision Research*, *49*(10), 1154–1165. https://doi.org/10.1016/j.visres.2008.07.012

Bell, A. H., & Bultitude, J. H. (2018). Methods matter: A primer on permanent and reversible interference techniques in animals for investigators of human neuropsychology. *Neuropsychologia*, *115*, 211–219. https://doi.org/10.1016/j.neuropsychologia.2017.09.019

Bell, P. T., & Shine, J. M. (2016). Subcortical contributions to large-scale network communication. *Neuroscience & Biobehavioral Reviews*, *71*, 313–322. https://doi.org/10.1016/j.neubiorev.2016.08.036

Benarroch, E. E. (2015). Pulvinar: Associative role in cortical function and clinical correlations. *Neurology*, *84*(7), 738–747. https://doi.org/10.1212/WNL.0000000000001276

Bender, D. B. (1982). Receptive-field properties of neurons in the macaque inferior pulvinar. *Journal of Neurophysiology*, *48*(1), 1–17. https://doi.org/10.1152/jn.1982.48.1.1

Bender, D. B. (1988). Electrophysiological and behavioral experiments on the primate pulvinar. *Prog Brain Res*, *75*, 55–65.

Bender, D. B., & Butter, C. M. (1987). Comparison of the effects of superior colliculus and pulvinar lesions on visual search and tachistoscopic pattern discrimination in monkeys. *Exp Brain Res*, *69*(1), 140–154.

Bender, D. B., & Youakim, M. (2001). Effect of Attentive Fixation in Macaque Thalamus and Cortex. *Journal of Neurophysiology*, *85*(1), 219–234. https://doi.org/10.1152/jn.2001.85.1.219

Benevento, L. A., & Fallon, J. H. (1975). The ascending projections of the superior colliculus in the rhesus monkey (Macaca mulatta). *The Journal of Comparative Neurology*, *160*(3), 339–361. https://doi.org/10.1002/cne.901600306

Benevento, L. A., & Miller, J. (1981). Visual responses of single neurons in the caudal lateral pulvinar of the macaque monkey. *J Neurosci*, *1*(11), 1268–1278.

Benevento, L. A., & Port, J. D. (1995a). Single neurons with both form/color differential responses and saccade-related responses in the nonretinotopic pulvinar of the behaving macaque monkey. *Visual Neuroscience*, *12*(3), 523–544. https://doi.org/10.1017/S0952523800008439

Benevento, L. A., & Standage, G. P. (1983). The organization of projections of the retinorecipient and nonretinorecipient nuclei of the pretectal complex and layers of the superior colliculus to the lateral pulvinar and medial pulvinar in the macaque monkey. *The Journal of Comparative Neurology*, *217*(3), 307–336. https://doi.org/10.1002/cne.902170307

Berger, H. (1934). Über das Elektrenkephalogramm des Menschen. *DMW - Deutsche Medizinische Wochenschrift*, *60*(51), 1947–1949. https://doi.org/10.1055/s-0028-1130334

Berman, R. A., & Wurtz, R. H. (2008). Exploring the pulvinar path to visual cortex. In *Progress in Brain Research* (Vol. 171, pp. 467–473). Elsevier. https://doi.org/10.1016/S0079-6123(08)00668-7

Berman, R. A., & Wurtz, R. H. (2010). Functional Identification of a Pulvinar Path from Superior Colliculus to Cortical Area MT. *Journal of Neuroscience*, *30*(18), 6342–6354. https://doi.org/10.1523/JNEUROSCI.6176-09.2010

Berman, R. A., & Wurtz, R. H. (2011). Signals conveyed in the pulvinar pathway from superior colliculus to cortical area MT. *The Journal of Neuroscience : The Official Journal of the Society for Neuroscience*, *31*(2), 373–384. https://doi.org/10.1523/JNEUROSCI.4738-10.2011

Berridge, C. W., & Waterhouse, B. D. (2003). The locus coeruleus–noradrenergic system: Modulation of behavioral state and state-dependent cognitive processes. *Brain Research Reviews*, *42*(1), 33–84. https://doi.org/10.1016/S0165-0173(03)00143-7

Bertini, C., Pietrelli, M., Braghittoni, D., & Làdavas, E. (2018). Pulvinar Lesions Disrupt Fear-Related Implicit Visual Processing in Hemianopic Patients. *Frontiers in Psychology*, *9*, 2329. https://doi.org/10.3389/fpsyg.2018.02329

Blatt, G. J., Andersen, R. A., & Stoner, G. R. (1990). Visual receptive field organization and cortico-cortical connections of the lateral intraparietal area (area LIP) in the macaque. *J Comp Neurol*, *299*(4), 421–445.

Bogadhi, A. R., Bollimunta, A., Leopold, D. A., & Krauzlis, R. J. (2019). Spatial Attention Deficits Are Causally Linked to an Area in Macaque Temporal Cortex. *Current Biology*, *29*(5), 726-736.e4. https://doi.org/10.1016/j.cub.2019.01.028

Bonnefond, M., Kastner, S., & Jensen, O. (2017). Communication between Brain Areas Based on Nested Oscillations. *Eneuro*, *4*(2), ENEURO.0153-16.2017. https://doi.org/10.1523/ENEURO.0153-16.2017

Bourgeois, A., Guedj, C., Carrera, E., & Vuilleumier, P. (2020). Pulvino-cortical interaction: An integrative role in the control of attention. *Neuroscience & Biobehavioral Reviews*, *111*, 104–113. https://doi.org/10.1016/j.neubiorev.2020.01.005

Brainard, D. H. (1997). The Psychophysics Toolbox. *Spatial Vision*, *10*(4), 433–436.

Bridge, H., Leopold, D. A., & Bourne, J. A. (2015). Adaptive Pulvinar Circuitry Supports Visual Cognition. *Trends in Cognitive Sciences*. https://doi.org/10.1016/j.tics.2015.10.003

Bridge, H., Leopold, D. A., & Bourne, J. A. (2016). Adaptive Pulvinar Circuitry Supports Visual Cognition. *Trends in Cognitive Sciences*, *20*(2), 146–157. https://doi.org/10.1016/j.tics.2015.10.003

Brüers, S., & VanRullen, R. (2018). Alpha Power Modulates Perception Independently of Endogenous Factors. *Frontiers in Neuroscience*, *12*, 279. https://doi.org/10.3389/fnins.2018.00279

Byrne, J. H. (2013). Introduction to neurons and neuronal networks. *Textbook for the Neurosciences*, 12.

Cajal, R. Y. (1906). Quelques antécédents historiques ignorés sur les Plasmazellen. *Anat. Anz*, *29*, 666.

Caldani, S., Isel, F., Septier, M., Acquaviva, E., Delorme, R., & Bucci, M. P. (2020). Impairment in Attention Focus During the Posner Cognitive Task in Children With ADHD: An Eye Tracker Study. *Frontiers in Pediatrics*, *8*, 484. https://doi.org/10.3389/fped.2020.00484

Chan, L. K. H., & Hayward, W. G. (2013). Visual search. *Wiley Interdisciplinary Reviews: Cognitive Science*, *4*(4), 415–429. https://doi.org/10.1002/wcs.1235

Cisek, P. (2006). Integrated Neural Processes for Defining Potential Actions and Deciding between Them: A Computational Model. *Journal of Neuroscience*, *26*(38), 9761–9770. https://doi.org/10.1523/JNEUROSCI.5605-05.2006

Cohen, M. R., & Newsome, W. T. (2004). What electrical microstimulation has revealed about the neural basis of cognition. *Current Opinion in Neurobiology*, *14*(2), 169–177. https://doi.org/10.1016/j.conb.2004.03.016

Corbetta, M., & Shulman, G. L. (2011). Spatial neglect and attention networks. *Annual Review of Neuroscience*, *34*, 569–599. https://doi.org/10.1146/annurev-neuro-061010-113731

Coull, J. T., Jones, M. E. P., Egan, T. D., Frith, C. D., & Maze, M. (2004). Attentional effects of noradrenaline vary with arousal level: Selective activation of thalamic pulvinar in humans. *NeuroImage*, *22*(1), 315–322. https://doi.org/10.1016/j.neuroimage.2003.12.022

Crunelli, V., Lőrincz, M. L., Connelly, W. M., David, F., Hughes, S. W., Lambert, R. C., Leresche, N., & Errington, A. C. (2018). Dual function of thalamic low-vigilance state oscillations: Rhythm-regulation and plasticity. *Nature Reviews Neuroscience*, *19*(2), 107–118. https://doi.org/10.1038/nrn.2017.151

Cudeiro, J., Gonzalez, F., Perez, R., Alonso, J. M., & Acuna, C. (1989). Does the pulvinar-LP complex contribute to motor programming? *Brain Res*, *484*(1–2), 367–370.

Dahl, M. J., Mather, M., & Werkle-Bergner, M. (2022). Noradrenergic modulation of rhythmic neural activity shapes selective attention. *Trends in Cognitive Sciences*, *26*(1), 38–52. https://doi.org/10.1016/j.tics.2021.10.009

Danziger, S., Ward, R., Owen, V., & Rafal, R. (2001). The effects of unilateral pulvinar damage in humans on reflexive orienting and filtering of irrelevant information. *Behav Neurol*, *13*(3–4), 95–104.

Danziger, S., Ward, R., Owen, V., & Rafal, R. (2004). Contributions of the human pulvinar to linking vision and action. *Cognitive, Affective, & Behavioral Neuroscience*, *4*(1), 89–99.

Desimone, R., & Duncan, J. (1995). Neural mechanisms of selective visual attention. *Annu Rev Neurosci*, *18*, 193–222.

Desimone, R., Wessinger, M., Thomas, L., & Schneider, W. (1990). Attentional Control of Visual Perception: Cortical and Subcortical Mechanisms. *Cold Spring Harbor Symposia on Quantitative Biology*, *55*(0), 963–971. https://doi.org/10.1101/SQB.1990.055.01.090

Dominguez-Vargas, A.-U., Schneider, L., Wilke, M., & Kagan, I. (2017). Electrical Microstimulation of the Pulvinar Biases Saccade Choices and Reaction Times in a Time-Dependent Manner. *Journal of Neuroscience*, *37*(8), 2234–2257. https://doi.org/10.1523/JNEUROSCI.1984-16.2016

Doricchi, F., Macci, E., Silvetti, M., & Macaluso, E. (2010). Neural Correlates of the Spatial and Expectancy Components of Endogenous and Stimulus-Driven Orienting of Attention in the Posner Task. *Cerebral Cortex*, *20*(7), 1574–1585. https://doi.org/10.1093/cercor/bhp215

Eckstein, M. P. (2011). Visual search: A retrospective. *Journal of Vision*, *11*(5), 14–14. https://doi.org/10.1167/11.5.14

Elorette, C., Forcelli, P. A., Saunders, R. C., & Malkova, L. (2018). Colocalization of Tectal Inputs With Amygdala-Projecting Neurons in the Macaque Pulvinar. *Frontiers in Neural Circuits*, *12*, 91. https://doi.org/10.3389/fncir.2018.00091

Fetsch, C. R., Kiani, R., Newsome, W. T., & Shadlen, M. N. (2014). Effects of Cortical Microstimulation on Confidence in a Perceptual Decision. *Neuron*, *83*(4), 797–804. https://doi.org/10.1016/j.neuron.2014.07.011

Fiebelkorn, I. C., & Kastner, S. (2019). The Puzzling Pulvinar. *Neuron*, *101*(2), 201–203. https://doi.org/10.1016/j.neuron.2018.12.032

Fiebelkorn, I. C., Pinsk, M. A., & Kastner, S. (2018). A Dynamic Interplay within the Frontoparietal Network Underlies Rhythmic Spatial Attention. *Neuron*, *99*(4), 842-853.e8. https://doi.org/10.1016/j.neuron.2018.07.038

Fiebelkorn, I. C., Pinsk, M. A., & Kastner, S. (2019). The mediodorsal pulvinar coordinates the macaque fronto-parietal network during rhythmic spatial attention. *Nature Communications*, *10*(1), 215. https://doi.org/10.1038/s41467-018-08151-4

Fischer, J., & Whitney, D. (2012). Attention gates visual coding in the human pulvinar. *Nature Communications*, *3*, 1051. https://doi.org/10.1038/ncomms2054

Foote, S. L., Aston-Jones, G., & Bloom, F. E. (1980). Impulse activity of locus coeruleus neurons in awake rats and monkeys is a function of sensory stimulation and arousal. *Proceedings of the National Academy of Sciences*, *77*(5), 3033–3037. https://doi.org/10.1073/pnas.77.5.3033

Foxe, J. J., & Snyder, A. C. (2011). The Role of Alpha-Band Brain Oscillations as a Sensory Suppression Mechanism during Selective Attention. *Frontiers in Psychology*, *2*. https://doi.org/10.3389/fpsyg.2011.00154

Froesel, M., Cappe, C., & Ben Hamed, S. (2021). A multisensory perspective onto primate pulvinar functions. *Neuroscience & Biobehavioral Reviews*, *125*, 231–243. https://doi.org/10.1016/j.neubiorev.2021.02.043

Frysinger, R. C., & Harper, R. M. (1989). Cardiac and respiratory correlations with unit discharge in human amygdala and hippocampus. *Electroencephalography and Clinical Neurophysiology*, *72*(6), 463–470. https://doi.org/10.1016/0013-4694(89)90222-8

Gattass, R., Oswaldo-Cruz, E., & Sousa, A. P. B. (1979). Visual receptive fields of units in the pulvinar of cebus monkey. *Brain Research*, *160*(3), 413–429. https://doi.org/10.1016/0006-8993(79)91070-9

Gattass, R., P.B. Sousa, A., & Oswaldo-Cruz, E. (1978). Single unit response types in the pulvinar of the cebus monkey to multisensory stimulation. *Brain Research*, *158*(1), 75–87. https://doi.org/10.1016/0006-8993(78)90007-0

Gattass, R., Soares, J. G. M., & Lima, B. (2018). Modulation of Pulvinar Neuronal Activity by Arousal. In R. Gattass, J. G. M. Soares, & B. Lima, *The Pulvinar Thalamic Nucleus of Non-Human Primates: Architectonic and Functional Subdivisions* (Vol. 225, pp. 49–51). Springer International Publishing. https://doi.org/10.1007/978-3-319-70046-5_10

Golgi, C. (1873). Sulla struttura della sostanza del cervello. *Lombardia: Gazzetta*.

Grieve, K. L., Acuña, C., & Cudeiro, J. (2000). The primate pulvinar nuclei: Vision and action. *Trends in Neurosciences*, *23*(1), 35–39.

Groh, A., Bokor, H., Mease, R. A., Plattner, V. M., Hangya, B., Stroh, A., Deschenes, M., & Acsády, L. (2014). Convergence of Cortical and Sensory Driver Inputs on Single Thalamocortical Cells. *Cerebral Cortex*, *24*(12), 3167–3179. https://doi.org/10.1093/cercor/bht173

Gutierrez, C., Cola, M. G., Seltzer, B., & Cusick, C. (2000). Neurochemical and connectional organization of the dorsal pulvinar complex in monkeys. *Journal of Comparative Neurology*, *419*(1), 61–86.

Gutierrez, C., Yaun, A., & Cusick, C. G. (1995). Neurochemical subdivisions of the inferior pulvinar in macaque monkeys. *The Journal of Comparative Neurology*, *363*(4), 545–562. https://doi.org/10.1002/cne.903630404

Halassa, M. M., & Kastner, S. (2017). Thalamic functions in distributed cognitive control. *Nature Neuroscience*, *20*(12), 1669–1679. https://doi.org/10.1038/s41593-017-0020-1

Halassa, M. M., & Sherman, S. M. (2019). Thalamocortical Circuit Motifs: A General Framework. *Neuron*, *103*(5), 762–770. https://doi.org/10.1016/j.neuron.2019.06.005

Hanks, T. D., & Summerfield, C. (2017). Perceptual Decision Making in Rodents, Monkeys, and Humans. *Neuron*, *93*(1), 15–31. https://doi.org/10.1016/j.neuron.2016.12.003

Hardy, S. G. P., & Lynch, J. C. (1992). The Spatial Distribution of Pulvinar Neurons That Project to Two Subregions of the Inferior Parietal Lobule in the Macaque. *Cereb Cortex*, *2*(3), 217–230. https://doi.org/10.1093/cercor/2.3.217

Hauser, C. K., & Salinas, E. (2014). Perceptual Decision Making. In D. Jaeger & R. Jung (Eds.), *Encyclopedia of Computational Neuroscience* (pp. 1–21). Springer New York. https://doi.org/10.1007/978-1-4614-7320-6_317-1

Histed, M. H., Ni, A. M., & Maunsell, J. H. R. (2013). Insights into cortical mechanisms of behavior from microstimulation experiments. *Progress in Neurobiology*, *103*, 115–130. https://doi.org/10.1016/j.pneurobio.2012.01.006

Homman-Ludiye, J., & Bourne, J. A. (2019). The medial pulvinar: Function, origin and association with neurodevelopmental disorders. *Journal of Anatomy*, *235*(3), 507–520. https://doi.org/10.1111/joa.12932

Homman-Ludiye, J., Mundinano, I. C., Kwan, W. C., & Bourne, J. A. (2020). Extensive Connectivity Between the Medial Pulvinar and the Cortex Revealed in the Marmoset Monkey. *Cerebral Cortex*, *30*(3), 1797–1812. https://doi.org/10.1093/cercor/bhz203

Hwang, K., Bertolero, M. A., Liu, W. B., & D'Esposito, M. (2017). The Human Thalamus Is an Integrative Hub for Functional Brain Networks. *The Journal of Neuroscience*, *37*(23), 5594–5607. https://doi.org/10.1523/JNEUROSCI.0067-17.2017

Imura, K., & Rockland, K. S. (2006). Long-range interneurons within the medial pulvinar nucleus of macaque monkeys. *The Journal of Comparative Neurology*, *498*(5), 649–666. https://doi.org/10.1002/cne.21085

Imura, K., & Rockland, K. S. (2007). Giant neurons in the macaque pulvinar: A distinct relay subpopulation. *Frontiers in Neuroanatomy*, *1*, 2.

Jaramillo, J., Mejias, J. F., & Wang, X.-J. (2019). Engagement of Pulvino-cortical Feedforward and Feedback Pathways in Cognitive Computations. *Neuron*, *101*(2), 321-336.e9. https://doi.org/10.1016/j.neuron.2018.11.023

Jones, E. G. (Ed.). (1985). *The Thalamus*. Springer US. https://doi.org/10.1007/978-1-4615-1749-8

Jones, E. G., & Burton, H. (1976). A projection from the medial pulvinar to the amygdala in primates. *Brain Res*, *104*, 142–147.

Kaas, J. H., & Baldwin, M. K. L. (2020). The Evolution of the Pulvinar Complex in Primates and Its Role in the Dorsal and Ventral Streams of Cortical Processing. *Vision*, *4*(1), Article 1. https://doi.org/10.3390/vision4010003

Kaas, J. H., & Lyon, D. C. (2007). Pulvinar contributions to the dorsal and ventral streams of visual processing in primates. *Brain Research Reviews*, *55*(2), 285–296. https://doi.org/10.1016/j.brainresrev.2007.02.008

Kagan, I., Gibson, L., Spanou, E., & Wilke, M. (2021). Effective connectivity and spatial selectivity-dependent fMRI changes elicited by microstimulation of pulvinar and LIP. *NeuroImage*, *240*, 118283. https://doi.org/10.1016/j.neuroimage.2021.118283

Kanai, R., Komura, Y., Shipp, S., & Friston, K. (2015). Cerebral hierarchies: Predictive processing, precision and the pulvinar. *Philosophical Transactions of the Royal Society B: Biological Sciences*, *370*(1668), 20140169. https://doi.org/10.1098/rstb.2014.0169

Karnath, H. O., Himmelbach, M., & Rorden, C. (2002). The subcortical anatomy of human spatial neglect: Putamen, caudate nucleus and pulvinar. *Brain*, *125*(Pt 2), 350–360.

Kastner, S., Fiebelkorn, I. C., & Eradath, M. K. (2020). Dynamic pulvino-cortical interactions in the primate attention network. *Current Opinion in Neurobiology*, *65*, 10–19. https://doi.org/10.1016/j.conb.2020.08.002

Kastner, S., O'Connor, D. H., Fukui, M. M., Fehd, H. M., Herwig, U., & Pinsk, M. A. (2004). Functional imaging of the human lateral geniculate nucleus and pulvinar. *J Neurophysiol*, *91*(1), 438–448.

Kastner, S., & Pinsk, M. A. (2004). Visual attention as a multilevel selection process. *Cogn Affect Behav Neurosci*, *4*(4), 483–500.

Kelly, S. P., & O'Connell, R. G. (2015). The neural processes underlying perceptual decision making in humans: Recent progress and future directions. *Journal of Physiology-Paris*, *109*(1–3), 27–37. https://doi.org/10.1016/j.jphysparis.2014.08.003

Kim, K., Ladenbauer, J., Babo-Rebelo, M., Buot, A., Lehongre, K., Adam, C., Hasboun, D., Lambrecq, V., Navarro, V., Ostojic, S., & Tallon-Baudry, C. (2019). Resting-State Neural Firing Rate Is Linked to Cardiac-Cycle Duration in the Human Cingulate and Parahippocampal Cortices. *The Journal of Neuroscience*, *39*(19), 3676–3686. https://doi.org/10.1523/JNEUROSCI.2291-18.2019

Kimura, K., Kanayama, N., & Katahira, K. (2023). Cardiac cycle affects risky decision-making. *Biological Psychology*, *176*, 108471. https://doi.org/10.1016/j.biopsycho.2022.108471

Kimura, K., Kanayama, N., Toyama, A., & Katahira, K. (2022). Cardiac Cycle Affects the Asymmetric Value Updating in Instrumental Reward Learning. *Frontiers in Neuroscience*, *16*, 889440. https://doi.org/10.3389/fnins.2022.889440

Klimesch, W. (1999). EEG alpha and theta oscillations reflect cognitive and memory performance: A review and analysis. *Brain Research Reviews*, *29*(2–3), 169–195. https://doi.org/10.1016/S0165-0173(98)00056-3

Klink, P. C., Aubry, J.-F., Ferrera, V. P., Fox, A. S., Froudist-Walsh, S., Jarraya, B., Konofagou, E. E., Krauzlis, R. J., Messinger, A., Mitchell, A. S., Ortiz-Rios, M., Oya, H., Roberts, A. C., Roe, A. W., Rushworth, M. F. S., Sallet, J., Schmid, M. C., Schroeder, C. E., Tasserie, J., … Petkov, C. I. (2021). Combining brain perturbation and neuroimaging in non-human primates. *NeuroImage*, *235*, 118017. https://doi.org/10.1016/j.neuroimage.2021.118017

Klink, P. C., Teeuwen, R. R. M., Lorteije, J. A. M., & Roelfsema, P. R. (2023). Inversion of pop-out for a distracting feature dimension in monkey visual cortex. *Proceedings of the National Academy of Sciences*, *120*(9), e2210839120. https://doi.org/10.1073/pnas.2210839120

Komura, Y., Nikkuni, A., Hirashima, N., Uetake, T., & Miyamoto, A. (2013). Responses of pulvinar neurons reflect a subject's confidence in visual categorization. *Nature Neuroscience*, *16*(6), 749–755. https://doi.org/10.1038/nn.3393

Kragel, P. A., Čeko, M., Theriault, J., Chen, D., Satpute, A. B., Wald, L. W., Lindquist, M. A., Feldman Barrett, L., & Wager, T. D. (2021). A human colliculus-pulvinar-amygdala pathway encodes negative emotion. *Neuron*, *109*(15), 2404-2412.e5. https://doi.org/10.1016/j.neuron.2021.06.001

Krauzlis, R. J., Bollimunta, A., Arcizet, F., & Wang, L. (2014). Attention as an effect not a cause. *Trends in Cognitive Sciences*, *18*(9), 457–464. https://doi.org/10.1016/j.tics.2014.05.008

LaBerge, D., & Buchsbaum, M. S. (1990). Positron Emission Tomographic Measurements of Pulvinar Activity During an Attention Task. *J Neurosci*, *10*(2), 613–619.

Li, C. S., Mazzoni, P., & Andersen, R. A. (1999). Effect of reversible inactivation of macaque lateral intraparietal area on visual and memory saccades. *J Neurophysiol*, *81*(4), 1827–1838.

Linares, D., Aguilar-Lleyda, D., & López-Moliner, J. (2019). Decoupling sensory from decisional choice biases in perceptual decision making. *ELife*, *8*, e43994. https://doi.org/10.7554/eLife.43994

Lovejoy, L. P., & Krauzlis, R. J. (2010). Inactivation of primate superior colliculus impairs covert selection of signals for perceptual judgments. *Nature Neuroscience*, *13*(2), 261–266. https://doi.org/10.1038/nn.2470

Lovejoy, L. P., & Krauzlis, R. J. (2017). Changes in perceptual sensitivity related to spatial cues depends on subcortical activity. *Proceedings of the National Academy of Sciences*, *114*(23), 6122–6126. https://doi.org/10.1073/pnas.1609711114

Lucas, N., Bourgeois, A., Carrera, E., Landis, T., & Vuilleumier, P. (2019). Impaired visual search with paradoxically increased facilitation by emotional features after unilateral pulvinar damage. *Cortex*, *120*, 223–239. https://doi.org/10.1016/j.cortex.2019.06.009

Luo, T. Z., & Maunsell, J. H. R. (2015). Neuronal Modulations in Visual Cortex Are Associated with Only One of Multiple Components of Attention. *Neuron*, *86*(5), 1182–1188. https://doi.org/10.1016/j.neuron.2015.05.007

Lyon, D. C. (2007). The Evolution of Visual Cortex and Visual Systems. In *Evolution of Nervous Systems* (pp. 267–306). Elsevier. https://doi.org/10.1016/B0-12-370878-8/00075-6

Ma, T. P., Lynch, J. C., Donahoe, D. K., Attallah, H., & Rafols, J. A. (1998). Organization of the medial pulvinar nucleus in the macaque. *The Anatomical Record*, *250*(2), 220–237. https://doi.org/10.1002/(SICI)1097-0185(199802)250:2<220::AID-AR12>3.0.CO;2-Q

Macmillan, N. A., & Creelman, C. D. (2004). *Detection Theory: A User's Guide* (2nd edition). Psychology Press.

Magariños-Ascone, C., Buño, W., & García-Austt, E. (1988). Monkey pulvinar units related to motor activity and sensory response. *Brain Research*, *445*(1), 30–38. https://doi.org/10.1016/0006-8993(88)91070-0

Magnin, M., Rey, M., Bastuji, H., Guillemant, P., Mauguière, F., & Garcia-Larrea, L. (2010). Thalamic deactivation at sleep onset precedes that of the cerebral cortex in humans. *Proceedings of the National Academy of Sciences*, *107*(8), 3829–3833. https://doi.org/10.1073/pnas.0909710107

Maior, R. S., Hori, E., Tomaz, C., Ono, T., & Nishijo, H. (2010). The monkey pulvinar neurons differentially respond to emotional expressions of human faces. *Behavioural Brain Research*, *215*(1), 129–135. https://doi.org/10.1016/j.bbr.2010.07.009

Markowitz, D. A., Shewcraft, R. A., Wong, Y. T., & Pesaran, B. (2011). Competition for Visual Selection in the Oculomotor System. *Journal of Neuroscience*, *31*(25), 9298–9306. https://doi.org/10.1523/JNEUROSCI.0908-11.2011

Mathers, L. H., & Rapisardi, S. C. (1973). Visual and somatosensory receptive fields of neurons in the squirrel monkey pulvinar. *Brain Research*, *64*, 65–83. https://doi.org/10.1016/0006-8993(73)90171-6

McFadyen, J., Mattingley, J. B., & Garrido, M. I. (2019). An afferent white matter pathway from the pulvinar to the amygdala facilitates fear recognition. *ELife*, *8*, e40766. https://doi.org/10.7554/eLife.40766

Mishkin, M., Ungerleider, L. G., & Macko, K. A. (1983). Object vision and spatial vision: Two cortical pathways. *Trends in Neurosciences*, *6*, 414–417. https://doi.org/10.1016/0166-2236(83)90190-X

Moreira, C. M., Rollwage, M., Kaduk, K., Wilke, M., & Kagan, I. (2018). Post-decision wagering after perceptual judgments reveals bi-directional certainty readouts. *Cognition*, *176*, 40–52. https://doi.org/10.1016/j.cognition.2018.02.026

Newsome, W., & Pare, E. (1988). A selective impairment of motion perception following lesions of the middle temporal visual area (MT). *The Journal of Neuroscience*, *8*(6), 2201–2211. https://doi.org/10.1523/JNEUROSCI.08-06-02201.1988

Nguyen, M. N., Hori, E., Matsumoto, J., Tran, A. H., Ono, T., & Nishijo, H. (2013). Neuronal responses to face-like stimuli in the monkey pulvinar. *European Journal of Neuroscience*, *37*(1), 35–51. https://doi.org/10.1111/ejn.12020

O'Brien, B. J., Abel, P. L., & Olavarria, J. F. (2001). The retinal input to calbindin-D28k-defined subdivisions in macaque inferior pulvinar. *Neuroscience Letters*, *312*(3), 145–148. https://doi.org/10.1016/s0304-3940(01)02220-0

Ohayon, S., & Tsao, D. Y. (2012). MR-guided stereotactic navigation. *J Neurosci Methods*, *204*(2), 389–397. https://doi.org/10.1016/j.jneumeth.2011.11.031

Oken, B. S., Salinsky, M. C., & Elsas, S. M. (2006). Vigilance, alertness, or sustained attention: Physiological basis and measurement. *Clinical Neurophysiology*, *117*(9), 1885–1901. https://doi.org/10.1016/j.clinph.2006.01.017

Olszewski, J. (1952). *The Thalamus of the Macaca Mulatta, An Atlas for Use with the Stereotaxic Instrument*. Karger Press.

Ott, I. S. A. A. C. (1891). *Vaso-tonic centres in the thalami.*

Passingham, R. E., Stephan, K. E., & Kötter, R. (2002). The anatomical basis of functional localization in the cortex. *Nature Reviews Neuroscience*, *3*(8), 606–616. https://doi.org/10.1038/nrn893

Pérez-Santos, I., Palomero-Gallagher, N., Zilles, K., & Cavada, C. (2021). Distribution of the Noradrenaline Innervation and Adrenoceptors in the Macaque Monkey Thalamus. *Cerebral Cortex*, *31*(9), 4115–4139. https://doi.org/10.1093/cercor/bhab073

Perryman, K. M., Lindsley, D. F., & Lindsley, D. B. (1980). Pulvinar neuron responses to spontaneous and trained eye movements and to light flashes in squirrel monkeys. *Electroencephalography and Clinical Neurophysiology*, *49*(1–2), 152–161. https://doi.org/10.1016/0013-4694(80)90361-2

Pessoa, L., & Adolphs, R. (2010). Emotion processing and the amygdala: From a "low road" to "many roads" of evaluating biological significance. *Nat Rev Neurosci*, *11*(11), 773–783. https://doi.org/10.1038/nrn2920

Pessoa, L., & Adolphs, R. (2011). Emotion and the brain: Multiple roads are better than one. *Nature Reviews Neuroscience*, *12*(7), 425–425. https://doi.org/10.1038/nrn2920-c2

Petersen, S. E., Robinson, D. L., & Keys, W. (1985). Pulvinar nuclei of the behaving rhesus monkey: Visual responses and their modulation. *Journal of Neurophysiology*, *54*(4), 867–886. https://doi.org/10.1152/jn.1985.54.4.867

Petersen, S. E., Robinson, D. L., & Morris, J. D. (1987). Contributions of the pulvinar to visual spatial attention.

Phillips, J. M., Kambi, N. A., Redinbaugh, M. J., Mohanta, S., & Saalmann, Y. B. (2021). Disentangling the influences of multiple thalamic nuclei on prefrontal cortex and cognitive control. *Neuroscience & Biobehavioral Reviews*, *128*, 487–510. https://doi.org/10.1016/j.neubiorev.2021.06.042

Poe, G. R., Foote, S., Eschenko, O., Johansen, J. P., Bouret, S., Aston-Jones, G., Harley, C. W., Manahan-Vaughan, D., Weinshenker, D., Valentino, R., Berridge, C., Chandler, D. J., Waterhouse, B., & Sara, S. J. (2020). Locus coeruleus: A new look at the blue spot. *Nature Reviews Neuroscience*, *21*(11), 644–659. https://doi.org/10.1038/s41583-020-0360-9

Posner, M. I. (1980). Orienting of Attention. *Quarterly Journal of Experimental Psychology*, *32*(1), 3–25. https://doi.org/10.1080/00335558008248231

Posner, M. I., Snyder, C. R., & Davidson, B. J. (1980). Attention and the detection of signals. *J Exp Psychol*, *109*(2), 160–174.

Preuss, T. M. (2007). Evolutionary specializations of primate brain systems. In M. J. Ravosa & M. Dagosto (Eds.), *Primate Origins: Evolution and Adaptations.* (pp. 625-675.). New York: Springer.

Prins, N., & Kingdom, F. A. A. (2009). *Palamedes: Matlab routines for analyzing psychophysical data*. http://www.palamedestoolbox.org

Rafal, R. D., Koller, K., Bultitude, J. H., Mullins, P., Ward, R., Mitchell, A. S., & Bell, A. H. (2015). Connectivity between the superior colliculus and the amygdala in humans and macaque monkeys: Virtual dissection with probabilistic DTI tractography. *Journal of Neurophysiology*, *114*(3), 1947–1962. https://doi.org/10.1152/jn.01016.2014

Rafal, R. D., & Posner, M. I. (1987). Deficits in human visual spatial attention following thalamic lesions. *Proceedings of the National Academy of Sciences*, *84*(20), 7349–7353. https://doi.org/10.1073/pnas.84.20.7349

Rikhye, R. V., Gilra, A., & Halassa, M. M. (2018). Thalamic regulation of switching between cortical representations enables cognitive flexibility. *Nature Neuroscience*, *21*(12), 1753–1763. https://doi.org/10.1038/s41593-018-0269-z

Robinson, D. L. (1993). Chapter 31 Functional contributions of the primate pulvinar. In *Progress in Brain Research* (Vol. 95, pp. 371–380). Elsevier. https://doi.org/10.1016/S0079-6123(08)60382-9

Robinson, D. L., McClurkin, J. W., & Kertzman, C. (1990). Orbital position and eye movement influences on visual responses in the pulvinar nuclei of the behaving macaque. *Exp Brain Res*, *82*(2), 235–246.

Robinson, D. L., & Petersen, S. E. (1992). The pulvinar and visual salience. *Trends in Neurosciences*, *15*(4), 127–132. https://doi.org/10.1016/0166-2236(92)90354-B

Robinson, D. L., Petersen, S. E., & Keys, W. (1986). Saccade-related and visual activities in the pulvinar nuclei of the behaving rhesus monkey. *Experimental Brain Research*, *62*(3). https://doi.org/10.1007/BF00236042

Rockland, K. S. (1996). Two types of corticopulvinar terminations: Round (type 2) and elongate (type 1). *The Journal of Comparative Neurology*, *368*(1), 57–87. https://doi.org/10.1002/(SICI)1096-9861(19960422)368:1<57::AID-CNE5>3.0.CO;2-J

Rockland, K. S. (1998). Convergence and branching patterns of round, type 2 corticopulvinar axons. *J Comp Neurol*, *390*(4), 515–536.

Rockland, K. S. (2019). Distinctive Spatial and Laminar Organization of Single Axons from Lateral Pulvinar in the Macaque. *Vision*, *4*(1), 1. https://doi.org/10.3390/vision4010001

Romanski, L. M., Giguere, M., Bates, J. F., & Goldman-Rakic, P. S. (1997a). Topographic organization of medial pulvinar connections with the prefrontal cortex in the rhesus monkey. *The Journal of Comparative Neurology*, *379*(3), 313–332. https://doi.org/10.1002/(SICI)1096-9861(19970317)379:3<313::AID-CNE1>3.0.CO;2-6

Rosenberg, D. S., Mauguière, F., Catenoix, H., Faillenot, I., & Magnin, M. (2009). Reciprocal Thalamocortical Connectivity of the Medial Pulvinar: A Depth Stimulation and Evoked Potential Study in Human Brain. *Cerebral Cortex*, *19*(6), 1462–1473. https://doi.org/10.1093/cercor/bhn185

Rosenberg, D. S., Mauguiere, F., Demarquay, G., Ryvlin, P., Isnard, J., Fischer, C., Guenot, M., & Magnin, M. (2006). Involvement of Medial Pulvinar Thalamic Nucleus in Human Temporal Lobe Seizures. *Epilepsia*, *47*(1), 98–107. https://doi.org/10.1111/j.1528-1167.2006.00375.x

Saalmann, Y. B., & Kastner, S. (2011). Cognitive and Perceptual Functions of the Visual Thalamus. *Neuron*, *71*(2), 209–223. https://doi.org/10.1016/j.neuron.2011.06.027

Saalmann, Y. B., & Kastner, S. (2015). The cognitive thalamus. *Frontiers in Systems Neuroscience*, *9*. https://doi.org/10.3389/fnsys.2015.00039

Saalmann, Y. B., Pinsk, M. A., Wang, L., Li, X., & Kastner, S. (2012). The pulvinar regulates information transmission between cortical areas based on attention demands. *Science*, *337*(6095), 753–756. https://doi.org/10.1126/science.1223082

Salinas, E., & Sejnowski, T. J. (2001). Book Review: Gain Modulation in the Central Nervous System: Where Behavior, Neurophysiology, and Computation Meet. *The Neuroscientist*, *7*(5), 430–440. https://doi.org/10.1177/107385840100700512

Schneider, L., Dominguez-Vargas, A.-U., Gibson, L., Kagan, I., & Wilke, M. (2019). Eye position signals in the dorsal pulvinar during fixation and goal-directed saccades. *Journal of Neurophysiology*, *123*(1), 367–391. https://doi.org/10.1152/jn.00432.2019

Schneider, L., Dominguez-Vargas, A.-U., Gibson, L., Wilke, M., & Kagan, I. (2021). *Visual, delay and oculomotor timing and tuning in macaque dorsal pulvinar during instructed and free choice memory saccades* [Preprint]. Neuroscience. https://doi.org/10.1101/2021.12.21.473504

Schultz, W. (2015). Neuronal Reward and Decision Signals: From Theories to Data. *Physiol Rev*, *95*(3), 853–951. https://doi.org/10.1152/physrev.00023.2014

Selemon, L., & Goldman-Rakic, P. (1988). Common cortical and subcortical targets of the dorsolateral prefrontal and posterior parietal cortices in the rhesus monkey: Evidence for a distributed neural network subserving spatially guided behavior. *The Journal of Neuroscience*, *8*(11), 4049–4068. https://doi.org/10.1523/JNEUROSCI.08-11-04049.1988

Sherman, S. M. (2017a). Functioning of Circuits Connecting Thalamus and Cortex. In R. Terjung (Ed.), *Comprehensive Physiology* (1st ed., pp. 713–739). Wiley. https://doi.org/10.1002/cphy.c160032

Sherman, S. M. (2017b). Functioning of Circuits Connecting Thalamus and Cortex. In R. Terjung (Ed.), *Comprehensive Physiology* (1st ed., pp. 713–739). Wiley. https://doi.org/10.1002/cphy.c160032

Sherman, S. M., & Guillery, R. W. (1996). Functional organization of thalamocortical relays. *Journal of Neurophysiology*, *76*(3), 1367–1395. https://doi.org/10.1152/jn.1996.76.3.1367

Sherman, S. M., & Guillery, R. W. (2002). The role of the thalamus in the flow of information to the cortex. *Philosophical Transactions of the Royal Society of London. Series B: Biological Sciences*, *357*(1428), 1695–1708.

Sherman, S. M., & Guillery, R. W. (2013). *Functional Connections of Cortical Areas: A New View from the Thalamus*. The MIT Press. https://doi.org/10.7551/mitpress/9780262019309.001.0001

Shine, J. M., Müller, E. J., Munn, B., Cabral, J., Moran, R. J., & Breakspear, M. (2021). Computational models link cellular mechanisms of neuromodulation to large-scale neural dynamics. *Nature Neuroscience*, *24*(6), 765–776. https://doi.org/10.1038/s41593-021-00824-6

Shipp, S. (2003). The functional logic of cortico-pulvinar connections. *Philosophical Transactions of the Royal Society B: Biological Sciences*, *358*(1438), 1605–1624. https://doi.org/10.1098/rstb.2002.1213

Skora, L. I., Livermore, J. J. A., & Roelofs, K. (2022). The functional role of cardiac activity in perception and action. *Neuroscience & Biobehavioral Reviews*, *137*, 104655. https://doi.org/10.1016/j.neubiorev.2022.104655

Snow, J. C., Allen, H. A., Rafal, R. D., & Humphreys, G. W. (2009). Impaired attentional selection following lesions to human pulvinar: Evidence for homology between human and monkey. *Proc Natl Acad Sci U S A*, *106*(10), 4054–4059. https://doi.org/10.1073/pnas.0810086106

Soares, S. C., Maior, R. S., Isbell, L. A., Tomaz, C., & Nishijo, H. (2017). Fast Detector/First Responder: Interactions between the Superior Colliculus-Pulvinar Pathway and Stimuli Relevant to Primates. *Frontiers in Neuroscience*, *11*. https://doi.org/10.3389/fnins.2017.00067

Sridharan, D., Steinmetz, N. A., Moore, T., & Knudsen, E. I. (2017). Does the Superior Colliculus Control Perceptual Sensitivity or Choice Bias during Attention? Evidence from a Multialternative Decision Framework. *Journal of Neuroscience*, *37*(3), 480–511. https://doi.org/10.1523/JNEUROSCI.4505-14.2017

Stanislaw, H., & Todorov, N. (1999). Calculation of signal detection theory measures. *Behavior Research Methods, Instruments, & Computers*, *31*(1), 137–149. https://doi.org/10.3758/BF03207704

Stein, B. E., Stanford, T. R., & Rowland, B. A. (2014). Development of multisensory integration from the perspective of the individual neuron. *Nature Reviews Neuroscience*, *15*(8), 520–535. https://doi.org/10.1038/nrn3742

Stepniewska, I. (2003). The pulvinar complex. In *The Primate Visual System*. CRC Press.

Stepniewska, I., Preuss, T. M., & Kaas, J. H. (1994). Thalamic connections of the primary motor cortex (M1) of owl monkeys. *The Journal of Comparative Neurology*, *349*(4), 558–582. https://doi.org/10.1002/cne.903490405

Stitt, I., Zhou, Z. C., Radtke-Schuller, S., & Fröhlich, F. (2018). Arousal dependent modulation of thalamo-cortical functional interaction. *Nature Communications*, *9*(1), 2455. https://doi.org/10.1038/s41467-018-04785-6

Strumpf, H., Mangun, G. R., Boehler, C. N., Stoppel, C., Schoenfeld, M. A., Heinze, H.-J., & Hopf, J.-M. (2013). The role of the pulvinar in distractor processing and visual search. *Human Brain Mapping*, *34*(5), 1115–1132. https://doi.org/10.1002/hbm.21496

Ungerleider, L. G., & Christensen, C. A. (1977). Pulvinar lesions in monkeys produce abnormal eye movements during visual discrimination training. *Brain Research*, *136*(1), 189–196. https://doi.org/10.1016/0006-8993(77)90146-9

Van der Stigchel, S., Arend, I., van Koningsbruggen, M. G., & Rafal, R. D. (2010). Oculomotor integration in patients with a pulvinar lesion. *Neuropsychologia*, *48*(12), 3497–3504. https://doi.org/10.1016/j.neuropsychologia.2010.07.035

Van Essen, D. C., Felleman, D. J., DeYoe, E. A., Olavarria, J., & Knierim, J. (1990). Modular and Hierarchical Organization of Extrastriate Visual Cortex in the Macaque Monkey. *Cold Spring Harbor Symposia on Quantitative Biology*, *55*(0), 679–696. https://doi.org/10.1101/SQB.1990.055.01.064

van Hemmen, J. L., & Sejnowski, T. J. (Eds.). (2006). *23 Problems in Systems Neuroscience*. Oxford University Press. https://doi.org/10.1093/acprof:oso/9780195148220.001.0001

Van Le, Q., Isbell, L. A., Matsumoto, J., Nguyen, M., Hori, E., Maior, R. S., Tomaz, C., Tran, A. H., Ono, T., & Nishijo, H. (2013). Pulvinar neurons reveal neurobiological evidence of past selection for rapid detection of snakes. *Proceedings of the National Academy of Sciences*, *110*(47), 19000–19005. https://doi.org/10.1073/pnas.1312648110

Vittek, A.-L., Juan, C., Nowak, L. G., Girard, P., & Cappe, C. (2022). *Multisensory integration in neurons of the medial pulvinar of macaque monkey* [Preprint]. Neuroscience. https://doi.org/10.1101/2022.03.21.485176

Vittek, A.-L., Juan, C., Nowak, L. G., Girard, P., & Cappe, C. (2023). Multisensory integration in neurons of the medial pulvinar of macaque monkey. *Cerebral Cortex*, *33*(8), 4202–4215. https://doi.org/10.1093/cercor/bhac337

Walker, A. E. (1938). *The primate thalamus*.

Wandschneider, B., Koepp, M., Scott, C., Micallef, C., Balestrini, S., Sisodiya, S. M., Thom, M., Harper, R. M., Sander, J. W., Vos, S. B., Duncan, J. S., Lhatoo, S., & Diehl, B. (2015). Structural imaging biomarkers of sudden unexpected death in epilepsy. *Brain*, *138*(10), 2907–2919. https://doi.org/10.1093/brain/awv233

Ward, R., & Arend, I. (2007). An object-based frame of reference within the human pulvinar. *Brain*, *130*(Pt 9), 2462–2469.

Ward, R., Calder, A. J., Parker, M., & Arend, I. (2007). Emotion recognition following human pulvinar damage. *Neuropsychologia*, *45*(8), 1973–1978. https://doi.org/10.1016/j.neuropsychologia.2006.09.017

Ward, R., & Danziger, S. (2005). Selective attention and response control following damage to the human pulvinar. In G. Humphreys & J. Riddoch (Eds.), *Attention in Action: Advances from Cognitive Neuroscience* (pp. 325–350). Psychology Press.

Ward, R., Danziger, S., & Bamford, S. (2005). Response to Visual Threat Following Damage to the Pulvinar. *Current Biology*, *15*(6), 571–573. https://doi.org/10.1016/j.cub.2005.01.056

Wardak, C., Ibos, G., Duhamel, J. R., & Olivier, E. (2006). Contribution of the monkey frontal eye field to covert visual attention. *J Neurosci*, *26*(16), 4228–4235.

Wardak, C., Olivier, E., & Duhamel, J. R. (2002). Saccadic target selection deficits after lateral intraparietal area inactivation in monkeys. *J Neurosci*, *22*(22), 9877–9884.

Wardak, C., Olivier, E., & Duhamel, J. R. (2004). A deficit in covert attention after parietal cortex inactivation in the monkey. *Neuron*, *42*(3), 501–508.

Webster, M. J., Bachevalier, J., & Ungerleider, L. G. (1993). Subcortical connections of inferior temporal areas TE and TEO in macaque monkeys. *J Comp Neurol*, *335*(1), 73–91.

Wilke, M., Kagan, I., & Andersen, R. A. (2012). Functional imaging reveals rapid reorganization of cortical activity after parietal inactivation in monkeys. *Proceedings of the National Academy of Sciences*, *109*(21), 8274–8279. https://doi.org/10.1073/pnas.1204789109

Wilke, M., Kagan, I., & Andersen, R. A. (2013). Effects of Pulvinar Inactivation on Spatial Decision-making between Equal and Asymmetric Reward Options. *Journal of Cognitive Neuroscience*, *25*(8), 1270–1283. https://doi.org/10.1162/jocn_a_00399

Wilke, M., Mueller, K. M., & Leopold, D. A. (2009). Neural activity in the visual thalamus reflects perceptual suppression. *Proc Natl Acad Sci U S A*, *106*(23), 9465–9470.

Wilke, M., Turchi, J., Smith, K., Mishkin, M., & Leopold, D. A. (2010). Pulvinar Inactivation Disrupts Selection of Movement Plans. *Journal of Neuroscience*, *30*(25), 8650–8659. https://doi.org/10.1523/JNEUROSCI.0953-10.2010

Woo, M. A., Macey, P. M., Fonarow, G. C., Hamilton, M. A., & Harper, R. M. (2003). Regional brain gray matter loss in heart failure. *Journal of Applied Physiology*, *95*(2), 677–684. https://doi.org/10.1152/japplphysiol.00101.2003

Wyart, V., Nobre, A. C., & Summerfield, C. (2012). Dissociable prior influences of signal probability and relevance on visual contrast sensitivity. *Proceedings of the National Academy of Sciences*, *109*(9), 3593–3598. https://doi.org/10.1073/pnas.1120118109

Yirmiya, R., & Hocherman, S. (1987). Auditory- and movement-related neural activity interact in the pulvinar of the behaving rhesus monkey. *Brain Research*, *402*(1), 93–102. https://doi.org/10.1016/0006-8993(87)91051-1

Zenon, A., & Krauzlis, R. J. (2012). Attention deficits without cortical neuronal deficits. *Nature*, *489*(7416), 434–437. https://doi.org/10.1038/nature11497

Zhou, H., & Desimone, R. (2011). Feature-Based Attention in the Frontal Eye Field and Area V4 during Visual Search. *Neuron*, *70*(6), 1205–1217. https://doi.org/10.1016/j.neuron.2011.04.032

Zhou, H., Schafer, R. J., & Desimone, R. (2016). Pulvinar-Cortex Interactions in Vision and Attention. *Neuron*, *89*(1), 209–220. https://doi.org/10.1016/j.neuron.2015.11.034